UNIVERSITY OF SOUTHAMPTON

FACULTY OF NATURAL & ENVIRONMENTAL SCIENCES

School of Chemistry

Studying the Lipoyl Synthase mediated conversion of Octanoyl substrates to Lipoyl products

by

Nhlanhla Sibanda

Thesis for the degree of Doctor of Philosophy

December 2013

UNIVERSITY OF SOUTHAMPTON

ABSTRACT

FACULTY OF NATURAL & ENVIRONMENTAL SCIENCES

CHEMICAL BIOLOGY

Thesis for the degree of Doctor of Philosophy

STUDYING THE LIPOYL SYNTHASE MEDIATED CONVERSION OF OCTANOYL SUBSTRATES TO LIPOYL PRODUCTS

By: Nhlanhla Sibanda

α-Lipoic acid is a cofactor used during oxidative metabolism reactions by several enzymes, including branched chain keto acid dehydrogenases, the glycine cleavage system, pyruvate dehydrogenase and α-ketoglutarate dehydrogenase.[1] The lipoic acid is attached to the ε-amino group of a specific lysine residue via an amide bond and acts as a carrier of acyl groups between active sites of these large multienzyme complexes.[2] The biosynthesis of lipoyl product requires as a cofactor the protein lipoyl synthase (LipA), which has two [4Fe-4S]$^{1+/2+}$ clusters, and uses *S*-adenosylmethionine as a substrate.[3] LipA is the product of the *lipA* gene [4] and has 36 % sequence homology to biotin synthase in *E.coli*, another protein involved in a sulfur insertion reaction.[5] The mechanism of sulfur insertion during lipoic acid biosynthesis is thought to be related to that for the BioB catalysed synthesis of biotin.[5, 6] LipA and BioB belong to a group of enzymes known to as the "radical SAM" superfamily.[7] All members of this group reductively cleave AdoMet to give methionine and the highly reactive 5′-deoxyadenosyl radical (5′- Ado•) which abstracts hydrogen atoms from appropriate substrates forming the side product 5'-deoxyadenosine and a substrate radical.[1, 8] The work in this thesis describes experiments that were carried out to study the mechanism of the LipA mediated reaction. LipA was expressed and purified in *E.coli* and two types of octanoylated substrates were synthesized; fluorescent and non-fluorescent substrates. These substrates were used in assays to probe the mechanism of the LipA mediated reaction. The binding constant of the co-substrate SAM to LipA was determined using fluorescence polarization assays. Experiments were also carried out to try and crystallize the LipA in the presence of octanoyl substrates and the co-substrate SAM.

Table of Contents

List of Tables

List of Figures

List of Schemes

DECLARATION OF AUTHORSHIP

I, **Nhlanhla Sibanda**

Declare that the thesis entitled

Studying the Lipoyl Synthase mediated conversion of Octanoyl substrates to Lipoyl products

And the work presented in the thesis is both my own, and has been generated by me as the result of my own original research. I confirm that:

- This work was done wholly or mainly while in candidature for a research degree at this University;
- Where any part of this thesis has previously been submitted for a degree or any other qualification at this University or any other institution, this has been clearly stated;
- Where I have consulted the published work of others, this is always clearly attributed;
- Where I have quoted from the work of others, the source is always given. With the exception of such quotations, this thesis is entirely my own work;
- I have acknowledged all main sources of help;
- Where the thesis is based on work done by myself jointly with others, I have made clear exactly what was done by others and what I have contributed myself;
- None of this work has been published before submission

Signed: ……

Dated: ……

Acknowledgements

I would like to thank Dr Ali Tavassoli and Dr Martin Grossel for their support and oversight during my studies and for supervising me in this project. I wish to also thank Graham Broader of the Roach group for helping me with the preparations of the fluorescent pentapeptide. I would like to thank Gerard Hobley for teaching me and helping me understand some of the organic synthesis work I had to do and for encouraging me when I was feeling low and tired during the course of my work. I would also like to thank my wife (Mrs Melody Portia Sibanda) for supporting me throughout all my studies and for helping me meet my financial needs when my grant was no longer available. I wish to thank my daughter (Pearl Nonhlanhla) and my son (Bongani Aaron) for inspiring me to work hard to succeed so that they could be proud of my achievements. Above all I thank God for granting me the ability and the strength to go through the difficult times I faced through my studies.

Abbreviations

ACP	Acyl carrier protein
ADH	Acetoin dehydrogenase complex
5′-Ado•	5′-Deoxyadenosyl radical
5′-AdoH	5′-Deoxyadenosine
AdoCbl	Adenosylcobalamin
AdoHcy	S-adenosylhomocysteine
AdoMet (SAM)	*S*-adenosylmethionine
APS	Alkaline protease solution
AMCA	7-Amino-4-methylcoumarin-3-acetic acid
AMCA-S	7-amino-4-methyl-6-sulfocoumarin-3-acetic acid or Alexa 350
ARR-AE	Anaerobic ribonucleotide reductase activation
ATP	Adenosyl triphosphate
BCKADH	Branched-chain α-keto acid dehydrogenase complex
BioB	Biotin synthase
B. sphaericus	*Bacillus sphaericus*
CLS	Cell lysis solution
CRS	Cell resuspension solution

Cys	Cysteine
d	Doublet
Dde	2-acetyldimedone
DECA	7-(diethylamino)-2-oxo-2*H*-chromene-3-carboxylic acid
DHL	Dihydrolipoyl
DIC	Diisopropylcarbodiimide
DIPEA	*N*,*N*-Diisopropylethylamine
DMAP	4-Dimethylaminopyridine
DMF	Dimethylformamide
DTB	Dethiobiotin (desthiobiotin)
DTT	Dithiothreitol
E. coli	*Escherichia coli*
EDTA	Ethylenediaminetetraacetic acid
ENDOR	Electron double nuclear resonance spectroscopy
EPR	Electron paramagnetic resonance spectroscopy
EtBr	Ethidium bromide
Fmoc	9-Fluorenylmethoxycarbonyl
[Fe-S]	Iron-Sulfur cluster
[2Fe-2S]	2 Iron- 2 Sulfur cluster

[4Fe-4S]	4 Iron- 4 Sulfur cluster
GCS	Glycine cleavage system
Glu	Glutamic acid (E)
GRE-AE’s	Glycyl radical enzyme activating enzymes
h	hour(s)
HemN	Coproporphyrinogen III oxidase
HOBt	Hydroxybenzotriazole
HPLC	High Performance Liquid Chromatography
HTP-FP	High-throughput fluorescence polarization
Ile	Isoleucine (I)
Isc	Iron-Sulfur cluster
KAM	Lysine 2,3-aminomutase
KDa	Kilodaltons
α-KGDH	α-Ketoglutarate dehydrogenase complex
LAE	Lipoate-activating enzyme
LCMS	Liquid column mass spectroscopy
LipA	Lipoyl synthase
LplA	Lipoate-protein ligase
Lys (K)	Lysine

m	Multiplet
MiaB	tRNA methylthiolation enzyme
min	minute
MoaA	Molybdopterin cofactor biosynthesis enzyme
MTA	5′-methylthioadenosine
MWCO	Molecular weight cut off
NADH	Nicotinamide adenine dinucleotide (reduced form)
NMP	*N*-methylpyrrolidone
NMR	Nuclear magnetic resonance spectroscopy
Non	Nonanoyl
Oct	Octanoyl
OD_{600}	Optical density at 600nm
PEG	Polyethylene glycol polymer
PDH	Pyruvate dehydrogenase complex
PFL	Pyruvate formate-lyase
PFL-AE	Pyruvate formate lyase activating enzyme
PLP	Pyridoxal 5′-phosphate
PyBOP	Benzotrizolyoxy-tris-[pyrrolidino]-phosphonium hexafluorophosphate
RED	Rapid equilibrium dialysis

rpm	rotations per minute (revolutions per minute)
SDS-PAGE	Sodium dodecyl sulfate polyacrylamide gel electrophoresis
s	Singlet
SAH	*S*-adenosylhomocysteine
SAM	*S*-adenosylmethionine
S. solfataricus	*Sulfolobus solfataricus*
SPPL	Spore photoproduct lyase
SPPS	Solid phase peptide synthesis
t	Triplet
*t*Bu	*tert*-Butyl
TCEP	Tris-(2-carboxyethyl)-phosphine
TAE	Tris-acetate-EDTA
TFA	Trifluoroacetic acid
THF	Tetrahydrofolate
Thr (T)	Threonine
TPP	Thiamine pyrophosphate
VTMCD	Variable-temperature magnetic circular dichroism

Chapter 1: Introduction

1.1 Nature and the sulfur containing compounds

All living organisms possess sulfur-containing biochemicals whose synthesis entails the insertion of sulfur atoms into metabolic precursors and the selective formation of carbon-sulfur (C-S) bonds.[6, 9] The chemical structures of some sulfur-containing compounds that are found in living organisms are shown in Figure 1.1. These compounds include essential co-factors, antibiotics and natural products, and some modified amino acids in proteins and thionucleosides in tRNAs.[6]

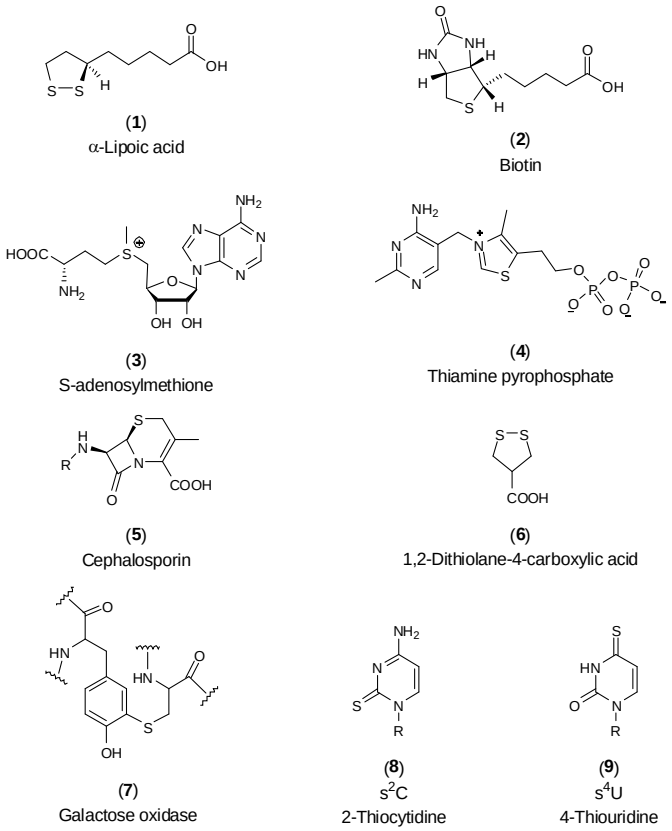

Figure 1.1 *The chemical structures of some naturally-occurring sulfur containing compounds are shown ~=-lipoic acid (***1***), biotin (***2***), S-adenosylmethionine (***3***), and thiamine pyrophosphate (***4***) are essential cofactors. Cephalosporin (***5***) is an antibiotic and 1,2-dithiolane-4-carboxylic acid (***6***) is a natural product. Galactose oxidase (***7***) is a modified amino acid, whilst 2-thiocytidine (***8***) and 4-thiouridine (***9***) are thionucleosides found in t-RNAs.*

1.2 SAM (AdoMet) as a source of various functional groups

The sulfonium compound *S*-adenosylmethionine (SAM or AdoMet) is recognised as the major methyl donor in a myriad of essential biochemical and biological processes.[10, 11] Processes such as the regulation of hormones, neurotransmitters and signal transduction; the regulation of gene expression, brain function and foetal development are affected by methylation. SAM also plays an important role as a source of various other essential chemical groups. Scheme 1.1 shows a few chemical transformations in which SAM is used as a source of different chemical groups. AdoMet can be used as a source of methylene, ribosyl, amino and aminoalkyl groups.[12] In fact adenosine-5′-triphosphate (ATP) and SAM are the two most widely used enzyme substrates in many essential biochemical transformations.[11, 12]

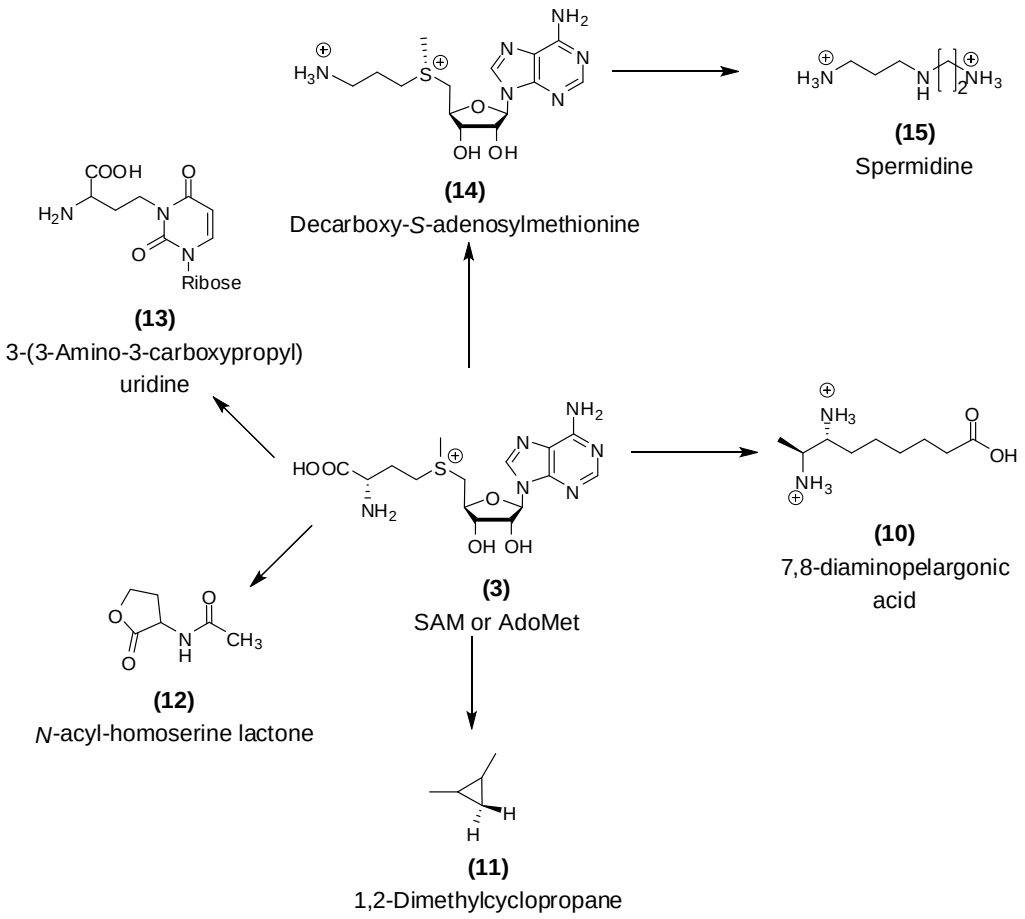

Scheme 1.1 *S-adenosylmethionine (SAM or AdoMet) has various applications in living organisms; the scheme shows the chemical structures of a number of essential compounds that are derived from SAM.*

Another essential function of AdoMet is as a source of radicals that are involved in a wide range of biochemical reactions. One such reaction is the lipoyl synthase (LipA) catalyzed biosynthesis of lipoyl products from octanoyl substrates, the study of which forms the basis for the work described in this thesis.

1.3 Radical enzymes and biochemical reactions

A wide range of biosynthetic and catabolic reactions in a host of organisms are mediated by radical enzymes.[13, 14] Examples of such transformations include amino acid catabolism, α-keto acid metabolism; vitamin and cofactor biosyntheses, deoxyribonucleotide biosynthesis and prostaglandin biosynthesis.[14, 15] However, it is not yet understood how unstable radical species can mediate some of the most important biological processes. These processes include respiration, photosynthesis, DNA synthesis and repair; and many other metabolic reactions and biosynthetic pathways that need to be closely regulated. There is evidence to suggest that the protein environment can provide the conditions necessary for such regulation.[16] The majority of the involved enzymes spawn their own organic radicals, but many rely on activases to provide the organic radicals which are stored as cysteinyl, glycyl, tryptophanyl or tyrosinyl radicals for use in multiple catalytic turnovers.[15] Electron paramagnetic resonance (EPR) spectroscopy of specifically labelled target molecules has been used to identify these species, but in many cases, the radicals are so reactive that they are not detectable.

1.3.1 The "radical SAM" superfamily

Sofia *et al.* (2001) using iterative profile searches and powerful bioinformatics and information visualisation techniques identified a group of metalloenzymes that they called the "radical SAM" superfamily.[17] The name was selected to differentiate this group of proteins from the classical SAM-dependent reactions that proceed via polar mechanisms (e.g. S_N2 pathways).[18] At that time, the "radical SAM" superfamily was predicted to have over 600 members. However, since then others

have indicated that this superfamily of enzymes could consist of over 2800 proteins in 781 microbial genomes.[18-20]

At present, only a few of the "radical SAM" proteins have been purified and partially characterized. For some enzymes, *e.g.* lysine 2,3-aminomutase (KAM), pyruvate formate-lyase (PFL), coproporphyrinogen III oxidase (HemN), and molybdopterin cofactor biosynthesis enzyme (MoaA) a lot of mechanistic and structural data has been obtained through various studies. For enzymes, such as spore photoproduct lyase (SPPL), anaerobic ribonucleotide reductase activation subunit (ARR-AE), lipoyl synthase, and tRNA methylthiolation enzyme (MiaB) a significant amount of biochemical information has been put forward.[19, 21-24]

The "radical SAM" enzymes catalyze a wide range of reactions that are found in all the kingdoms of the living organisms.[25, 26] These proteins can broadly be put into two groups based on how they use SAM to bring about their characteristic biotransformations. One of these groups can be further divided into two sub-groups. The biotransformations shown in reaction Scheme 1.2 show some classical examples of reactions catalysed by members of the "radical SAM" enzymes. These reactions were chosen to show the different types of "radical SAM" enzyme groupings.

1.3.2 The "radical SAM" enzymes sub-groups

The first group consists of the enzymes that use AdoMet catalytically as a co-factor or co-enzyme.[19, 27] During each catalytic cycle, AdoMet is used as a reversible source of the 5′-deoxyadenosyl radical (5′-Ado•) and is subsequently regenerated. The only enzymes known to use AdoMet in this way are lysine 2,3-aminomutase (KAM) which catalyses the reversible transformation of lysine to β-lysine Scheme 1.2 (i)) and spore photoproduct lyase (SPPL) that repairs methylene-bridged thymine dimers in DNA.[27]

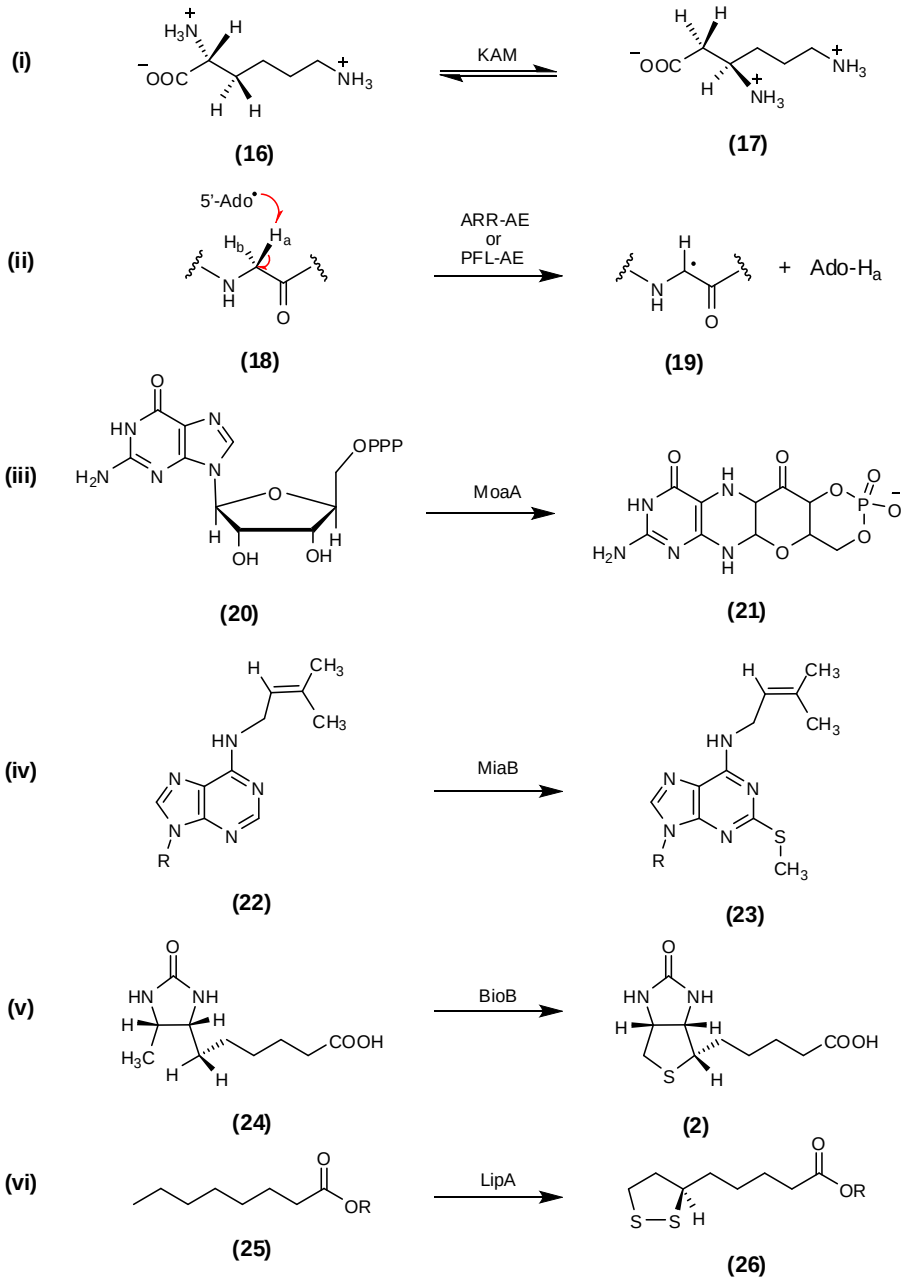

Scheme 1.2 *Examples of reactions catalysed by the 'radical SAM' enzymes, (i) Lysine 2,3-aminomutase catalyses the conversion of lysine to -lysine. (ii) Anaerobic ribonucleotide reductase activating enzyme and pyruvate formate lyase activating enzyme generate glycyl radicals on anaerobic ribonucleotide reductase and pyruvate formate lyase respectively. (iii) Molybdopterin biosynthesis protein A mediates the formation of "precursor Z", an intermediate in the biosynthesis of molybdopterin from 5'-GTP. (iv) MiaB is implicated in the thiolation and methylation of tRNA; (v) Biotin synthase catalyses the conversion of dethiobiotin to biotin; (vi) Lipoyl synthase catalyses the biosynthesis of lipoyl product from an octanoyl substrate.*[20, 28]

The second group of "radical SAM" enzymes are the glycyl radical enzyme activating enzymes (GRE-AEs). The enzymes in this group use the 5′-Ado• to abstract a hydrogen atom from a conserved glycine residue of an enzyme substrate (Scheme 1.2 (ii)). This activates the glycyl radical enzyme since the intermediate glycyl radical can be used to form a catalytic active site radical. Anaerobic ribonucleotide reductase activating enzyme (ARR-AE) and pyruvate formate lyase activating enzyme (PFL-AE) are examples of enzymes that fall into this group.[29]

The third group of "radical SAM" enzymes use stoichiometric quantities of the co-substrate AdoMet to facilitate their typical biochemical transformations.[19] This group consists of many more enzymes, and the reactions catalysed are very diverse. Reactions (iii) – (vi) of Scheme 1.2 show some examples of enzymes that use SAM as a substrate. In these reactions stoichiometric amounts of SAM are used in producing 5′-Ado• radicals that in-turn are used in oxidising the substrates.[27, 30]

1.3.3 Features common to the "radical SAM" enzymes

The identified members of the "radical SAM" superfamily of enzymes have the following three features in common. Firstly, almost all members of the "radical SAM" family possess a conserved amino acid sequence CX_3CX_2C (where C is a cysteine residue) that coordinates to three iron (Fe) atoms of a $[4Fe\text{-}4S]^{+/2+}$ cluster. Table 1.1 lists six examples of "radical SAM" enzymes and also shows for each enzyme the residues indicated as possessing the conserved CX_3CX_2C amino acid sequence. The fourth, uncoordinated Fe atom of this cluster is unique and is said to coordinate to SAM when available.[7, 16, 28] The [4Fe-4S] clusters of radical SAM enzymes are extremely oxygen labile and easily decompose into [3Fe-4S] or [2Fe-2S] clusters and are only active under strictly anaerobic conditions, which has made the characterisation of the "radical SAM" enzymes very difficult.[27]

Table 1.1 *Sequence alignment of amino acids for "radical SAM" enzymes to show the characteristic conserved CX_3CX_2C binding motif.*

Protein	Residues	Sequence
LipA	92 – 103	A I **C** T R R **C** P F **C** D V
BioB	51 – 62	G A **C** P E D **C** K Y **C** P Q
MiaB	155 -166	E G **C** N K Y **C** T Y **C** V V
ARR-AE	24 -35	S G **C** V H E **C** P G **C** Y N
PFL-AE	28 – 39	Q G **C** L M R **C** L Y **C** H N
KAM	131 - 142	N Q **C** S M Y **C** R Y **C** T R

The second common feature is that "radical SAM" enzymes require AdoMet as a co-factor or as the co-substrate. The AdoMet has to be in close proximity to, and directly coordinated to the [4Fe-4S] cluster, thereby enabling the transfer of a single electron from the cluster to AdoMet. Spectroscopic studies on a number of "radical SAM" enzymes indicated that it was the AdoMet's α-amino and α-carboxylate groups that coordinate to the [4Fe-4S] cluster's available Fe atom.

The pictures in Figure 1.2 show the $[4Fe\text{-}4S]^+$ clusters of four "radical SAM" enzymes and the relative positions of the cysteine residues and the AdoMet. For each [4Fe-4S] cluster, three Fe centres are coordinated to the CX_3CX_2C binding motifs and the unique Fe centre coordinates to the AdoMet. The $[4Fe\text{-}4S]^+$ cluster is thought to transfer an electron into the sulfonium of AdoMet generating an unstable species, which leads to fragmentation of the molecule into methionine and the highly unstable 5′-deoxyadenosyl radical intermediate.[31]

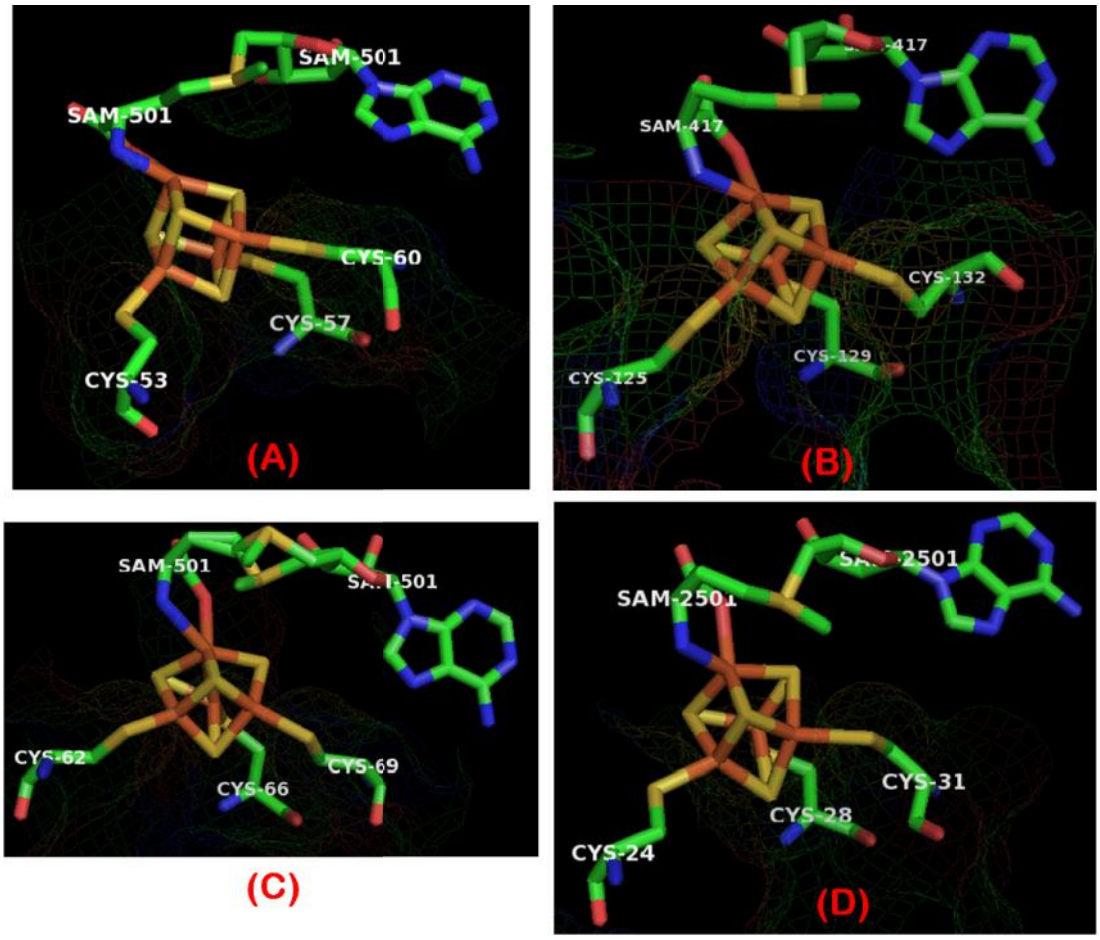

Figure 1.2 *Images showing the [4Fe-4S]$^{1+}$ clusters of the "radical SAM" enzymes (A) BioB; (B) KAM; (C) HemN and (D) MoaA. The images show the three Fe centres of each cluster that are coordinated to the CX_3CX_2C binding motifs. The unique Fe sites for each cluster are shown coordinated to AdoMet.* The *coordinates were downloaded from the protein data bank and the structures prepared using the Pymol Molecular Graphics system.*

The third common feature is that to reductively cleave AdoMet into the highly reactive 5′-Ado• radical and methionine, "radical SAM" enzymes require a low-potential electron donor, a ferredoxin or a flavodoxin. The 5′-Ado• radical in turn initiates enzymatic catalysis by abstracting a hydrogen atom from the appropriate substrate leading to the formation of 5′-deoxyadenosine (5′-AdoH) which is either released irreversibly as a by-product or recycled to regenerate the AdoMet.[32]

The sequences of reactions that are common to the "radical SAM" superfamily of enzymes are shown in the reaction Scheme 1.3.

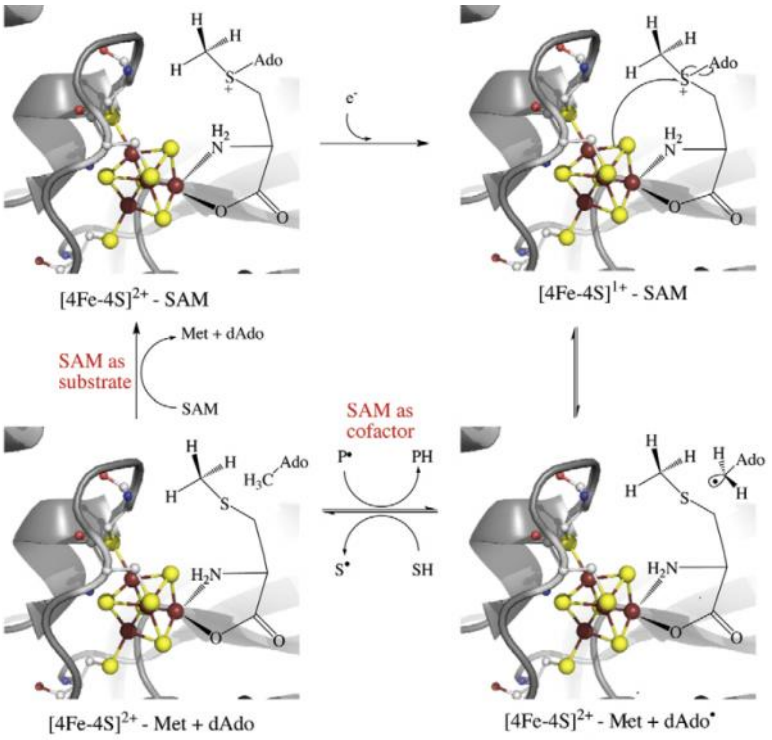

Scheme 1.3 *The sequence of reactions common to the "radical SAM" superfamily of enzymes that lead to the formation of methionine, 5′-deoxyadenosine and the product of the reaction. This picture was reproduced from a paper by Duschene et. al (2009).*[20]

In the vicinity of a $[4Fe\text{-}4S]^{2+}$ cluster AdoMet binds to the cluster's free Fe site using the methionine's α-amino and α-carboxylate groups. This enables the transfer of a single electron from a reductant such as sodium dithionite, flavodoxin, flavodoxin reductase and NADPH system or reduced deazaflavin. The stable $[4Fe\text{-}4S]^{2+}$ cluster is reduced to the highly reactive $[4Fe\text{-}4S]^{1+}$ cluster.[20, 33] An inner sphere single electron transfer from the $[4Fe - 4S]^{1+}$ species to the sulfonium of AdoMet occurs, resulting in the homolytic cleavage of the AdoMet's 5′C-S bond with the concomitant formation of a 5′-deoxyadenosyl radical (5′- Ado•) and methionine.[20] The formed highly reactive 5′-Ado• radical then abstracts a hydrogen atom from an appropriately positioned carbon on a substrate, which could be an organic molecule, protein or nucleic acid.[16, 28]

When the 5′-Ado• radical abstracts a proton from the substrate the products of this reaction are 5′-AdoH and a highly reactive substrate radical intermediate. For most of the "radical SAM" enzymes this substrate radical species intermediate will then be involved in other reactions. The only exceptions are the GRE-AEs for which the enzyme catalysed reaction ends with the formation of the glycyl radicals and the 5′-AdoH.[20] In some instances AdoMet is regenerated by the re-abstraction of the H atom from 5′-AdoH, in which case AdoMet is acting as a true cofactor. In other reactions AdoMet will be consumed and acts as a co-substrate.[15]

1.3.4 Formation of 5′-deoxyadenosyl (5′- Ado•) radicals

The first member of the "radical SAM" superfamily of enzymes to be identified was lysine 2,3-aminomutase which catalyzes the conversion of lysine to β-lysine (Scheme 1.2 (i)).[27, 34, 35] In this process lysine's α-amino moiety migrates to the β-carbon in β-lysine. There is an inversion in the absolute configuration at the C3 atom and the 3-pro-*R* hydrogen of lysine migrates to the 2-pro-*R* position.[19] The reaction Scheme 1.4 shows a proposed reaction mechanism by which KAM catalyzes the conversion of lysine to β-lysine.

KAM contains pyridoxal 5′-phosphate (PLP) and traces of iron. It was observed that adding exogenous PLP and ferrous ions to purified lysine amino mutase enhanced enzymatic activity.[19] Significantly, it was found that sodium dithionite and AdoMet were prerequisites for *in vitro* KAM activity.[35, 36] This raised the possibility that the lysine amino mutase mediated reaction involved 5′- Ado• radical. Until this intervention the only identified source of 5′- Ado• radicals had been adenosylcobalamin (AdoCbl). These findings led to the conclusions that the mechanism of the reaction catalysed by KAM was similar to that for the adenosylcobalamin-dependent rearrangements. AdoCbl and SAM function as sources of 5′- Ado• radicals that abstract H atoms from suitable substrates in order to facilitate the enzymatic reactions.[37, 38] In fact "radical SAM" enzymes catalyze many more reactions than the adenosylcobalamin-dependent enzymes.

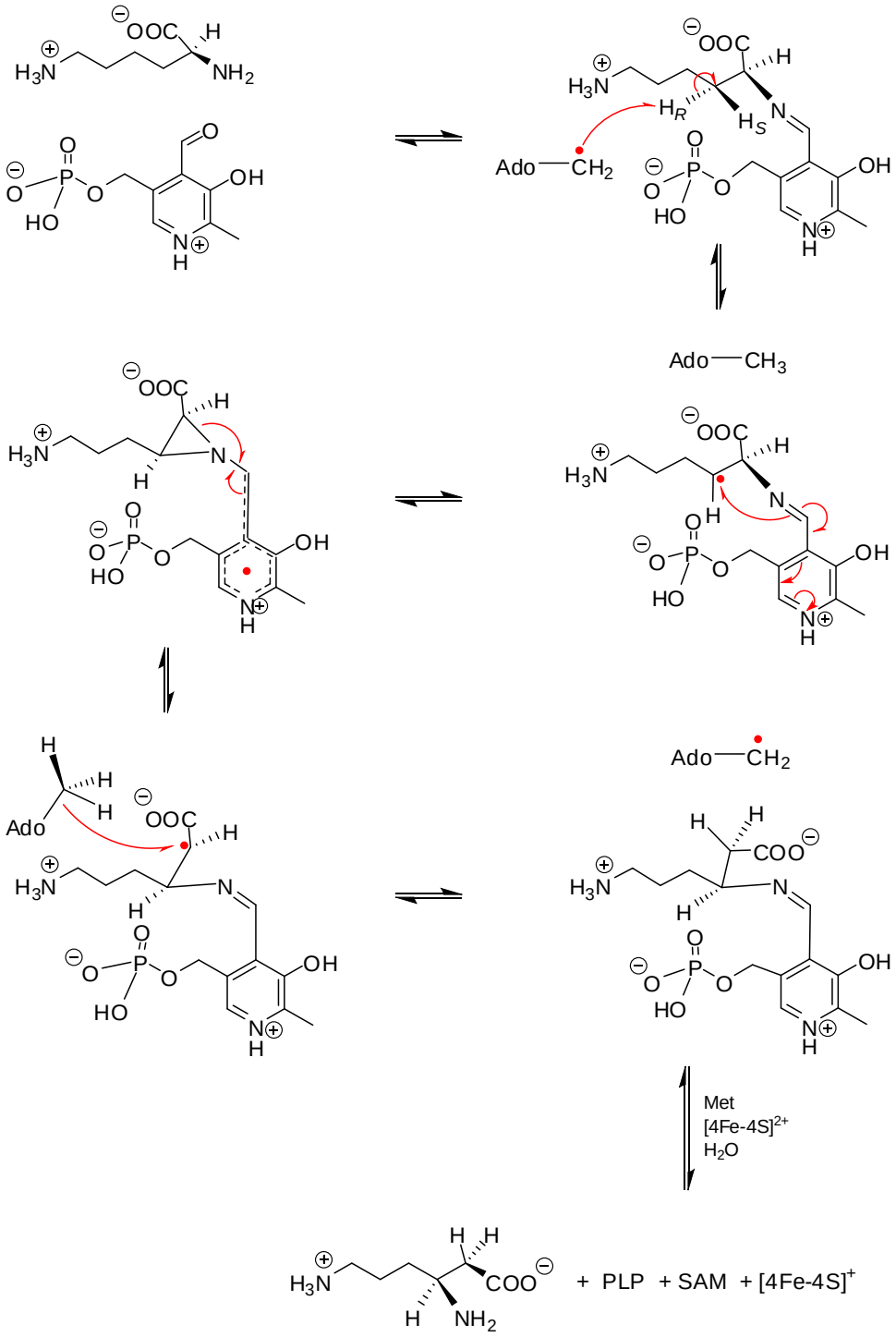

Scheme 1.4 *A proposed reaction mechanism for the KAM mediated conversion of lysine to -lysine.*

The chemical structures of SAM and AdoCbl are shown in Figure 1.3. The diagram also shows how the 5′- Ado• radicals would be formed from both compounds by the cleavage of C-S and Co-S bonds respectively.

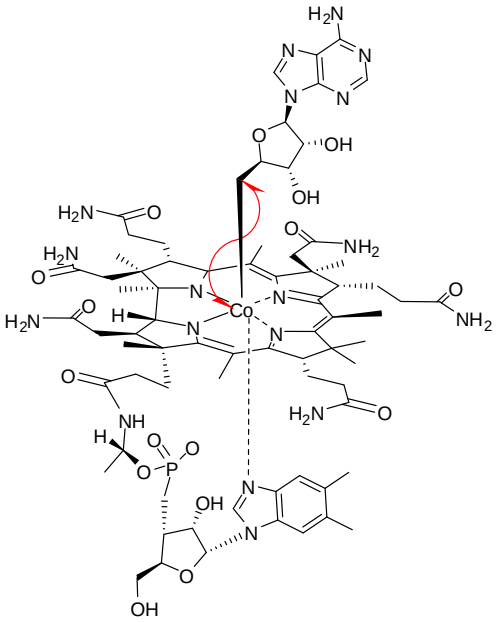

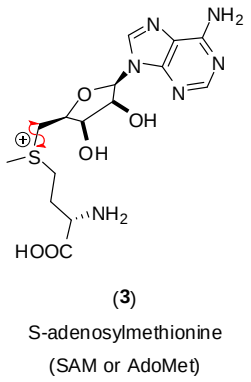

Figure 1.3 *The structures of adenosylcobalamin and S-adenosylmethionine. Adenosylcobalamin undergoes a homolytic cleavage of the C-Co bond, whilst SAM under goes a single electron reductive cleavage of the C-S bond to give the 5′-Ado• radicals (the cleavages are shown by the red-half arrows).*

When a substrate binds an adenosylcobalamin-dependent enzyme, the weak C-Co bond (dissociation energy ~ 30 kcal mol^{-1}) easily undergoes homolytic cleavage to give the highly active 5′-deoxyadenosyl radical [27, 34]; this is known to be a reversible process.[38, 39] However for the “radical SAM” enzyme mediated reactions, the significantly stronger S-C bond (≥ 60 kcal mol^{-1}) in SAM cannot undergo homolytic cleavage. Instead this bond undergoes an irreversible reductive cleavage that gives the 5′- Ado• radical and the by-product methionine. The only exceptions are lysine 2,3-aminomutase and spore photoproduct lyase that reversibly give 5′- Ado• radicals, without an overall change in the substrate’s oxidation state.[38]

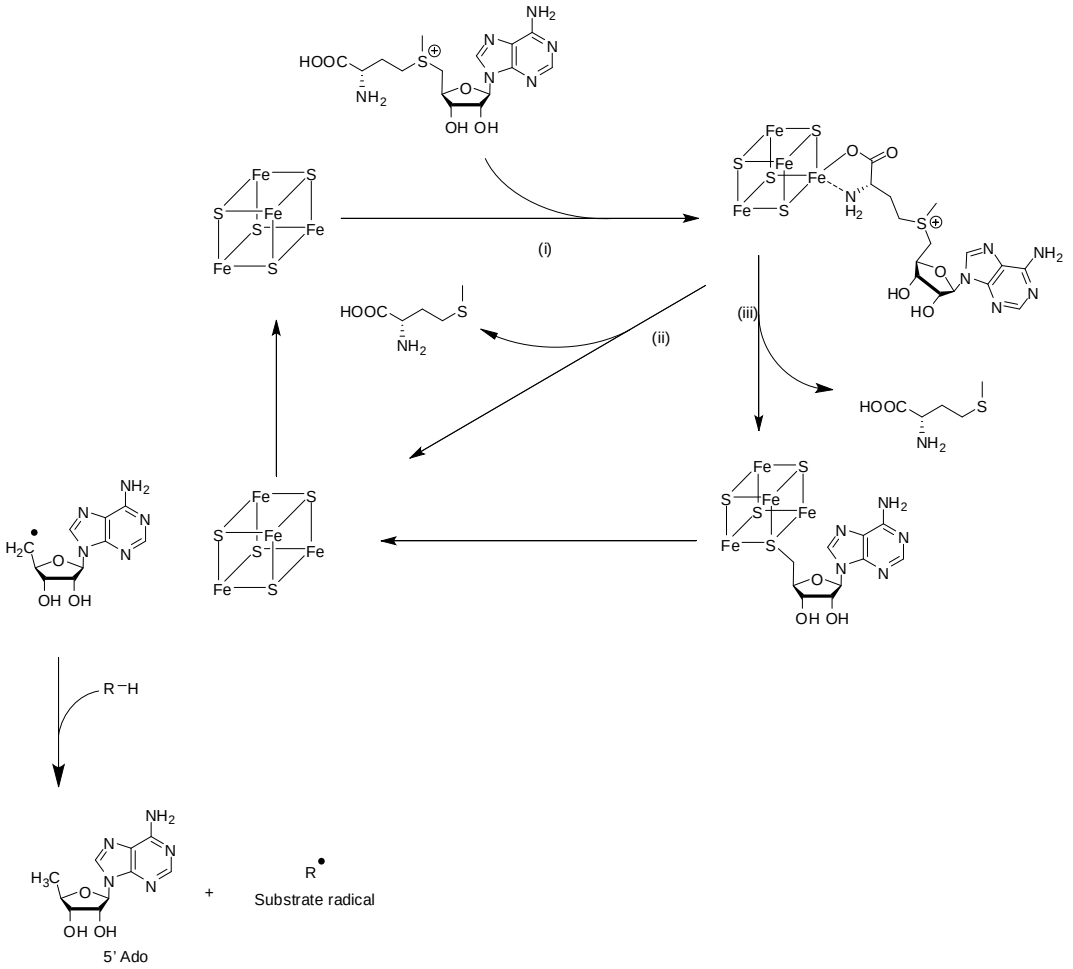

Scheme 1.5 *Two proposed mechanisms using the [4Fe-4S] cluster for the cleavage of SAM to produce 5′-deoxyadenosyl (5′- Ado•) radicals.*[12]

The reaction Scheme 1.5 shows two mechanisms in which the [4Fe-4S] cluster cleaves SAM. X-ray crystallography, Mössbauer spectroscopy, electron double nuclear resonance (ENDOR), EPR and Raman resonance spectroscopy have all provided proof that SAM binds at the free Fe of the $[4Fe\text{-}4S]^{+}$ cluster using the α-amino group and the α-carboxylate groups; this is the first step in the reductive cleavage of AdoMet (Scheme 1.5 (i)). After this, there are two possible routes by which the cleavage of AdoMet can be achieved (Scheme 1.5 paths (ii) or (iii)). Route (ii) involves an inner sphere transfer of an electron from the $[4Fe\text{-}4S]^{+}$ cluster to AdoMet; whereas route (iii) involves a bridging sulfide alkylation unstable intermediate which is then homolytically cleaved at the 5′-C-S bond. Both pathways lead to the formation of methionine and the 5′- Ado• radical.

1.3.5 The function of the iron-sulfur cluster in the cleavage of SAM

[Fe-S] clusters are generally accepted as stable redox factors that facilitate electron transfer reactions and are utilized by many proteins as cofactors.[14, 27] The most common types of [Fe-S] clusters have the [4Fe-4S], [3Fe-4S] and [2Fe-2S] cores and at least one of these is found in 120 different types of enzymes and proteins.[27, 40] Most of the "radical SAM" superfamily enzymes can accommodate all of these different clusters. However, the type of cluster present at any given stage depends on the electrochemical potential and the available iron and sulfide.[14] The different [Fe-S] cluster states are interconvertible and reaction Scheme 1.6 shows how these changes in state are proposed to occur.

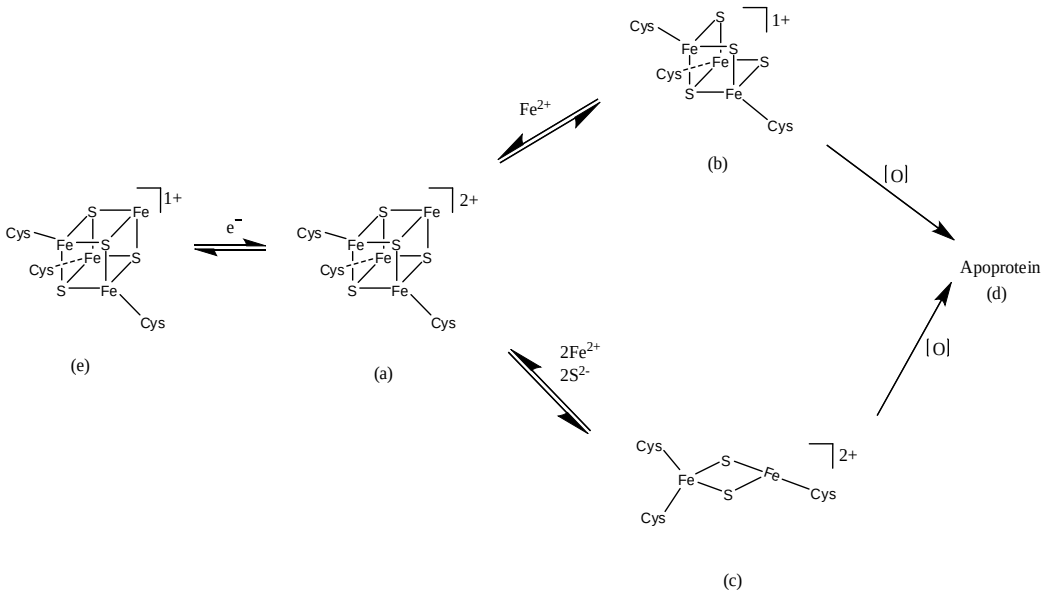

Scheme 1.6 *Diagram showing how the [Fe-S] cluster states of the "radical SAM" enzymes can be interconverted. This diagram was adapted from a paper by Jarrett et al. (2003).*[14]

The $[3Fe\text{-}4S]^{+}$ or $[2Fe\text{-}2S]^{2+}$ clusters (Scheme 1.6 (b) and (c)) result when a $[4Fe\text{-}4S]^{2+}$ loses one or two electron(s) and one or two Fe^{3+} ions. Further oxidation of these clusters would give the apoprotein (Scheme 1.6 (d)). The $[4Fe\text{-}4S]^{2+}$ and/or $[4Fe\text{-}4S]^{+}$ clusters (Scheme 1.6 (a) and (e)) are formed by reducing $[2Fe\text{-}2S]^{2+}$ and $[3Fe\text{-}4S]^{+}$. However, the Fe^{2+} and the S^{2-} ions required for this transformation are derived from disintegrated [Fe-S] clusters of other protein molecules, which results in a less

than stoichiometric yield of [4Fe-4S] clusters.[14] This yield can be increased to stoichiometric values by supplying exogenous Fe^{2+} and S^{2-}.

The [Fe-S] clusters discussed so far are those in which the Fe atoms are ligated to at least one cysteine residue of the protein backbone. The "radical SAM" enzymes, however, have [4Fe-4S] clusters in which three of the Fe atoms are coordinated to three cysteine residues from the conserved CX_3CX_2C binding motif of the protein. The fourth unique Fe atom is not coordinated, which most probably causes the cluster's extreme lability and its rapid decomposition under mild oxidizing conditions.[27] The $[4Fe\text{-}4S]^{1+}$ cluster was identified by electron paramagnetic resonance spectroscopy (EPR) as the catalytically active species. [14, 27]

As has already been stated, the "radical SAM" enzymes can be classified into two groups (or three sub-groups) based on how AdoMet is used during the course of a catalytic reaction. Spectroscopic experiments indicated that the [Fe-S] clusters in two of these sub-groups bind differently to AdoMet.[27] This could be the reason why the members of these two groups differ in how they use AdoMet. The members of one group use AdoMet catalytically as a co-factor or co-enzyme, whereas the members of the second group use SAM as a substrate. Scheme 1.7 shows how SAM is thought to bind to the [4Fe-4S] clusters for the two groups of "radical SAM" enzymes.

ENDOR and X-ray absorption spectroscopy experiments indicated that for KAM the α-amino group, the α-carbonyl group and the sulfonium sulfur of AdoMet interacted with the uncoordinated Fe atom of the [4Fe-4S] cluster.[22, 41] Scheme 1.7 (i) shows how an inner-sphere electron transfer from the $[4Fe\text{-}4S]^{1+}$ to the sulfonium on AdoMet, as well as the ligation of the unique Fe atom to the SAM's sulfur and the cleavage of the 5′ C-S bond, give rise to the 5′- Ado• radical.

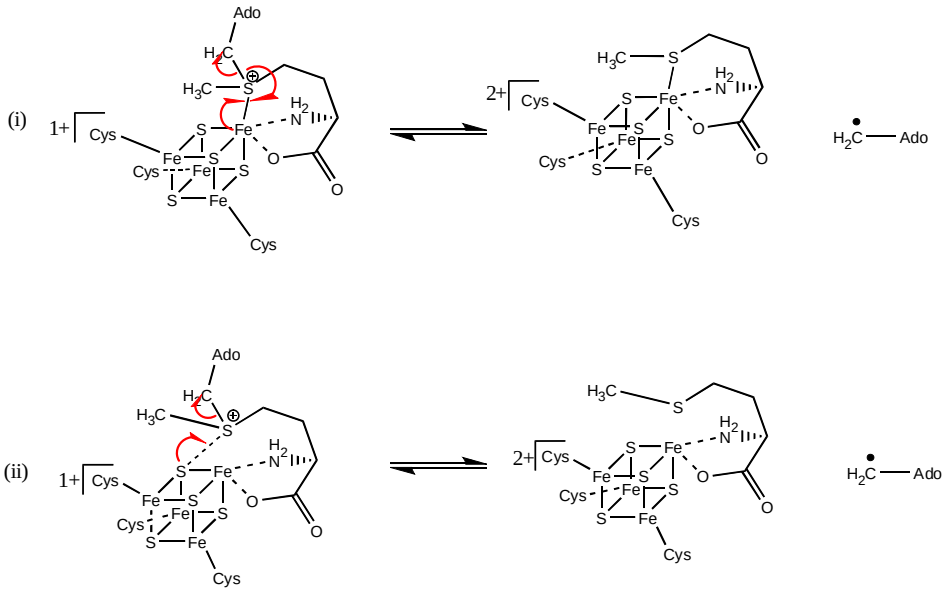

Scheme 1.7 *Two ways by which AdoMet binds to [4Fe-4S] clusters. (i) shows the binding observed for the enzymes in which SAM is used catalytically e.g. KAM and (ii) shows the binding of SAM in the enzymes that use SAM as a substrate e.g. BioB and PFL activase. This diagram was adapted from a paper by Marsh et al. (2004).*[27]

Mössbauer and EPR spectroscopy of biotin synthase (BioB) and PFL-AE indicated that the sulfonium of AdoMet interacts closely with one of the [4Fe – 4S] cluster's sulfides and not the unique Fe atom (Scheme 1.7 (ii)). This would imply that the inner sphere electron transfer from the $[4Fe\text{-}4S]^{1+}$ to the sulfonium ion on SAM occurs via a sulfide – sulfonium interactions and subsequently, the homolytic cleavage of the 5′ C-S bond results in the formation of the 5′- Ado• radical.[42-44]

Some of the "radical SAM" enzymes catalyze transformations that involve the insertion of sulfur atoms. BioB and LipA catalyze sulfur insertion reactions during the formation of biotin and lipoic acid respectively. BioB is the product of the *bioB* gene and LipA the product of *lipA* gene.[45] The two enzymes are believed to be closely related and the mechanisms that they catalyse are very similar.[17, 46] The BioB mediated reaction mechanism has been widely studied and is better understood than the LipA catalysed reaction.[33]

1.4 Biotin synthase (BioB)

The essential vitamin biotin is the end product from a complex cascade of enzymes that are thought to mediate processes originating from the fatty acid synthetic pathway.[47, 48] The final step in the biosynthesis of biotin is catalysed by BioB (Scheme 1.8). The enzyme mediates the conversion of dethiobiotin (DTB) to biotin, a transformation that involves the insertion of a sulfur atom between the unreactive C-H bonds at the C6 and C9 positions of the compound.[19, 49]

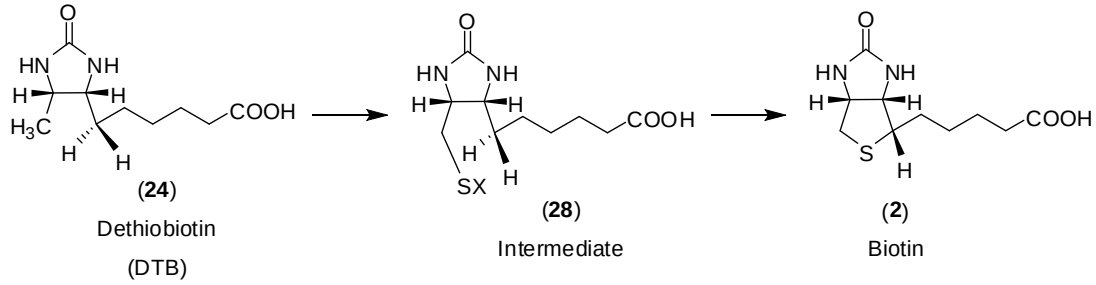

Scheme 1.8 *BioB catalyses the conversion of dethiobiotin (24) to biotin (2), the reaction involves the formation of a thiolated intermediate (28). When X=H the intermediate is 9-mercaptodethiobiotin.*

In vivo labelling experiments carried out by Parry *et al*. (1976) and Marquet *et al.* (1982) showed that during the reaction hydrogen atoms were abstracted from the C6 and C9 positions of DTB.[50-52] Using stereo-specifically tritiated DTB, Marquet *et al.* (1982) demonstrated that it was the *pro-S* hydrogen atom, which was abstracted from the C6 position. Furthermore, this process was accompanied by the retention of configuration.[53, 54] In other experiments, it was also observed that SAM was not the sulfur donor during biotin synthesis.[55]

The successful conversion of DTB to biotin in cell-free extracts of *Escherichia coli* was first achieved by Ifuku *et al*. (1992). They found that along with other components, both the cofactor SAM and the substrate DTB were required for activity.[56] In separate experiments, when ^{14}C-labelled DTB was incubated in cell-free extracts from an *E. coli* strain containing the cloned *bioB* gene, ^{14}C-labelled

biotin was obtained. Along with some low molecular weight compounds and two other proteins, this biotransformation also required SAM.[57] Different experiments carried out by a number of researchers proved that SAM and DTB were prerequisites for BioB activity.[58] However, there was variance among the groups as to the need for the other proteins and small molecules.[58]

The first purification of the protein encoded by the *bioB* gene in *E. coli* was reported in 1994.[59] A little while later highly purified BioB from *Bacillus sphaericus* was used to convert DTB to biotin.[60] The protein BioB was found to be a homodimer with a native molecular mass of approximately 80 kDa.[58, 61] A proposed mechanism for the BioB mediated conversion of DTB to biotin is shown in reaction Scheme 1.9 [62]

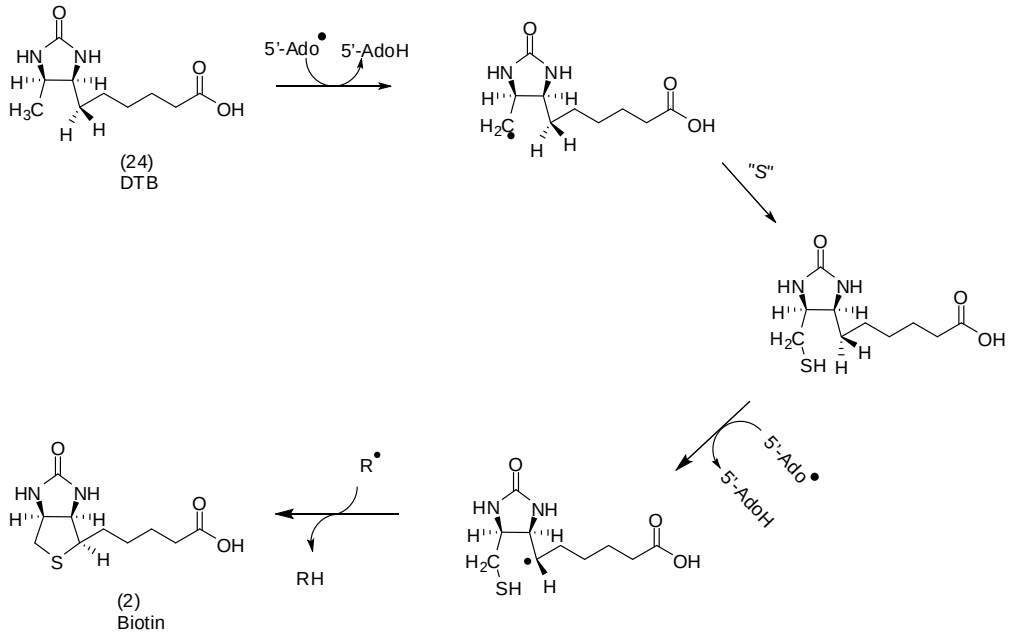

Scheme 1.9 *A proposed mechanism for the E. coli BioB catalyzed conversion of DTB to biotin. A highly reactive 5′- Ado• radical species, derived from SAM abstracts an H-atom from the C9 methyl group in DTB. This leads to the formation of a C9-substrate radical species which reacts with a source of sulfur "S" to give the 9-mercapto-DTB intermediate. A second 5′- Ado• radical species then abstracts an H-atom from the C6-methylene group in the 9-mercapto-DTB intermediate. The resultant C6- radical 9-mercapto-DTB species then reacts so as to produce the biotin.*

During some quantitative experiments BioB from *E. coli* and *B. sphaericus* was incubated with S-[2,8-^{3}H] adenosylmethionine and *S*-adenosyl-[methyl-^{3}H]-methionine and the products of the transformations were identified.[63] In both instances the cleavage products 5′-AdoH and methionine were obtained in 1:1 ratio. However, the two compounds were obtained in a ratio ~ 3:1 with respect to the biotin obtained. These results indicated that two SAM equivalents were consumed in the reaction that entailed the homolytic cleavage of two C-H bonds.[64] Abortive processes were said to be the cause of the observed excess SAM consumption.[58, 63]

Using 6,9-[$^{2}H_5$]-DTB, 9-[$^{2}H_3$]-DTB, 6(S)-[$^{2}H_1$],9-[$^{2}H_1$]-DTB and 6(R)-[$^{2}H_1$],9-[$^{2}H_1$]-DTB as substrates coupled with the mass spectrum analysis of the evolved labelled 5′-AdoH, it was demonstrated that BioB catalysed the transfer of hydrogen from the substrates.[65] However it was not possible to determine if the radical mediating this hydrogen transfer was a protein-based radical or it was the 5′- Ado• radical derived from the cofactor SAM. Although there is experimental evidence for the involvement of a free radical species in the BioB mediated reaction, the species has not been detected.[66]

In other experiments, the HPLC analysis of the reaction mixtures, in which ^{14}C-labelled DTB was the substrate for cell-free extracts from *E. coli* containing BioB, detected the presence of an intermediate compound. This intermediate was ^{14}C-labelled implying it was derived from the substrate; further when isolated this compound could be used as an AdoMet-dependent substrate for BioB and it was converted to biotin.[64] It was also determined that one equivalent of SAM was consumed in forming the ^{14}C-labelled intermediate. A second equivalent of SAM was used when the intermediate compound was converted to biotin.[64]

The intermediate species in Scheme 1.8 and Scheme 1.9 has been shown to be 9-mercaptodethiobiotin, which during some labelling experiments was converted to biotin by *B. Sphaericus*. [67] All this work confirmed BioB to be a member of the

"radical SAM" enzymes, but also sub-classified the enzyme as part of a sub-group that utilize SAM as a co-substrate in the insertion of sulfur.[58]

1.4.1 The Iron-Sulfur Clusters of BioB

Aerobically purified BioB obtained from either *E. coli* or *B. sphaericus* was found to contain [Fe-S] clusters in their inactive form. EPR and UV-visible spectroscopy studies on aerobically purified BioB samples identified the presence of a single [2Fe-2S]$^{2+}$ cluster per monomer.[59, 68] Various techniques including variable-temperature magnetic circular dichroism (VTMCD), resonance Raman, UV-visible and EPR spectroscopies were used to obtain the detailed characterization of BioB. These experiments confirmed the presence of a single S=0 [2Fe-2S]$^{2+}$ cluster per dimer subunit from samples that were purified under aerobic conditions.[69]

Further it was also observed that almost stoichiometric quantities of a single S=0 [4Fe-4S]$^{2+}$ cluster were formed when two [2Fe-2S]$^{2+}$ clusters were anaerobically reduced with dithionite in the presence of glycerol or 60 % ethylene glycol. The prolonged incubation of the [4Fe-4S]$^{2+}$ clusters with dithionite converted this spin state *S*=0 cluster into a [4Fe – 4S]$^{1+}$ cluster with the mixed spin states S = 1/2 and *S* = 3/2 [4Fe – 4S]$^{1+}$.[69] Interestingly there was no major variation in the enzymatic activities observed in assays beginning with the three different [Fe-S] clusters.[70]

It was found that, under anaerobic conditions, the incubation of BioB with the reductant dithionite, dithiothreitol (DTT), Na_2S and excess $FeCl_3$ gave a protein that contained two [4Fe-4S]$^{2+}$ clusters per dimer.[71, 72] The [4Fe-4S]$^{2+}$ clusters could be further reduced to [4Fe-4S]$^{1+}$ clusters and conversely the oxidation of the [4Fe-4S]$^{1+}$ clusters resulted in the formation of [4Fe-4S]$^{2+}$ clusters the rapid decay of which gave [2Fe-2S]$^{2+}$ clusters. Which two [Fe-S] clusters and how much of each was assembled in BioB strongly depended on the reconstitution conditions. It was possible to produce a protein with just two [4Fe-4S]$^{2+}$ clusters, or a protein having one [4Fe-4S]$^{2+}$ cluster and one [4Fe-4S]$^{1+}$ cluster. Under other conditions it was

possible to produce protein having two $[4Fe\text{-}4S]^{1+}$ clusters and it was also possible to produce protein with a mixed $[4Fe\text{-}4S]^{2+}$ and $[2Fe\text{-}2S]^{2+}$ clusters.[70, 71, 73] Under aerobic conditions the [Fe-S] in BioB is the $[2Fe\text{-}2S]^{2+}$ cluster, which is thought to be an oxidative degradation product of the active $[4Fe\text{-}4S]^{2+}$ cluster.

1.4.2 The source of Sulfur in biotin

The source of the sulfur atom in biotin has been widely debated. DeMoll *et al.* (1984) first identified cysteine as a likely sulfur donor.[74] Work carried out by Florentin *et al.* (1994) and Birch *et al.* (1995) provided evidence to support this hypothesis.[57, 75] However, Méjean *et al.* (1995) did not obtain labelled biotin from [^{35}S]-cysteine. Instead, they proposed that the [Fe-S] cluster or some other sulfur containing moiety in biotin synthase was the source of sulfur.[68] This was confirmed by Sanyal *et al.* (1996) who observed that no sulfur was incorporated into biotin from [^{35}S]-SAM or [^{35}S]-cysteine. They also proposed that the [Fe-S] cluster was the more likely source of the sulfur.[76]

Tse Sum Bui *et al*. (1998) using *E. coli* and *B. Sphaericus* assays found that additional Fe^{2+} and S^{2-} resulted in increased activity.[77, 78] To explain this effect it was assumed that the [Fe-S] cluster depleted by the reaction was somehow being reconstituted. However, when purified enzymes were used in assays the [^{35}S]-label was not transferred unless one of the components of the assay was a cysteine desulfurase such as IscS or NifS.[79, 80] The observed transfer of [^{35}S] or [^{34}S]-label from Na_2S to biotin indicated that S^{2-} was the sulfur source.[78] In separate experiments by Gibson *et al.* (1999), BioB from *E. coli* was grown in [^{35}S]-labelled cysteine, and was then used in an assay in which there was no other source of sulfur. Transfer of the [^{35}S]-label into biotin was observed but it was not clear if this [^{35}S]-label was derived from a cysteine of the polypeptide chain or any other sulfur bearing species or indeed if it was provided by an [Fe-S] cluster.[81]

The work carried out by various groups indicated that the [Fe-S] cluster could be the source of the sulfur in biotin, but it could not be ruled out that other sulfur sources could have been formed due to the addition of exogenous sulfur.[59, 78] This hypothesis was better explained by the proposal that BioB chelated two [Fe-S] clusters. The first cluster is a [4Fe-4S] cluster that would be used in the initial homolytic cleavage of SAM to give the 5′-deoxyadenosyl radical and methionine. The second cluster is a [2Fe-2S] cluster that is proposed to function as the source of the sulfur used in the biosynthesis of biotin.[73, 77, 82]

A proposed reaction mechanism that incorporates the use of the [2Fe-2S] cluster as the source of sulfur for the BioB mediated transformation is shown in Scheme 1.10. EPR and UV-visible spectroscopy studies indicated the preservation of the [4Fe-4S] cluster; conversely the decay of the [2Fe-2S] cluster was observed.[77] It was also concluded that two equivalents of SAM were consumed during the course of the BioB mediated transformation and that the sulfur in biotin is provided by an [Fe-S] cluster.

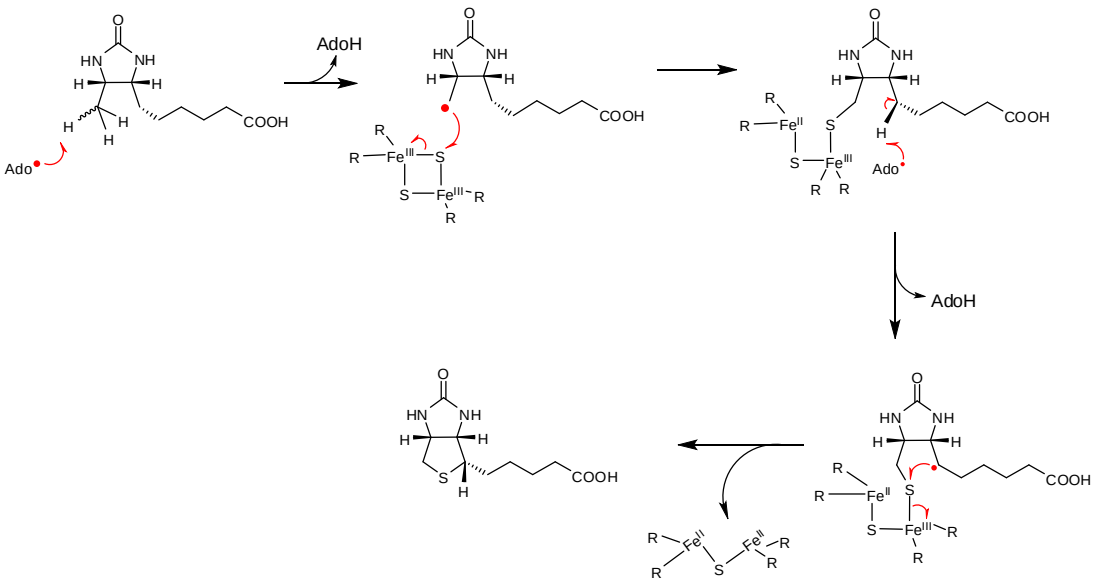

Scheme 1.10 *The reaction mechanism for the conversion of DTB to biotin, in which the* [*2Fe-2S*] *cluster, is the sulfur donor.*

1.4.3 The crystal structure of BioB

In BioB the common [4Fe-4S] cluster binding motif is Cys 53- X_3 -Cys 57- X_2 -Cys 60. BioB also has other conserved cysteine residues, namely Cys 97, Cys 128 and Cys 188. There are also non-conserved cysteine residues Cys 276 and Cys 288.[83, 84] The role of these cysteine residues was determined by site mutagenesis studies. When single Cys $\rightarrow$Ala mutations on the Cys 53, Cys 57 and Cys 60 residues in BioB were assayed for activity; it was found that the resultant enzymes were inactive. However, the UV-visible spectra obtained were identical to that of the $[2Fe\text{-}2S]^{2+}$ cluster from the wild-type enzyme.[85]

In detailed studies, when all eight cysteine residues of *E. coli* BioB were mutated (Cys $\rightarrow$Ala) and assayed for activity, it was found that only the C276A and C288A mutant proteins were very similar to the wild-type protein. The other six mutants still assembled [4Fe-4S] clusters under reducing conditions but gave inactive enzymes.[86] From the EPR and Mössbauer spectroscopy it was observed that the C53A, C57A and C60A mutants could not be reduced to assemble the $[4Fe\text{-}4S]^{+}$ state. That *E. coli* BioB mutant Cys 97, Cys 128 and Cys 188 enzymes could assemble [4Fe-4S] clusters but could not convert DTB to biotin seemed to suggest these cysteine residues were involved in binding the $[2Fe\text{-}2S]^{2+}$ clusters.[87] There was no reductive cleavage of SAM with the Cys 53, Cys 57 and Cys 60 mutants which indicated that these residues should be involved in the binding of the $[4Fe\text{-}4S]^{2+/1+}$ clusters.[83]

Under anaerobic conditions *E. coli* BioB purified to contain a $[2Fe\text{-}S]^{2+}$ cluster per monomer was reconstituted to have in addition a $[4Fe\text{-}4S]^{2+}$ cluster per monomer. The clusters were stabilized against aerial oxidation by binding to AdoMet and DTB, and X-ray diffraction was successfully used to determine the crystal structure of this stable form of the enzyme to a resolution of 3.4 Å.[88] The crystal structure of biotin synthase from *E. coli* is shown in Figure 1.4. The main feature of the structure for each monomer of BioB is a triosephosphate isomerase (TIM) type $(\alpha/\beta)_8$ barrel, with the [Fe-S] clusters, SAM and the DTB bound at the centre of this barrel.

Residues 2 – 38 constitute two helices at the N terminal, whilst residues 316 – 343 constitute a disordered region at the C terminal.[61]

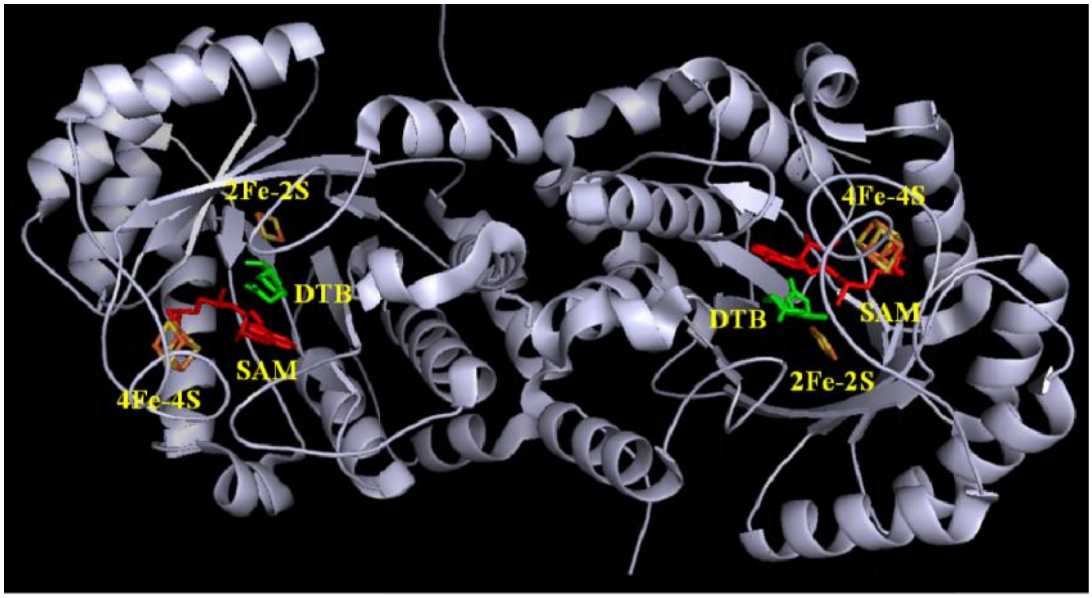

Figure 1.4 *A ribbon diagram showing the crystal structure of BioB (1R30). The structure shows the relative positions of the [4Fe-4S]$^{2+}$ and [2Fe-2S]$^{2+}$ clusters, the substrate DTB and the co-factor SAM. The Fe atoms of the clusters are shown in brown in the stick diagrams and the S atoms are shown in the orange colour. DTB is shown in green and AdoMet is represented in red. This structure was prepared using the Pymol Molecular Graphics system.*

Situated approximately 30 Å from the dimer interface, at the C terminal of the $(\alpha/\beta)_8$ barrel, is the [4Fe-4S]$^{2+}$ cluster. Three of the Fe atoms of this cluster are coordinated to the conserved cysteine residues Cys 53, Cys 57, Cys 60 in a 28- residue loop that stretches through β-strand 1 and helix 1. The unique fourth Fe atom of the [4Fe-4S]$^{2+}$ cluster is coordinated to SAM via the oxygen atom of the carbonyl moiety and the nitrogen of the amino moiety. Hydrogen bonds hold the SAM in close proximity to the [4Fe-4S]$^{2+}$ cluster.[61, 88] The pictures in Figure 1.5 show the relative positions of the [4Fe-4S]$^{2+}$ cluster (shown by the spheres) with SAM bound. The blue ribbon shows the extended protein loop backbone (residues 49–77), in which the [4Fe-4S]$^{2+}$ cluster coordinates to the Cys53, Cys57, and Cys60. [61]

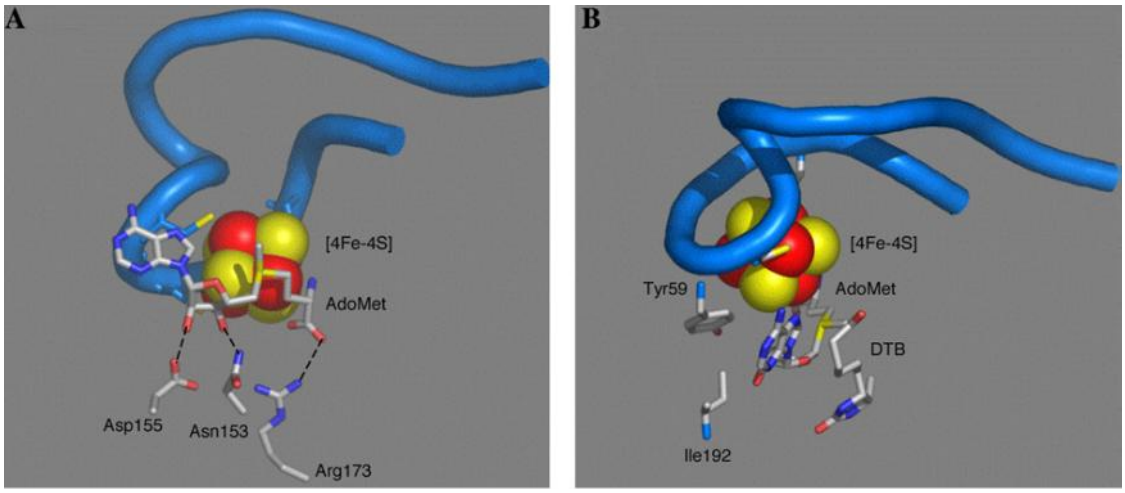

Figure 1.5 *Pictures showing the relative positions of the [4Fe-4S]$^{2+}$ cluster with SAM bound. (A) AdoMet is coordinated to one Fe of the cluster through the methionyl amine and carboxylate. Hydrogen bonds between the carboxylate and Arg173 and between the ribose hydroxyls and Asp155 and Asn153 fix the AdoMet in close proximity to the cluster. (B) The adenine of AdoMet is tightly packed in a hydrophobic pocket created by Tyr59, Ile192, and the carboxylate chain of DTB. The red spheres represent Fe and the yellow spheres represent sulfur. The stick structures in the diagrams represent the SAM and the other residues found in close proximity to the [4Fe-4S]$^{2+}$ cluster. The atom colours are as follows; blue represents nitrogen; gray represents carbon. Oxygen is shown in red on the stick representations. The pictures were adopted from a paper by Joseph T. Jarrett*.[61]

The pictures in Figure 1.6 shows the biotin synthase's [2Fe-2S]$^{2+}$ cluster with the substrate DTB bound. Positioned approximately 25 Å from the C terminal, deep inside the TIM barrel is the [2Fe-2S]$^{2+}$ cluster which is bound within an unusual coordination environment. The residues Asn 151, Asn 153 and Asn 222 are in H-bonding with dethiobiotin in such a way that the substrate's C9 is ~ 4.6 Å from the closest sulfide and ~ 3.9 Å from the SAM's 5′ -carbon. One of the Fe atoms of the [2Fe-2S]$^{2+}$ cluster is coordinated to Cys 97 and Cys 128 whilst the other is coordinated to Cys 188 and Arg 260. The Arg 260 residue is in itself fixed and stabilized by its coordination to Ser 43, Ser 218, Ser 283 and Arg 95, though mutation studies seemed to indicate that this placement of arginine may not be essential for enzymatic activity.[84]

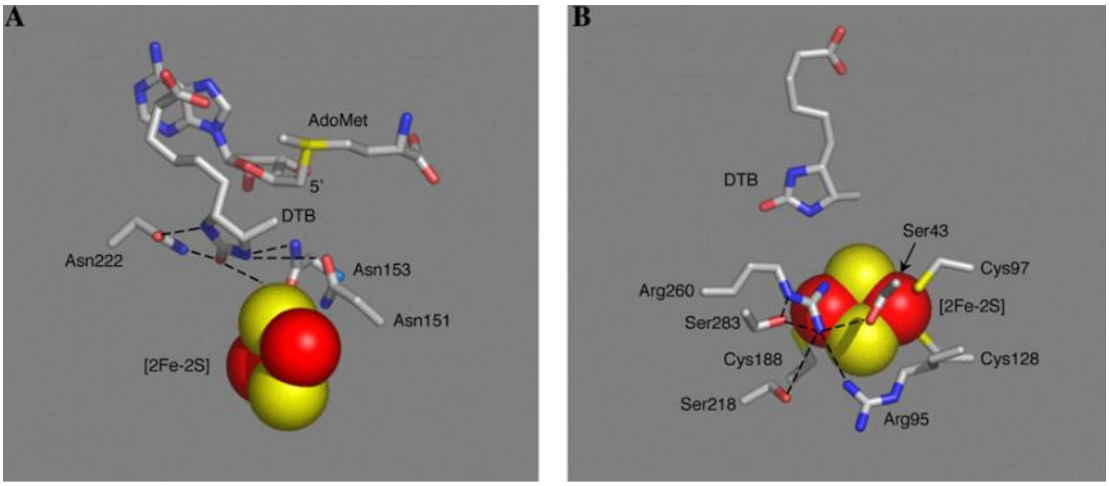

Figure 1.6 *The pictures show the structure of the dethiobiotin and [2Fe–2S]*$^{2+}$ *cluster binding sites in biotin synthase. In (A) DTB is shown with the residues that contribute to its positioning. In (B) the [2Fe–2S]*$^{2+}$ *cluster is shown within the unusual coordination environment, and the structure also shows the positioning of the Arg260.*[61]

1.5 ~-Lipoic Acid

The organosulfur compound α-lipoic acid (1,2-dithiolane-3-pentanoic acid or 6,8-thioctic acid) **1** integrates a carboxylic acid and a cyclic dithiolane ring in which a disulfide bond links the two sulfur atoms at C6 and C8. The C6-carbon atom is chiral, and the molecule exists as two enantiomers *R*-(+)-lipoic acid and *S*-(-)-lipoic acid or as a racemic mixture *R*/*S*-lipoic acid.[89] The biosynthesized R-enantiomer is an essential cofactor for many multienzyme complexes. This compound is at times used somewhat controversially as a dietary supplement.[90] Intracellularly sulfur compounds exist in their reduced form, which for α-lipoic acid is dihydrolipoic acid. Under physiological conditions, carboxylic acids exist as their conjugate base, which for lipoic acid is called “lipoate.” Therefore free lipoic acid in the cell can also be referred to as dihydrolipoate.

Unless obtained from supplementary exogenous sources, most of the intracellular lipoic acid is not in its free state. Almost all the lipoic acid is bound to the multi-

enzyme complexes that use it. The lipoic acid is covalently attached to the ε-amino group of a specific lysine residue via an amide bond and acts as a carrier of acyl groups between active sites of the large multi-enzyme complexes.[2]

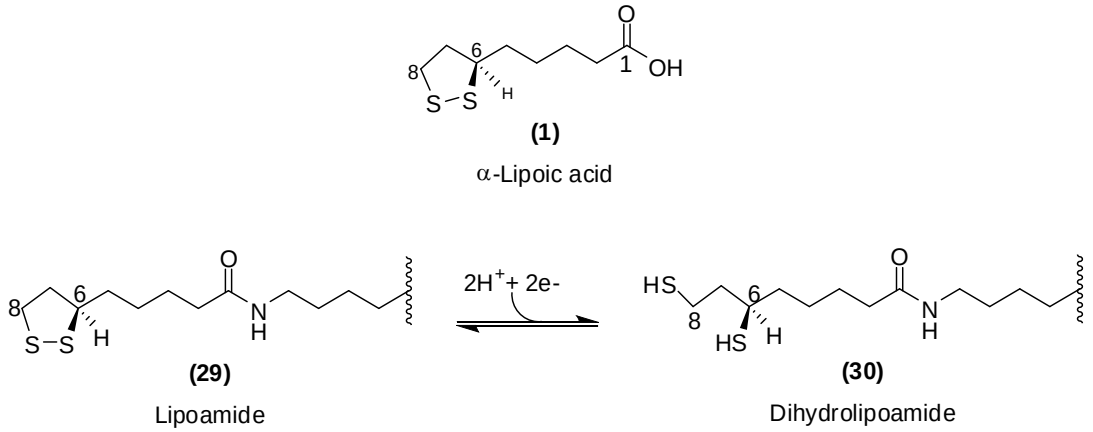

Scheme 1.11 *The chemical structures of free ~-lipoic acid* (**1**) *and the equilibrium between the protein bound cyclic disulfide* (**29**) *and its reduced form, dihydrolipoamide* (**30**)*. The lipoamide and dihydrolipoamide are both shown connected by an amide linkage to the lipoyl carrier protein.*[31]

The chemical structures of lipoic acid in three different forms are shown in Scheme 1.13. The structure of free lipoic acid is shown by compound **1** and the structures of cyclic lipoamide and the reduced dihydrolipoamide are shown by compounds **29** and **30** respectively. Scheme 1.13 shows these two compounds in equilibrium. The lipoyl cofactor can be inter-converted between the lipoamide and the dihydrolipoamide via some redox reactions. During turnover, the disulfide accepts two electrons and is reduced to the dihydrolipoamide. The re-oxidation of the dihydrolipoamide which must occur before further rounds of turnover is catalysed by lipoamide dehydrogenase.[31]

1.5.1 Lipoic acid-dependent complexes

So far, only five lipoate-dependent multienzyme complexes have been characterized.[91] These complexes are the pyruvate dehydrogenase complex (PDH), the α-ketoglutarate dehydrogenase complex (α-KGDH), the branched-chain α-keto acid dehydrogenase complex (BCKADH), the acetoin dehydrogenase complex (ADH) and the glycine cleavage system (GCS). The PDH, α-KGDH and BCKADH complexes are α-keto acid dehydrogenases that consist of repetitive copies of three enzymatic subunits called E1, E2 and E3.[92] ADH possesses three subunits like the α-keto acid dehydrogenases and is closely related to PDH. However, the GCS complex is structurally different and comprises four loosely interacting moieties referred to as the P, H, T, and L proteins.[31]

1.5.2 The ~-keto acid dehydrogenases

In *E. coli* and other microorganisms α-keto acid dehydrogenase complexes are essential for the oxidative decarboxylation of pyruvate, α-ketoglutarate and the branched-chain keto acids. These complexes mediate the metabolism of all the tricarboxylic acid cycle (TCA-cycle) substrates, branched-chain amino acids and carbohydrates.[93] The PDH complex uses lipoic acid as a cofactor for the oxidation of pyruvate to form Acetyl-CoA.[94] The α-KGDH complex is essential for the energy production and oxidative metabolism in mitochondria. The BCKADH complex plays an important role in the breakdown of the branched-chain keto acids which have a regulatory function in nitrogen homeostasis.[93]

1.5.3 The Pyruvate Dehydrogenase Complex (PDH)

The oxidative decarboxylation of pyruvate to give acetyl-CoA is mediated by the PDH complex, which consists of repetitive copies of three enzymes encoded by the *aceEF lpd* operon.[93] The first enzyme E1p (encoded by *aceE*) is a thiamine diphosphate-dependent decarboxylase that mediates both the oxidative decarboxylation of pyruvate, and the reductive acetylation of lipoyl moieties bound to lysyl residues on the second enzyme E2p (encoded by *aceF*).[95]

The dihydrolipoyl acetyltransferase E2p mediates the formation of acetyl-CoA via the transfer of acetyl groups from lipoyl moieties to coenzyme A (CoA). The last of these repetitive enzymes is E3 (encoded by *lpd*), a dihydrolipoyl dehydrogenase that mediates the oxidation of lipoate disulfide bonds before the ensuing catalytic cycle.[94, 95]

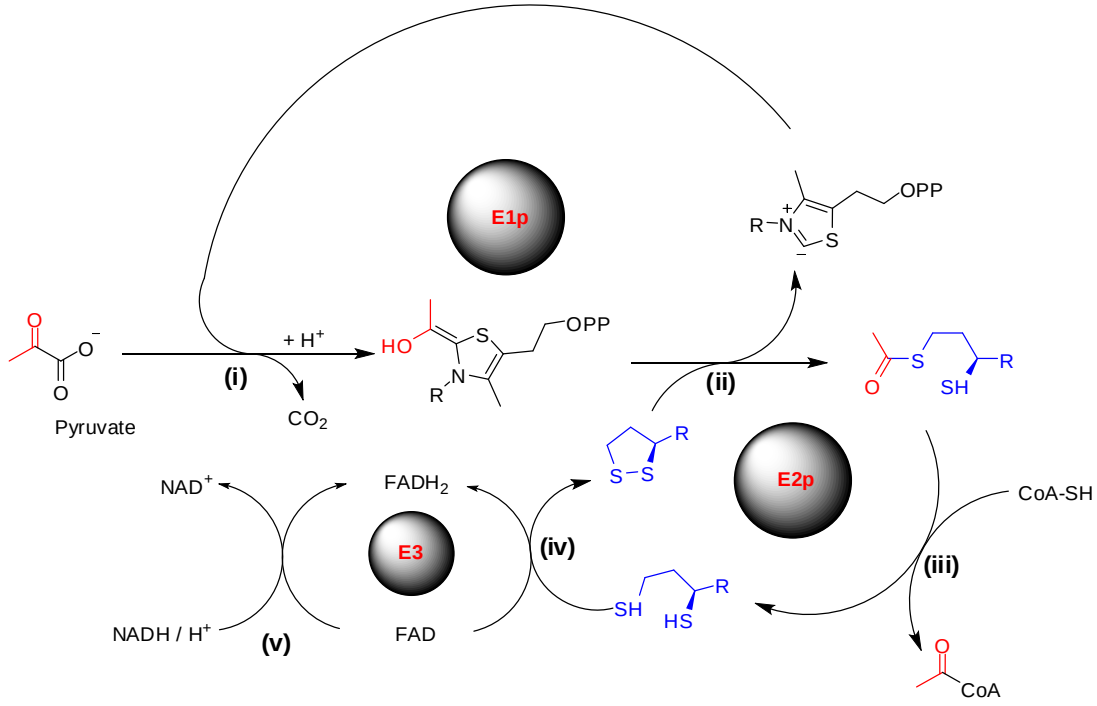

Scheme 1.12 *The sequence of reactions in the pyruvate dehydrogenase complex (PDH) which are mediated by the three enzymes E1p a thiamine diphosphate-dependent decarboxylase, E2p a dihydrolipoyl acetyltransferase and E3 a dihydrolipoyl dehydrogenase.*[93]

The series of biotransformations that occur during the breakdown of pyruvate, in the PDH complex are shown in the reaction Scheme 1.12. The first step is a thiamine pyrophosphate (TPP) dependent reaction that is mediated by the E1p subunit. This decarboxylation of pyruvate results in the formation of hydroxyethyl pyrophosphate intermediate, accompanied by the evolution of CO_2. Thereafter, the hydroxyethyl pyrophosphate enables the E1p subunit to reductively cleave the lipoyl moiety which is covalently bound to the E2p subunit (reaction ii). The dihydrolipoyl acetyltransferase (E2p) subunit then catalyses the transfer of an acetyl group to

coenzyme A, resulting in the synthesis of acetyl-CoA (reaction (iii)). This reaction also gives off the dihydrolipoamide which is subsequently reoxidized to lipoamide by the E3 subunit in a process that couples the NADH / H^+ and NAD^+ redox system.[2, 8]

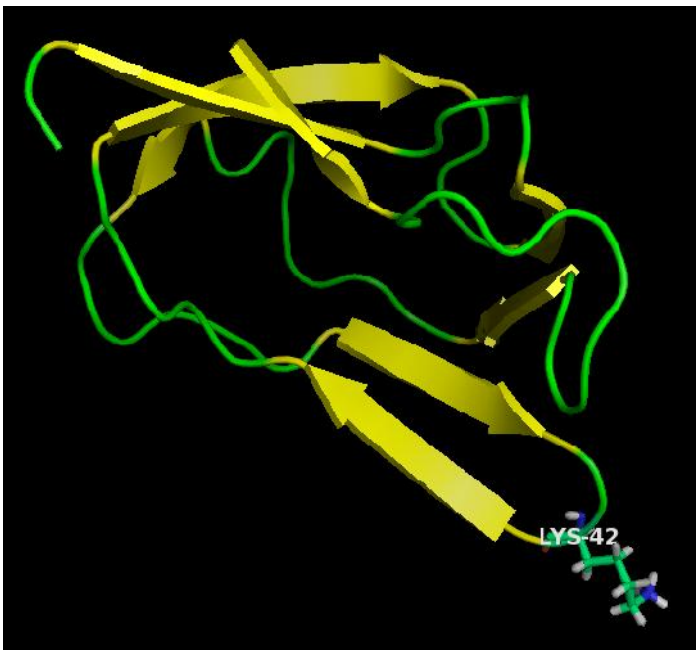

Figure 1.7 *A picture showing the structure of the lipoyl domain of E_2 subunit of the pyruvate dehydrogenase complex of Bacillus stearothemophilus (PDB 1LAB). The lipoyllysine (Lys 42) is located at the tip of a -hairpin structure, and is shown here in the stick format. This structure was prepared using the Pymol Molecular Graphics.*

The three dimensional structure of the lipoyl domain from *Bacillus stearothermophilus* comprising of residues 1-79 of the dihydrolipoamide acetyltransferase motif (Figure 1.7) was determined by nuclear magnetic resonance (NMR) spectroscopy.[96] This structure is taken as the standard structure for a number of other microorganisms for which the structures of lipoyl domains have been determined.[31] The structure consists of a distinct core of hydrophobic residues, which is surrounded by an eight-stranded β-barrel. The lipoyllysine is positioned at the tip of one β-turn, and the C- and N- termini are in adjacent β-

strands on the opposite side of the domain from the lipoyllysine group. Next to the lipoyl-accepting lysine is an alanine residue on its C-terminal side, whilst an aspartate residue is on its N-terminal side. Site directed mutagenesis was used to prove that the absolute positioning of the target lysine is essential for proper recognition.[31, 92]

The α-KGDH and the BCKADH complexes follow mechanisms that are very similar to that used by the PDH complex. The α-KGDH complex mediates the conversion of α-ketoglutarate to CO_2 and succinyl-CoA with the concomitant release of NADH.[97] The BCKADH complex mediates the oxidative decarboxylation of the α-keto acids derived from the branched-chain amino acids, to give their corresponding acyl-CoA derivatives. The PDH, the α-KGDH and the BCKADH complexes are all composed of multiple copies of the E_1, E_2 and the E_3 subunits. The E_1 and E_2 subunits for each of these complexes are the products of different genes and are specific for the complex in which they are found. The E_3 subunits are all products of the *lpd* gene in *E. coli*.[91, 94]

1.5.4 The Glycine Cleavage System (GCS)

The main pathway for the catabolic cleavage of glycine (Scheme 1.13 and Scheme 1.14) is an oxidative decarboxylation that produces ammonia, carbon dioxide and N^5,N^{10}-methylene tetrahydrofolate (THF). This reaction is mediated by the glycine cleavage system (GCS) which is also known as the glycine decarboxylase complex.[98, 99] The glycine cleavage system comprises of three enzymes and a carrier protein that weakly interact with each other. The three enzymes are a dimeric P-protein which is a pyridoxal phosphate-dependent decarboxylase, a monomeric T-protein which is an aminomethyl-transferase and a dimeric L-protein which is a dihydrolipoyl dehydrogenase.[94] The fourth component of the glycine cleavage system is the lipoic acid bearing monomeric H-protein.[98]

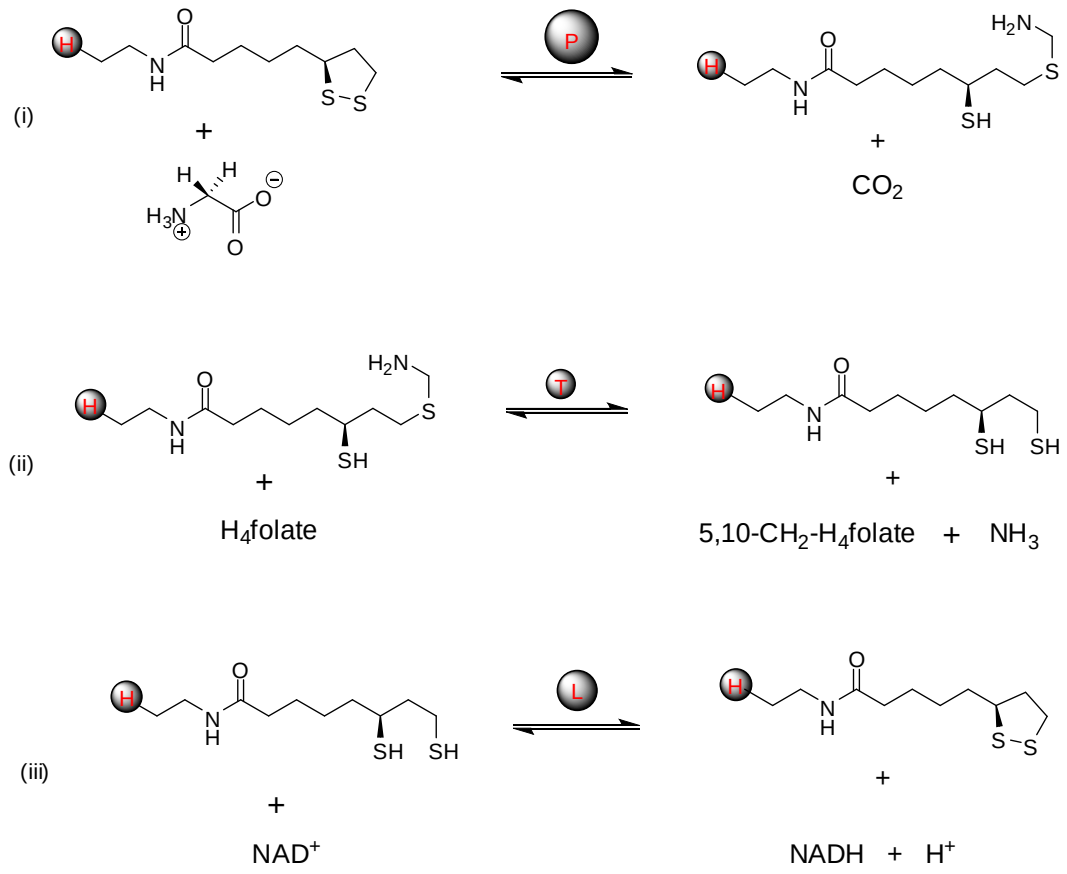

Scheme 1.13 *The reaction mechanism of the glycine cleavage system. H is the lipoylated H-protein; L is the dihydrolipoyl dehydrogenase; P is the pyridoxal phosphate-dependent decarboxylase; T is an aminomethyl-transferase.*[98]

The reactions (i) to (iii) in Scheme 1.13 show the steps for a proposed mechanism of how the glycine cleavage system mediates glycine catabolism. The first reaction, the decarboxylation of glycine, is catalysed by P-protein and requires H-protein as a co-substrate. In the second reaction, T-protein further degrades the decarboxylated glycine moiety in a transformation that involves H_4-folate. The products of this process are N^5,N^{10}–methylene-H_4-folate, ammonia and H-protein with dihydrolipoate. L-protein then catalyses the reoxidation of the reduced lipoate attached to H-protein. A representation of the glycine cleavage cycle is shown in reaction Scheme 1.14.

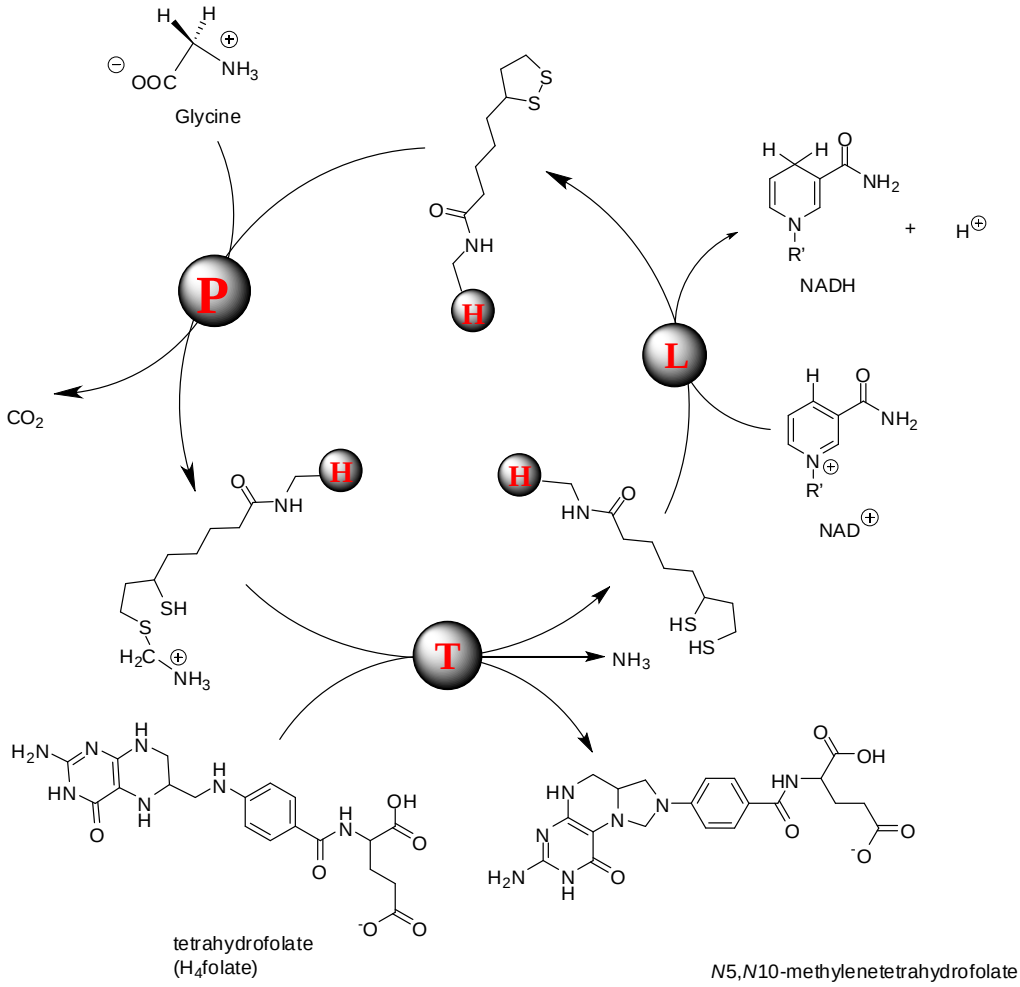

Scheme 1.14 *A cyclic scheme showing the reactions of the glycine cleavage system. The H-protein links the other proteins which catalyse the cyclic processes of reductive methylamination, methylamine transfer and electron transfer.*[94, 100]

During a catalytic cycle of the glycine cleavage system, the H-protein plays an important role as a mobile substrate that links the successive steps carried out by the other three proteins. The lipoyl moiety covalently bonded by an amide linkage to a lysine on the H-protein repeatedly cycles through the processes of reductive methylamination, methylamine transfer and electron transfer. Glycine cleavage is initiated when the molecule's amino group forms a Schiff base with the P-protein's pyridoxal phosphate.[100] Carbon dioxide is produced from the carboxyl group and the remnant methyl amine group is passed to the H-protein's lipoamide co-factor. The enzymatic release of ammonia is carried out at the T-protein, which causes an overall conformational change of the H-protein.

The final stage in the cycle is the regeneration of the oxidised form of the lipoamide which is facilitated by the L-protein. This process is accompanied by the reduction of NAD^+ to NADH.

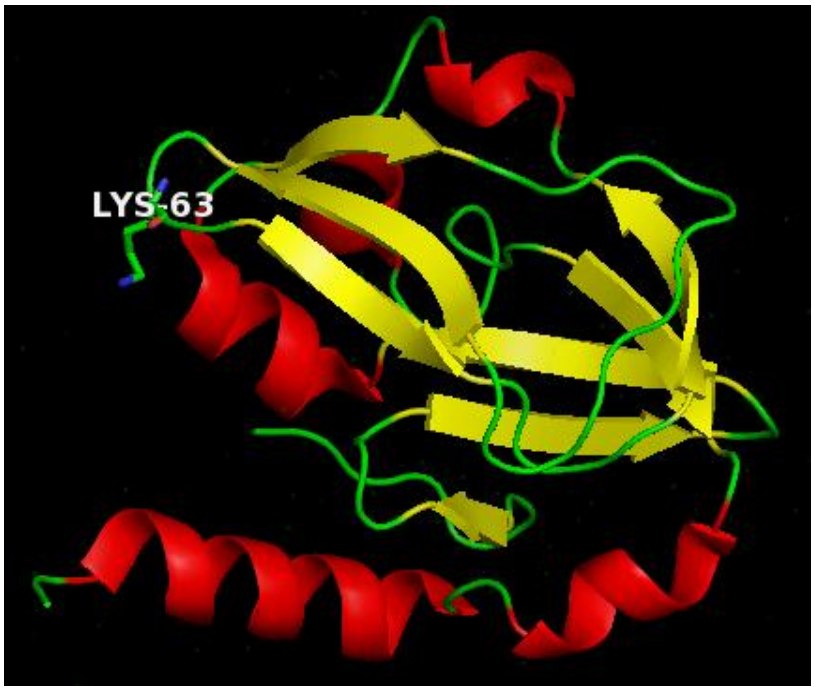

Figure 1.8 *A picture showing the structure of the H-protein of the glycine cleavage complex from Pisum sativum (PDB 1DXM). The lipoyllysine (Lys 63) is located at the tip of a -hairpin structure, and is shown here in the stick format. Individual atoms are colour coded (blue, nitrogen; red, oxygen; grey, hydrogen and green, bonds). This structure was prepared using the Pymol Molecular Graphics system.*

The structure of the H-protein of the glycine cleavage complex of *Pisum sativum* is shown in the picture in Figure 1.8. The structure is similar to the lipoyl domains in that it contains the eight-stranded β-barrel but the H-protein is much larger than the lipoyl domains of the E_2 subunits of PDH and the KDH. In addition to having two additional β- strands at the N-terminus the H-protein contains added helixes i.e. a short helix at the C-terminus and another at the N-terminal's exposed loop. [96, 99, 101]

1.6 The biosynthesis of lipoic acid catalysed by lipoyl synthase (LipA)

Crystalline α-lipoic acid (compound **1**) was first isolated by Reed *et al.* (1951) [102, 103] and thereafter the chemical formula and structure of the compound were determined.[103, 104] Reed (1964) also identified the biosynthetic precursor for α-lipoic acid in *E. coli* as octanoic acid.[9] Almost ten years later Parry *et al.* (1977) and White *et al.* (1980) in independent radio-labelling and degradation studies observed that protein bound lipoic acid was obtained when [1-^{14}C]-octanoate was administered to cultures of *E. coli*.[105, 106] The Scheme 1.15 shows the reactions of specifically labelled octanoic acids used as substrates in feeding experiments that were carried out to investigate the formation of lipoic acid, based on the assumption that octanoic acid was the biosynthetic precursor to lipoic acid.

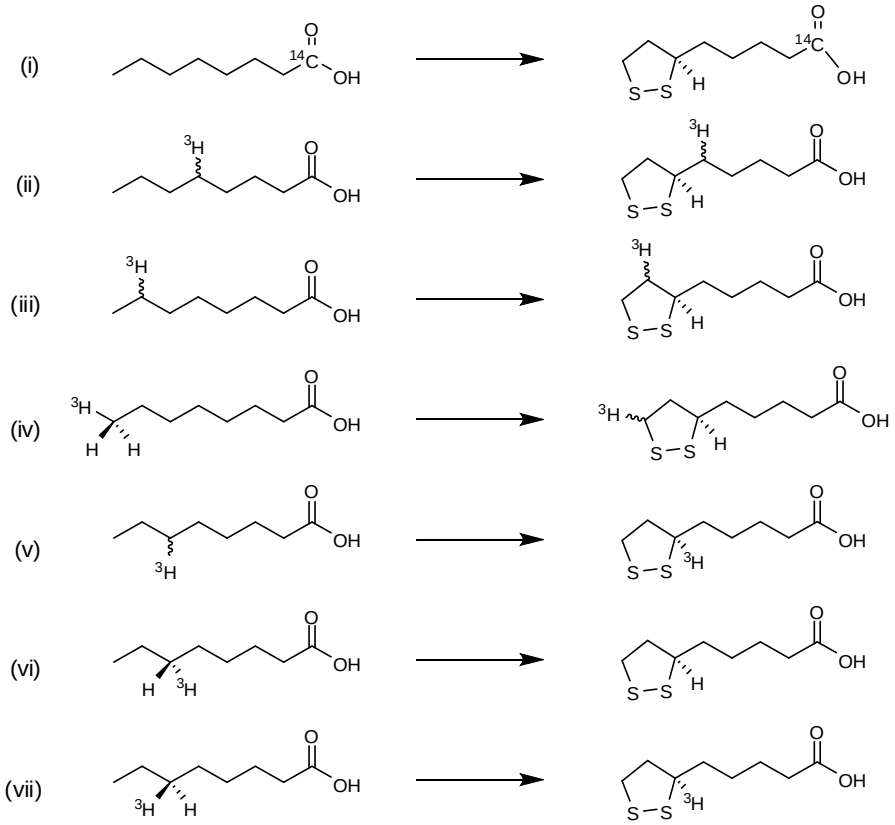

Scheme 1.15 *The chemical structures of the radio - labelled molecules used as substrates in feeding studies of the biosynthesis of lipoic acid (i) [1-^{14}C]-octanoic acid, (ii) [5(R,S)-^{3}H]-octanoate, (iii) [7(R,S)-^{3}H]-octanoate, (iv) [8-^{3}H]-octanoate, (v) [6(R,S)-^{3}H]-octanoic acid, (vi) [6(R)-^{3}H]-octanoic acid and (vii) [6(S)-^{3}H]-octanoic acid.*

In the initial experiments (Scheme 1.15 (i)), [1-^{14}C]-lipoic acid was isolated from *E. coli* in growth media supplemented with [1-^{14}C]-octanoic acid, but no lipoic acid was isolated from *E. coli* in growth media supplemented with either [1,6-^{14}C] adipic acid or [1-^{14}C]-hexanoic acid.[9] These results indicated that "intact" octanoic acid was a precursor to lipoic acid in *E. coli*. Thereafter samples of octanoic acid specifically labelled at C5, C6, C7 and C8 were prepared (Scheme 1.15 reactions (ii) to (vii)) and coadministered with [1-^{14}C]-octanoic acid. The percentage ^{3}H retention (% ^{3}H retention) and the ^{3}H to ^{14}C ratios for the precursor and for the lipoic acid were determined.[105]

In reaction (ii) of Scheme 1.15 the precursor's ^{3}H / ^{14}C ratio (4.05) was identical to that for lipoic acid (4.11). The percentage ^{3}H retention (% ^{3}H retention) was found to be 102 %. In reaction (iii) of Scheme 1.15 the ^{3}H / ^{14}C ratio for the precursor was 3.95, whilst that for the lipoic acid was 3.81. The percentage ^{3}H retention was found to be 96.5 %. These two results illustrated that during the biosynthesis of lipoic acid the C5 and C7 hydrogen atoms were not removed during the sulfur insertions. The results also suggested that unsaturated species were unlikely to be intermediates in this transformation.[9, 105] Experiment (iv) of Scheme 1.15 was carried out to show the incorporation of [^{3}H]-octanoic acid. The ^{3}H / ^{14}C ratio for the precursor was 5.02 and that for lipoic acid was 4.81. The percentage ^{3}H retention was found to be 95.8%. This indicates that no tritium loss occurs during the transformation of [^{3}H]-octanoic acid into [^{3}H]-lipoic acid, possibly a result of the strong tritium isotope effect associated with removing H-atoms from the C8 position.[107]

When [1-^{14}C]-octanoate was coadministered with [6(R,S)-^{3}H]-octanoate (Scheme 1.15 (v)), the ^{3}H / ^{14}C ratio for the precursor was 5.08, whilst that for the lipoic acid was 2.53 and the percentage ^{3}H retention was found to be 49.8 %. The observed 50 % tritium loss is consistent with the stereoselective removal of one of the octanoic acid's C6 H-atoms.[108] Administering [1-^{14}C]-octanoic with [6(R)-^{3}H]-octanoic acid (Scheme 1.17 (vi) resulted in ^{3}H / ^{14}C ratios for the precursor and for lipoic acid of 4.4 and 0.48 respectively. The % ^{3}H retention was found to be 10.9 %. In experiment (vii), [1-^{14}C]-octanoic acid was coadministered with [6(S)-^{3}H]-octanoic

acid and the ^{3}H / ^{14}C ratio for the precursor was found to be 4.13, whilst that for the lipoic acid was 3.47. The percentage ^{3}H retention was found to be 84.0 %.

These results of these feeding experiments indicated that during the biosynthesis of lipoic acid, the major pathway entails the removal of the 6-*pro*-R hydrogen. Removal of the 6-*pro*-S hydrogen might be a minor pathway.[105] Given that the natural isomer of lipoic acid has an *R*-configuration at C6, it was suggested that sulfur insertion occurs with inversion of configuration.[109] In contrast the insertion of sulfur at C8 occurs with racemization which would be expected if this process involves an intermediate carbon radical species.[106, 108, 110] 6-Thiooctanoic acid and 8-thiooctanoic were converted to lipoic acid. However 8-thiooctanoic was up to 10 times more efficient than 6-thiooctanoic in this conversion.[111]

1.6.1 Identification of the lipA gene

Biochemical and genetic studies carried out in the 1960s identified mutant strains of *E. coli* that stopped the biosynthesis of lipoic acid.[112, 113] The affected gene is now called *lipA* and its product is lipoyl synthase (LipA). Another gene located downstream of *lipA* was also identified and designated *lipB*. The product of this gene, octanoyl-acyl carrier protein (ACP): protein-N-octanoyltransferase (LipB) is thought to be a ligase used to attach lipoic acid to the E2p subunit of the enzyme complexes that use lipoic acid.[114, 115] Early attempts to use the *lipA* mutants to bioassay lipoic acid were complicated by reversion to lipoic acid prototrophy and prevailing residual growth without lipoate.[116] It was only in the early 1990s that the successful cloning of the *lipA* gene in *E. coli* was reported. Molecular cloning allowed for the preparation of stable null mutants devoid of lipoic acid biosynthesis that also had an absolute requirement of lipoate for growth.[117, 118]

In other experiments it was observed that octanoate substrate was not converted to lipoate by the product of the mutant *lipA* gene. However the *lipA* mutants used either 6-thiooctanoic acid or 8-thiooctanoic acid instead of lipoic acid to support growth in

minimal media. It was concluded from these observations that LipA was involved in the insertion of the first sulfur of the lipoate biosynthesis.[115, 119, 120] The purification and characterization of LipA using various spectroscopic techniques, EPR, UV-visible and resonance Raman spectroscopy provided unequivocal evidence that LipA is an [Fe-S] enzyme.[121, 122] Iron content and sulfide analysis of LipA purified under aerobic conditions suggested the presence of 2Fe and 2S per monomer of the protein.[115] It has been reported that the [Fe-S] cluster for the aerobically purified protein is a $[2Fe\text{-}2S]^{2+}$ cluster, which is reduced to give [4Fe-4S] clusters.

Under aerobic conditions the [4Fe-4S] clusters are oxidatively degraded to the $[2Fe\text{-}2S]^{2+}$ cluster. Experiments using EPR methods, Mossbauer, UV-visible and resonance Raman spectroscopies showed the presence of one [4Fe-4S] cluster per monomer under anaerobic conditions.[121] Further studies showed that in *E. coli* the form relevant to turnover binds two [4Fe-4S] clusters per polypeptide.[123] One of the clusters is ligated by the conserved CX_3CX_2C binding motif (one of the characteristic features of all the enzymes of the "radical SAM" superfamily). The other [Fe-S] cluster is ligated to a CX_4CX_5C motif (which is a unique feature of the LipA protein).[123]

1.6.2 The substrate for LipA

In the literature, it has been suggested that free octanoic acid cannot be the natural substrate for LipA, an assertion that has been very difficult to verify due to the lack of *in vitro* assays.[124-126] A breakthrough was made by Miller *et al*. (2000) who used the discovery of lipoate-protein ligase (LplA) and LipB to develop a sensitive and quantitative *in vitro* assay for lipoyl formation.[3] Assuming that the substrate for LipA was octanoyl-ACP, they developed an assay to indirectly determine the formation of lipoyl product.[116] Purified LipA and the lipoyl accepting protein (apo-pyruvate dehydrogenase complex) were incubated with a substrate mixture. Two substrate systems were used for these assays, either (i) octanoic acid mixed with LplA and ATP, or (ii) octanoyl-ACP mixed with LipB. The extent of activation of apo-PDH upon lipoylation was determined by monitoring the reduction of an NAD^+

analogue. A direct relationship existed between the rate of formation of reduced pyridine dinucleotide and the amount of lipoylated PDH.[97] The main drawback of this assay is that the intermediate product for the LipA reaction was not characterised because free lipoyl-ACP product was never isolated. However the assay demonstrated that LipA activity required [Fe-S] clusters and SAM. Further work carried out by two other groups established that octanolyated derivatives of lipoyl accepting proteins were substrates for LipA.[127, 128]

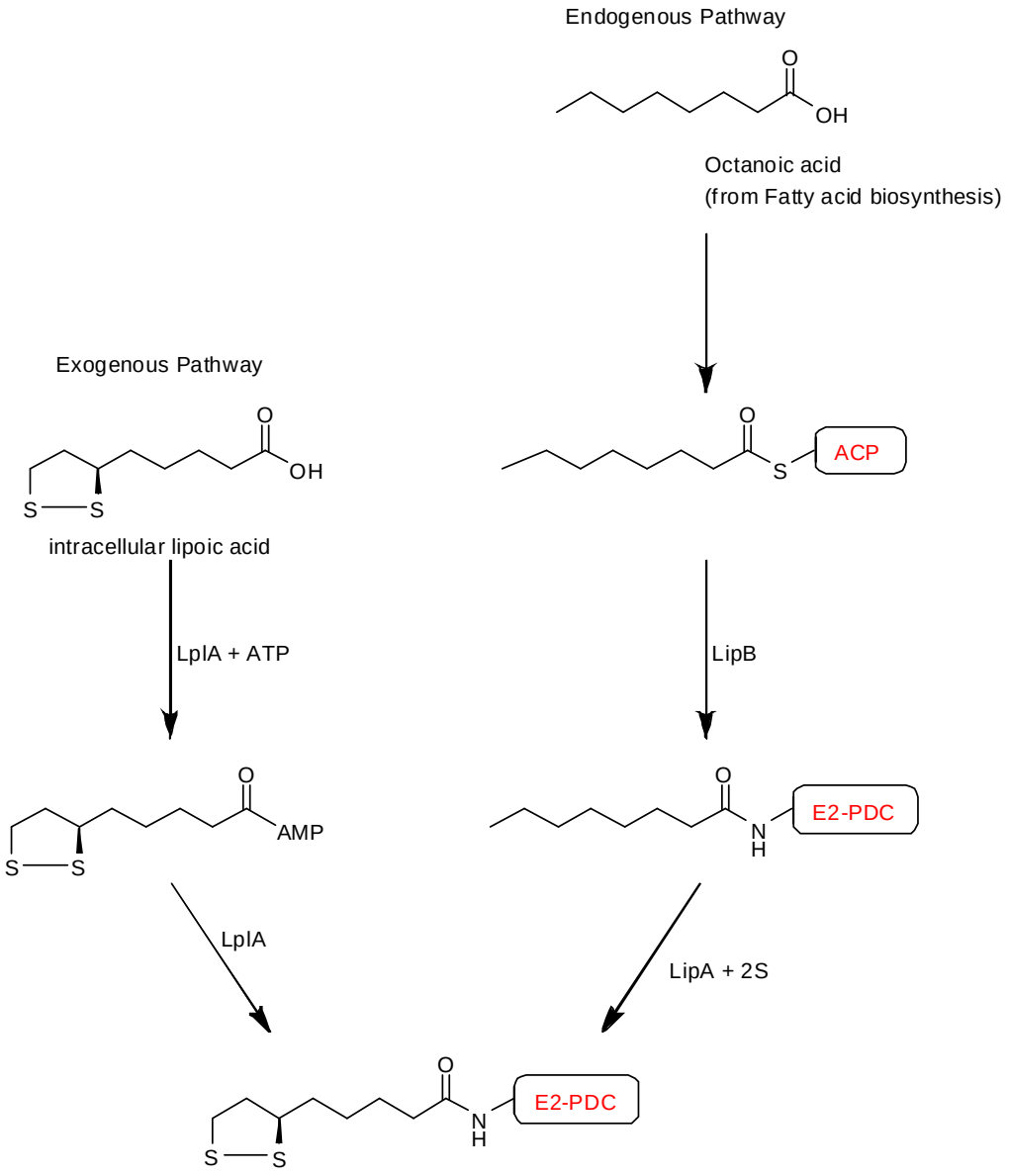

Scheme 1.16 *The two pathways for the incorporation of lipoate onto apo-proteins in E. coli.*[127, 129, 130]

There are several mechanisms by which the post-translational modification of apoproteins with lipoic acid occurs. In mammals the first step is mediated by lipoate-activating enzyme (LAE) which activates lipoic acid to lipoyl-AMP. The action of lipoyl-AMP: N-ε-lysine lipoyl transferase then leads to the transfer of the lipoyl group to the apoproteins.[131, 132] In *E. coli* there are two complimentary pathways involved in the incorporation of lipoate onto apoprotein; the endogenous pathway and the exogenous pathway (Scheme 1.18).[97, 133]

In the exogenous pathway the ATP-dependent activation of lipoic acid from nutrient sources is catalysed by LplA. A lipoyl-AMP intermediate is formed and the enzyme then catalyses the subsequent transfer of the activated lipoic acid to the appropriate lipoyl carrier protein.[120] In contrast, in the endogenous pathway, LipB catalyses the transfer of octanoyl chains originating from fatty acid biosynthesis, to the appropriate lipoyl carrier protein.[127, 134] LipA then catalyses the insertion of two sulfur atoms into C-H, resulting in the formation of lipoamide.[133]

1.6.3 The biosynthesis of ~-lipoyl groups from octanoyl groups

The simplified chemical reactions illustrating the biosynthesis of α-lipoyl groups from octanoyl groups and the biosynthesis of biotin from DTB are shown in Scheme 1.17.[129]

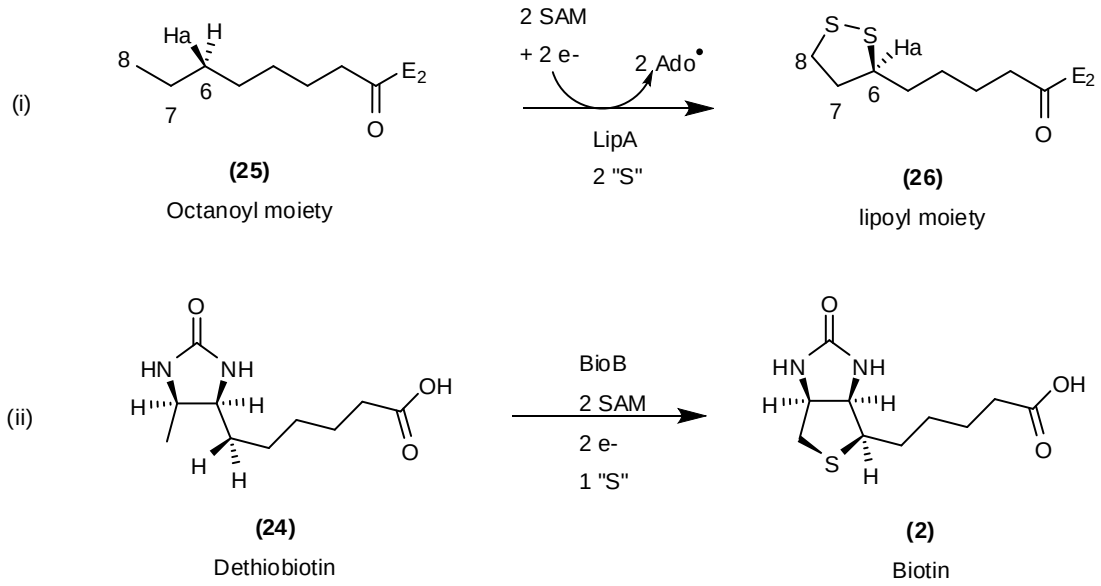

Scheme 1.17 *Reactions showing the syntheses of lipoyl product and biotin; reactions catalysed by LipA and BioB respectively. Both reactions involve the use of two SAM molecules and require two electrons, which are provided by reductants. The LipA mediated reaction requires the insertion of two S atoms whilst the biotin mediated reaction requires one.*[3, 129]

LipA is a 36 kDa protein that has 36 % sequence homology to BioB in *E. coli* and both proteins are involved in sulfur insertion reactions.[5] The mechanism of sulfur insertion during lipoic acid synthesis is thought to be related to that of biotin synthesis as catalysed by BioB.[5, 6] LipA, which has two $[4Fe\text{-}4S]^{1+/2+}$ clusters, and uses SAM as a substrate, is utilized as a cofactor during lipoyl biosynthesis.[3] LipA is the product of the *lipA* gene [4] and it was shown through genetic studies on *E. coli* that cells that had mutations in *lipA* did not produce lipoic acid. [135]

1.6.4 [4Fe-4S] clusters and the reaction mechanism

Most members of the "radical SAM" superfamily when in their functional resting state have a $[4Fe\text{-}4S]^{2+}$ cluster. During turnover this cluster must be reduced to the active $[4Fe\text{-}4S]^{+}$ cluster; in *E. coli* this is mediated by the flavadoxin / flavadoxin NADPH oxidoreductase system. Experimentally *in vitro* turnover can be accomplished using reductants such as sodium dithionite or 5-deazariboflavin.[31, 136] It was shown that in *E. coli*, LipA could contain two [4Fe-4S] clusters, both of which are needed for enzymatic activity.[137] There are putatively two pivotal functions carried out by the [4Fe-4S] clusters during the LipA mediated formation of C-S bonds. Firstly, one [4Fe-4S] cluster is coordinated to the common CX_3CX_2C motif,[7] this $[4Fe\text{-}4S]^{+}$ cluster provides an electron for the reductive cleavage of S-AdoMet, forming the 5′-deoxyadenosyl radical that abstracts hydrogen atoms at C6 and C8 of protein-bound octanoyl moieties.[33, 137] Secondly, for BioB, which is closely related to LipA, it was shown that an [Fe-S cluster] is the source of sulfur that is ultimately transferred to biotin.[78, 138]

In LipA the second [4Fe-4S] is coordinated to a CX_4CX_5C motif which is only conserved in lipoyl synthases.[137] It was speculated that this cluster could function as the donor of the sulfur atoms involved in the reaction, a conclusion made plausible by two *in vitro* LipA assays. Firstly, it was observed that in a pseudo-first order kinetic reaction, LipA catalysed less than one turnover, a phenomenon that could be explained in terms of the depletion of the sulfur source.[134]

Secondly, it was possible to synthesize lipoyl product without introducing an external source of sulfur (i.e. only AdoMet was added into the assays).[139] However the sulfur source has not been positively identified in the LipA catalysed reaction.[136, 137] Using assays in which the time-dependent formation of 5′-deoxyadenosine and [lipoyl]-H-protein were monitored, it was concluded that in *E. coli*, LipA irreversibly cleaves two equivalents of AdoMet to synthesize one lipoyl group.[140]

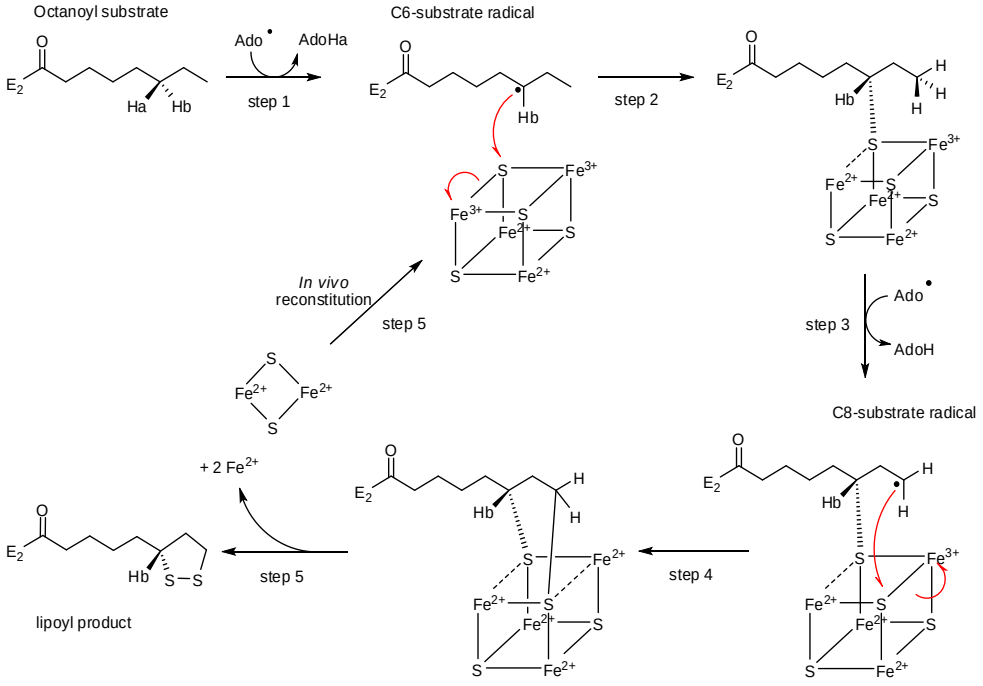

Scheme 1.18 *The mechanism for the LipA catalysed sulfur insertion reaction (adopted from P. Bryant's thesis). Though shown here as a [4Fe-4S] cluster the actual source of the sulfur is not yet known.*[136, 137]

Scheme 1.18 shows a proposed reaction mechanism for the formation of lipoyl product from an octanoyl substrate.[1, 136] The reductive cleavage of AdoMet results in the formation of methionine and the highly reactive 5′-deoxyadenosyl radical which abstracts the pro-*R* hydrogen atom (H_a) from the C6 position of the octanoyl substrate. This results in the formation of one equivalent of 5′-deoxyadenosine ($AdoH_a$) and the substrate radical that attacks one of the bridging μ-sulfide atoms of the [4Fe-4S] cluster coordinated to the $^{68}CX_4{}^{73}CX_5{}^{79}C$ motif.[1] This in turn causes the reduction of one of the adjacent Fe^{3+} atoms to Fe^{2+}. This entire process is then repeated at the C8 position of the octanoyl substrate. The reductive cleavage of a second AdoMet results in another highly reactive Ado radical that abstracts a hydrogen atom from the C8 position to give a C8 alkyl radical. Again this radical attacks another of the bridging μ-sulfide atoms of the [4Fe-4S] cluster causing the reduction of one of the adjacent Fe^{3+} atoms to Fe^{2+}.[1] Release of the product leads to the release of a 2Fe-2S cluster that is assumed to be reconstituted in vivo to give the $[4Fe\text{-}4S]^{+}$.

The Roach group reported the successful turnover of short octanoyl peptide substrate analogues with LipA.[33] Subsequently peptide substrate analogues were used to investigate the order of the sulfur insertion at the C6 and the C8 positions of the octanoyl substrate; and to characterise the structure of the reaction's intermediates.[141] *Sulfolobus solfataricus* P2 LipA and the octanoyl tripeptide substrate (compound **39,** Scheme 2.2) were incubated under assay conditions and the reaction stopped after 20 minutes. LCMS analysis of the supernatant separated from the protein pellet identified four different compounds i) the unconverted substrate [m/z = 515.3]; ii) a monothiolated intermediate [m/z = 547.3]; iii) the lipoamide product [m/z = 577.5]; and iv) the dihydrolipoamide product [m/z = 579.3]. Over extended reaction times (up to 2h) the amount of lipoyl products observed increased whilst the amount of the intermediate decreased.[141]

8,8,8-Trideuterooctanoyl tripeptide was synthesized and used to investigate the order of sulfur insertion at the C6 and the C8 positions. This substrate analogue was incubated with LipA using the same conditions as those used with the octanoyl substrate and the reaction was analysed. The results showed the monothiolated intermediate with sulfur at C6 and very little of the lipoyl product.[31, 141] To eliminate the possibility that the C6 sulfur insertion was due to a random order of sulfur insertion biased by a strong isotope effect at C8, reactions were carried out with proteo-substrate and stopped after 20 minutes of incubation. The products from the reaction were reduced and treated with iodoacetamide, and then purified by high performance liquid chromatography (HPLC). NMR analysis was then carried out to identify the C6, C7 and C8 protons of the monothiolated species. Since the only monothiolated species identified was the C6 sulfur inserted compound, it was concluded that sulfur insertion occurs at C6 first and then sulfur insertion at C8.

Booker *et al.* (2005) investigated the role of LipA as a source of sulfur during the catalysed conversion of octanoyl substrate to lipoyl product.[139] LipA was overproduced in minimal media supplemented with $Na_2{}^{34}S$ only. The isolated protein was used in reaction with SAM and the octanoyl-H-protein substrate, both of which contained ~ 95 % ^{32}S. The lipoic acid product was cleaved from the lipoyl-H-protein and analysed by GC-MS. It was concluded that LipA was the source of sulfur since the lipoic acid product contained the ^{34}S isotope at the same percentage to that in the growth media.[31] In order to determine if both sulfur atoms were supplied by the same LipA subunit, the whole experiment was repeated but this time using equimolar concentrations of ^{34}S labelled and ^{32}S labelled LipA.[136, 139] If one polypeptide provided both sulfur atoms, the isolated lipoic acid would contain either two ^{34}S atoms or two ^{32}S atoms with mixed products expected if the sulfur atoms were supplied by two LipA polypeptides. A ratio of 1:2:1 would be observed corresponding to $^{34}S^{34}S$: $^{34}S^{32}S$: $^{32}S^{32}S$. The reactions gave almost equal amounts of $^{34}S/^{34}S$ and $^{32}S/^{32}S$ H-protein consistent with one LipA polypeptide providing both sulfur atoms.[31, 139]

1.7 The Aims and Objectives of the Study

The three main objectives to this study were:

1. To express the active LipA protein and to then purify and isolate the enzyme for *in vitro* experiments.

2. To effect the laboratory synthesis and to purification of appropriate substrates for the enzyme.

To set-up *in vitro* experiments to probe the LipA mediated transformation of substrates into products

Chapter 2: Results and Discussions

In this chapter, the results obtained from various experiments carried out to study the kinetics of the LipA mediated conversion of octanoyl substrates to lipoyl products are discussed. The experiments carried out during this study can be separated into three different groups. The first set of experiments entailed the expression and the purification of the LipA protein (isolation of the enzyme). The second group of experiments involved the organic synthesis of the different substrates for the enzyme. The last set of experiments involved the setup of the assays to probe the LipA mediated transformation of substrates into products.

2.1 The expression, purification and the isolation of LipA

2.1.1 Transforming competent cells with plasmid DNA

In order to express the *Sulfolobus solfataricus* P2 LipA protein in *E.coli*, the enzyme's DNA had to be transformed into the bacterial cells. A literature search revealed three methods by which foreign genetic material can be inserted into bacterial cells. The first method, conjugation, involves the transfer of DNA between two cells, which are in direct contact with each other.[142, 143] Transduction, the second method, entails the injection of foreign DNA into the host bacterium by a bacteriophage virus.[144, 145] The third method, transformation, is defined as the uptake, incorporation and expression of exogenous DNA in cells.[146, 147] During the transformation of bacterial cells, exogenous DNA initially binds to the cell's surface and is then transferred across the cell wall/membrane complex into the cytoplasm.[148]

In some microorganisms, *e.g. Bacillus*, *Micrococcus* and *Haemophilus* transformation occurs naturally.[149, 150] Such microorganisms possess a dedicated mechanism for binding foreign DNA on the cell surfaces and then transferring it into the cells. However, for most bacteria the uptake of exogenous DNA does not occur naturally, but can be induced by placing the bacterial cells in certain artificial

environments. Under these conditions, the cells are capable of taking up free DNA and are said to be competent. There are a number of methods that are used for preparing competent cells; these include chemical methods, electroporation, sonoporation and biolistic transformation.[151] One way of making *E. coli* cells competent for DNA uptake is to heat-shock them in the presence of Ca^{2+} ions.[145]

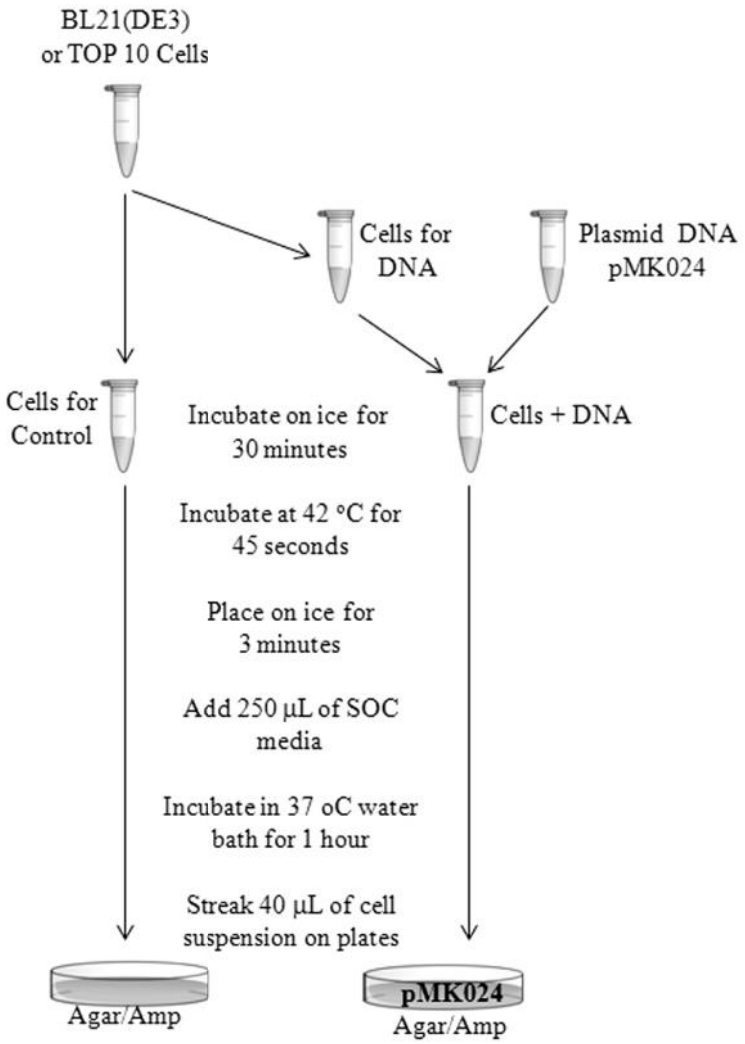

Figure 2.1 *The transformation of bacterial cells with foreign DNA using the heat-shock method.*

The work in this thesis details an application of the heat-shock method (schematic shown in Figure 2.1) to transform TOP 10 and BL21(DE3) competent cells with DNA from the expression plasmid pMK024 (Figure 2.2). This pBR322 derived plasmid was designed by Dr M. Kriek for the co-expression of the *E.coli* iron sulfur

cluster (isc) operon proteins and *S. solfataricus* lipoyl synthase.[136] It has been reported that the co-expression of LipA and the *E.coli* isc operon yielded more soluble protein containing more iron and sulfide equivalents.[33, 152]

Competent cells and the plasmid DNA were incubated on ice (15 min) after which the plasmid DNA was added to the cells. The negative controls were prepared by incubating competent cells alone. The resultant mixtures were incubated on ice (30 min) and then heat-shocked in a water bath (42 ^{o}C, 45 s) after which they were incubated in ice (3 min). SOC growth media was added to the reaction mixtures and the tubes agitated (1 h, 37 ^{o}C). Some of the cell suspension was then spread on ampicillin agar plates. The plates were then incubated (37 ^{o}C, 16 h). When competent TOP 10 and BL21(DE3) cells were transformed with pMK024 DNA, cell colonies grew overnight on the agar/ampicillin plates, and no colonies were obtained for the negative controls. After expressing the transformed cell colonies, the DNA was extracted using the Wizard® Plus SV Miniprep DNA purification system. The extracted DNA was analysed by restriction endonucleases digestion.

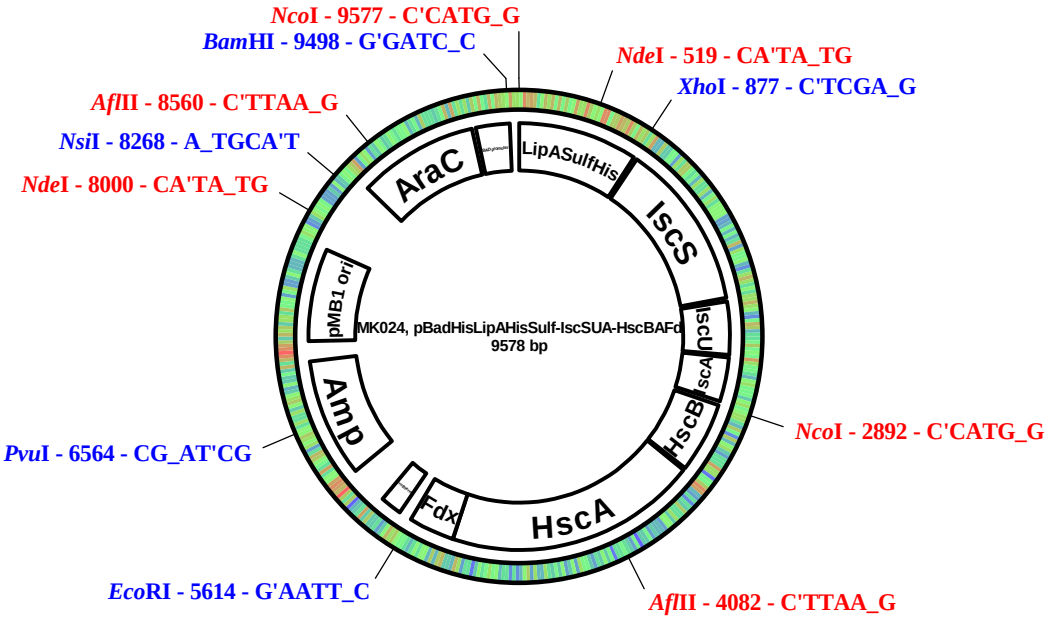

Figure 2.2 *The plasmid map for pMK024, constructed by Dr. M. Kriek for the co-expression of S. solfataricus LipA and proteins encoded by the E. coli isc operon. The map also shows the restriction enzymes used to analyse the expressed LipA.*[136]

The plasmid map for pMK024 is shown in Figure 2.2. This diagram also shows the cleavage sites for the endonucleases XhoI, NcoI, EcoRI, BamHI, NdeI, PvuI and NsiI. These restriction enzymes were used to digest the DNA extracted from the transformed cell colonies, enabling the analysis of pMK024. The plasmid pMK024 provides for a controlled, dose-related recombinant protein expression and purification in *E.coli*. The ampicillin resistance gene (*Amp*) enables selection based on antibiotic resistance. The *AraC* gene encodes the protein to tightly regulate the P_{BAD} promoter. Furthermore, included in this plasmid are the genes for iron sulfur cluster assembly, *IscS, IscU* and *IscA*. The gene LipASulfHis encodes for the *S. solfataricus* LipA and the N-terminal His_6-tag. Chaperones encoding genes *HscA* and *HscB* were also included in the plasmid as well as the ferrodoxin encoding *Fdx* gene.

Table 2.1 *The sizes of the DNA strands that would be expected from the digestion of the plasmid pMK024 using the restriction endonucleases XhoI, NcoI, EcoRI, BamHI, NdeI, PvuI and NsiI.*

Restriction enzymes	**Cut 1**	**Cut 2**	**Strand 1 (Cut2 –Cut1)**	**Strand 2 (9578 – Strand 1)**
XhoI	877	-	-	9578
NcoI	2892	9577	6685	2893
NdeI	519	8000	7481	2097
EcoRI + BamHI	5614	9498	3884	5694
PvuI + NsiI	6564	8268	1704	7874

The sizes of the DNA fragments that would be obtained from digesting the pMK024 DNA with various restriction endonucleases are shown in Table 2.1 After the digestions, the DNA fragments were separated by electrophoresis in an agarose gel, visualised by staining the gel with ethidium bromide (EtBr). The gel was finally observed under an ultraviolet light. Figure 2.3 shows a picture of a developed agarose gel for the digestion analysis of plasmid DNA from three different sources.

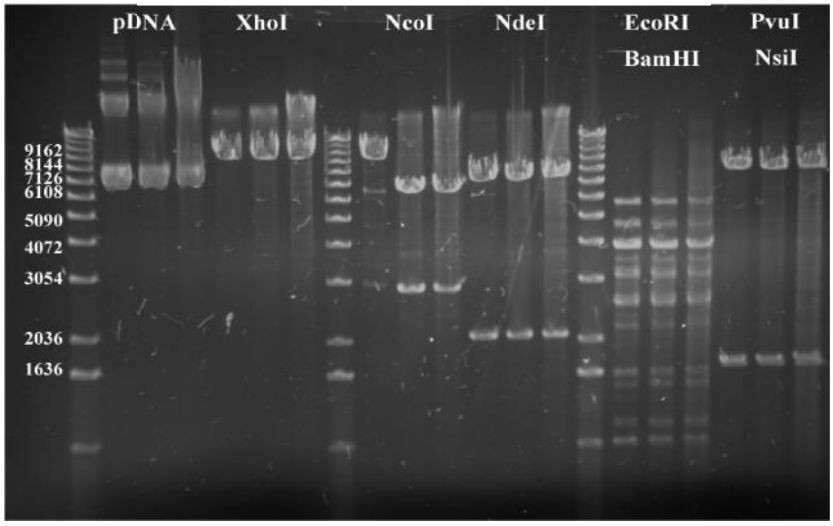

Figure 2.3 *A picture of an agarose gel showing the digestion of pMK024 by restriction enzyme, pDNA is the plasmid DNA.*

XhoI cleaves DNA at 877 base pairs (bp) and would give a single strand of 9578 bp when cutting pMK024. This indeed is what was observed and is shown in the image of the agarose gel shown in Figure 2.3 (lanes 5 – 7). Digestion of pMK024 with NcoI produces two cuts at 2892 bp and 9577 bp. This means that two strands of 6685 bp (9577-2892 bp) and 2893 bp (9578 -6685 bp) were to be expected. These two strands were observed on the agarose gel (lanes 9 – 11). Likewise, digestion with NdeI gives two cuts at 519 bp and 8000 bp, meaning two strands of sizes 7481 bp and 2097 bp were expected from the digestion of pMK024. This was confirmed by the image of the agarose gel shown in Figure 2.3 (lanes 12 – 14).

The restriction enzymes EcoRI, BamHI, PvuI and NsiI all cut DNA at one site; pairing any of these for a digestion would give DNA cut at two different points. Table 2.1 and Figure 2.1 show that the expected strands were observed when pMK024 was digested using the restriction enzymes shown. However, digestion with EcoRI and BamHI showed “star” activity under the conditions used; hence in addition to the predicted strands other strands of varying sizes were also observed. This activity could have resulted from either EcoRI or BamHI; both of which are known to exhibit “star” activity under the wrong buffer conditions. It could be that

the buffer's ionic conditions were too low (*i.e.* < 50 mM), or the glycerol concentration was too high and this could have lead to the "star" activity of either restriction enzyme. Another explanation for the occurrence of this phenomenon could be that too many units of either enzyme had been added to the reaction mixture.[153, 154]

The digestion of the extracted DNA with restriction enzymes and the analysis thereof on an agarose gel shows that it had a size of 9578 bp, which is equivalent to that of pMK024. Further characterization of this DNA could have been achieved via DNA sequencing, but it was not necessary in this instance because the plasmid had previously been sequenced within the Roach group. The restriction enzyme digestions and the analysis were carried out to verify that the right plasmid had been transformed and subsequently the correct cells were expressed and purified.

2.1.2 Expression and purification of S. solfataricus LipA

The large-scale expression of the transformed cells was carried out in 2YT media (5L). The cells were induced when the optical density at 600nm wavelength (OD_{600}) reached the range 0.8 – 1.00 and yields were typically 25 – 35 g for this expression. LipA purification was carried out anaerobically using a Ni^{2+} affinity chromatography column followed by an S75 gel filtration process. The method applied was developed by Dr M. Kriek and is similar to the procedure previously used with *E. coli* LipA.[136]

Cells were incubated with benzonase and lysozyme for 1 h and then lysed by sonication (10 min, 1 s pulses). The lysate was centrifuged, and the supernatant was then applied to a Ni^{2+} charged affinity column. A single peak recorded on a UV spectrum at a wavelength of 420 nm, used to monitor the protein as it passed through the column, corresponded to the LipA fractions. This indicated that the Ni^{2+} column was effective in separating the LipA from the other proteins in the lysate but could not differentiate between the dimeric and monomeric forms of LipA.

The collected LipA fractions exhibited a characteristic black colour which is indicative of the presence of [Fe-S] clusters. Typically, 40 - 50 mL of the eluate LipA were collected from the Ni^{2+} column and this was concentrated to ~ 10 mL, which was applied to an S-75 gel filtration column. The chart in Figure 2.4 shows the UV spectrum trace recorded for the eluate from the S75 gel filtration of *S. solfataricus* LipA. Two peaks were observed, the first corresponding to dimeric LipA and the second peak equivalent to monomeric LipA.[136]

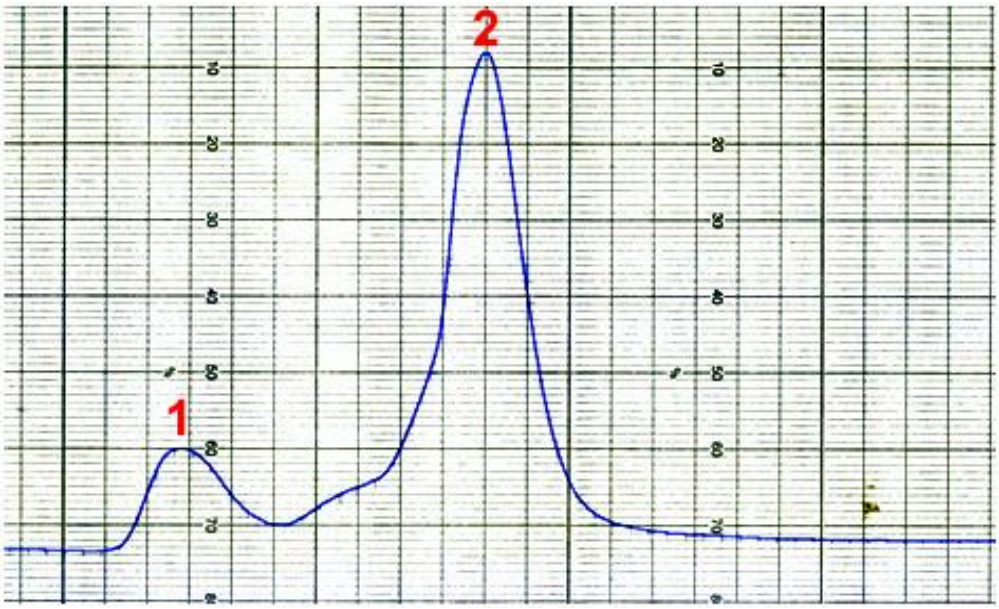

Figure 2.4 *UV absorption (^{a}=420 nm) trace for the S75 gel filtration of LipA. The two peaks correspond to (1) dimeric LipA and (2) monomeric LipA.*

An image of the SDS-PAGE gel obtained for the electrophoresis analysis of the collected *S. solfataricus* LipA fractions from the S75 gel filtration is shown in Figure 2.5. The protein has a mass of 36 kDa and the fractions 2–7 show the purified protein; fractions 3-7 correspond to monomeric LipA and fraction 2 corresponds to dimeric LipA. Typically, 200 – 250 mg of LipA (10 – 30 mg dimeric and 170 – 220 mg of monomeric LipA) were purified from 30 – 40 g of cells and stored at -80 ^{o}C. The iron and sulfide content analysis of the protein was carried out according to the

methods developed by Fish [155] and Beinert [156] respectively. It was determined that each mole of LipA contained 3.8 ± 0.2 moles of Fe and 3.5 ± 0.4 of sulfide.

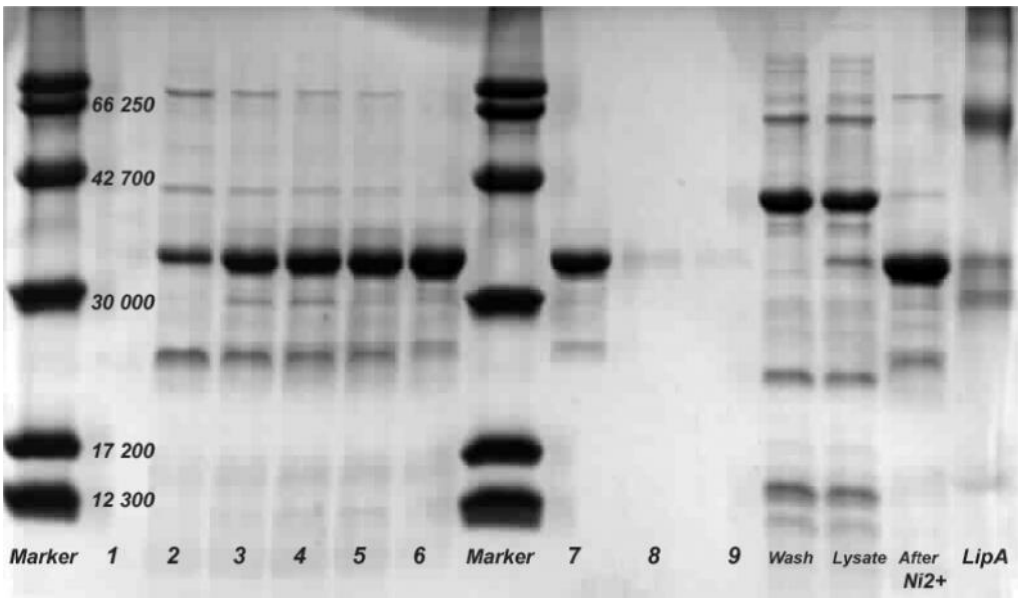

Figure 2.5 *A picture of an SDS-PAGE gel for the Purification of LipA. Lanes 1- 9 shows collected fractions of LipA alongside the lysate obtained from cell lysis, and the LipA purified on a* Ni^{2+} *column. The wash column shows the protein that was washed out during the* Ni^{2+} *column purification. It is seen that the LipA is bound to the* Ni^{2+} *column. Lane 2 corresponds to dimeric LipA and lanes 3-7 correspond to monomeric LipA.*

2.1.3 Conclusions on the expression, isolation and purification of LipA

S. solfataricus LipA was successfully transformed into bacterial cells and was subsequently expressed and purified from these cells. The isolated enzyme was in an inactive form but could be reconstituted into the active form when needed (see experimental section 3.3.14). Having successfully expressed and purified the enzyme for the activity assays the next step was to synthesize the substrates for the enzymes. Two types of substrates were prepared, the octanoylated peptide substrate analogues corresponding to the identified E_2 domain sequence in LipA from the archaeon *S. solfataricus* P2 [136] and the fluorescently labelled octanoylated peptide substrate analogues Schemes 2.2 and 2.3).

2.2 Preparation of Substrates for LipA

2.2.1 Testing the stability of fluorophores in the presence of sodium dithionite

In order to be able to prepare the fluorescently labelled substrate analogues to add to the LipA assays, it was necessary to identify fluorophores that were stable in the presence of sodium dithionite. This reducing agent is one of the components of the *in vitro* substrate turnover assays with LipA. Figure 2.6 shows the chemical structures of fluorophores that were tested for stability in the presence of sodium dithionite.

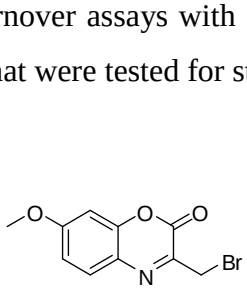

(31)
3-Bromomethyl-7-methoxy-1,4-benzoxazin-2-one

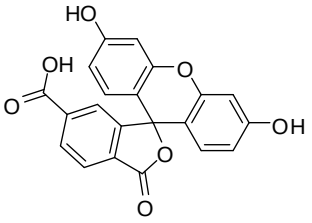

(32)
6-Carboxyfluorescein

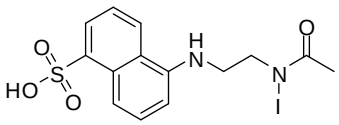

(33)
5-(2-(*N*-iodoacetamido)ethylamino) naphthalene-1-sulfonic acid

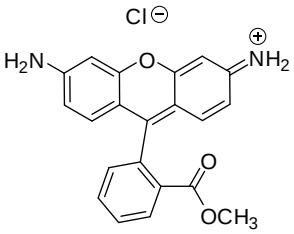

(34)
Rhodamine B

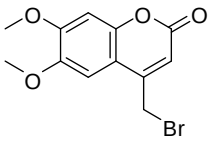

(35)
4- bromomethyl-6,7-dimethoxycoumarin

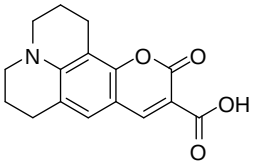

(36)
Coumarin 343

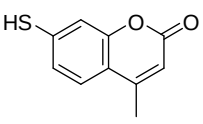

(37)
7-mercapto-4-methylcoumarin

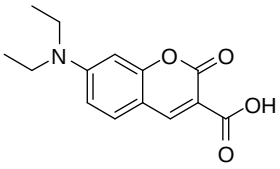

(38)
7-(diethylamino)-2-oxo-2*H*-chromene-3-carboxylic acid

Figure 2.6 *The chemical structures of the fluorophores that were tested for stability in the presence of sodium dithionite.*

All of the fluorophores in Figure 2.6 were obtained from commercial sources except for 7-(diethylamino)-2-oxo-2*H*-chromene-3-carboxylic acid (38) which was synthesized. This coumarin was successfully prepared by reacting 4-(diethylamino)-salicyclaldehyde and 2,2-dimethyl-1,3-dioxane-4,6-dione with dry ethanol as the solvent (Experimental 3.5). The fluorophores were incubated in a cuvette with sodium dithionite and dithiothreitol (DTT) in HEPES buffer (25 mM, pH 7.5) and the fluorescence intensity recorded over a period of 30 min. The graphs in Figure 2.7 and Figure 2.8 show how the recorded fluorescence varied with time for these fluorophores.

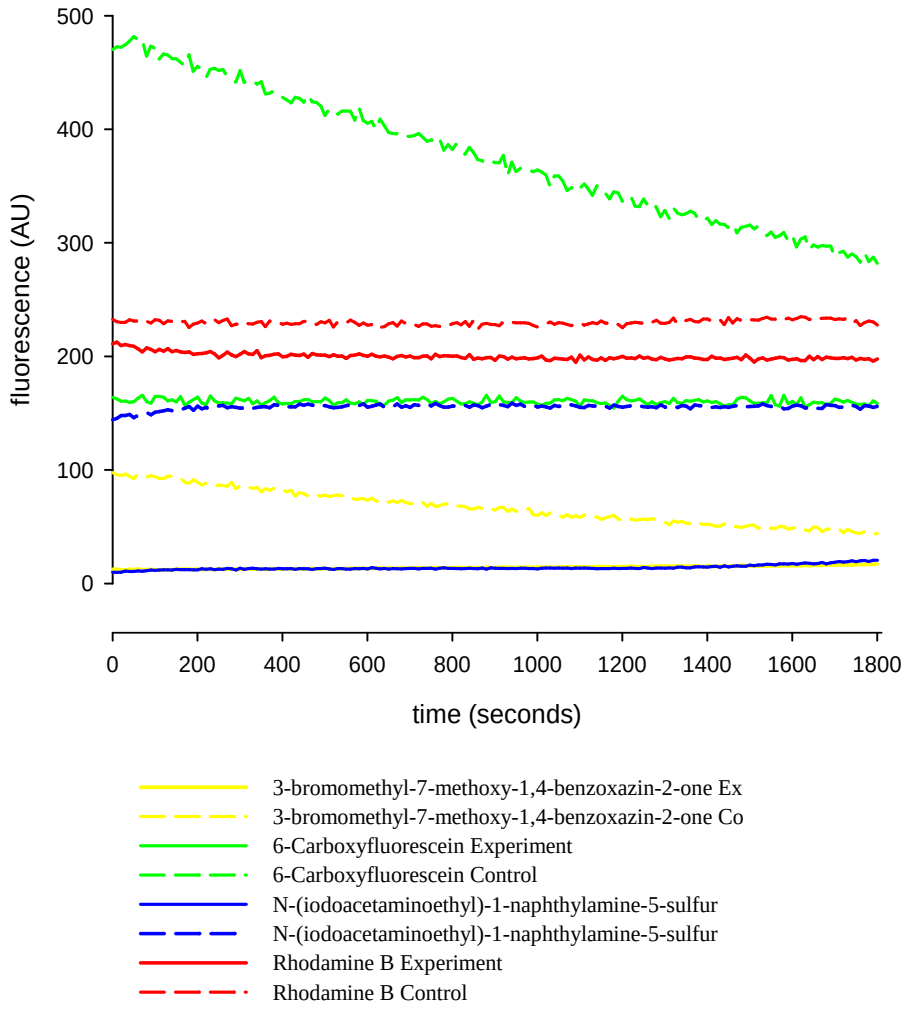

Figure 2.7 *A plot of fluorescence (AU) against time (seconds) for testing the stability of 6-Carboxyfluorescein, Rhodamine B, 3-Bromomethyl-7-methoxy-1,4-benzoxazin-2-one and N-(iodoacetaminoethyl) -1-naphthylamine-5-sulfuric acid in the presence of sodium dithionite.*

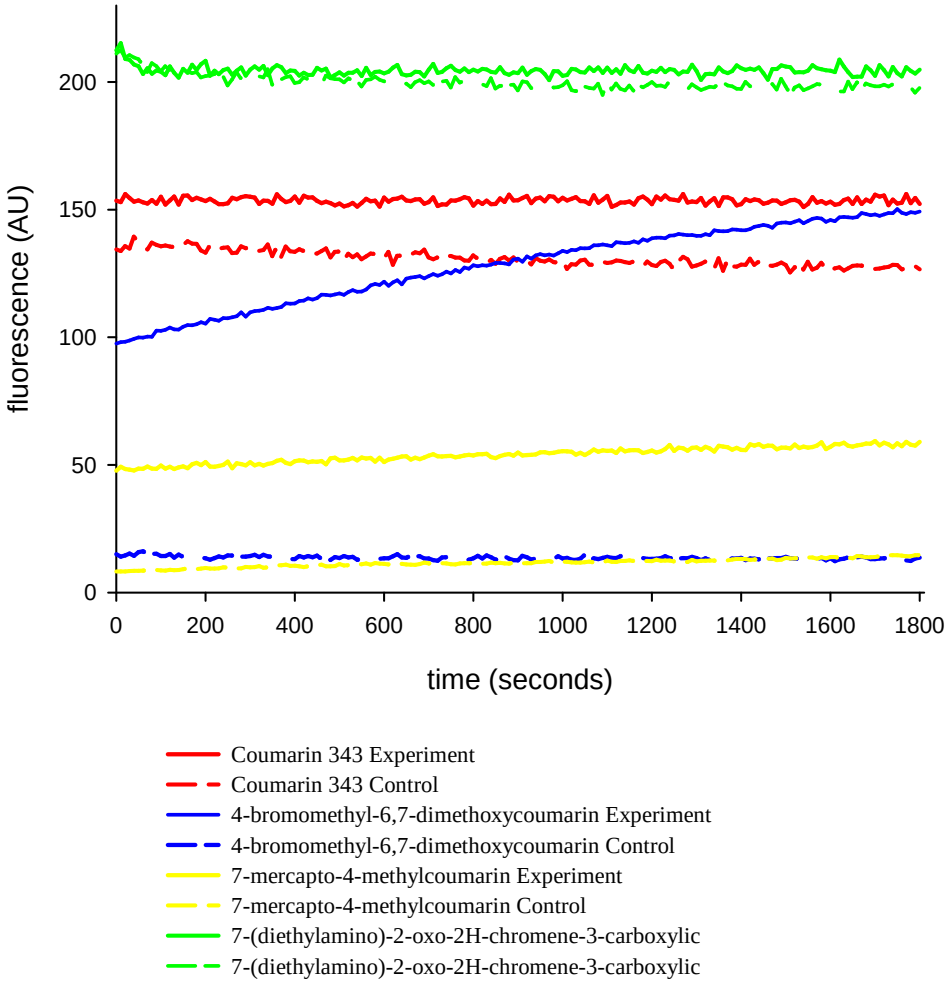

Figure 2.8 *A plot of fluorescence (AU) against time (seconds) for testing the stability of coumarin 343, 7-mercapto-4-methylcoumarin, 4-bromomethyl-6,7-dimethoxycoumarin and 7-(diethylamino)-2-oxo-2H-chromene-3-carboxylic acid, in the presence of sodium dithionite.*

The results showed that the coumarins or benzo-α-pyrones (compounds whose structure is shown by compound **46** (Scheme 2.6) retained most of their fluorescence intensity for the duration of the observations which led to the conclusion that they were the more stable compounds under the LipA assay conditions. Coumarin 343 (compound **36**, Figure 2.6) retained most of its initial fluorescence signal over time and there was very little difference in signal between the control experiment and the test experiment (Figure 2.8). This raised the possibility that coumarin 343 was the

best fluorophore for the proposed assays, and it was anticipated that it would be possible to attach this coumarin to the peptide substrate analogues to be used in assays with LipA. However none of the commercial suppliers had stock of coumarin 343 and a literature search yielded no practical synthetic route. The structurally related compound 7-(diethylamino)-2-oxo-2*H*-chromene-3-carboxylic acid (38), for which a synthetic route is described in literature, was then considered as an alternative fluorophore. The synthesized compound was tested for retention of its fluorescence intensity in the presence of sodium dithionite, and indeed, it proved stable (Figure 2.8). The coumarin 7-(diethylamino)-2-oxo-2H-chromene-3-carboxylic acid (38) was therefore selected as the fluorophore to be used in the synthesis of fluorescent peptide substrate analogues for lipoyl synthase.

2.2.2 Synthesis of substrate analogues

One of the first compounds to be identified as a substrate for lipoyl synthase was an octanoylated derivative of the lipoyl-bearing subunit (E2) of the pyruvate dehydrogenase complex.[46] After this, it was shown that the octanoylated derivative of the glycine cleavage system's lipoyl-bearing subunit (H-protein) was also a substrate for LipA.[157] In more recent studies, Bryant and Douglas used three and four amino acid substrate analogues to investigate *in vitro* LipA activity.[33, 136] When tripeptides and tetrapeptides were synthesized [5, 6, 19] it was observed that these peptides were of limited solubility in aqueous solution and were insoluble in organic solvents.[136] Among the synthesized peptides, tetrapeptides were more soluble compared to the shorter peptides.

In the experimental section of this thesis is a description of the solid phase peptide synthesis of substrate analogues (shown in Figure 2.9 and Figure 2.10) corresponding to the identified E_2 domain sequence in LipA from the archaeon *S. solfataricus* P2. Figure 2.9 shows the structures of the tripeptide EK(Oct)I (**39**), tetrapeptide TEK(Oct)I (**40**) and the pentapeptide ETEK(Oct)I (**42**). These three compounds are unlabelled substrate analogues which are centred on the octanoylated lysine residue of the E2 subunit's amino acid sequence. The substrates were successfully

synthesized and the purified compounds were applied to *in vitro* activity assays with LipA. Another substrate that was synthesized is the tripeptide EK(Non)I (41) in which a nonanoyl residue substituted the octanoyl on the lysine residue.

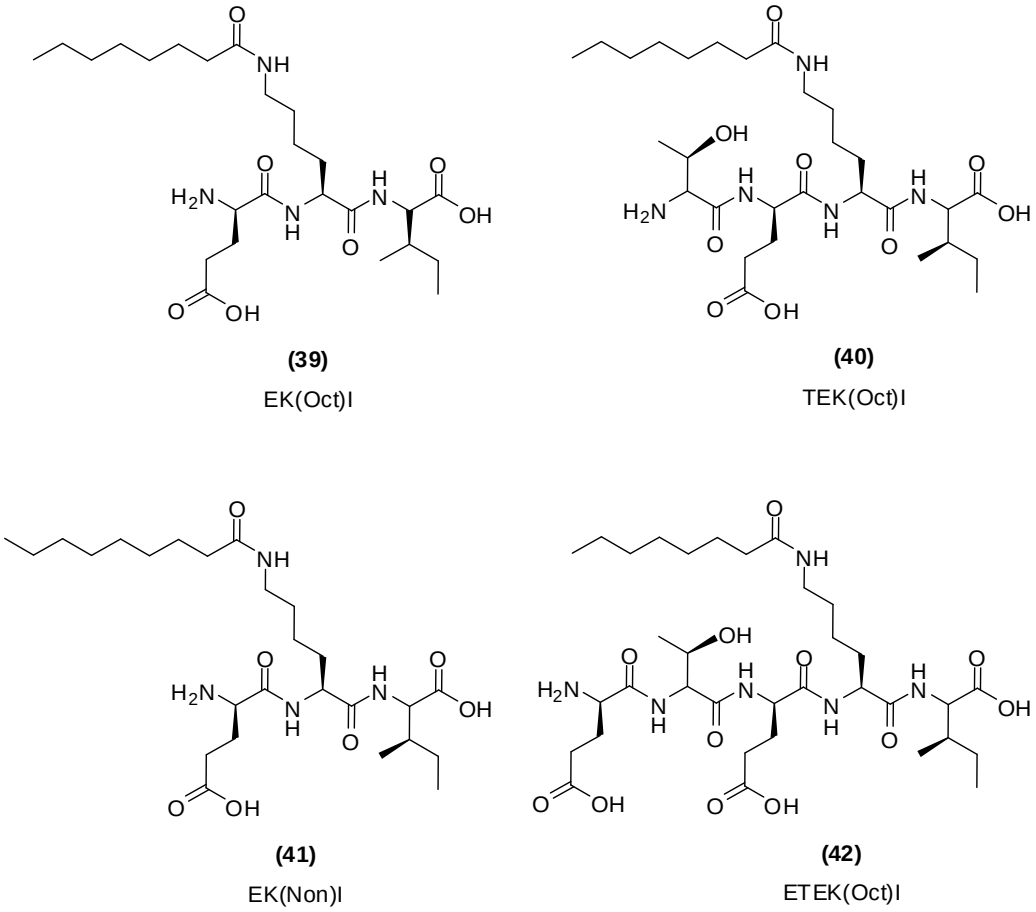

Figure 2.9 *The synthetic non-fluorescent peptide substrate analogues for LipA. These peptides were all synthesized on a resin by applying the solid phase peptide synthesis procedure developed by Merrifield.*

The ideal synthetic substrate analogue would need to be soluble in aqueous solution, at neutral pH. It must be stable under the assay conditions and importantly should not result in any modification of the natural substrate binding site. The previously used non-fluorescent substrates and the resultant intermediates and/or end products had been difficult to detect in the reaction mixtures. Fluorescent labelling of the peptide substrate analogues would significantly improve the detection levels of intermediates and end products. Figure 2.10 shows new substrates that possess previously unused fluorescent coumarin labels (box 1) which could be used with fluorescence detectors

in the analysis of reactants, intermediates and products formed in the LipA assays. The substrate analogues in Figure 2.10 possess an octanoyl group (Box 2) on the lysine residue side chain, which is the site for the sulfur insertion.

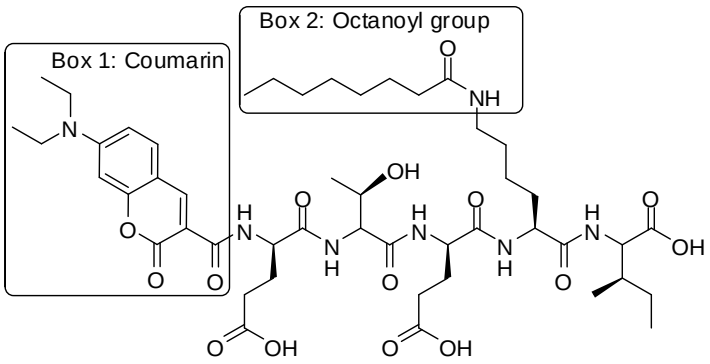

DECA-1-ETEK(Oct)I
(43)

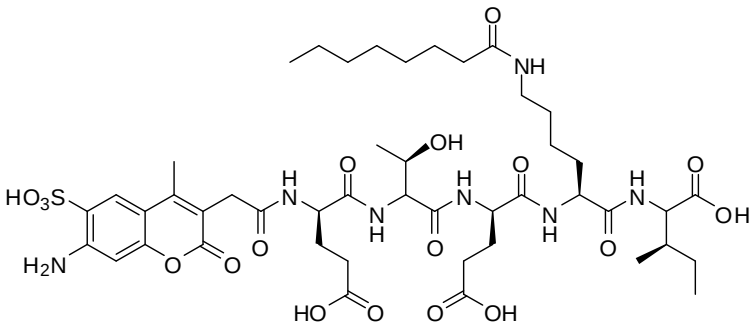

Alexa 350-ETEK(Oct)I
(44)

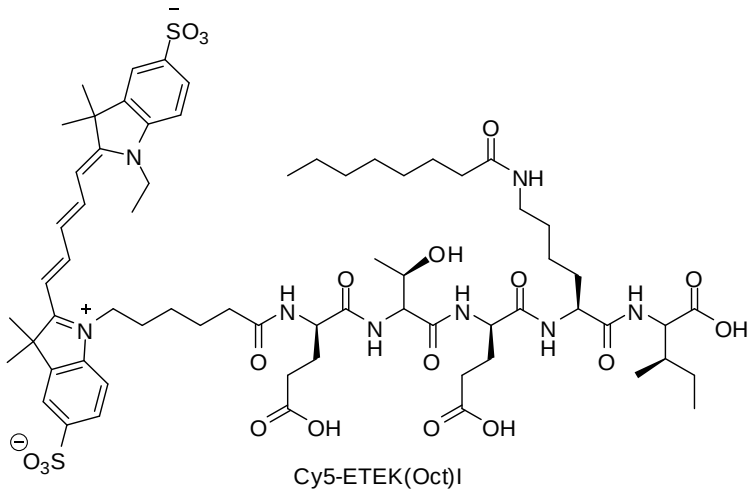

Cy5-ETEK(Oct)I
(45)

Figure 2.10 *The synthetic fluorescent octanoyl pentapeptide substrate analogues for LipA. These peptides were all synthesized on a resin by applying the solid phase peptide synthesis procedure developed by Merrifield.*

2.2.3 Peptide synthesis

The chemical synthesis of peptides and proteins involves the assembly of protected peptide fragments, the deprotection of the protecting groups and the purification and characterisation of the synthesized product. There are three approaches used to achieve the chemical synthesis of peptides (shown in Figure 2.11) [158]

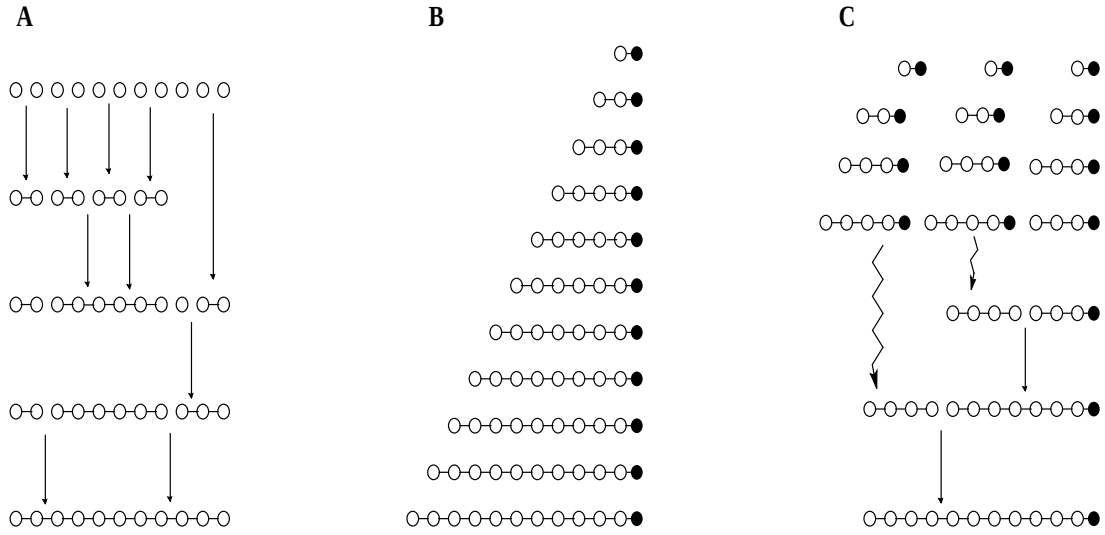

Figure 2.11 *The three basic methods for assembling peptide chains. (A) Convergent fragment condensation is a process achieved in solution. (B) In stepwise solid phase synthesis, the peptide chain is assembled from the C-terminal residue while bound to a polymeric resin support. (C) During sequential solid phase fragment condensation protected fragments made by stepwise solid phase synthesis are released and are condensed on a resin support.*[158]

Fragment condensation is a classical solution synthetic strategy in which the appropriate chemistry is applied to encourage the formation of bonds between the fragments in solution.[159] After each peptide bond-forming step the intermediates are purified and characterised. In order for this approach to be successful in preparing peptides the intermediates have to be soluble in the solution phase. However, in some instances, the protected fragments may be insoluble in solution making it impossible to form peptide bonds. Another problem is racemisation of the activated C-terminal amino acids in the peptide which raises the need for effective and efficient methods to separate the components of racemic mixtures.[159]

In this study, LipA substrate analogues were prepared using the second approach for peptide synthesis, called solid phase peptide synthesis (SPPS). This procedure involves attaching a protected C-terminal amino acid to a solid support or resin and subsequently adding the ensuing amino acids in a stepwise manner. This method is more applicable to assembling peptides from protected amino acids.[160] The main advantages of this approach are that there is no need for the protected amino acid fragments to be soluble, and the synthesized peptide can be separated from fragments by simply washing and filtering the resin.

In the third approach, sequential solid phase fragment condensation, peptides are prepared on a solid support by successively condensing protected fragments prepared by solid phase peptide synthesis. The resin-bound intermediates are easily purified by filtering and washing the resin. One advantage of this approach is that it is carried out in solution and there are no insoluble fragments since the approach uses shorter protected fragments, which are more soluble.[158]

Peptides are formed when α-amino acids are coupled together through the formation of amide bonds. The reactivity of the N-protected amino acid's carboxyl group and the steric accessibility of the reactive nucleophile determine the success of the coupling of amino acid derivatives.[161] To achieve the synthesis of an amide bond the carboxyl group must first be activated, which can be accomplished in many different ways. Ultimately, the reactivity of the activated species determines the coupling yield. Coupling reagents such as carbodiimides are often used to achieve couplings during peptide synthesis. The coupling reagent reacts with the free carboxyl group of the amino acid to give a highly reactive species which facilitates the formation of the amide bonds at ambient temperatures.[161, 162]

The reaction mechanism in Scheme 2.1 shows how carbodiimides activate the carboxylic acids on amino acids and the subsequent formation of peptide bonds. The carbodiimide (ii) rapidly reacts with the *N*-protected amino acid (i) to give the *O*-acylisourea (v). This labile intermediate can be involved in a number of different

reactions. It could react with a second equivalent of the *N*-protected amino acid (i) to give the symmetrical anhydride (viii). This intermediate will then be involved in a reaction with a second amino acid (vii) to form the amide bond. This pathway is shown by the clockwise cycle in Scheme 2.1. Another reaction that could occur is the direct coupling between the *O*-acylisourea (v) and the second amino acid (vii). This reaction is shown by the arrow going from compound (v) down to (x) in Scheme 2.1.

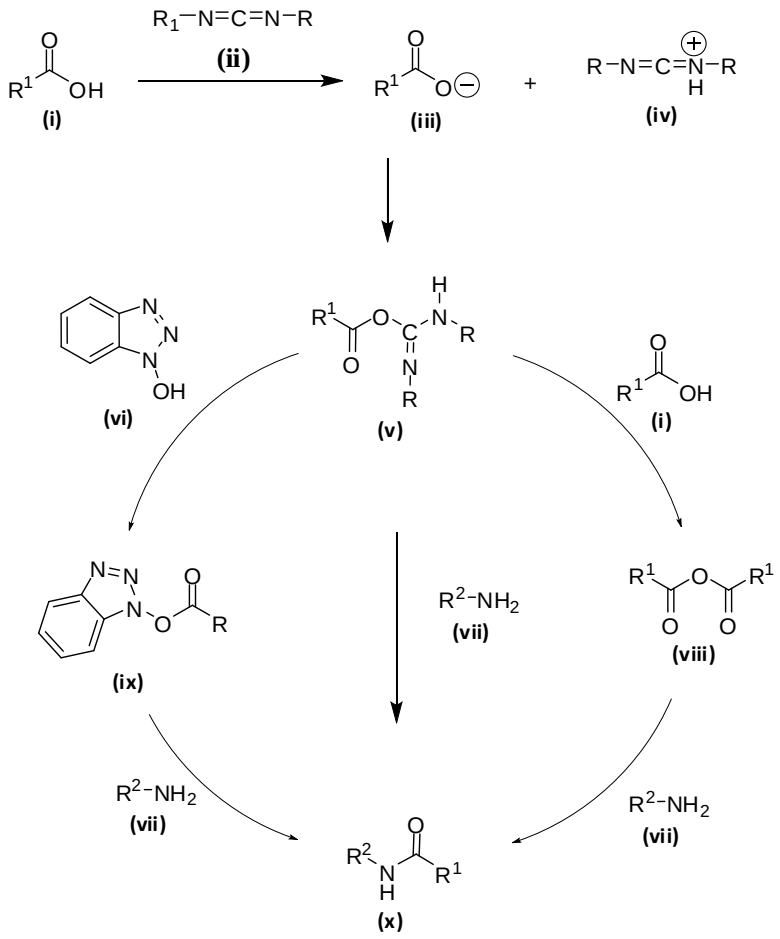

Scheme 2.1 *The formation of peptide bonds by carbodiimides activation.*

In the presence of an additive such as HOBt (ix), the *O*-acylisourea (v) could still be involved in a third reaction, shown by the anti-clockwise cycle in Scheme 2.1. In this instance, an active ester (ix) intermediate is formed which in turn reacts with the amino terminal of the second amino acid (vii) to form the peptide bond. Additives such as HOBt are often introduced with the carbodiimides to suppress racemisation and to exclude the dehydration of carboxamide residues such as Gln and Asn.[163]

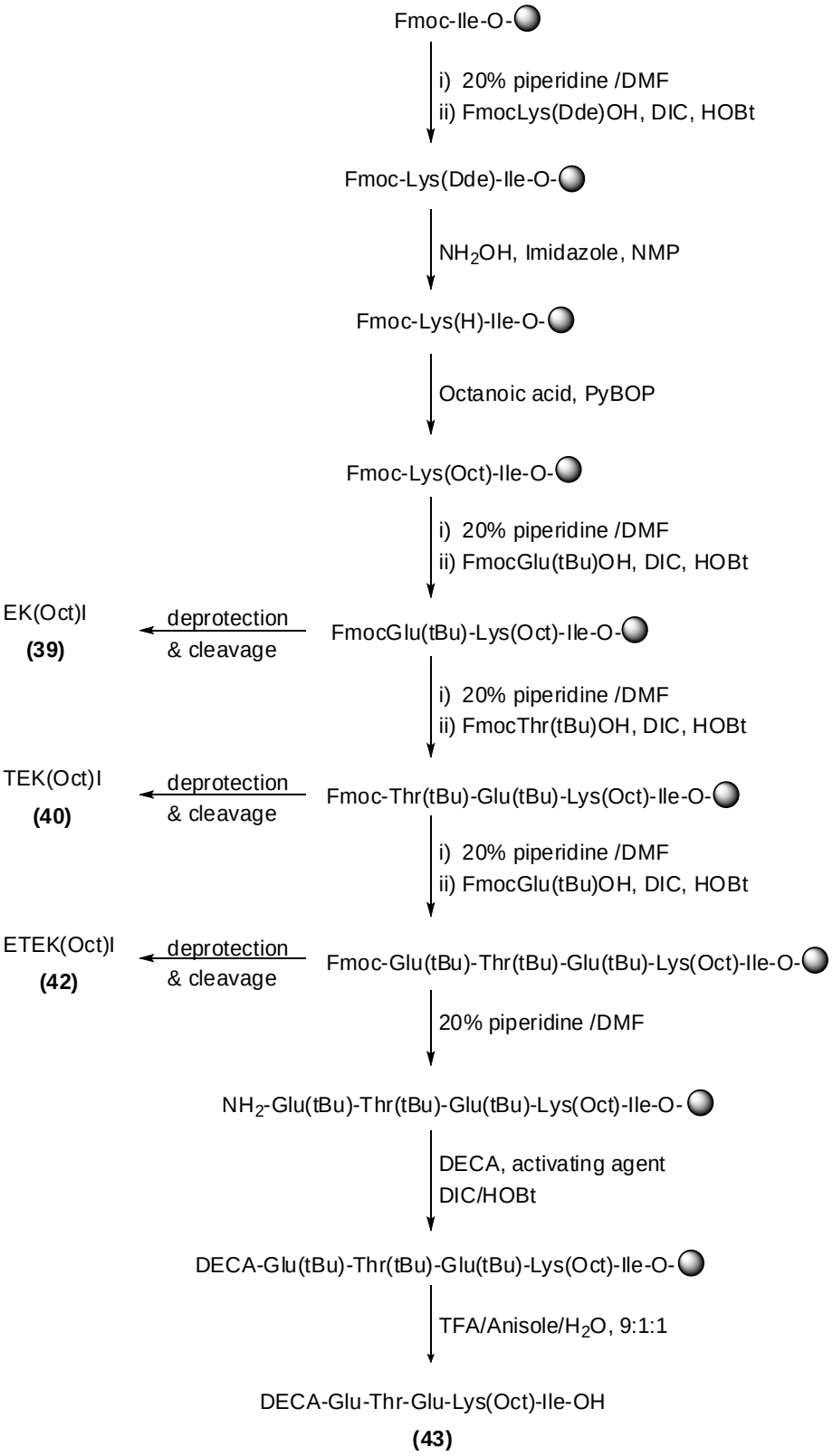

Scheme 2.2 *The solid phase synthesis of the fluorescent-labelled pentapeptide substrate analogue DECA-ETEK(Oct)I. The final deprotection of the desired peptide's protecting groups and cleavage from the resin was achieved using TFA/water/anisole (9/1/1) solution.*

The octanoylated substrate analogues for LipA (Figure 2.9 and Figure 2.10) were prepared according to the steps shown in the reaction Scheme 2.2. This application of Merrifield's solid phase peptide synthesis approach was carried out in a sintered glass bubbler peptide synthesizer.[160] The synthesis uses orthogonally protected Fmoc protected *N*-(α)-amino acids, and *tert*-Butyl (tBu) protected alcohol and carboxylic acid groups. The *tert*-Butyl protecting group is stable in the basic conditions used for Fmoc deprotection, but is easily removed under the strong acidic conditions required to cleave the peptides from the resin. The lysine side chain to which the octanoic acid was coupled was initially protected using 2-acetyldimedone (Dde), which is removed with 2 % v/v hydrazine, but is relatively stable to the conditions for Fmoc/ tBu deprotection.[164]

The shorter peptide substrate analogues (*i.e.* tripeptides and tetrapeptides) were reported to be less soluble in aqueous solutions, and so it was preferred to synthesize the pentapeptide analogue. Significantly, the pentapeptide possesses the alcohol group (OH) and the additional carboxyl group (COOH), which are hydrophilic groups. Fluorescence labelling was desirable as it would improve the sensitivity of the compounds to detection with fluorescence detectors and would also make possible the use of plate readers to analyse assays.

To prepare the peptides the first amino acid, isoleucine, was attached via its β-carboxyl group onto Wang's resin using DMAP and coupling with diisopropylcarbodiimide. The levels of loading varied from 50 % to 60 % of the resin's loading capacity (0.44 mmol/g). The loading of the isoleucine was repeated until a high level (73 %) was achieved. The loading was improved when the minimal amount of DMF was used in the reaction mixture. Capping of the free amino acids and the resin's unreacted groups was achieved with pyridine and benzoyl chloride. This step was necessary to avoid the formation of undesirable peptide fragments.

The lysine side chain to which the octanoic acid was coupled was initially protected using the 1-(4,4-dimethyl-2,6-dioxacyclohexylidene)-ethyl (Dde) group. Dde was selectively removed with imidazole and hydroxylamine hydrochloride suspended in *N*-methylpyrrolidone (NMP), but was relatively stable to the both conditions for Fmoc and *t*Bu deprotection.[164, 165] Octanoic acid was coupled to the deprotected ε-amino group of the lysine side chain using benzotriazolyloxy-tris-[pyrrolidino]-phosphonium hexafluorophosphate (PyBOP) in the presence of diisopropylethylamine (DIPEA).

The coupling of the octanoic acid was achieved by first (Dde)-deprotecting the growing peptide on the resin. This made the lysine residue available for the coupling with octanoic acid in the presence of DIPEA and PyBoP. After this the coupling of the octanoic acid was checked by cleaving 25 mg of the resin bound dipeptide and characterizing the cleaved compound by ESI-mass spectroscopy. The TFA was evaporated on a rotary evaporator, which gave a pale yellow solution. A drop of this solution was dissolved in acetonitrile, and the resultant solution analysed by ESI mass spectroscopy. The spectrum in Figure 2.12 shows the mass ions observed from this analysis.

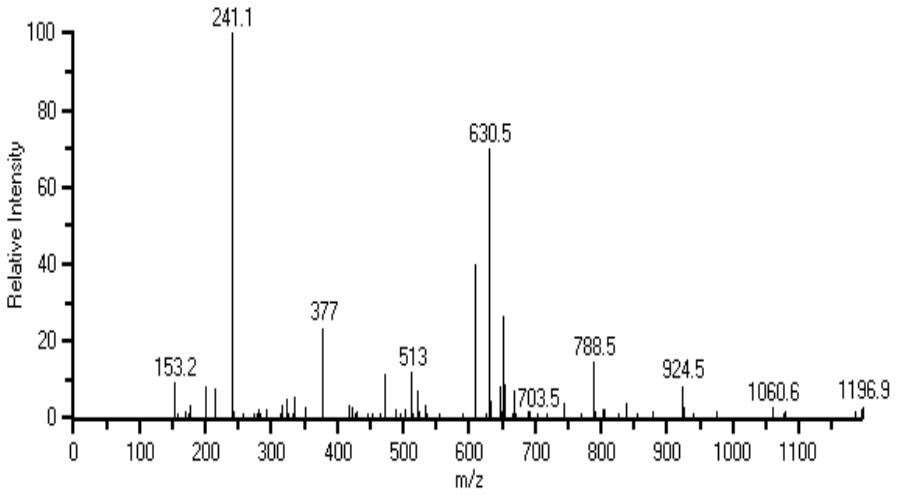

Figure 2.12 *An ESI+ mass spectrum used to show the successful coupling of octanoic acid to the lysine residue.*

The peak at m/z = 608.5 corresponds to the $[M+H]^+$ ion, and the peak at m/z = 630.5 corresponds to the $[M+Na]^+$ ion. The other peaks on the spectrum were attributed to contaminants within the samples. The mass spectrum of Figure 2.12 showed that the coupling of octanoic acid had been achieved, but it also showed that there were other uncharacterized compounds from which the desired peptide would have to be separated. The peptidyl resin was repeatedly washed with DMF and dried under vacuum after which it was possible to carry-out the coupling of the third amino acid. The desired peptides (EK(Oct), TEK(Oct)I, ETEK(Oct)I) and DECA-ETEK(Oct)I) were cleaved from the resin using a mixture of TFA/anisole/water (9:1:1). In this mixture the anisole functions as a scavenger for cationic species formed in the reaction mixture.

The crude peptides were purified either by reverse phase chromatography on a Supelclean ™ LC-18 solid phase extraction column (a mixture of water/acetonitrile mobile phase), or by preparative HPLC on a reversed phase Phenomenex Gemini C18 (5 µm, 150 × 10 mm) column. The yields of purified peptides were much lower when preparative HPLC was used (≤ 20 %), compared to the yields of purified peptides obtained from the solid phase extraction column (70 %).

Conclusions on the synthesis of substrate analogues for LipA

Solid phase peptide synthesis was successfully used in the synthesis of the fluorescent and the non-fluorescent substrate analogues for LipA (shown in Figure 2.9 and Figure 2.10 respectively). The non fluorescent peptides were synthesized first and then purified. These substrates were then used in the activity assays with LipA. After these assays what remained of the non fluorescent substrates was then used in the preparation of the fluorescent substrates by coupling with the chosen fluorophores. The non fluorescent peptides were then also used in assays with LipA.

2.2.4 Synthesis of 7-amino-4-methyl-6-sulfocoumarin-3-acetic acid

Coumarins, also known as benzo-α-pyrones are compounds whose structures consist of a benzene ring fused to a pyrone (Figure 2.13). These compounds have a wide range of fluorescence emission properties, which has led to their use as labels or tracers and in the preparation of fluorescent substrates for use in enzyme assays.[166]

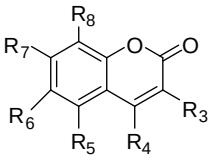

(46)

Coumarin structure

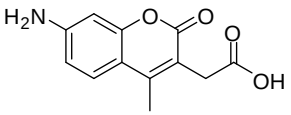

(47)

2-(7-amino-4-methyl-2-oxo-2*H*-chromen-3-yl)acetic acid

AMCA

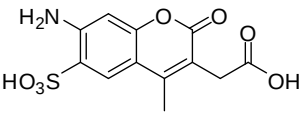

(48)

2-(7-amino-4-methyl-2-oxo-6-sulfo-2*H*-chromen-3-yl)acetic acid

Alexa 350

Figure 2.13 *The basic structure of coumarins (***46***), 7-amino-4-methylcoumarin-3-acetic acid (AMCA,* **47***) and the sulfonated derivative 7-amino-4-methyl-6-sulfocoumarin-3-acetic acid (AMCA-S,* **48***).*

Multicolour fluorescence applications, such as cell tracing and *in situ* hybridization have been made possible because the blue fluorescence emission of coumarin dyes is easily distinguished from the red rhodamine and the green fluorescein derivatives.[167] One of the most widely used coumarins, 7-amino-4-methylcoumarin-3-acetic acid (AMCA), has the excitation and emission wavelengths of 350 nm and 435 nm respectively. There are a number of disadvantages with using coumarin dyes in biological systems. The most commonly used coumarin dyes, including AMCA, are characterised by the quenching of fluorescence upon conjugation to proteins. Some coumarin derivatives are unsuitable for preparing bioconjugates in aqueous media because of their poor water solubility, and they are not photostable enough to be used for long periods.[168]

In this thesis, an account is provided of the attempt to synthesize 7-amino-4-methyl-6-sulfocoumarin-3-acetic acid (AMCA-S, compound **48**), the sulfonated derivative of AMCA (compound **47**). This sulfonated derivative is more water soluble than AMCA, making it more applicable to the labelling of proteins in aqueous or buffer solutions without the need for any organic solvent.[169] In addition, the conjugation derivatives of AMCA-S have considerably improved fluorescence quantum yields when compared to their AMCA counterparts. AMCA-S is a member of a relatively newly identified series of fluorescent compounds called Alexa dyes. In fact, AMCA-S is known as Alexa 350, where 350 nm represents the compound's approximated excitation wavelength maxima.[167, 169]

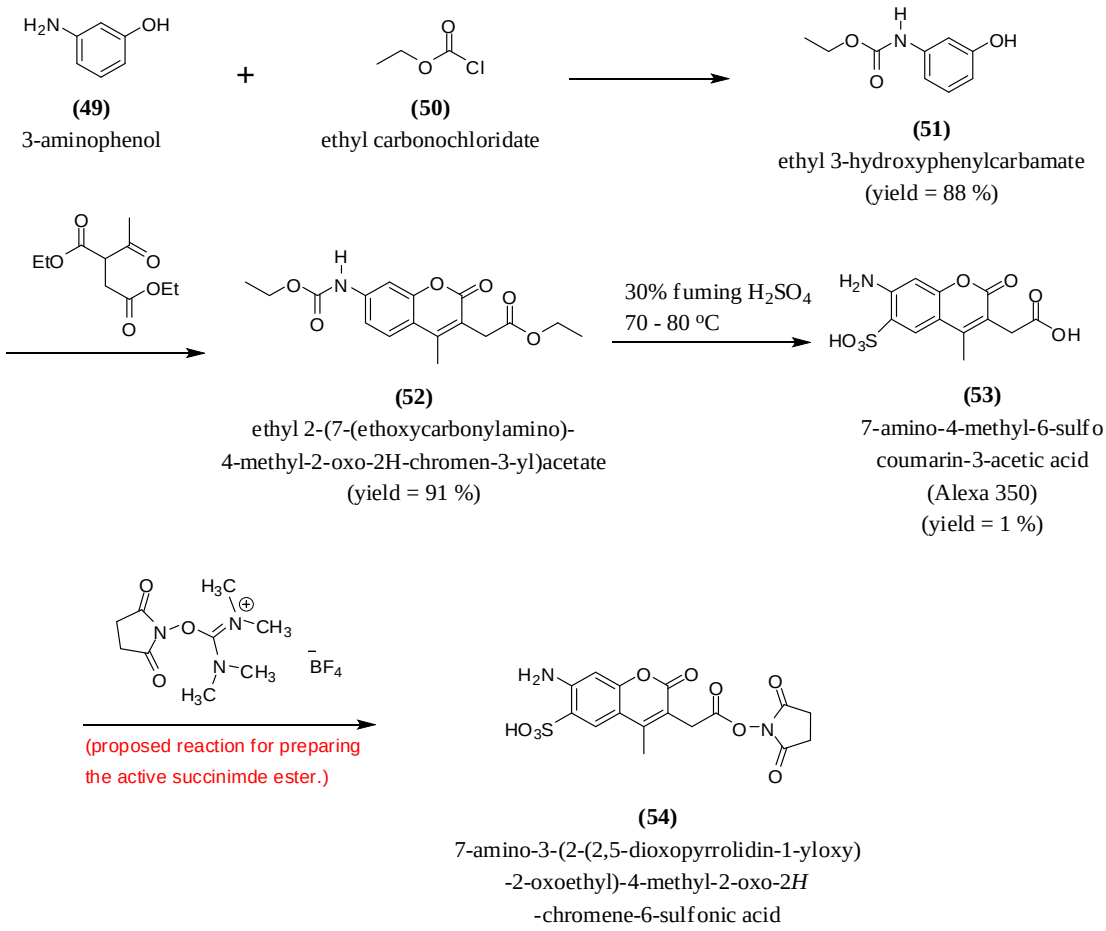

Scheme 2.3 *The proposed reaction pathway for the synthesis of 7-amino-4-methyl-6-sulfocoumarin-3-acetic acid* (**53**). *The final reaction shows how 7-amino-3-(2-(2,5-dioxopyrrolidin-1-yloxy)-2-oxoethyl)-4-methyl-2-oxo-2H-chromene-6-sulfonic-acid* (**54**) *would have been synthesized had Alexa 350 been isolated.*

The synthesis of Alexa 350 (**53**) and its succinimidyl ester (**54**) is outlined in Scheme 2.3. In the first reaction, 3-aminophenol (**49**) was reacted with ethyl carbonochloridate (**50**) to give the protected ethyl carbamate (**51**). The crude yield for this reaction was 88 %. In the second reaction, this protected compound was then condensed with commercially acquired diethyl 2-acetyl succinate in a Pechmann reaction to give 7-carboethoxyamido-4-methylcoumarin-3-ethylacetate (**52**) at a yield of 91 %. The sulfonation of 7-carboethoxyamido-4-methylcoumarin-3-ethylacetate using fuming sulfuric acid was attempted. However, this attempt to simultaneously sulfonate the ethyl 2-(7-(ethoxycarbonylamino)-4-methyl-2-oxo-2*H*-chromen-3-yl acetate and remove the terminal protecting groups yielded trace amounts of the Alexa 350 (**53**) which were observed by ESI mass spectroscopy, but could not be isolated or be purified from the reaction mixture. The yield for this sulfonation reaction was 1 %. This was a very low yield which meant that the manner in which the synthesis was being carried out was not viable for preparation of Alexa 350. A main cause of this could be that the reaction required a pressure and temperature controlled environment which could not be achieved with the available apparatus.

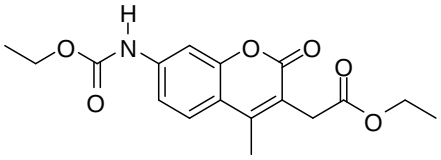

(52)
MW: 333.34

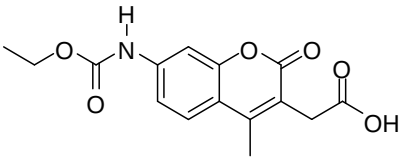

(55)
MW: 305.28

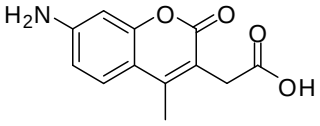

(47)
MW: 233.2

Figure 2.14 *The chemical structures and the corresponding molecular weights of the compounds observed after the acid hydrolysis of ethyl-2-(7-(ethoxycarbonylamino)-4-methyl-2-oxo-2H-chromen-3-yl)acetate.*

Most of the compound obtained from this reaction consisted of the hydrolysis products shown in Figure **2.14**. It was thought that if these compounds could still be sulfonated and under the right conditions, Alexa 350 could still be synthesized. However, efforts to sulfonate the mixture of the compounds of Figure **2.14** were futile as it proved difficult to work up the reactions and isolate the product. Had it been possible to isolate enough Alexa 350 it was anticipated that the succinimidyl ester would have been prepared by reacting the Alexa 350 (compound **53**) with *N*,*N*,*N'*,*N'*-tetramethylsuccinimidouronium tetrafluoroborate in pyridine, which acts both as a base and a solvent. It was therefore decided to purchase the Alexa Fluor ® 350 carboxylic acid, succinimidyl ester (compound **54**) from a commercial source. This succinimidyl ester is more reactive to free amines and could be useful when coupling the Alexa 350 to synthetic peptides.

However, the cost of the Alexa Fluor ® 350 carboxylic acid succinimidyl ester was very prohibitive and only 5 mg was purchased. This was coupled to HPLC purified ETEK(Oct)I to give the fluorescently labelled substrate **44** (Figure 2.10). Section 2.4.7 describes the results of fluorescence polarization experiments in which this compound was used. However it was not possible to use this compound in LipA turn-over experiments which required the use of substantially larger amounts of the substrate than had been prepared. It was then decided to use the derivatization of the thiol residues of the lipoyl product of the turn-over experiments as a means of studying the LipA mediated reaction. The advantage with this method was that the LipA turn-over assays could be carried out under the standard conditions and thereafter the products separated from the protein and derivatized with the fluorescent probe. In this case any conditions under which the derivatization occurred could be used since there was no concern about the enzyme being denatured by the organic solvents used. The following section describes the synthesis of a fluorescent thiol reactive compound and its use in the current study.

2.2.5 Synthesis of Maleimide Derivative and the Derivatization Experiments

Proteins and nucleic acids often contain fewer thiol groups than amino groups, which has resulted in the proliferation of thiol reactive reagents used as probes for biological functions, interactions and structures. A literature search reveals different types of thiol-reactive dyes, including disulfides, iodoacetamides, maleimides, vinyl sulfones and a range of electron-deficient aryl halides and sulfonates. The most frequently used of these compounds are the iodoacetamides and the maleimides. Fluorescent thiol-reactive dyes have been used in the mapping of cellular membrane proteins, determination of the spaces within proteins or between proteins and in monitoring protein conformational changes. Iodoacetamides and other haloalkyl reagents react to form stable thioether conjugates with the thiol moieties of small biomolecules and biopolymers. Although iodoacetamides have a strong affinity for thiol groups, at high pH values and when free thiols are not readily available, they may react with methionine residues, histidine or even tyrosine. The bioconjugation reactions of thiol-reactive probes can be quenched by the addition of cysteine, glutathione or mercaptosuccinic acid to the reaction mixture. This would result in the formation of water-soluble adducts that are easily removed by dialysis or gel filtration.

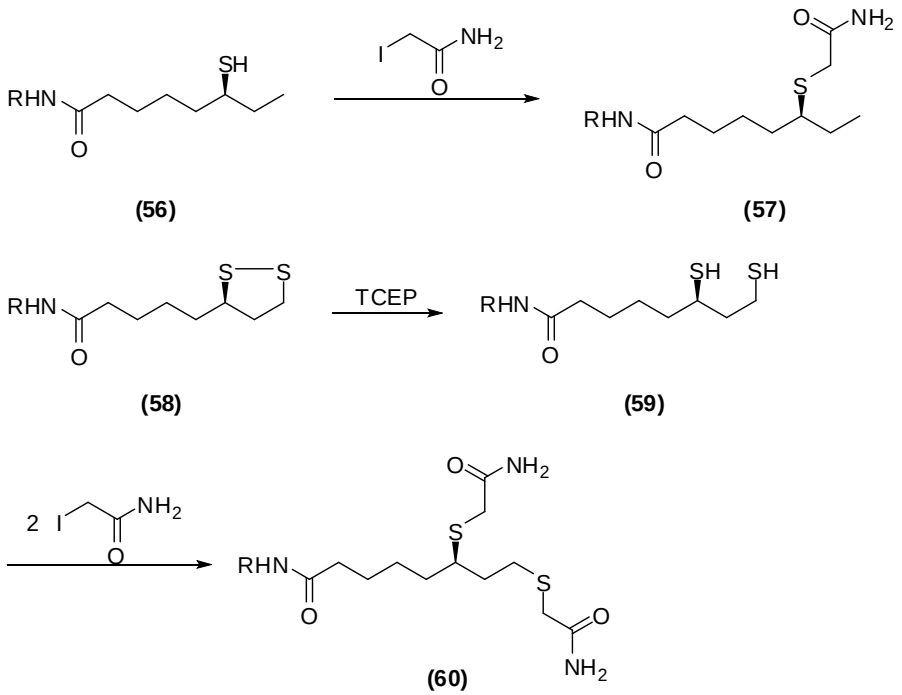

Scheme 2.4 *The use of iodoacetamide derivatization to probe LipA reaction.*

The proposed mechanism for the conversion of octanoyl substrate to lipoyl product involves the formation of an intermediate 6-monothiolated (6-MT) species. This species is ultimately converted to the lipoyl product. Penny Bryant[136] used derivatization with iodoacetamide as a means to detect thiolated species. This approach allowed for the improved separation between the dihydrolipoyl and the 6-MT compounds during HPLC and LC-MS analysis. The use of iodoacetamide as the derivatising reagent to probe the LipA reaction is illustrated in Scheme 2.4. The present work describes the synthesis of 7-(diethylamino)-*N*-(2-(2,5-dioxo-2,5-dihydro-1*H*-pyrrol-1-yl)ethyl)-2-oxo-2*H*-chromene-3-carboxamide (Figure 2.15), a fluorescent thiol-reactive maleimide and the attempt to use this probe to derivatize thiol species.

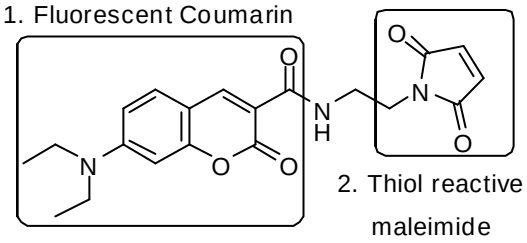

compound (**61**)

Figure 2.15 *The chemical structure of 7-(diethylamino)-N-(2-(2,5-dioxo-2,5-dihydro-1H-pyrrol-1-yl)ethyl)-2-oxo-2H-chromene-3-carboxamide a fluorescent thiol sensitive maleimide.*

Compound **61** contains a coumarin moiety which would allow for the use of fluorescence detection. This very sensitive technique would enable the detection of trace amounts of derivatized products. The compound also contains a thiol reactive maleimide moiety which was selected because maleimides, just like iodoacetamides, will react with thiols groups to give thioether-coupled products. However, maleimides are more thiol selective and the optimum pH for reaction of maleimides is approximately 7.0. Maleimides require conjugation conditions less stringent than those of iodoacetamides and also maleimides do not react with histidine and methionine under physiological conditions.

The fluorescent coumarin 7-(diethylamino)-2-oxo-2*H*-chromene-3-carboxylic acid (**38**) was synthesized by reacting 4-(diethylamino)-salicyclaldehyde and 2,2-dimethyl-1,3-dioxane-4,6-dione with ethanol as solvent (Experimental 3.5). The purified compound **38** was then reacted with commercially acquired *N*-2-aminoethyl maleimide (**62**) in the presence of HOBt/DIC and DIPEA to produce compound **61**, the fluorescent thiol reactive maleimide. The crude product was purified by flash chromatography (silica stationary phase and a mobile solvent system of CH_2Cl_2/MeOH). Purified 7-(diethylamino)-*N*-(2-(2,5-dioxo-2,5-dihydro-1*H*-pyrrol-1-yl)ethyl)-2-oxo-2*H*-chromene-3-carboxamide was obtained in a yield of 36 %.

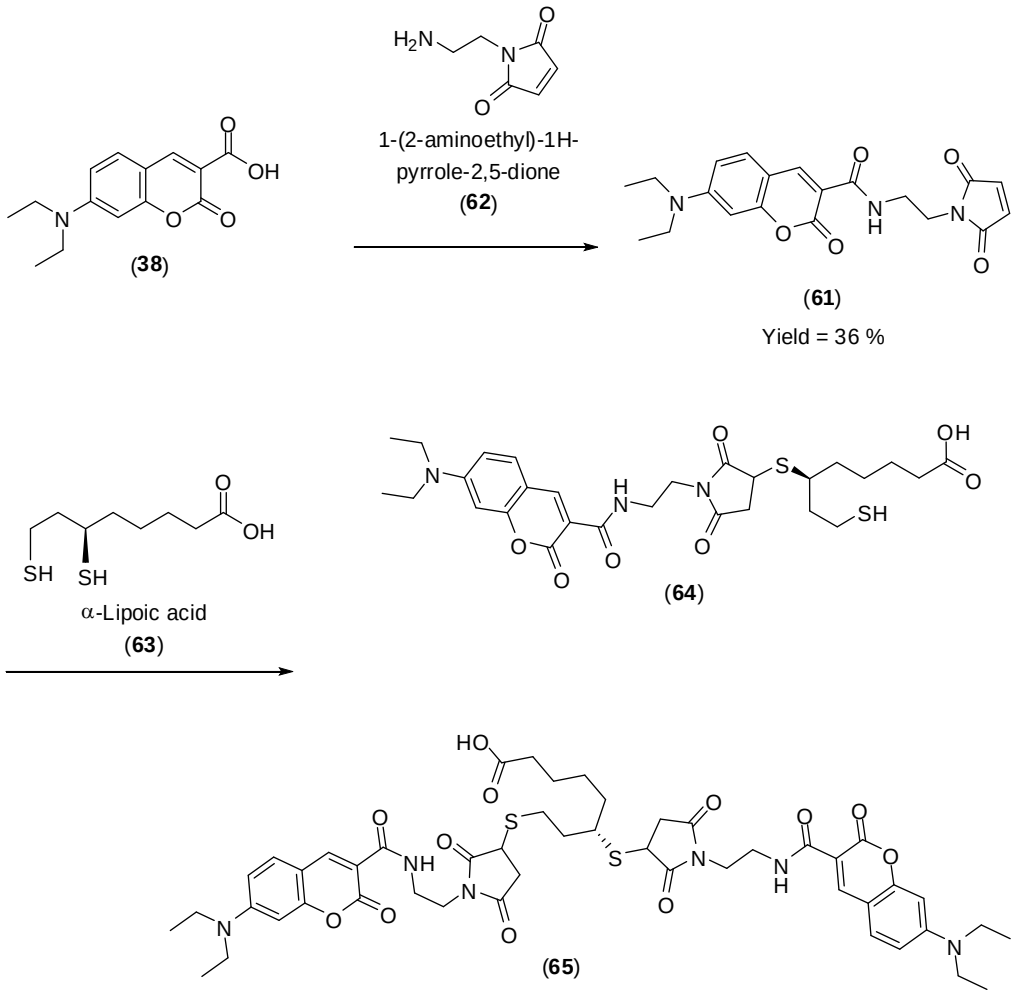

Scheme 2.5 *The synthesis of 7-(diethylamino)-N-(2-(2,5-dioxo-2,5-dihydro-1H-pyrrol-1-yl)ethyl)-2-oxo-2H-chromene-3-carboxamide (**33**). The second reaction shows how the thiol probe would be used in derivatising ~-lipoic acid.*

The first reaction in Scheme 2.5 shows the synthesis of compound **61**. Maleimides react with thiol groups to give thioether-coupled products. The second reaction in Scheme 2.5 shows how the thiol reactive maleimide (compound **61**) would be expected to react with α-lipoic acid. Commercially acquired α-lipoic acid was reduced by incubation with the reductant tris-(2-carboxyethyl)-phosphine (TCEP) to produce the dihydrolipoic acid (compound **63**). Thereafter the dihydrolipoic acid **63** was reacted with the thiol reactive maleimide (compound **61**).

The positive experiment comprised of a mixture of all the reagents *i.e.* α-lipoic acid, TCEP, 7-(diethylamino)-*N*-(2-(2,5-dioxo-2,5-dihydro-1*H*-pyrrol-1-yl)ethyl)-2-oxo-2*H*-chromene-3-carboxamide mixed in HEPES buffer (25 mM, pH 7.5). The three negative control experiments were prepared by removing single components (reagents) from the positive experiment in succession. The reaction mixtures were analyzed by high performance liquid chromatography and the components masses were identified by LC-MS analysis (Figure 2.16).

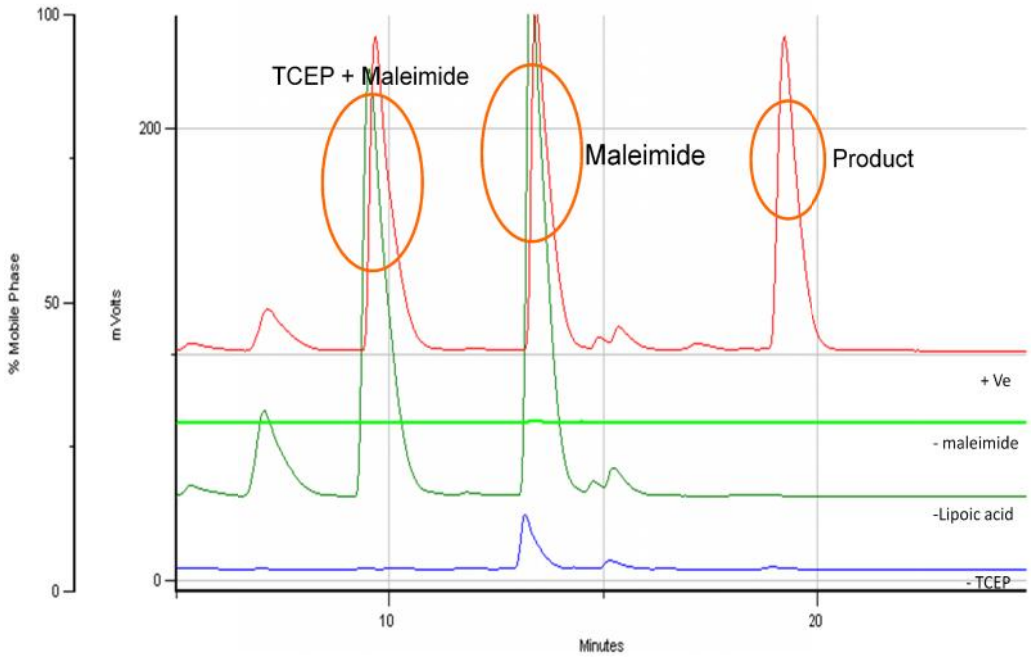

Figure 2.16 *Trace of the fluorescence signal recorded during HPLC analysis of the assays in HEPES buffer. +Ve = positive assay, -maleimide = assay without the maleimide (**61**), -Lipoic acid = assay without lipoic acid and -TCEP = assay without TCEP. The volume in the negative controls was made up with the buffer.*

The chromatographs in Figure 2.16 show the fluorescence traces recorded for the analysis of 60 μL samples of the positive derivatization experiment and the three negative controls. The results show that when no maleimide was added to the reaction mixture no fluorescence was recorded. A low fluorescence peak, at a retention time t = 13 min, was recorded when no TCEP was added to the reaction mixture. This would indicate the presence a single fluorescent compound identified as 7-(diethylamino)-*N*-(2-(2,5-dioxo-2,5-dihydro-1*H*-pyrrol-1-yl)-ethyl)-2-oxo-2*H*-chromene-3-carboxamide. When α-lipoic acid was excluded from the reaction mixture there was a marked increase in the peak fluorescence identified as due to compound **61**. There are two additional peaks observed. The peak at t = 6 min was associated with a mass of 401.8 a.m.u. This mass is 18 units more than the mass of compound **61**. This difference is equivalent to the addition of an equivalent of water. The peak at t = 9 min is associated with a mass of 385.8, which is equivalent to the reduction of compound **61** with two H-atoms.

Table 2.2 *The retention times (min), masses observed by LC-MS and the products assigned to the observed peaks for the derivatization of lipoic acid.*

Retention time (min)	**Observed mass (a.m.u)**	**Identified mass ion**
6.0	401.8	Maleimide (**61**) + H_2O
9.2	385.8	(Maleimide + 2H) (**66**)
13.0	383.5	Maleimide (**61**)
18.0	975.5	Derivatization Product (**65**)

Table 2.2 shows the masses observed by LC-MS analysis and the possible assignments for each peak. For the positive experiment all of the fluorescence peaks from the negative controls were observed and in addition a unique peak was observed at retention time t = 18 min. This peak is associated with a mass of 975.5 which is attributed to the products of derivatising lipoic acid with compound **61**.

The synthesized thiol reactive coumarin compound **61** was not water soluble and so could not be added directly into the LipA assays which were carried out in aqueous buffer. After the LipA turnover assays, the protein was separated by centrifugation and the supernatant was then analysed for the presence of thiol moieties by adding TCEP and the compound **61**. It was observed that thiol derivatization product (compound **65**) was being produced on turnover of the octanoyl tripeptide substrate.

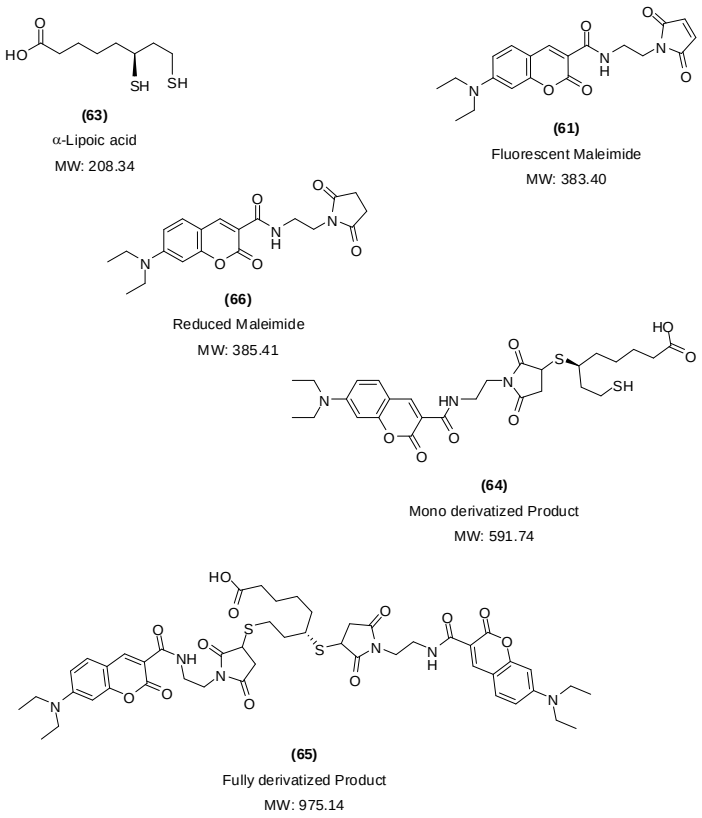

Figure 2.17 *The structures and molecular weights (MW) of the reactants and the expected products of derivatising lipoic acid with 7-(diethylamino)-s-(2-(2,5-dioxo-2,5-dihydro-1H-pyrrol-1-yl)ethyl)-2-oxo-2H-chromene-3-carboxamide.*

However the TCEP (used as the reductant for the maleimide derivatization) reacts with the maleimide (**61)**, to give a reduced maleimide product (**66)**. Since some of the maleimide probe was being reduced it was not possible to use the maleimide probe to quantify the amount of thiol in the assay mixture. After numerous attempts, trying to stop the reaction between the maleimide probe and the TCEP, without much success it was decided not to proceed with these experiments

2.3 Activity Assays

2.3.1 Product Inhibition of LipA

The enzymes of the "radical SAM" superfamily catalyse a wide range of bio-transformations that involve the reduction of AdoMet and the oxidation of the substrate molecules. Methionine and 5′-deoxyadenosine are given off as the by-products. The series of reactions that occur during the reductive cleavage of SAM are shown in the reaction Scheme 2.6.

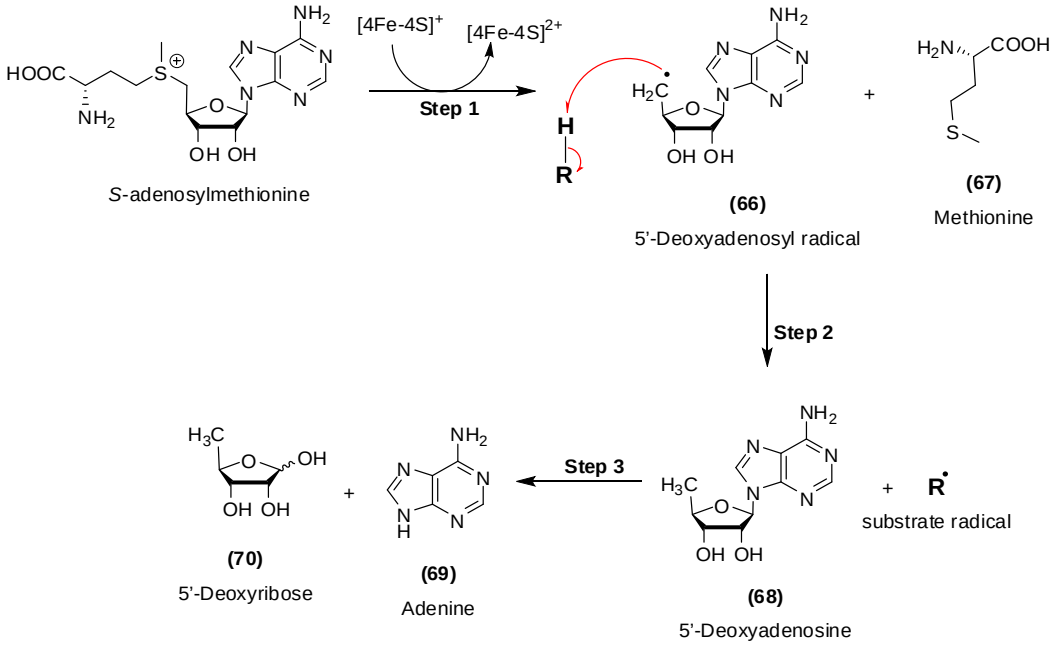

Scheme 2.6 *The reaction pathway showing the formation of products when the "radical SAM" enzymes cleave AdoMet. In step 1 the reductive cleavage of AdoMet results in the formation of the highly unstable 5′-Ado• radical and methionine. Step 2 shows the formation of 5′-deoxyadenosine and the substrate radical (R•) from a substrate (R-H). The final reaction, Step 3 shows the MTA/AdoHcy nucleosidase mediated cleavage of 5′-AdoH to give adenine and the thioribose.*

In the first step methionine is evolved along with the highly unstable 5′-deoxyadenosyl radical that abstracts a hydrogen atom from the appropriate substrate molecule in step 2. This results in the formation of 5′-deoxyadenosine and the

substrate radical species (R•). Subsequently, the substrate radical is then involved in carrying out the enzyme's characteristic reaction. Methionine (**67**) and 5′-deoxyadenosine (**68**) are modest inhibitors of biotin synthase and other members of the radical SAM superfamily of enzymes.[170] This inhibition of enzymatic activity, in which a product of an enzymatic reaction binds to the enzyme so as to inhibit its activity, is called product inhibition.[171]

Both BioB and LipA which catalyze the insertion of sulfur atoms during the biosynthesis of biotin and lipoic acid respectively, require AdoMet for activity. Cicchillo *et al*. (2004) showed that *in vitro* LipA required two equivalents of SAM for the synthesis of one equivalent of lipoic acid.[157] *In vitro* activity assays carried out by Ugulava *et al*. (2001) indicated that biotin was produced in stoichiometric ratio to the BioB monomer.[77] It was thought that this non-catalytic behaviour of the enzymes was due the depletion of the sulfur donors.[172] The investigations carried out by two groups into the possible *in vitro* product inhibition of BioB caused by methionine and AdoH resulted in conflicting conclusions. Ollagnier-de Choudens *et al*. (2002) observed the near complete inhibition of BioB at a molar ratio of 1.5 AdoH : 1.0 BioB monomer. They argued that the absence of multiple turnover was due to strong inhibition by AdoH.[49] Contrary to this argument, Tse Sum Bui *et al*. (2004) observed that AdoH does not inhibit the BioB-catalysed reaction, but rather that the absence of multiple turnover could be due to the depletion of the $[2Fe\text{-}2S]^{2+}$ clusters.[173]

In vivo studies showed the catalytic activity of BioB required the expression of 5′-methylthioadenosine/*S*-adenosylhomocysteine (MTA/AdoHcy) nucleosidase, the product of the *pfs* gene.[8, 170, 172] Approximately 20 - 60 molecules of biotin were synthesised per monomer of BioB.[174] MTA/AdoHcy nucleosidase catalyses the cleavage of the glycosidic bonds in 5′-methylthioadenosine (MTA) and *S*-adenosylhomocysteine (AdoHcy) to produce adenine and thioribose (homocysteine).[175, 176] Step 3 in the reaction Scheme 2.6 shows the reaction catalysed by MTA/AdoHcy nucleosidase during the breakdown of SAM. Choi-Rhee and Cronan reported that MTA/AdoHcy nucleosidase was required for the *in vivo*

function of BioB and they observed that *E.coli* strains lacking this nucleosidase were deficient of BioB activity because of the accumulation of AdoH.[174] Biotin synthase activity was restored by adding the *pfs* protein to the reaction mixture.

In the current study experiments were carried out to investigate the inhibitory effect of methionine and 5′-deoxyadenosine (AdoH) on lipoyl synthase (LipA) and the effect of adding the product of the *pfs* gene to the reaction mixture. The reaction Scheme 2.7 shows products (**69** and **70**) obtained from the hydrolysis of 5′-deoxyadenosine (**68**). This reaction is catalysed by 5′-methylthioadenosine/S-adenosylhomocysteine nucleosidase; the product of the *pfs* gene.

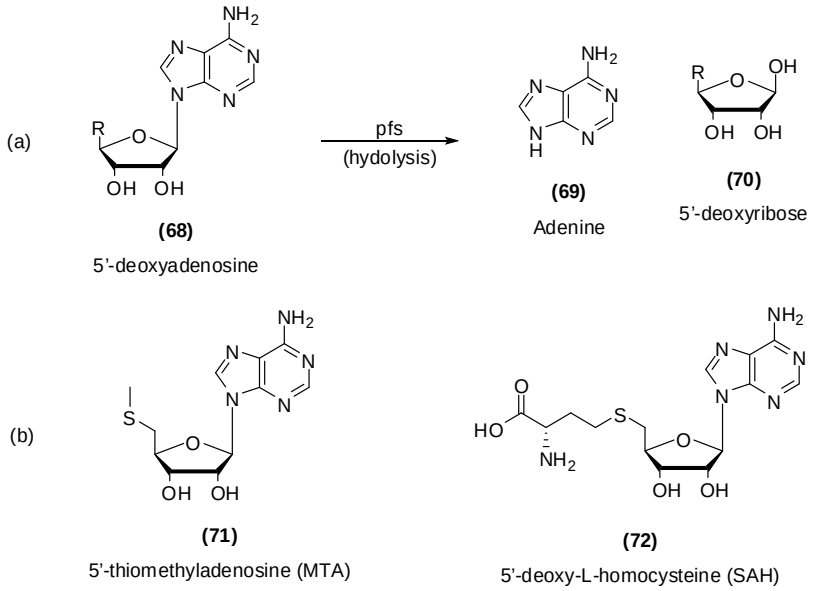

Scheme 2.7 *Reaction (a) shows the reactions catalysed by the product of the pfs gene and reaction (b) shows the structures of two of the enzyme's substrates.*

A lipoyl synthase based assay was prepared by mixing reconstituted LipA (100 μM), SAM-chloride (1 mM), the octanoyl substrate EK(Oct)I (50 μM) and sodium dithionite (1 mM). The reaction mixture was then incubated in a water bath (30 min, 37 ^{o}C). The reaction was quenched by adding neat trifluoroacetic acid (25 μL) and the mixture was centrifuged (13 000 rpm, 10 min). The protein (pellet) was separated from the supernatant which was analysed on an LC-MS to identify and characterise the components of the reaction mixture.

Table 2.3 Results for the Product inhibition experiments, the conditions for each assay are as follows. **Experiment 1** = positive LipA turnover experiment; **Experiment 2** = positive LipA turnover experiment + Methionine + 5′-deoxyadenosine; **Experiment 3** = positive LipA turnover experiment + Methionine + 5′-deoxyadenosine + product of *pFs* gene; **Experiment 4** = positive LipA turnover experiment + product of *pFs* gene; **Experiment 5** = positive LipA turnover experiment - *S*-adenosylmethionine; **Experiment 6** = positive LipA turnover experiment – sodium methionine. The masses at the top of the columns are masses of identified compounds whose structures are shown in Scheme 2.1.

Experiment	**M = 149.2 x 10^6**	**M = 251.2 x 10^6**	**M = 297.3 x 10^6**	**M = 399.4 x 10^5**	**M = 514.3 x 10^5**	**M = 546.7 x 10^6**	**M = 576.3 x 10^6**	**M = 578.3 x 10^7**	**Total peptide x 10^7**	**Fraction of Lipoyl formed**
1	1.48	2.63	190.00	-	-	5.66	0.22	2.64	3.22	0.82
2	-	13.00	200.00	6.79	-	37.00	-	1.59	5.29	0.30
3	0.56	0.58	105.00	5.26	1.08	4.55	1.20	2.38	2.97	0.84
4	0.52	1.03	0.41	6.18	-	3.86	2.51	8.62	3.11	0.95
5	-	0.60	0.71	6.08	1180.00	-	0.19	-	11.80	0.01
6	2.76	0.09	76.40	6.35	1180.00	-	-	-	11.80	0.00

The Total Ion Current (TIC) for the recorded mass spectra was quantified using the computer program Xcalibur, to give an estimate of the relative abundance of each component of the reaction mixture. Table 2.3 shows a quantification of the TIC signals for the products of assays as observed on the LCMS. The fraction of lipoyl product formed during the positive turnover LipA assay was calculated to be 0.82 (Experiment 1, Table 2.3). The synergistic inhibitory effect of methionine and 5′-deoxyadenosine on the reaction catalysed by LipA (Experiment 2, Table 2.3) was tested by preparing the positive LipA turnover assay as above and then adding an excess of methionine (1 mM) and 5′-deoxyadenosine (1 mM). It was observed that adding AdoH and Met greatly reduces the amount of lipoyl product obtained. The fraction of lipoyl product obtained drops from 0.82 in the positive assay to 0.30 in the test for the synergistic inhibitory effect of AdoH and Met. This result indicates that AdoH and Met (both by-products of the LipA catalysed reaction) have an inhibitory effect on the enzyme's activity, which is indicated by the decrease in the fraction of lipoyl product formed.

To test the effect of 5′-methylthioadenosine/S-adenosylhomocysteine (MTA/AdoHcy) nucleosidase; this product of the *pfs* gene (10 μM) was added to the positive LipA turnover assay along with AdoH and Met. This was done to observe if the product of the *pfs* gene would reverse the inhibition of formation of the lipoyl product that was caused by the Met and the AdoH. The fraction of lipoyl product formed in this assay was calculated to be 0.84, which was equivalent to 0.82, the fraction of lipoyl product determined for the positive LipA turn over assay (Table 2.3). This result indicated that the 5′-methylthioadenosine/S-adenosylhomocysteine (MTA/AdoHcy) nucleosidase was reversing the inhibitory effect of Met and the AdoH on the LipA catalyzed reaction.

When 5′-methylthioadenosine/S-adenosylhomocysteine nucleosidase was added to the positive LipA turnover assay without adding AdoH and Met (Table 2.3, experiment 5), the fraction of lipoyl product formed was determined to be 0.95. This was an increase on the 0.82 observed for the positive LipA turnover assay. This

result further confirmed that the added 5′-methylthioadenosine/*S*-adenosylhomocysteine nucleosidase was hydrolysing at least one of the products from the breakdown of AdoMet and this in turn was reversing the inhibitory effects of AdoH and Met. Two negative control assays were prepared (Table 2.3, experiments 5 and 6). These assays contained all the components of the positive LipA turnover assay but sodium dithionite and *S*-adenosylmethionine chloride were removed in turn. The values of 0.00 % fractions of lipoyl formed, indicated that no lipoyl product was formed from the octanoyl substrate, which showed that both SAM and sodium dithionite were necessary for the turnover LipA assay.

Figure 2.18 shows the chemical structures and the molecular masses of the expected compounds of the LipA turnover assay using EK(Oct)I as the substrate. The starting materials are octanoyl substrate EK(Oct)I and *S*-adenosylmethionine, and the reaction's expected final products are the dihydrolipoyl-EKI product and the lipoyl-EKI-product. All the other structures are for the intermediate products of the LipA turnover reaction.

Conclusions from the product inhibition of LipA experiments

The results in Table 2.3 indicated that AdoH and Met have a synergistic inhibitory effect on the LipA mediated formation of the lipoyl product. The addition of AdoH and Met to a LipA turn over assay led to a > 50 % loss in enzymatic activity. This synergistic effect was reversed by the addition of MTA/AdoHcy nucleosidase. It was observed that AdoH and Met inhibited LipA regained all its enzymatic activity (~ 100 %) in the presence of MTA/AdoHcy nucleosidase. These conclusions are in agreement with the observations of Douglas *et al*, who used assays with varying concentrations of inhibitors, incubated for 2 h, at 37 ^{o}C. They had concluded that the product of the *pfs* gene catalyses the *in vivo* hydrolysis of AdoH. They had also observed that the addition of the product of the *pfs* gene into assays without any inhibitor resulted in a 1.4 fold increment in the lipoyl and dihydrolipoyl products formed and also determined the IC_{50} = 327 ± 22 μM.

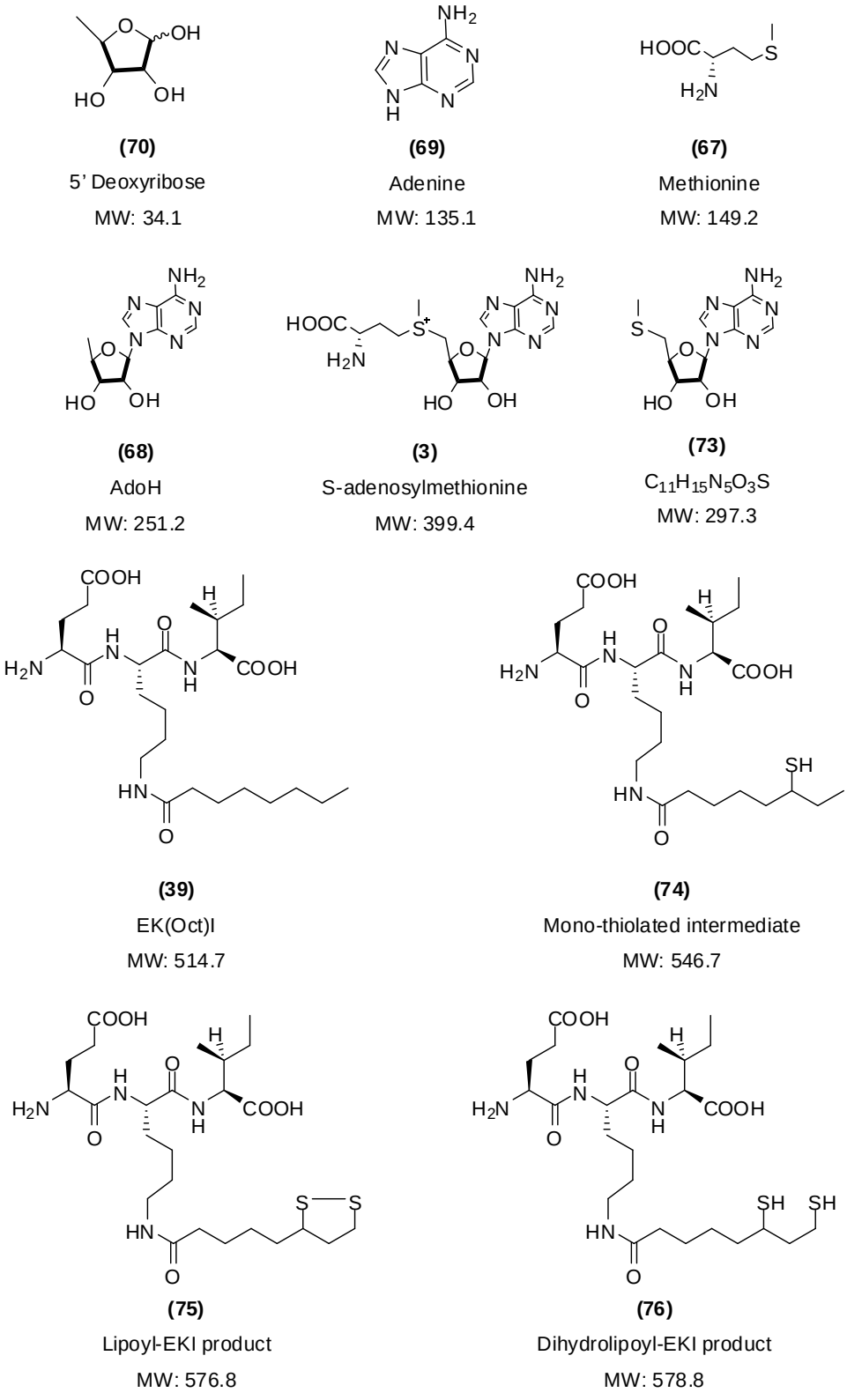

Figure 2.18 *The structures and molecular weights (MW) of compounds that would be observed when using EK(Oct)I as the LipA substrate for the product inhibition assays.*

2.3.2 Characterisation of the products of the nonanoyl substrate turn-over

Although enzymes exhibit a high specificity for their natural substrate, they do show some flexibility in binding other molecules. The substrate binding sites of enzymes can accommodate slightly modified versions of the natural substrate and known substrate analogues. This feature of enzymes has been exploited in studies to investigate the mechanisms of enzyme catalysed reactions. Modified substrates can be used to block a desired pathway resulting in inhibition of the enzyme and/or the detection of alternative reaction pathways.[141]

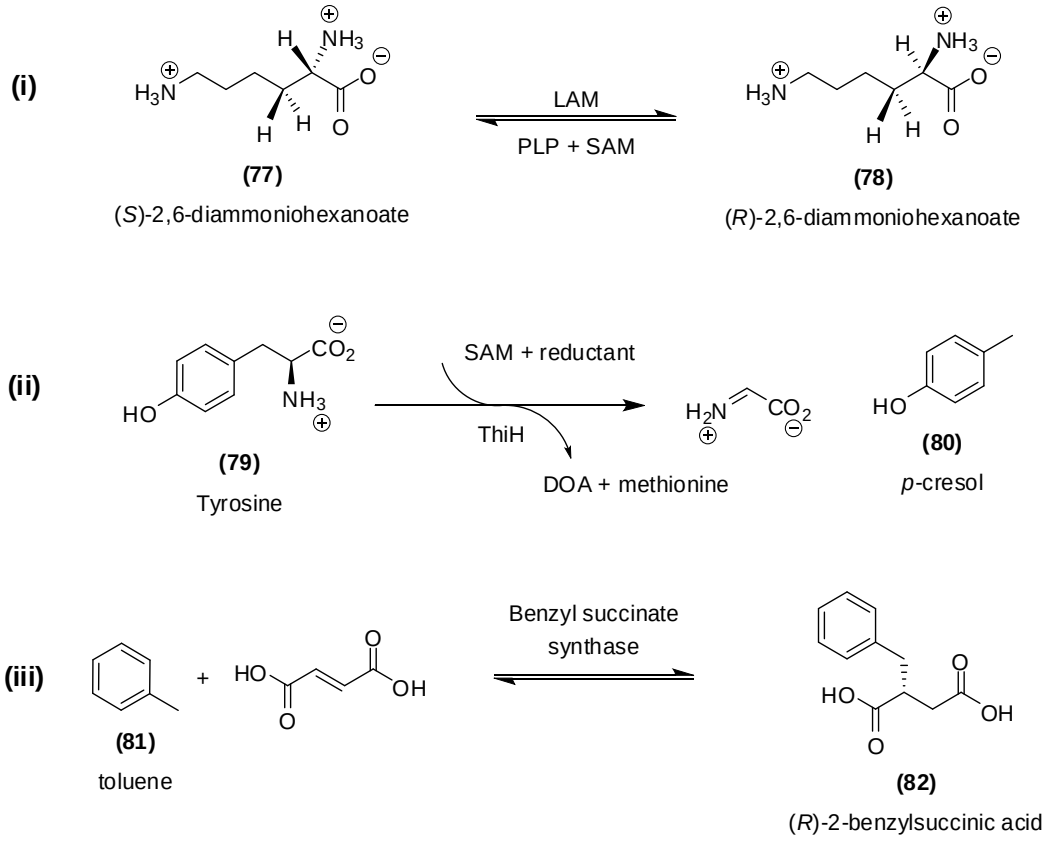

Scheme 2.8 *Examples of biological transformations that have been studied through the use of synthetic analogues of the natural substrates. (**i**) The formation of an allylic radical by lysine 2,3-aminomutase (LAM) using a SAM analogue, (**ii**) the formation of p-cresol from tyrosine and (**iii**) the benzyl succinate synthase mediated reaction.*

The mechanisms of many biological reactions have been investigated using substrate analogues. Scheme 2.8 shows three examples of enzyme catalysed conversions for which the mechanisms were determined using analogues of the natural substrates. In 1982 Parry[9] wrote an informative review entitled "Biosynthesis of some sulfur-containing natural products: Investigations of the mechanism of carbon-sulfur bond formation." In the stated review, the author gives many examples of reaction mechanisms that were determined using substrate analogues. The examples include the biosynthesis of biotin, asparagusic acid, penicillin and lipoic acid. The reaction mechanism of the LipA-catalysed formation of lipoyl product has been investigated in many experiments using various substrate analogues of the natural substrate (octanoic acid). Table 2.4 shows a summary of the results for some of the *in vivo* labelling experiments using the analogues [8-$^2H_2$]-8-hydroxyoctanoic acid, [6(*RS*)-$^2H_1$]-6-hydroxyoctanoic acid, [8-$^2H_2$]-8-thiooctanoic acid, [6(*RS*)-^{2}H]-6-thiooctanoic acid and [8-$^2H_2$]-(±)-6,8-dihydroxyoctanoic acid as the substrates for LipA.

Table 2.4 *Summarized results of in vivo labelling experiments in which [8-$^2H_2$]-8-hydroxyoctanoic acid, [6(RS)-$^2H_1$]-6-hydroxyoctanoic acid, [8-$^2H_2$]-8-thiooctanoic acid and [6(RS)-^{2}H]-6-thiooctanoic acid and [8-$^2H_2$]-(±)-6,8-dihydroxyoctanoic acid were used as substrates for LipA.*

Experiment	Precursor	% Lipoic acid derived from the precursor
1	[8-$^2H_2$]-8-hydroxyoctanoic acid	< 0.5
2	[6(*RS*)-$^2H_1$]-6-hydroxyoctanoic acid	< 0.2
3	[8-$^2H_2$]-8-thiooctanoic acid	19.0[a] and 27.9[b]
4	[6(*RS*)-^{2}H]-6-thiooctanoic acid	2.1
5	[8-$^2H_2$]-(±)-6,8-dihydroxyoctanoic acid	< 0.5

[a]15.8 mg of precursor added to the culture. [b] 30.0 mg of precursor were added to the culture.

The results for [8-$^{2}H_2$]-8-thiooctanoic acid (19.0 and 27.9 % of lipoic acid derived from the precursor) and [6(*RS*)-^{2}H]-6-thiooctanoic acid (2.1 % of lipoic acid derived from the precursor) led to the conclusion that the C8 hydrogen atom was abstracted first and hence the higher percentage of lipoic acid derived from the precursor. This was contradicted by an *in vitro* assay using a peptide analogue of the natural substrate, in which the C6 hydrogen atom was identified as the one that is abstracted first.[33, 141] An explanation for this anomaly is that the branched C6 thiol does not fit into the active site as well as the linear C8 thiol.

Douglas[141], a previous member of the Roach group carried out experiments in which he analysed the conversion of a nonanoyl substrate to the corresponding lipoyl product. He reported that LipA formed a range of products, which were detected in reactions using the octanoyl substrate, and could only be isolated using the nonanoyl substrate. Scheme 2.9 shows how the nonanoyl substrate could be converted to different products. Five products were observed i) the lipoyl product **87**, ii) an alkene product **84**, iii) two thietane products **85** & **86** and iv) a monothiolated product **83**. As shown in Scheme 2.9, all the products result from a common intermediate. During the conversion of an octanoyl substrate to lipoyl product two sulfur atoms are inserted at unactivated C-H sites. These sites are known to be the C6 and the C8 positions of the substrate. It has been shown that the two sulfurs in lipoic acid are provided by the same polypeptide.[31, 139] In the first instance sulfur insertion at the substrate's C6 position leads to the formation of a protein bound intermediate, which has been observed.[141]

The reaction involving the nonanoyl tripeptide substrate is thought to use the same mechanism as that of the octanoyl substrate and the formation of the protein bound intermediate has been shown. Release of the product at this stage of the reaction would lead to the monothiolated product (m/z = 560.75). However, if the protein bound intermediate was involved in further reactions other products are formed as shown in Figure 2.20.

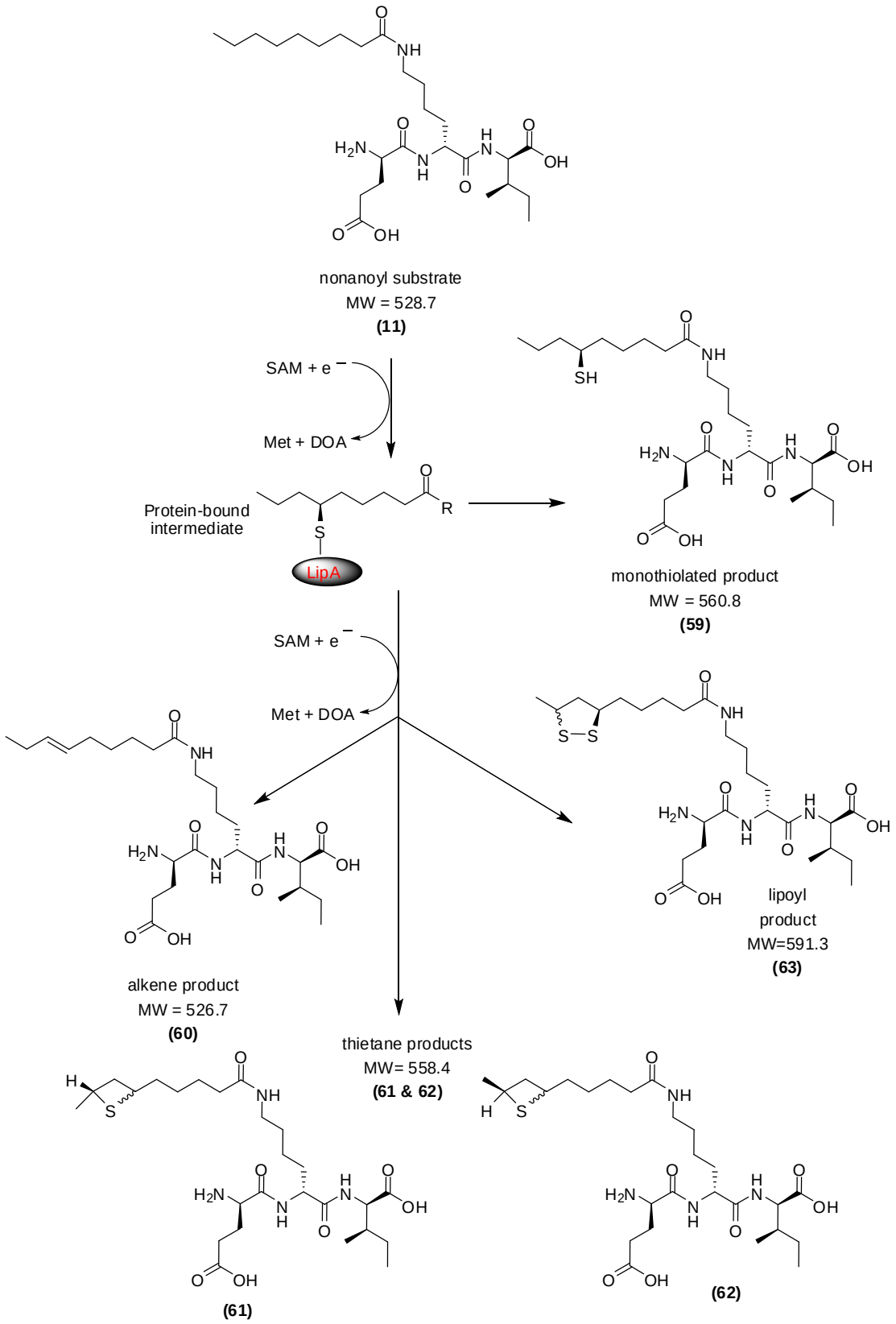

Scheme 2.9 *The formation of products using nonanoyl peptide substrate analogue for LipA. The group "R" in the scheme is used to represent the tripeptide sequence and the lysine residue to which the nonanoyl moiety is attached (R≡ EKI).*

The work detailed in this thesis describes a related set of experiments, carried out to obtain a set of readings for the characterisation of the thietane products. The nonanoyl tripeptide substrate analogue EK(Non)I (**41**) was synthesized by solid phase method and purified on a prepacked C18 reverse phase column. This substrate was then used in turnover assays with reconstituted LipA using the standard method developed within the Roach group. Reactions were incubated (37 ^{o}C, 30 min), the protein precipitated by adding neat TFA (25 μL) and separated by centrifugation (12000 r.p.m, 30 min). Aliquots (80 μL) of the supernatant were analysed on the LC-MS for products and intermediates. The graph in Figure 2.19 shows a trace of the TIC chromatogram obtained from this LC-MS analysis of the supernatant.

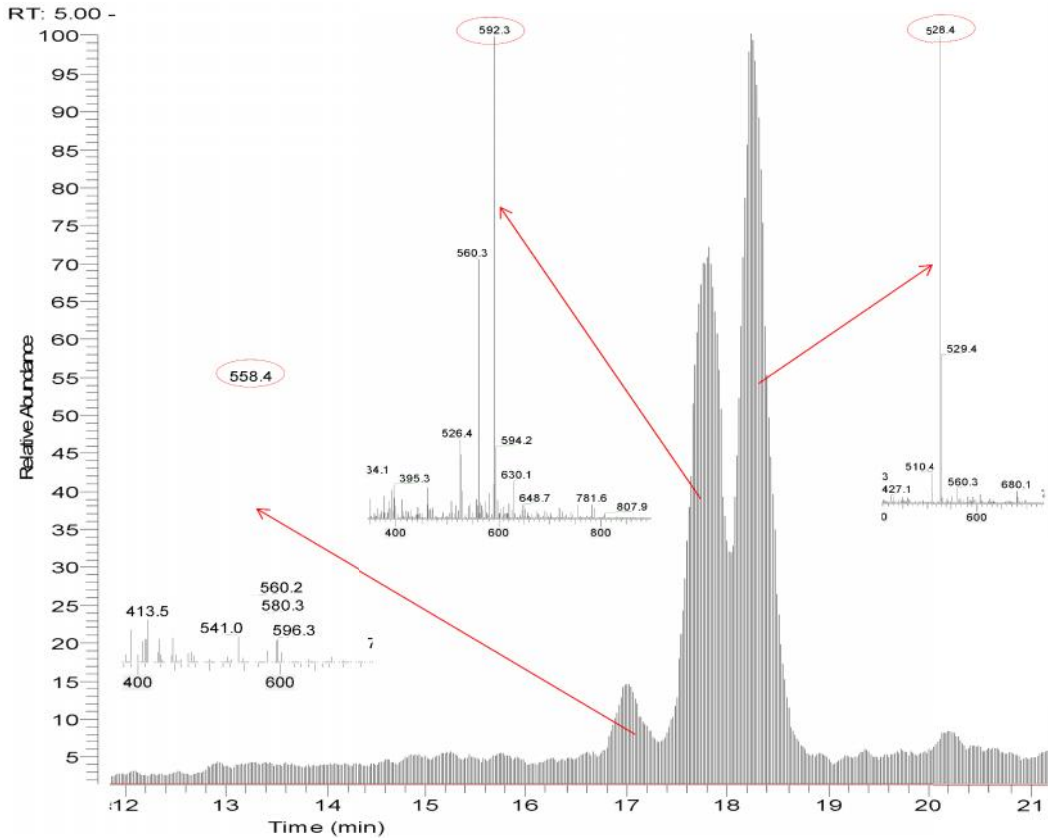

Figure 2.19 *A trace of the total ion current (TIC) chromatogram with SIM = 500 – 600, for the EK(Non)I (***41***) turn-over assay, incubated at 37 °C (30 min). The protein was precipitated by adding TFA and separated by centrifugation. The inserts show the spectrum corresponding to each peak on the chromatograph.*

Five different compounds were identified by LC-MS analysis of the nonanoyl tripeptide assay. A product was identified at *m/z* = 526.4 thought to be an alkene (compound **84**) resulting from the loss of hydrogen atoms from the C6 and C7 positions of the nonanoyl moiety. The compound with *m/z* = 528.4 corresponds to the starting material (compound **41**) which has not been turned over during the reaction. The compound(s) with *m/z* =558.2 correspond to the formation of the thietane(s). There are two possible stereoisomers of the thietane which could not be distinguished from each other by LC- MS analysis.

The compound with *m/z* = 560.3 corresponds to the monothiolated intermediate (compound **83**). It is thought that the first sulfur insertion occurs at the C6 position of the nonanoyl moiety. The doubly thiolated product (the lipoyl product, **87**) was identified at *m/z* = 592.3. It is important to note that all the masses of the compounds identified by use of the LC-MS show a systematic error of 1 a.m.u. The masses observed are 1 a.m.u less than the expected values, *e.g*. for the nonanoyl tripeptide substrate the observed $[M + H]^+ = 528.4$ but the expected value $[M + H]^+ = 529$. This was attributed to the LC-MS which needed recalibrating.

Assays were carried out to enable the collection of 1.5 mL of the supernatant. High resolution mass spectroscopic (HRMS) analysis of the nonanoyl peptide assay supernatant was used to determine the exact masses of the product formed. The $[M + H]^+$ ion of the starting material was identified at *m/z* = 529.3596, and the formula was $C_{26}H_{49}N_4O_7$. The $[M + H]^+$ ion of the alkene product was identified at *m/z* = 527.3439, and the formula was $C_{26}H_{47}N_4O_7$. The $[M + H]^+$ ion of the two thietane products was identified at m/z = 559.3160, and the formula was $C_{24}H_{47}N_4O_7S_1$. The $[M + H]^+$ ion of the monothiolated product was identified at *m/z* = 561.3316, and the formula was obtained as $C_{26}H_{49}N_4O_7S$. The $[M + H]^+$ ion of the lipoyl (dithiolated) product was identified at *m/z* = 591.2881 and the formula of was $C_{26}H_{47}N_4O_7S$.

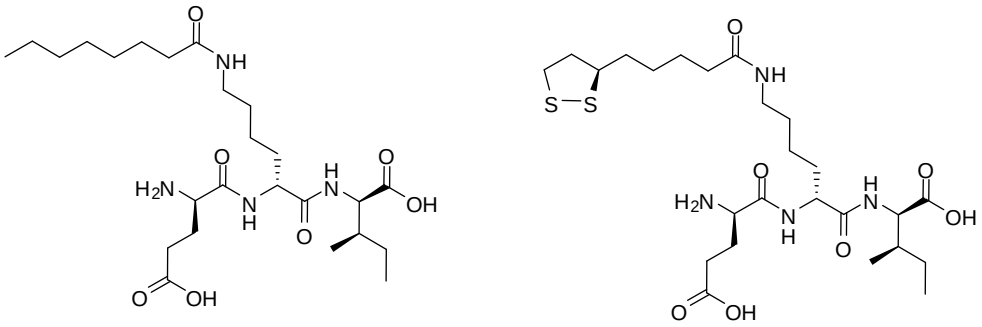

(39)
Octanoyl substrate
MW = 514.7

(58)
Lipoyl Product
MW = 576.8

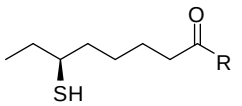

(88)
monothiolated product
MW = 560.8

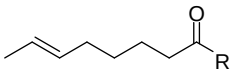

(89)
alkene product
MW = 526.7

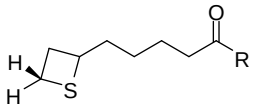

(85 or 86)
thietane products
MW= 558. 4

where R = the peptide sequence EKI

Figure 2.20 *The structures of the octanoyl substrate EK(Oct)I (***39***), the intermediates (***88, 89 & 85 / 86***) and the lipoyl product (***58***) that would be expected from using the octanoyl substrate in an identical assay to the nonanoyl substrate if the reaction mechanism with both substrates is the same. In the above structures R is used to represent the peptide sequence EKI which binds to the octanoyl and the lipoyl moiety using the lysine residue.*

It was also possible to compare the products of the assays using the nonanoyl substrate with the products observed from an identical assay in which the octanoyl tripeptide (Figure 2.20 compound **39**) was used as the substrate. The structures of the lipoyl product and the anticipated intermediate compounds obtained for the octanoyl substrate are shown in Figure 2.20. When the octanoyl compound was used in the assays of Experimental Section 3.12, replacing the nonanoyl substrate **41**, the spectrum obtained from the ESI mass spectrum analysis of the reaction mixture is shown in Figure 2.21.

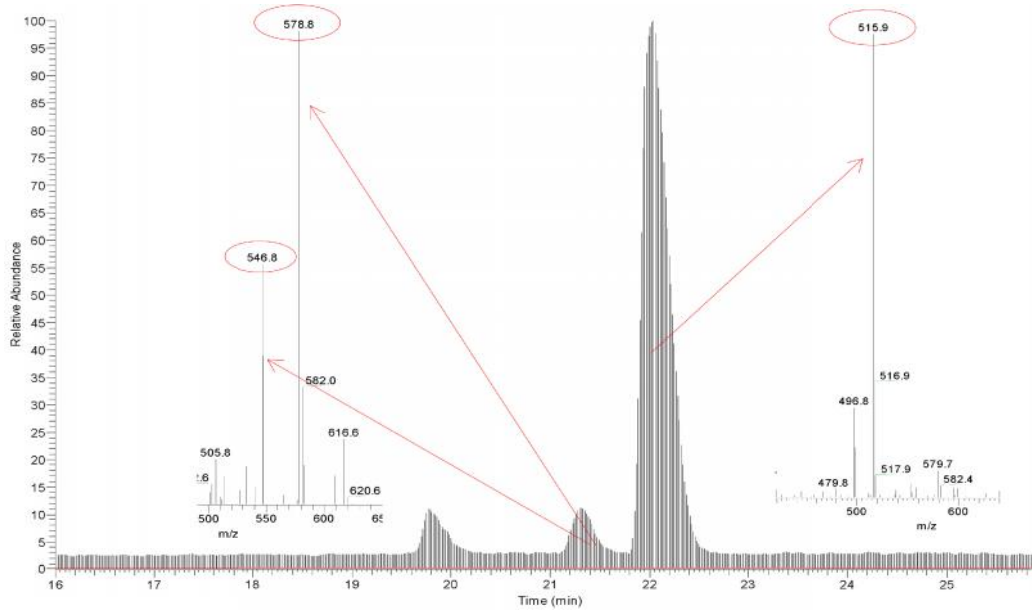

Figure 2.21 *A trace of the total ion current (TIC) chromatogram with SIM = 500 – 600, for the EK(Oct)I turnover assay, incubated at 37 °C (30 min). The protein was precipitated by adding TFA and separated by centrifugation. The inserts show the spectrum corresponding to each peak on the chromatograph.*

The spectrum indicated the presence of a compound of *m/z* = 576.8, corresponding to the expected lipoyl end product **58**. The presence of a mono-thiolated product, thought to be compound **88**, was indicated by the peak of *m/z* = 546.7. However no compounds were observed that corresponded to *m/z* = 512.7 and *m/z* = 544.7; values that would be indicative of the alkene **89** and the thietane **85** and / or **86** respectively. In Figure 2.21 the compound with *m/z* = 514.3 corresponds to EK(Oct)I the starting octanoyl compound.

Conclusions from the characterisation of the products of the nonanoyl and octanoyl substrate turn-over experiments

The LipA mediated formation of lipoyl product starting with a nonanoyl substrate uses a mechanism that involves the formation of the alkene **60** and the thietane (**61** and / or **62)** intermediates. However the formation of lipoyl product starting with an octanoyl substrate utilizes a different mechanism which does not necessarily involve the formation of the alkene **89** and the thietane (**85** and / or **86)** intermediates.

2.4 Ligand-Protein binding relationships

Any species that selectively, stoichiometrically and reversibly binds to a larger molecule such as a protein can be referred to as a ligand. The equilibrium 2.1 and the simple rate equations 2.1 – 2.5 can be used to describe the interactions between a ligand (L) and a protein (P).[177]

$$\text{Ligand [L]} + \text{Protein [P]} \rightleftharpoons \text{Ligand: Protein [LP]} \qquad \textit{(equilibrium 2.1)}$$

$$\textit{foward reaction} \quad L + P \rightarrow LP$$

$$\textit{rate}\,(r_1) = k_1[L][P] \qquad \textit{(equation 2.1)}$$

$$\textit{reverse reaction} \quad LP \rightarrow L + P$$

$$\textit{rate}\,(r_{-1}) = k_{-1}[LP] \qquad \textit{(equation 2.2)}$$

$$\textit{foward reaction rate}\,(r_1) = \textit{reverse reaction rate}\,(r_{-1})$$

$$k_1[L][P] = k_{-1}[LP] \qquad \textit{(equation 2.3)}$$

$$K_d = \frac{k_1}{k_{-1}} = \frac{[L][P]}{[LP]} \qquad \textit{(equation 2.4)}$$

$$K_a = \frac{k_{-1}}{k_1} = \frac{[LP]}{[L][P]} \qquad \textit{(equation 2.5)}$$

The equilibrium 2.1 represents the direct binding of the ligand (L) to the protein (P) resulting in a Ligand: Protein (LP) product. The rate of the forward reaction (r_1) is shown by equation 2.1 in which k_1 is the rate constant; [L] and [P] are the

concentrations of the ligand and protein respectively. Equation 2.2 shows the rate for the reverse reaction (r_{-1}) for which k_{-1} is the rate constant. At equilibrium, the rate of the forward reaction is equal to the rate of the reverse reaction as indicated in equation 2.3. Equations 2.4 and 2.5 show how the equilibrium association constant (K_a) and the dissociation constant are derived by rearranging equation 2.3. Both these constants provide an indication of how strongly or weakly the protein and the ligand interact.[177] The equations 2.6 and 2.7 show how the dissociation constant relates to the Gibbs-free energy (ΔG^o), the standard enthalpy (ΔH^o) and entropy (ΔS^o). In these equations, T is the absolute temperature, and R is the universal gas constant.[177, 178]

$$\Delta G^0 = \Delta H^0 - T\Delta S^0 \qquad \textit{(equation 2.6)}$$

$$\Delta G^0 = -RT\ln K_d \qquad \textit{(equation 2.7)}$$

The equations 2.4 and 2.5 indicate that the experimental measurement of K_d or K_a values requires the determination of [LP], [L] and [P]. Two commonly used approaches for determining K_d values are the use of equilibrium dialysis and the monitoring of changes in spectroscopic properties of the ligand or protein. Many techniques that use these approaches require labelling and rigorous synthesis. Label free determination of binding strength can be achieved by isothermal titration calorimetry (ITC). In this approach the heat change that occurs during the interaction between the ligand and the protein is measured.

The experimental section 3.13 and 3.14 of this thesis describe three different types of experiments that were carried out in an effort to determine the dissociation constants for the interaction of *E.coli* lipoyl synthase with AdoMet and an octanoyl substrate to the enzyme. In the first set of experiments changes to the UV-visible spectrum associated with LipA were observed when AdoMet and the octanoylated substrate EK(Oct)I were added. In the second set of experiments an attempt was made to use

rapid equilibrium dialysis (RED) in determining the dissociation constants. In the third approach, fluorescently labelled substrates were prepared and used in fluorescence polarization assays in an effort to measure the dissociation constants.

2.4.1 Determination of the binding constant K_d using UV-visible spectroscopy

In BioB, the easiest method to promote coupled radical formation *in vivo* is to couple the binding of AdoMet and dethiobiotin. Ugulava *et al.* (2003) investigated the binding of SAM and DTB to both the active and inactive cluster forms of biotin synthase.[179] They observed that DTB only binds in the presence of SAM and the stoichiometry of binding being ca. 2: 1: 1 (SAM: DTB: BS dimer). Their work also showed that SAM on its own weakly binds to biotin synthase, but the introduction of DTB greatly enhances the stoichiometry and affinity of binding. It was noticed that $[4Fe\text{-}4S]^{2+}$ and $[2Fe\text{-}2S]^{2+}$ clusters were necessary for the high-affinity binding of either DTB or SAM. A very interesting observation was that a slight decrease in the magnitude of the UV-visible absorption band associated with the $[4Fe\text{-}4S]^{2+}$ cluster accompanied SAM binding. This observation enabled the study of the kinetics of substrate binding using a stopped-flow spectrophotometer to monitor this spectral disturbance.[179]

LipA is closely related to BioB, and both enzymes catalyse sulfur insertion bio-transformations. A number of similarities have been identified in the reaction mechanisms that are proposed to be followed from substrate to product during the reactions involving these two enzymes.[9, 27] These close similarities have prompted the need to investigate if the binding of SAM and EK(Oct)I to LipA was identical to that of SAM and DTB to BioB. In this section of this thesis, the results of the UV-visible absorption spectral experiments carried out to study the interactions between the octanoyl substrate EK(Oct)I, the co-substrate SAM and the enzyme LipA, are discussed.

2.4.2 UV-visible spectrum for SAM and the substrate EK(Oct)I binding to LipA

Reconstituted LipA (15 μM) was mixed with the octanoyl tripeptide substrate EK(Oct)I (200 μM), and SAM (concentration increasing from 0 – 400 μM) was added in small aliquots. After each addition of SAM, the protein mixture was stirred for 5 min and the UV- visible spectrum was then recorded. The graph in Figure 2.22 shows a plot of the mixture's absorbance as the wavelength was varied. There is a slight decrease in the magnitude of the UV-visible absorption band associated with the $[4Fe\text{-}4S]^{2+}$ cluster (λ = 400 nm) as the concentration of SAM in the mixture is increased.

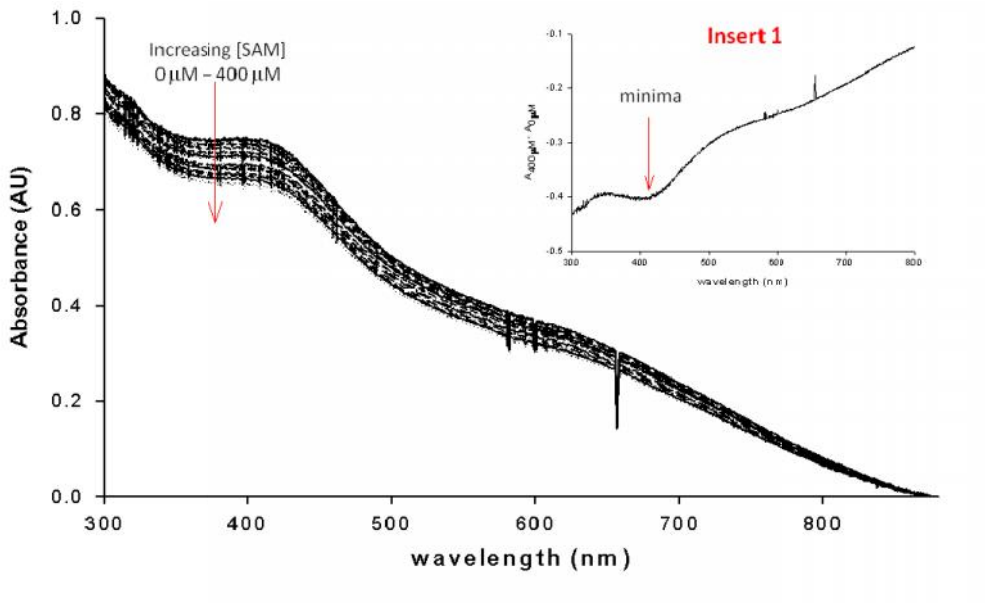

Figure 2.22 *A plot of the absorbance against wavelength (nm) for SAM in presence of the tripeptide EK(Oct)I. Insert 1 is a plot of the difference spectrum showing a maximal decrease at ~ 400 nm. The graph was prepared using SigmaPlot® version 11.*

A plot of the difference spectrum obtained by subtraction the absorbance values at 0 μM [SAM] from the values at 400 μM [SAM] is shown in Insert 1 of Figure 2.22. The graph in the insert shows a maximal decrease at ~ 400 nm which would suggest that there is a decrease in the absorption by the $[4Fe\text{-}4S]^{2+}$ cluster as the [SAM] is increased. In the presence of EK(Oct)I, SAM binds to LipA with higher affinity.

In the graph shown in Figure 2.23 the absorbance values at 400 nm were plotted against the concentration of SAM in the reaction mixture. This data was fitted to an exponential linear function $\boldsymbol{y = y_0 + ae^{-bx} + cx}$, from which the constants a = 0.0692 ± 0.0047; b = 0.0621 ± 0.0096; c = -0.0001 ± 0.0041 and y_0 = 0.6555 ± 0.0041 were determined.

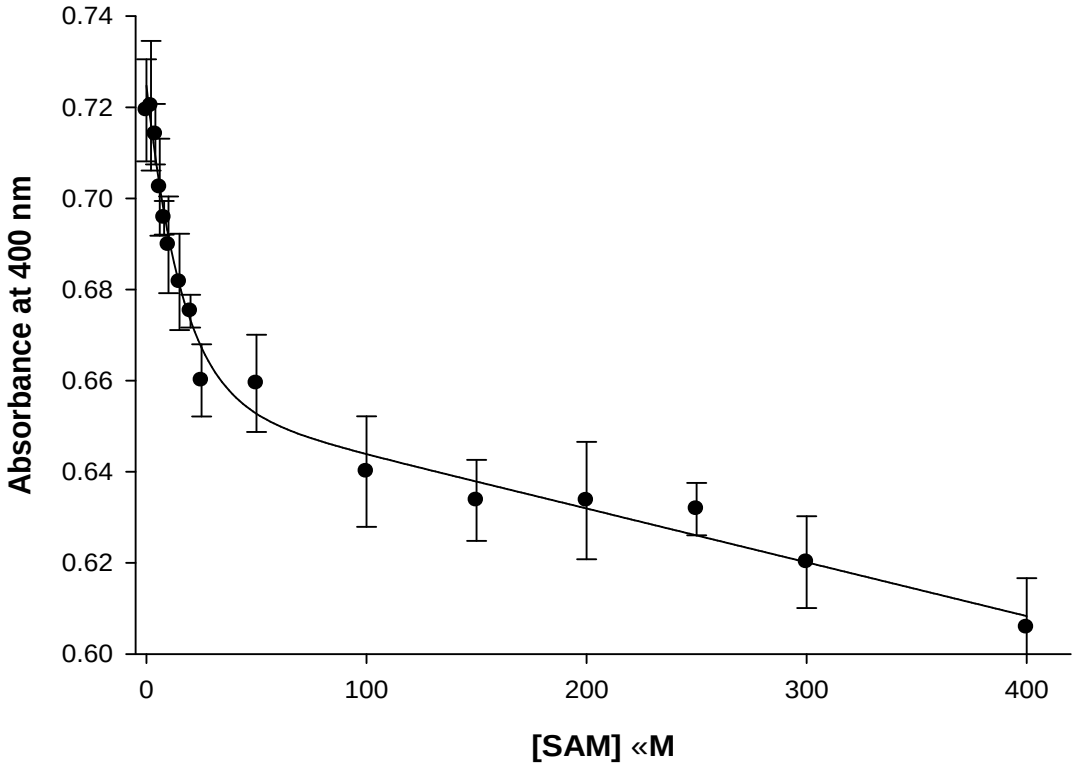

Figure 2.23 *A plot of absorbance at 400 nm against the concentration of SAM for the assay containing the tripeptide substrate (EK(Oct)I). The plotted curve shows the data fitted to an exponential linear function* $\boldsymbol{y = y_0 + ae^{-bx} + cx}$. *The constants were determined to be a = 0.0692 ± 0.0047; b = 0.0621 ± 0.0096; c = -0.0001 ± 0.0041 and* y_0 *= 0.6555 ± 0.0041. The graph was prepared using SigmaPlot® version 11.*

The constants a, b, c and y_0 obtained from the graph in Figure 2.14 were then used to fit the data to a ligand substrate binding function $\mathbf{y = \frac{B_{max}x}{K_D + x} + N_s x}$ (Figure 2.24) from which was obtained the binding constant $K_d = 3.6 \pm 1.1$ and the constant $B_{max} = 18.1 \pm 1.9$ were determined. The constant $N_s = 0.027 \pm 0.008$ refers to non specific DNA binding which occurs during the course of the assays.

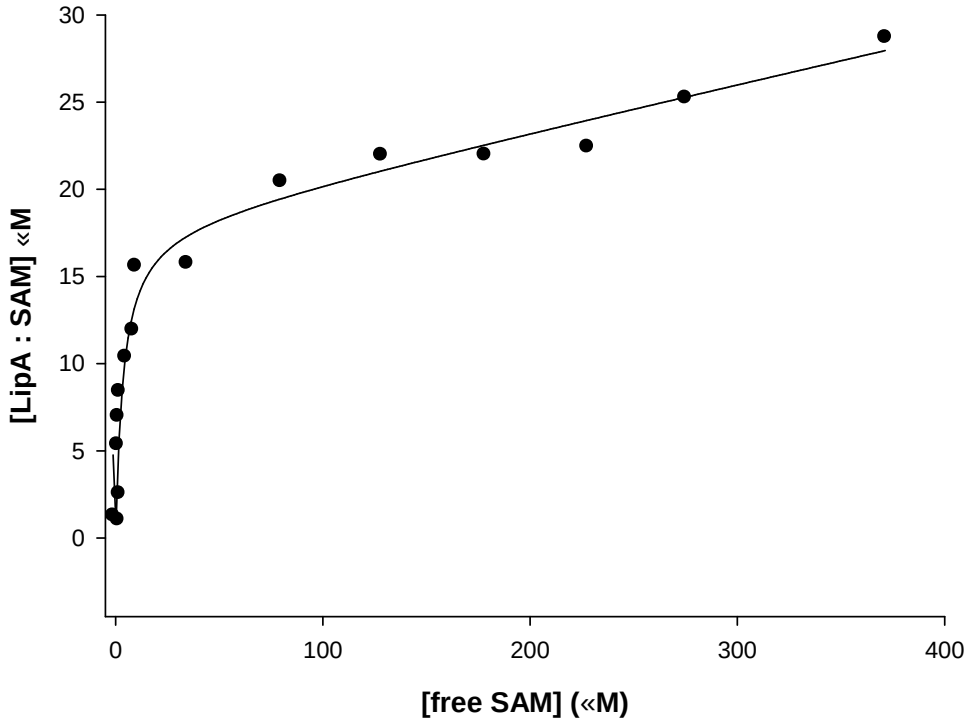

Figure 2.24 *A plot of [LipA: SAM] «M against [free SAM] «M. The data was fit to a ligand substrate binding function* $\boldsymbol{y = \frac{B_{max}x}{K_D + x} + N_s x}$ *and values for the binding constant* $K_d = 3.6 \pm 1.1$ *and the constant* $B_{max} = 18.1 \pm 1.9$ *were determined. The non specific DNA binding constant was determined to be* $N_s = 0.027 \pm 0.008$*. The graph was prepared using SigmaPlot® version 11.*

2.4.3 UV- visible spectral changes observed when SAM was added to LipA in absence of the tripeptide EK(Oct)I

SAM (concentration increasing from 0 – 400 μM) was added in small aliquots to reconstituted LipA (15 μM). After each addition of SAM the protein mixture was stirred for 5 minutes and the UV-visible spectrum was recorded. The graph in Figure 2.25 shows a plot of the mixture's absorbance as the wavelength is varied. There is a slight decrease in the magnitude of the UV-visible absorption band associated with the $[4Fe\text{-}4S]^{2+}$ cluster as the concentration of SAM in the mixture is increased.

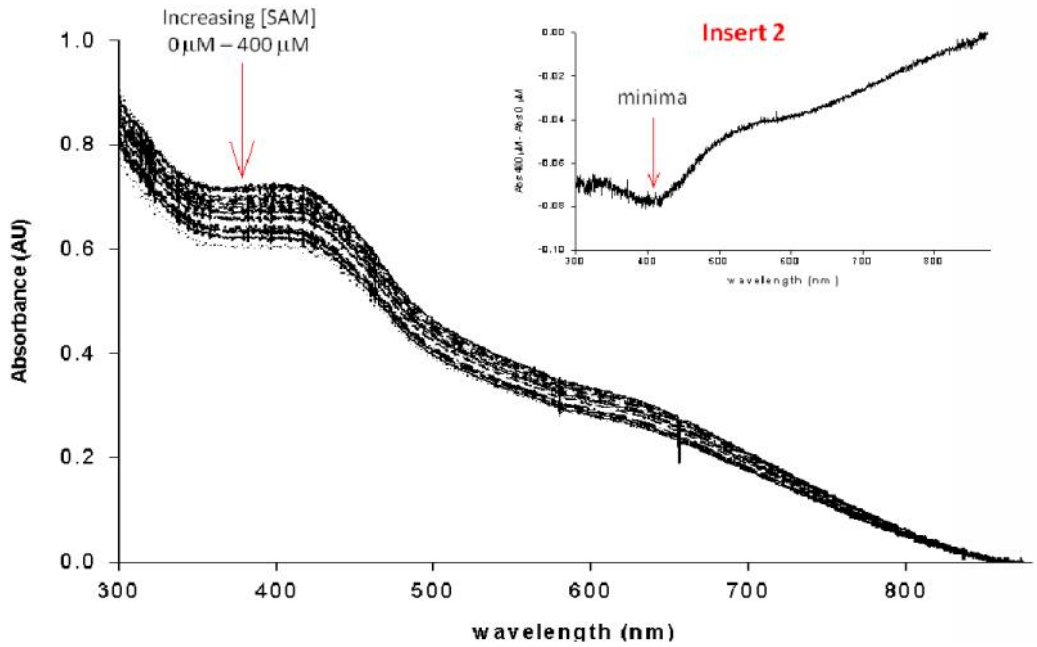

Figure 2.25 *A plot of the absorbance against wavelength (nm) for SAM in absence of the tripeptide EK(Oct)I. Insert 2 plots the difference spectrum showing a maximal decrease at ~ 400 nm. The difference spectrum was obtained by subtracting the absorbance values at 0 «M [SAM] from the values at 400 «M [SAM]. The graph was prepared using SigmaPlot® version 11.*

The insert 2 in Figure 2.25 shows the plot of the difference spectrum which indicates a maximal decrease at ~ 400 nm; this would suggest there is a decrease in absorption by the $[4Fe\text{-}4S]^{2+}$ cluster. In the graph shown in Figure 2.26 the absorbance readings at 400 nm were plotted against the concentration of SAM in the reaction mixture.

This data was fitted to an exponential linear function $y = y_0 + ae^{-bx} + cx$, from which the constants a = 0.0524 ± 0.0028; b = 0.0584 ± 0.0071; c = -0.0001 ± 1.0189 x 10^{-5} and y_0 = 0.6988 ± 0.0025 were determined.

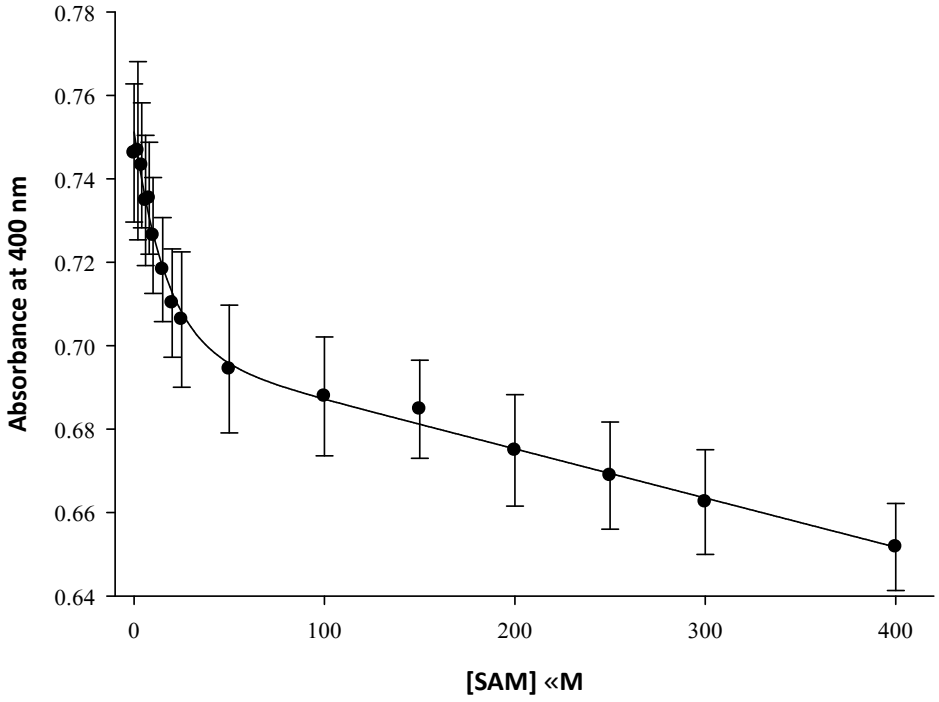

Figure 2.26 *A plot of absorbance at 400 nm against the concentration of SAM for the assay without the tripeptide substrate (EK(Oct)I. The plotted graph shows how the data was fitted to an exponential linear function* $y = y_0 + ae^{-bx} + cx$, *from which the constants a = 0.052 ± 0.003; b = 0.058 ± 0.007; c = -0.00010 ± 0.00001 and* y_0 *= 0.6988 ± 0.0025 were determined.*

These constants obtained from graph of Figure 2.17 were used to fit the data to a ligand substrate binding function $y = \frac{B_{max}x}{K_d + x} + N_s x$ (shown in Figure 2.18) from which the binding constant K_D = 6.6 ± 1.2 and the constant B_{max} = 15.5 ±1.0 were determined. The non specific DNA binding was determined as Ns = 0.027 ± 0.004.

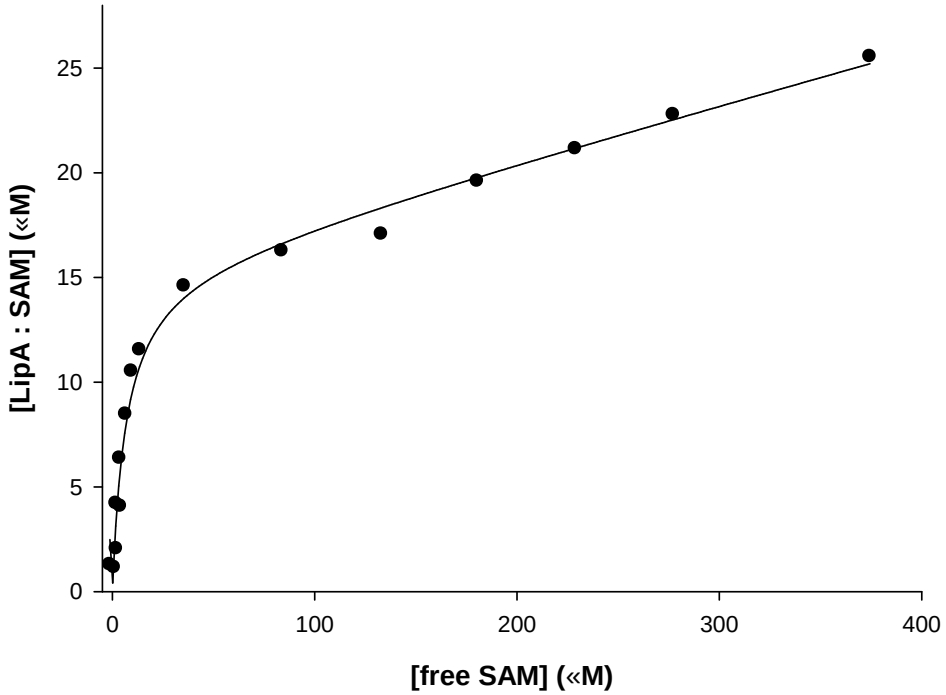

Figure 2.27 *A plot of [LipA: SAM] «M against [free SAM] «M. The data was fit to a ligand substrate binding function* $\boldsymbol{y = \frac{B_{max}x}{K_d + x} + N_s x}$*. The binding constant was determined as* K_d *= 6.6389 ± 1.1743 and the constant* B_{max} *= 15.5 ±1.0. The non specific DNA binding was determined as Ns = 0.027 ± 0.004. The graph was prepared using SigmaPlot® version 11.*

Conclusions from the SAM binding experiments

The K_d value for the binding of SAM to reconstituted LipA was determined in two experiments to be 8.8 ± 1.3 μM and 16.2 ± 3.4 μM. In comparison, the K_d value for the binding of SAM to LipA in the presence of the co-substrate EK(Oct)I was determined in two experiments to be 3.0 ± 0.9 and 3.5 ± 1.5 μM. When comparing K_d values, a lower value indicates a stronger (tighter) binding, whilst a higher value indicates a less stronger (looser) binding. Even taking into account the margin of the errors in the values determined, it is possible to conclude that SAM binds to LipA more tightly in the presence of the co-substrate EK(Oct)I.

2.4.4 The rapid equilibrium dialysis (RED) experiments

The interactions between proteins and small molecules or ions can be effectively studied by equilibrium dialysis assays.[180] The assays are carried out under equilibrium conditions making possible the precise study of the interactions involved. In some instances, these interactions include undetectable low affinity interactions. The primary aim of an equilibrium dialysis experiment is to determine how much of a ligand binds to a macromolecule. This is usually achieved using an indirect method because for any macromolecule-ligand mixture, it is often very difficult to distinguish between unbound and bound ligand. However, if the free ligand is dialysed until its equilibrium concentration is achieved across the membrane it can be quantified.[181] Through carefully planned experiments other kinetic information about the interactions, such as binding constant, binding capacity, the number of binding sites and the change of free energy can also be determined.

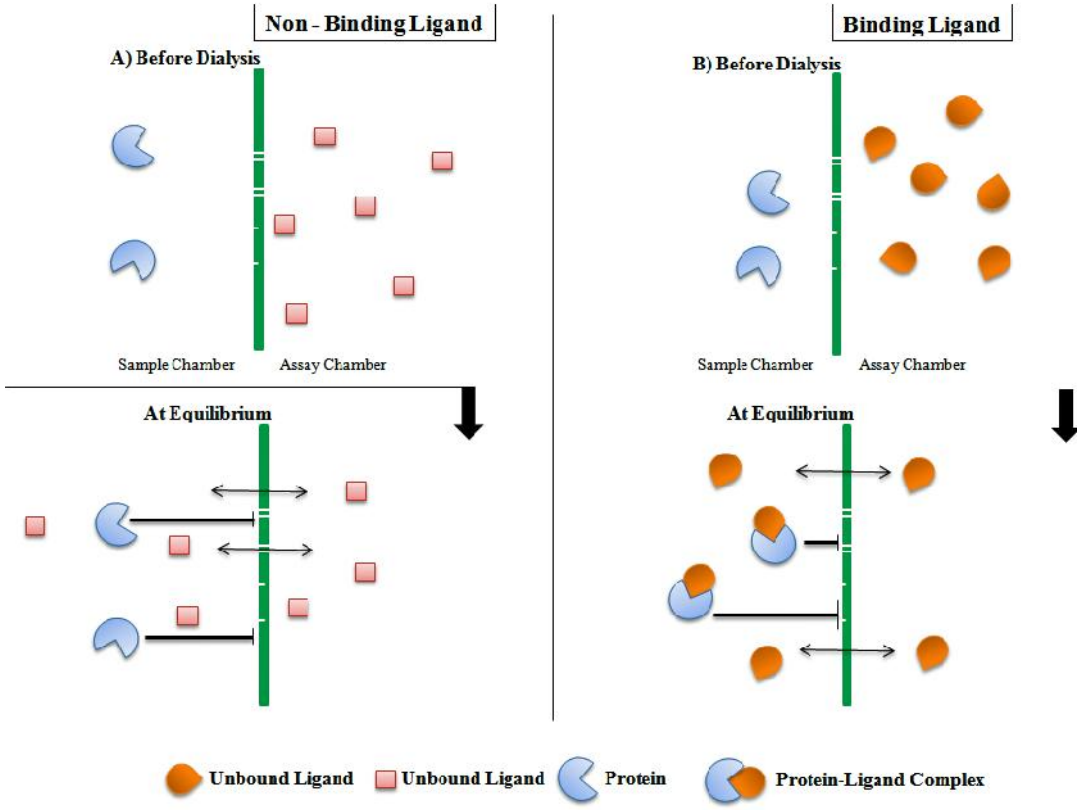

Figure 2.28 *Diagram to show the principle behind equilibrium dialysis.*

A schematic diagram that can be used to explain the principle of equilibrium dialysis is shown in Figure 2.28. Every protein or enzyme can interact with two types of ligands; the non-binding ligand (Figure 2.28A) and the binding ligand (Figure 2.28B). During equilibrium dialysis a semi permeable membrane, with a molecular weight cut off (MWCO) that allows the ligand to pass through but retains the receptor molecules on one side, is used to separate two chambers. These are known as the sample and assay chambers. Ligand of a known concentration and volume is placed into the assay chamber, and the receptor protein or macromolecule of known concentration and a volume equivalent to that of the ligand is placed in the sample chamber. Since the ligand is small enough to pass through the membrane some of the ligand will diffuse across the membrane into the sample chamber.[181]

If the ligand cannot bind to the receptor protein it will be free to cross the membrane (Figure 2.28A). When equilibrium is reached, the concentration of ligand in both chambers is half that of the initial ligand placed in the sample chamber. However, if the ligand binds to the receptor protein it can no longer freely diffuse across the membrane but is confined to the assay chamber (Figure 2.28B). At equilibrium the two chambers have an equivalent concentration of free ligand, but taking into account the bound ligand, the overall concentration of ligand in the sample chamber is higher. The concentration of free ligand in the assay chamber is reduced by the total amount of ligand bound to the receptor protein divided by two.[180]

The experiments carried out for the current thesis write-up involved the use of a rapid equilibrium dialysis (RED) device (Figure 2.29) which was purchased from Thermo Fisher Scientific. This device was specifically designed to overcome some of the difficulties associated with standard rapid equilibrium procedure. The RED device consists of a 96-well Teflon® base plate (Figure 2.29A) and disposable dialysis tube inserts (Figure 2.29B). In comparison to standard equilibrium dialysis approaches each cell of the RED device has an increased surface area-to-volume ratio. This should lead to less time being spent on equilibrations and a much higher assay throughput.[182]

The tube inserts of the RED device are made up of two side-by-side chambers divided by a vertical cylinder of dialysis membrane optimised for minimal non-specific binding. From the three sizes available, 8K, 12K or 25K MWCO the dialysis membrane chosen was of 8K MWCO because LipA has a molecular weight of 36,000 KDa and the substrates were typically less than 2,000 KDa. The RED device's inserts were arranged so as to form alternating columns of red and white conical wells. The sample chambers were the red wells and the buffer chambers are the white wells. The buffers used were selected to be able to freely diffuse into and out of the sample chamber.

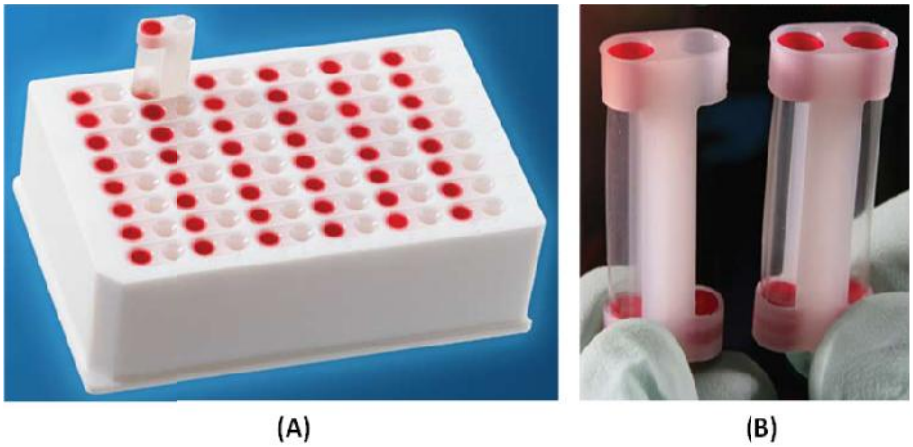

Figure 2.29 *The Rapid Equilibrium Dialysis (RED) device designed by Pierce Biotechnology (Thermo Fisher Scientific, Waltham, MA) consisting of (A) a 96-well Teflon® base plate and (B) disposable dialysis tube inserts.* [181]

Initially 500 μL of the tripeptide EK(Oct)I, (250 μM in HEPES buffer (25 mM, pH 7.5)), were placed in the sample chamber of the RED device. Reconstituted LipA (150 μM, 75 μL) was placed into the buffer chamber. The buffer solution was made up to 750 μL with HEPES buffer (25 mM, pH 7.5). The RED device was sealed using self-adhesive tape and incubated at 37 ^{o}C in a warm water bath for 6 hours. Every 30 minutes 20 μL samples were collected from both chambers of the device and each sample diluted to 80 μL in HEPES buffer (25 mM, pH 7.5). Finally 60 μL of these samples was analysed by HPLC.

The graph in Figure 2.30 shows the HPLC traces recorded for the 60 μL injected samples taken from the sample chamber of the RED device. The area under the peaks corresponds to the amount of EK(Oct)I present in each sample.

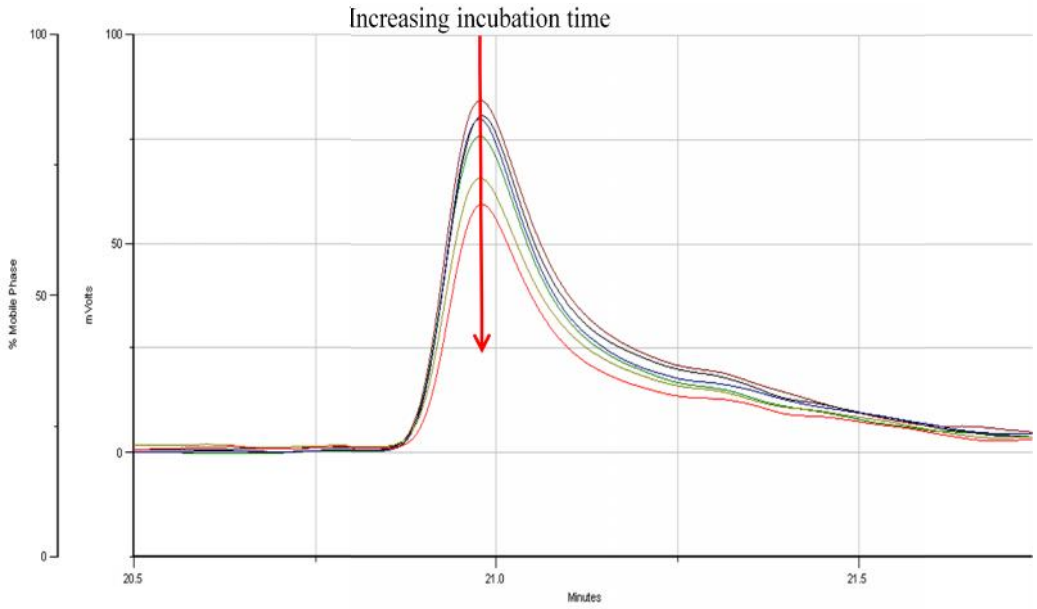

Figure 2.30 *HPLC traces recorded for injected samples taken from the sample chamber of the RED device. The time in minute on the x-axis of the graph shows the retention time of the sample in the HPLC, the incubation time indicated by the red arrow in the graph is with respect to how long the assay was allowed to equilibrate before the analysis sample was taken.*

The traces of Figure 2.30 show a decrease in the amount of EK(Oct)I present in the sample chamber as the time of incubation of the RED device increases. This was to be expected because the sample compound EK(Oct)I would have been expected to diffuse across the membrane into the buffer chamber until an equilibrium was established in the whole system. Using the computer software Unipoint 5.1 it was possible to determine the total area under each peak. The graph in Figure 2.31 shows the plot of the peak area against time (minutes). The concentration of EK(Oct)I represented by each peak area was determined using an EK(Oct)I calibration plot. The graph in Figure 2.32 shows how the concentration of EK(Oct)I decreases with time.

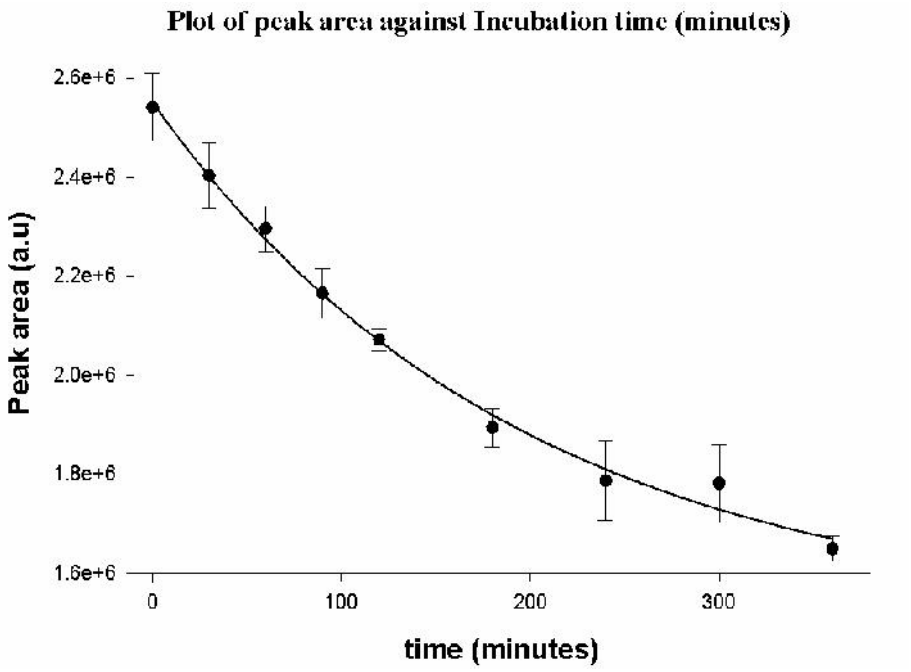

Figure 2.31 *A plot of the area under a peak against the total time the RED device had been incubated in a water bath when the sample was injected.*

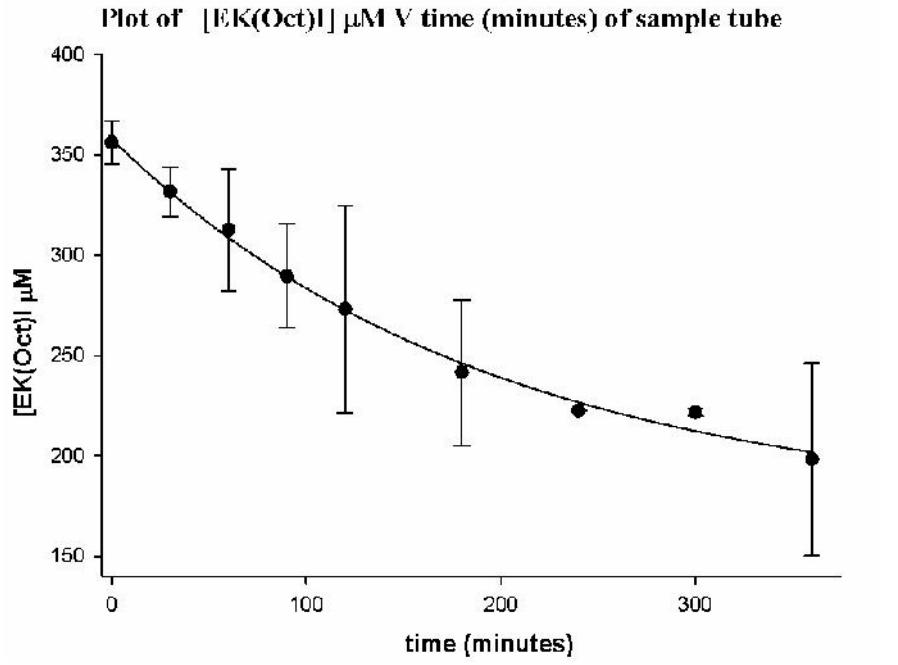

Figure 2.32 *A plot of the concentration of EK(Oct)I («M) against the total time the RED device had been incubated in a water bath when the sample was injected.*

The graph in Figure **2.33** shows the HPLC traces obtained for the analysis of samples taken from the buffer chamber. The single peak at the top of the plot is the trace of a sample of EK(Oct)I which was superimposed just to show where the sample peaks were expected to appear.

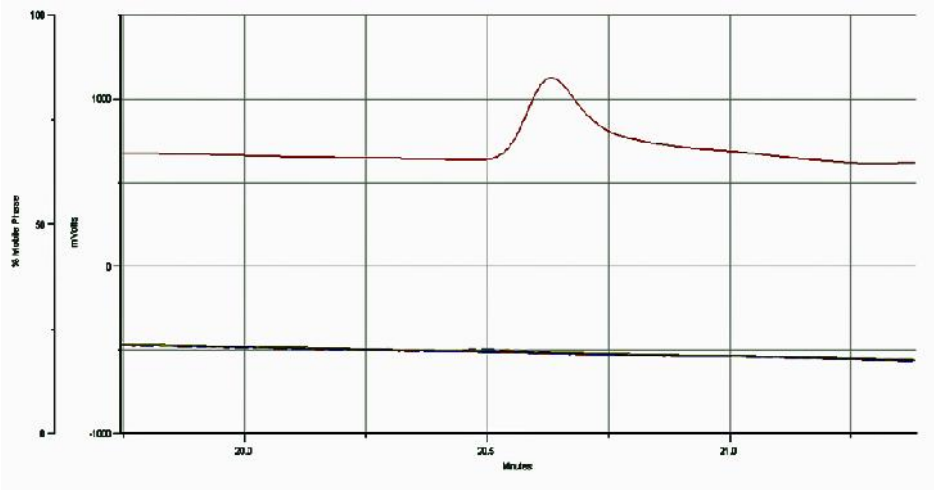

Figure 2.33 *HPLC traces recorded for injected samples taken from the buffer chamber of the RED device. The single peak at the top is a trace of EK(Oct)I superimposed to show where the sample peaks were expected to appear.*

The straight-line traces were unexpected; these indicated that there was no apparent EK(Oct)I in the buffer chamber. However, since the concentration of EK(Oct)I in the sample chamber was decreasing with time it meant that the migrating EK(Oct)I was being trapped within the semi-permeable membrane. Changing the assay buffer to ammonium bicarbonate (25 mM, pH 7.5) did not resolve this problem. An alternative approach was to wash the inserts in different organic solvents for an hour before preparing the RED device for the dialysis. Acetonitrile, DMF and diethyl ether were all used but that did not make the membrane permeable to the tripeptide EK(Oct)I. The RED device inserts were also soaked in reagents commonly used to prevent non specific binding in assays, *i.e.* tween (1 % v/v), sodium chloride (200mM) and sodium octanoate (1mM), but the EK(Oct)I was still being retained in the dialysis membrane. Since the tripeptide EK(Oct)I was being trapped in the membrane and could not be recovered it was therefore not possible to use the RED device to study the interactions between LipA and the substrate EK(Oct)I.

Had there been sufficient time to allow for further experiments, the membrane would have been tested using named standard compounds to check if the compounds would have passed through it. That way it would have been possible to determine whether or not the membrane was at all defective. Another solution to this problem could have been to use a different membrane for these experiments. The new membrane would have a lager pore size than 12,000 KDa, to let the octanoyl substrate EK(Oct)I pass through freely, but would still need to have pores that were less than 36,000 KDa so that the LipA did not pass through the membrane.

2.4.5 Fluorescence polarization

Complex protein-protein and protein-ligand interactions that involve a wide range of affinities are a key part of biological and biochemical processes. These interactions have been primary targets for drug development and pharmacological interventions as well as basal biological and biophysical studies. In recent years, chemical biology and high-throughput (HTP) screening techniques have been developed, in which the targeted manipulation of protein interactions is achieved using small organic molecules.[183, 184] One such widely used, very robust and highly sensitive HTP technique is fluorescence polarization (FP). Figure 2.34 schematically shows how fluorescence polarization is detected.

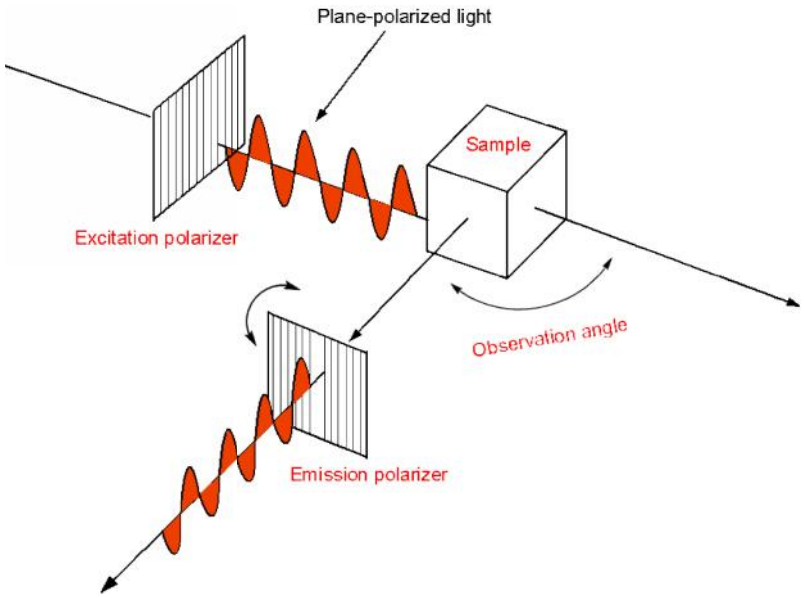

Figure 2.34 *A diagram showing a fluorescence polarization instrument set up.* [183]

When plane-polarized light is used to excite fluorescent molecules, the emitted light is also polarized. Fluorescent sample molecules are excited using plane polarized, monochromatic light. Only the appropriately oriented molecules absorb the light and are excited and subsequently emit light. A moving polarizer is used to measure the emitted light in both the horizontal and the vertical planes.[183] If the detected parallel intensity is $I_{\parallel}$ and the detected perpendicular intensity is $I_{\perp}$; the polarization (P) of emission can be defined as shown in the equation 2.8.[185, 186]

$$P = \frac{(I_{\parallel} - I_{\perp})}{(I_{\parallel} + I_{\perp})} \qquad (equation\ 2.8)$$

Another term also used in the context of polarized emission is anisotropy (A) which is defined as shown in equation 2.9. [187, 188]

$$A = \frac{(I_{\parallel} - I_{\perp})}{(I_{\parallel} + 2I_{\perp})} \qquad (equation\ 2.9)$$

By rearranging equations 2.8 and 2.9 the anisotropy can also be related to polarization as shown by equations 2.10 and 2.11.

$$A = \frac{2P}{(3-P)} \qquad (equation\ 2.10)$$

$$\text{or} \quad A = \frac{2}{3}\left(\frac{1}{P} - \frac{1}{3}\right)^{-1} \qquad (equation\ 2.11)$$

A molecule's polarization is closely related to its Brownian molecular rotation and is also proportional to its rotational relaxation time (ρ). For a rigid spherical molecule, the rotation relaxation time is related to the absolute temperature (T), the gas constant (R), molecular volume (V) and viscosity of the medium (η) as shown in the equation 2.12. [189]

$$P \propto \rho = \frac{3\eta V}{RT} \qquad (equation\ 2.12)$$

It follows from equation 2.12 that by keeping the absolute temperature and the viscosity constant the polarization can be directly affected by changes in the molecular size (or volume). The molecular size (or volume) can be changed by the binding or dissociation of molecules, degradation or conformational changes.[177, 189] During high-throughput fluorescence polarization (HTP-FP) assays, *e.g.* the enzymatic release of a free fluorophore or displacement of molecular complexes, the changes in polarization resulting from changes in the molecular mass of a labelled species are detected.[183]

Equation 2.13 shows a quantitative relationship known as the Perrin-Weber equation in which the observed steady-state polarization is P, and the limiting or intrinsic polarization in the absence of depolarization influences such as rotation and energy transfer is P_0. The excited-state lifetime (corresponding to the time after excitation at which the number of excited molecules has been reduced to 1/e of its starting number) is τ. The Debye rotational relaxation time is ρ. [178, 185, 189]

$$\left(\frac{1}{P} - \frac{1}{3}\right) = \left(\frac{1}{P_0} - \frac{1}{3}\right)\left(1 + \frac{3\tau}{\rho}\right) \qquad (equation\ 2.13)$$

2.4.6 Advantages of using fluorescence polarization

Fluorescence polarization is widely used in high-throughput and clinical assays for a number of reasons. Firstly, the use of advanced instruments and well developed fluorescence probe technology, along with target specific labelling strategies; all make it possible to detect fluorescence changes, precisely over background levels even in live cell environments.[185] Secondly, the "mix and measure" assays are homogeneous, meaning that there is no need to separate the bound or the free ligand. Other attractions when using fluorescence techniques are that there is no need for radioisotopes, and polarization assays are reproducible and are easy to automate. Another main advantage of fluorescence assays is the ability to make time-resolved measurements.[183, 185]

The current write-up describes the coupling of the two fluorescent compounds **54** and **89** (Figure 2.35) to HPLC purified pentapeptide ETEK(Oct)I (**42**, Figure 2.9) to yield the labelled substrates **44** and **45**. The author of this thesis prepared compound **44** by coupling the Alexa Fluor® 350 carboxylic acid succinimidyl ester to purified ETEK(Oct)I. The progress of the reaction was monitored by TLC and the fluorescent product was characterized by recording the ESI mass spectrum and the fluorescence intensity on a plate-reader. Compound **45** was prepared with the help of Graham Broader, another member of the Roach group.

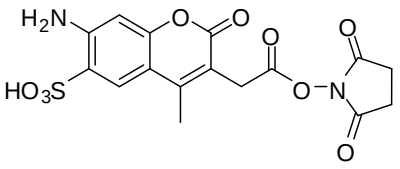

(54)

Alexa Fluor® 350 carboxylic acid succinimidyl ester

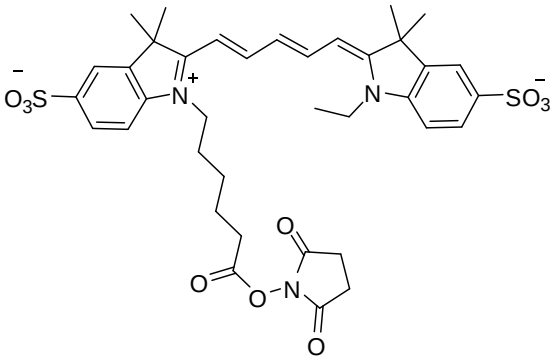

(89)

Cy5

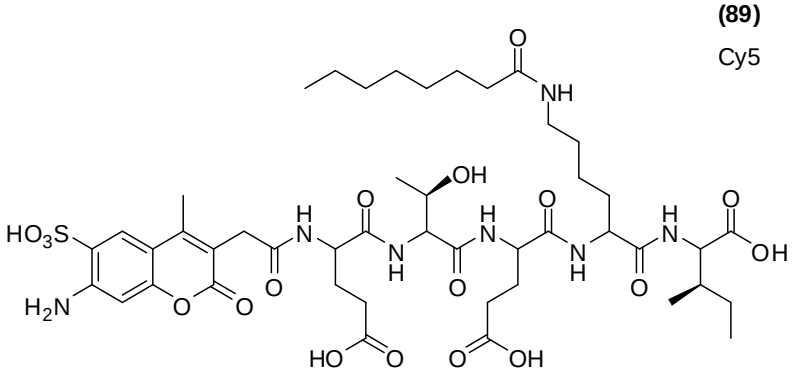

(44)

Alexa 350-ETEK(Oct)I

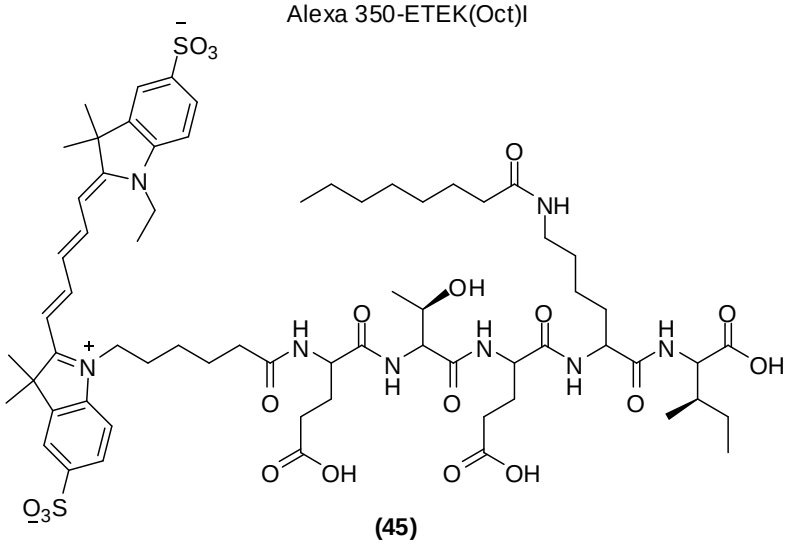

(45)

Cy5-ETEK(Oct)I

Figure 2.35 *The chemical structures of the Alexa 350 carboxylic acid succinimidyl ester and Cy5 and the labelled peptides that were prepared by coupling the fluorophores to the pentapeptide ETEK(Oct)I.*

The ESI-mass spectrum for compound **44** showed that there was a compound of mass 520.9 corresponding to the $[M+2H]^{2+}$ ions. The fluorescence intensity recorded

for compound **44** on the plate-reader (Figure 2.26) showed a single peak for the wavelengths in the range of 330 nm to 400 nm. This information, coupled with the reverse phase TLC analysis of compound **44**, indicated that the desired compound had been prepared and the sample was pure enough to be used in the LipA assays.

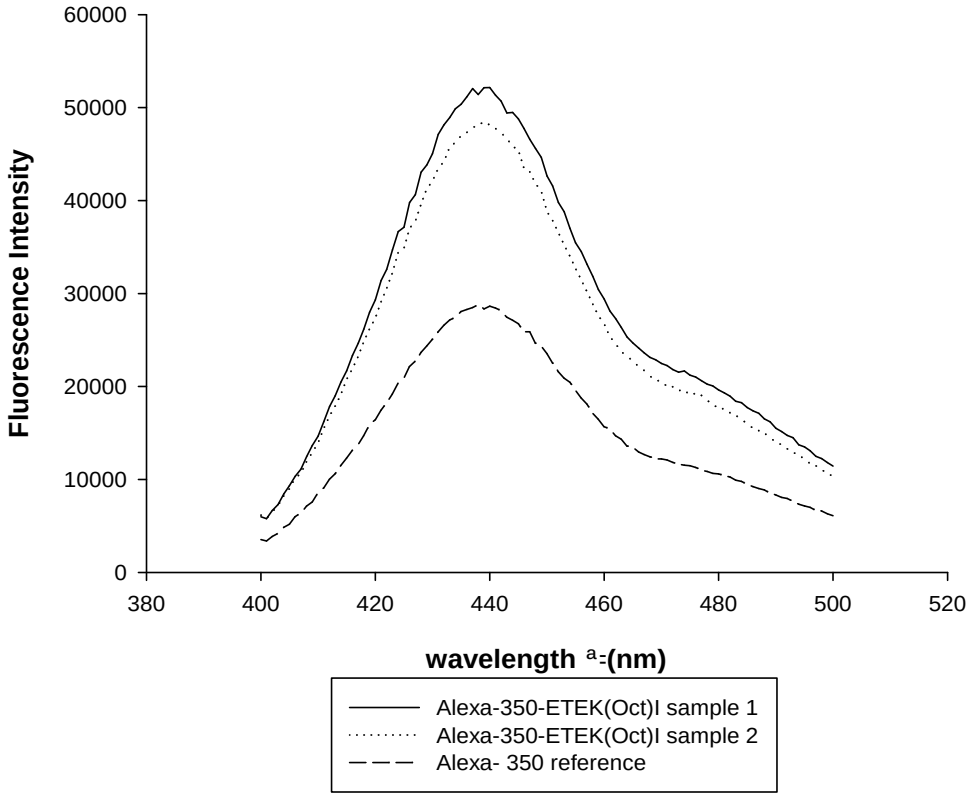

Figure 2.36 *The recorded fluorescence intensities for the Alexa Fluor® 350 carboxylic acid succinimidyl ester* **54** *(given here as Alexa-350 reference) and the fluorophore coupled pentapeptide* **44**.

2.4.7 The fluorescence polarization assays

The LipA binding assays were set up as described in the experimental section 3.14. The graph shown in Figure 2.37 is a plot of the fluorescence polarization recorded over time for the Alexa 350-ETEK(Oct)I binding to *E.coli* LipA in the presence of AdoMet. The plots are for the different wells or the different concentrations of LipA. This assay was repeated three times and the same trend was observed. The expected

trend for the ligand-protein binding assay was a sigmoidal function and clearly from the plot shown in Figure 2.37 there was a fluctuation up and down of the fluorescence with time. This suggested the assay was not able to detect the binding interactions between the ligand and the protein. Similar results were observed in the LipA binding assays which did not contain SAM.

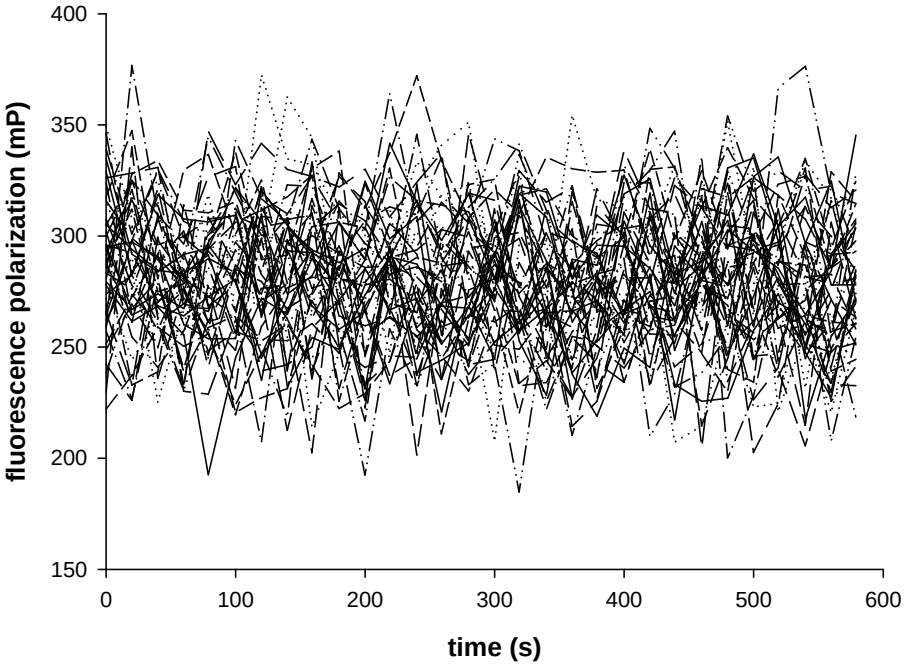

Figure 2.37 *A plot of the fluorescence polarization recorded over time for the binding of Alexa 350-ETEK(Oct)I to E.coli LipA in the presence of AdoMet.*

There are a number of possible reasons why this assay was not able to detect the interaction between the ligand and the protein. The first possibility is that the synthesized substrate was very small and so its interactions with the protein were too weak to be detected using this approach. If that was the problem the solution would have been to synthesize a much longer peptide substrate *e.g.* 25, 40 or even 50-amino acid-long peptide. One of the desired properties of the synthetic substrates for the assays used throughout this report is that they be soluble in aqueous solutions. However the synthesis of much longer peptides could have potentially resulted in compounds that were relatively insoluble in aqueous solution.

The second possible reason for the assay not being effective in detecting the interactions between the synthesized substrate and the protein is that the fluorophore could have been unsuitable. Ideally, the desired fluorophore would enhance the interactions between the substrate and the protein. In this instance it could be that the fluorophore did not do so. There was a need to screen through the vast array of available fluorophores to determine which ones would be appropriate for these assays. Due to time constraints it was not possible to investigate other options.

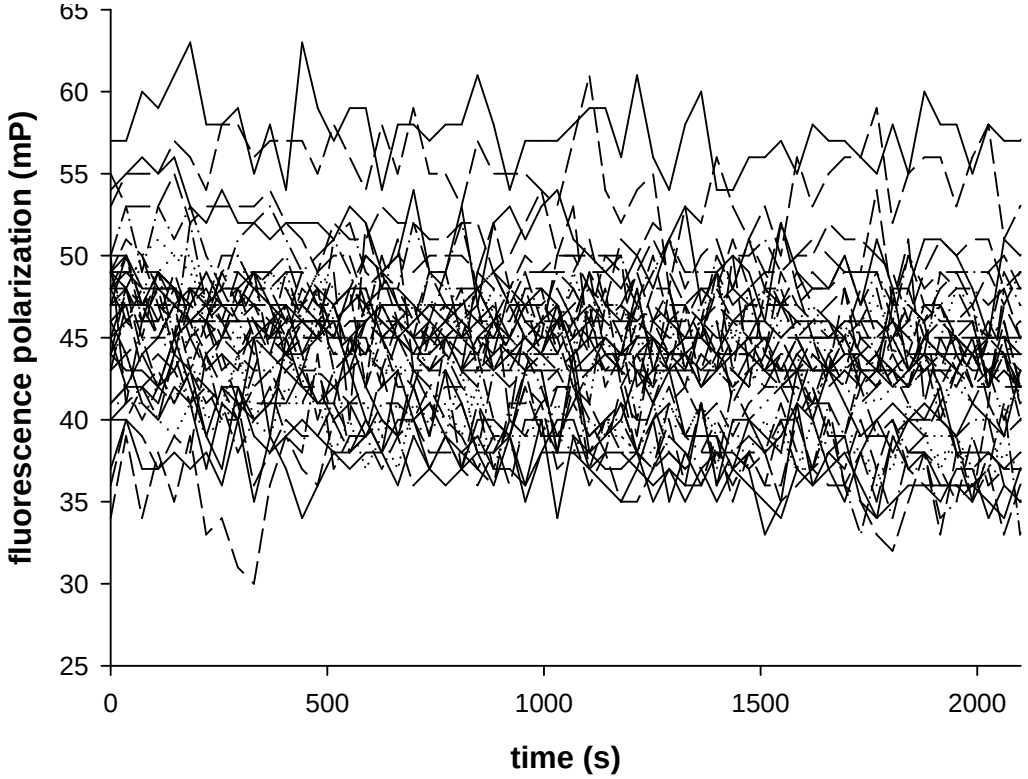

Figure 2.38 *A plot of the fluorescence polarization recorded over time for the binding of Cy5-ETEK(Oct)I to E.coli LipA in the presence of AdoMet.*

The graph shown in Figure 2.38 is a plot of the fluorescence polarization recorded over time for the Cy5-ETEK(Oct)I binding to *E.coli* LipA in the presence of AdoMet. The observed results are very similar to those obtained with Alexa 350-ETEK(Oct)I. The conclusions are also the same. The assay using coupled Cy5 could not be used in the study of the interactions of the substrate and the *E.coli* LipA.

2.5 Crystallization of LipA

2.5.1 Crystallization of Macromolecules

Crystallization often represents the "bottle-neck" when trying to determine the three-dimensional (3-D) structure of a macromolecule.[190, 191] Macromolecules such as proteins, nucleic acids, viruses and ribosomes can be induced to crystallize under the right conditions. However, the crystals formed (with volumes typically $\leq 10\ \mu m^3$) are relatively small in comparison to those obtained from small molecules, and they have to be examined using a binocular microscope.[192] Macromolecular crystals are characterized by poor mechanical properties (they are very fragile and are easily affected by changes to their environment), and they have a very high solvent content.[192, 193] Initially, protein crystallization was developed as a means for purifying proteins and for testing the purity of proteins. There were some who perceived the crystallization of macromolecules as nothing more than "an interest" to be pursued in the biological chemist's laboratory.[65] In the 1930's Bernal and Crowfoot using pepsin, pioneered the use of crystallization and X-ray diffraction in the structural studies of proteins.[192, 194] For many years thereafter there were a lot of reports of successful growths of macromolecular crystals.

However, such preparations were carried out in an empirical manner and were often based on experience and intuition. The structures of many macromolecules crystallized using this approach, without the rational control of the involved processes, have been determined.[192] The apparent lack of extensive theory or strong foundational data to guide any crystallization efforts requires the macromolecular crystallographer to be persistent, relentless and occasionally very intuitive. Even more "daunting at times" is the complexity and the range of the macromolecules that exist in nature. For example, the smaller proteins possess almost a thousand atoms, with hundreds of bonds and thousands of degrees of freedom.[195] Notwithstanding, the situation today is much better than what it was in the earlier days of macromolecular crystallization. The crystallization of macromolecules can now be approached in a rational manner based upon the understanding of the fundamental properties of the systems involved.[191, 194, 196]

Basically, the crystallization of macromolecules requires the systematic screening of the various conditions that affect the formation of crystals. Once a set or sets of conditions that give rise to any type of crystals are identified, the individual variables are optimized to obtain the best possible crystals.[193, 195] This is usually achieved by preparing a broad range of assays or establishing a vast matrix of crystallization conditions and evaluating the results. The collected information is used to improve the experimental conditions in subsequent attempts at crystallization. Even then, experience and insight in designing and evaluating all the results can be critical to the successful crystallization of macromolecules, because the number of variables to consider is significantly large and the ranges are so broad.[193, 195]

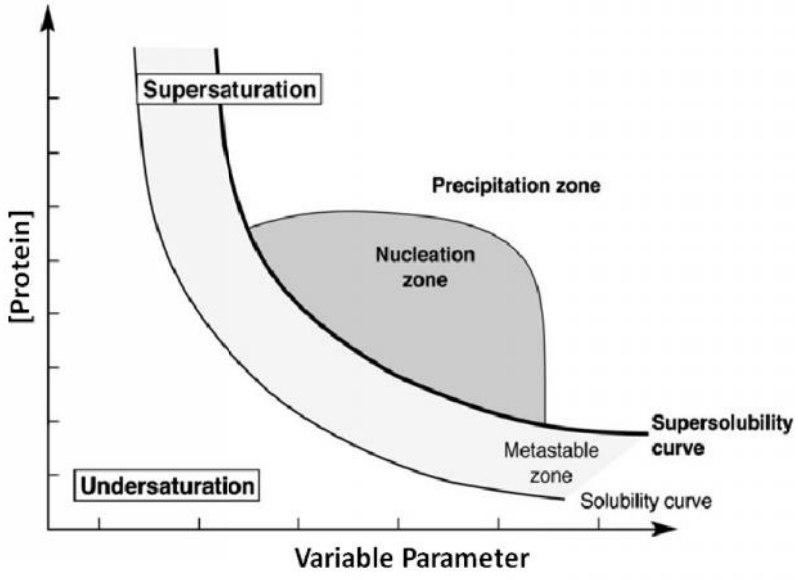

Figure 2.39 *A diagram showing a schematic representation of a macromolecule's phase diagram.*[191, 197] *The graph plots the protein concentration against a variable parameter (e.g. temperature, pH, a precipitant or additive concentration).*

Figure 2.39 shows a phase diagram which can be used to illustrate crystallization. The diagram indicates which state (amorphous solid, crystalline or liquid) is stable under different conditions (variable parameters).[197] The diagram also provides for the quantification of the influence various parameters have on crystallization. A detailed analysis and study of phase diagrams can aid and improve the designing of crystal optimization experiments. Crystals form when supersaturated protein molecules aggregate in an ordered manner. When a protein solution of unsaturated

concentration is mixed with crystallizing reagents, it simply dissolves in the liquid phase. On the other hand, crystallization would occur if the protein concentration is supersaturated. The supersaturation region of the phase diagram can be divided further into the metastable region, the labile region, and the precipitate region.[191, 197, 198]

The crystallization of a molecule occurs in two main stages, nucleation and crystal growth.[199] During nucleation, crystalline nuclei are formed due to an ordered aggregation of large numbers of protein molecules. During crystal growth, the nuclei aggregate in an arranged manner with numerous protein molecules until a critical size is reached. Whilst nucleation only occurs in the labile region (Figure 2.39) crystal growth can occur in both the metastable and the labile regions. Therefore, to crystallize any macromolecule the whole system must be maintained in the metastable and/or labile regions of the phase diagram.[197] In the ideal crystallization experiment, the protein concentration would be increased until it reaches the labile region allowing for a few nuclei to be formed.[199] When the nuclei separate out the supersaturated protein concentration would be allowed to fall into the metastable region. In this region, protein molecules separate out and aggregate with the available nuclei and to grow large crystals, no more new nuclei should be formed. During this whole process, the protein concentration should be kept very close to the supersolubility curve of the labile region (Figure 2.39).[199]

There are a large number of variables to explore when searching for the appropriate macromolecular crystallization conditions. Table 2.5 provides a list of physical, biochemical and chemical factors that have been identified as affecting crystallization.[195] Not all of these variables are critical for the crystallization of a macromolecule at the same time. [64] Some variables, such as pH and salt type, or the concentration of other precipitants are more important for the crystallization of macromolecules. Other variables such as viscosity, gravity, electric and magnetic fields are of lesser significance. The biggest challenge in a crystallization experiment is to decide which variables are significant and how much of each relevant variable is required for a success. The only way to determine which variables are of significance

when crystallizing a macromolecule is to carry-out a series of empirically designed screening experiments.

Table 2.5 *Some of the different variables that affect crystallization experiments.*

Physical	**Chemical**	**Biochemical**
Temperature/temperature variation	pH	Purity of the macromolecule/impurities
Surfaces	Precipitant type	Ligands, inhibitors, effectors
Methodology/approach to equilibrium	Precipitant concentration molecule	Aggregation state of the macromolecule
Gravity	Ionic strength	Post-translational modifications
Pressure	Specific ions	Source of macromolecule
Time	Degree of supersaturation	Proteolysis/hydrolysis
Vibrations/sound/mechanical perturbations	Reductive/oxidative environment	Chemical modifications
Electrostatic / magnetic fields	Concentration of the macromolecules	Genetic modifications
Dielectric properties of the medium	Metal ions	Inherent symmetry of the macromolecule
Viscosity of the medium	Cross-linkers / polyions	Stability of the macromolecule
Rate of equilibration	Detergents/surfactants/amphophiles	Isoelectric point
Homogeneous or heterogeneous nucleants	Non-macromolecular impurities	History of the sample

There are several techniques for crystallizing macromolecules, including the temperature-induced and pH-induced crystallizations, bulk crystallizations and the addition of effectors. There are various dialysis techniques that can also be used to crystallize macromolecules. These techniques include bulk dialysis, microdialysis

and concentration dialysis. Evaporation and vapour diffusion techniques, as well as sequential extractions have all been used for the crystallization of macromolecules. The most commonly used techniques are the hanging drop and sitting drop methods (both of which are vapour diffusion methods) and the micro-batch under oil techniques.[198]

2.5.2 Vapour diffusion methods

In the vapour diffusion techniques, a small aqueous droplet (containing purified protein, a precipitant and a buffer) is equilibrated with a reservoir solution (containing the precipitant and buffer at much higher concentrations). The protein concentration within the droplet slowly increases due to the diffusion of water from the droplet into the reservoir solution. In addition, the solubility of the protein also decreases because of the increasing concentration of the precipitant.[199] When the optimal concentrations for the protein and precipitant are reached, nucleation and crystal growth will occur.

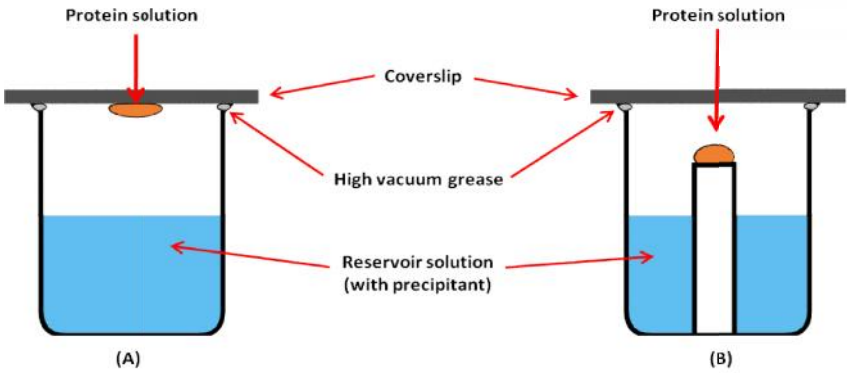

Figure 2.40 *Diagrams showing (A) the hanging drop and (B) the sitting drop methods. Usually the reservoir solution contains the buffer and the precipitant. The protein solution contains the buffer and the precipitant, but in lower concentrations, and may also contain trace ions or metals needed for precipitating particular proteins.*

The two main techniques that apply vapour diffusion are the hanging drop and the sitting drop methods; both of which are illustrated in Figure 2.40.[197, 200] The obvious difference between these two techniques is the placement of the drop. In the hanging drop method, the drop is suspended from the underside of a microscope cover slip (Figure 2.40A). In the sitting drop method the drop is placed on a stable pedestal above the reservoir solution (Figure 2.40B). For both methods, equilibrium is established by sealing the system using high-vacuum grease or oil placed around the circumference of the wells.

2.5.3 Initial screening Experiment

In the current project the hanging drop method was used in crystallizing *S. solfataricus* P2 LipA. The protein was purified following the standard procedure using an S-75 gel purification column (Experimental 3.3.8). The LipA was then reconstituted using the standard procedure (Experimental 3.3.14) and thereafter concentrated to ~ 0.75 mM in HEPES buffer (25 mM, pH 7. 5). Separate solutions of the tripeptide EK(Oct)I (3.9 mM), *S*-adenosyl methionine chloride (70 mM) and *S*-adenosyl homocysteine (20 mM) were prepared in HEPES buffer (25 mM, pH 7. 5). The crystallization assays were set up in 24 well Linbro plates**.** The schematic diagram of Figure 2.41 shows the cross section of each well of the Linbro plate, in which two hanging drops were placed on a cover slip.

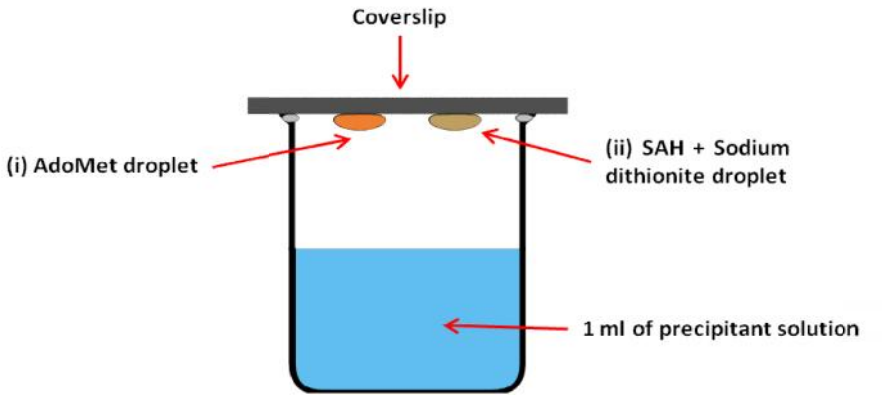

Figure 2.41 *A schematic diagram showing the cross section of each well of the 24 well Linbro plate when set up for the crystallisation assay with two hanging drops.*

Table A.1 in *Appendix 1* shows the initial screening conditions that were set-up in a 24 well Linbro plates. The precipitants used included the salts Li_2SO_4, HCOONa and $(NH_4)_2SO_4$; the organic solvent isopropanol and the polyethylene glycol (PEG) polymers 400, 1500, 4000 and 8000. For the first screening experiments, the buffer used was phosphate buffer (100 mM, pH 6.6). Several plates were set up on successive days using freshly prepared batches of LipA. However no "hits" were obtained (*i.e.* no crystallization occurring under the set conditions).

The buffer for the assays was then changed to HEPES buffer (100 mM, pH 7.5). The LipA turn over assays use HEPES buffer (25 mM, pH 7.5) and so in the crystallization experiments it would have been desirable to use the same buffer. Using the HEPES buffer (100 mM, pH 7.5), the wells B4, B5, B6, C1, C2 and C3 of Table A.1 were identified as possible "hits". Observing these wells under a microscope indicated the formation of globules thought to be due to some form of crystallization. These wells contained PEG 400 and PEG 1500 polymers. However, the number of globules formed and the size of each globule varied with each different experimental setup. This led to the conclusion that in HEPES buffer (100 mM, pH 7.5) it was likely that the crystallization of *E.coli* LipA would be possible, but that the conditions were not reproducible.

The set up of the screening plates in Table A.1 was then repeated but replacing the HEPES buffer (100 mM, pH 7.5) with TRIS buffer (100 mM, pH 8.1). In this instance globules were observed in the wells B4, B5, B6, C1, C2, C3, C4, C5, C6, D1, D2 and D3. All the wells in which polyethylene glycol (PEG) polymer was present had globules. The conclusion was that PEG polymer was needed for the initiation of crystallization of *E.coli* LipA. The picture in Figure 2.42 shows an image captured from the binocular microscope of one of the wells of the Linbro plate showing the presence of globules thought to be due to some form of crystallization.

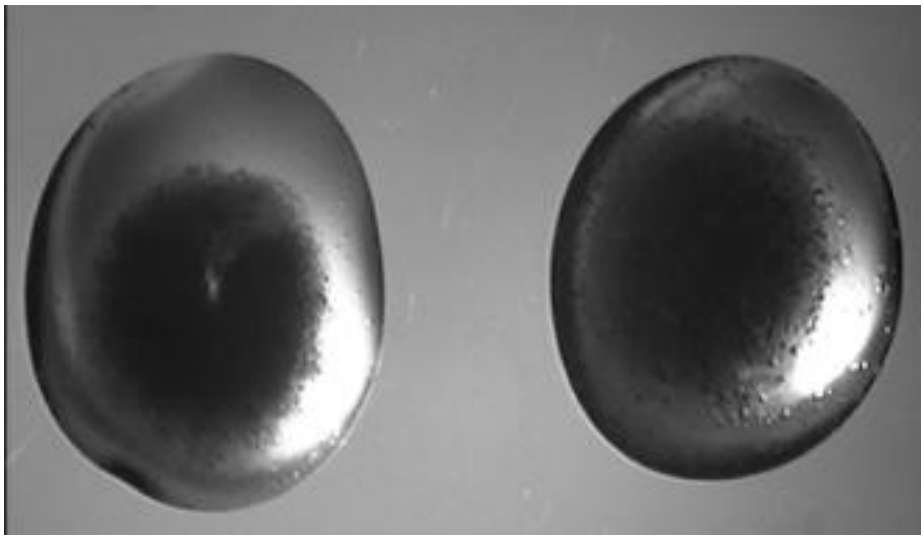

Figure 2.42 *A picture captured from the binocular microscope of one of the wells of the Linbro plate showing the formation of globules thought to be due to crystallization. Two droplets were on the coverslip. The drop on the right was prepared with SAH in it and the droplet on the left was prepared with SAM in it.*

2.5.4 Testing the effect of changing the concentration of PEG polymer

Having identified that polyethylene glycol (PEG) polymer induced the formation of globules in the LipA it was necessary to determine what effect the concentration of PEG would have on the formation of the globules. The Table A.2 in *Appendix 1* shows the set up of the 24 wells to test how changing the concentration of the polyethylene glycol (PEG) polymer would affect the formation of the *E.coli* LipA crystals. The best sets of results were obtained with PEG 400. The pictures of Figure 2.43 show the crystallization observed for three different concentration of PEG 400. It was observed that the droplets that contained SAH gave better observed globules than those droplets which had SAM along with the tripeptide EK(Oct)I. In addition there was no precipitation of the enzyme in the SAH containing droplets.

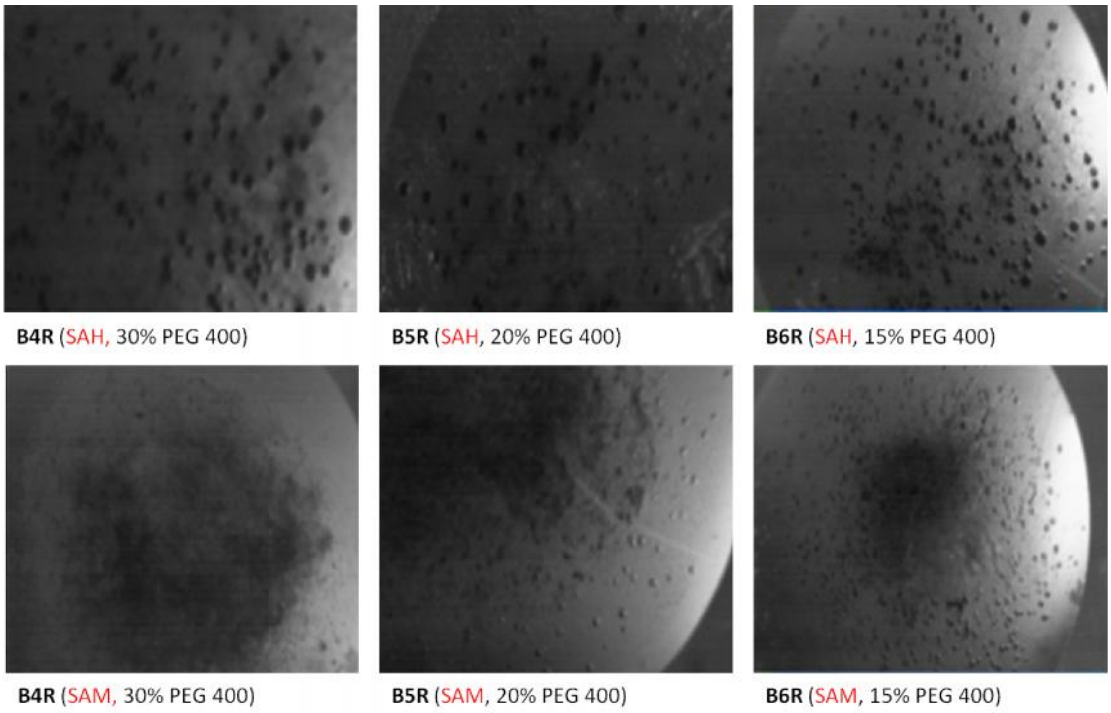

Figure 2.43 *Pictures showing the formation of globules in a few selected wells thought to be the best results. These pictures were taken from a binocular microscope with a camera attached to the eye piece.*

The co-substrate put into one of the droplets was AdoMet (SAM) and the SAH was put in the other droplet. The structures of these two compounds are shown in Figure 2.44. The aim for these preparations was to test if the removal of a methyl group from SAM to give SAH would affect the crystallisation.

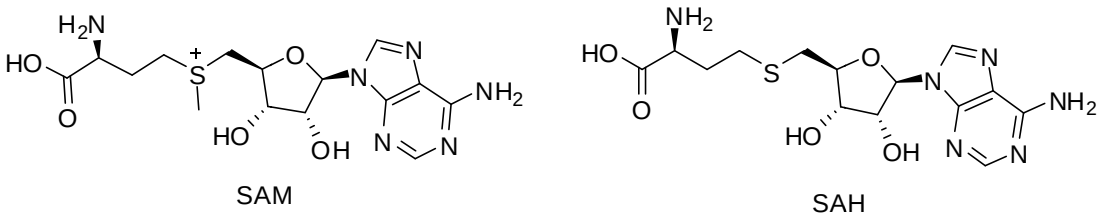

Figure 2.44 *The chemical structures of S-adenosyl methionine (SAM) and S-adenosyl homocysteine (SAH).*

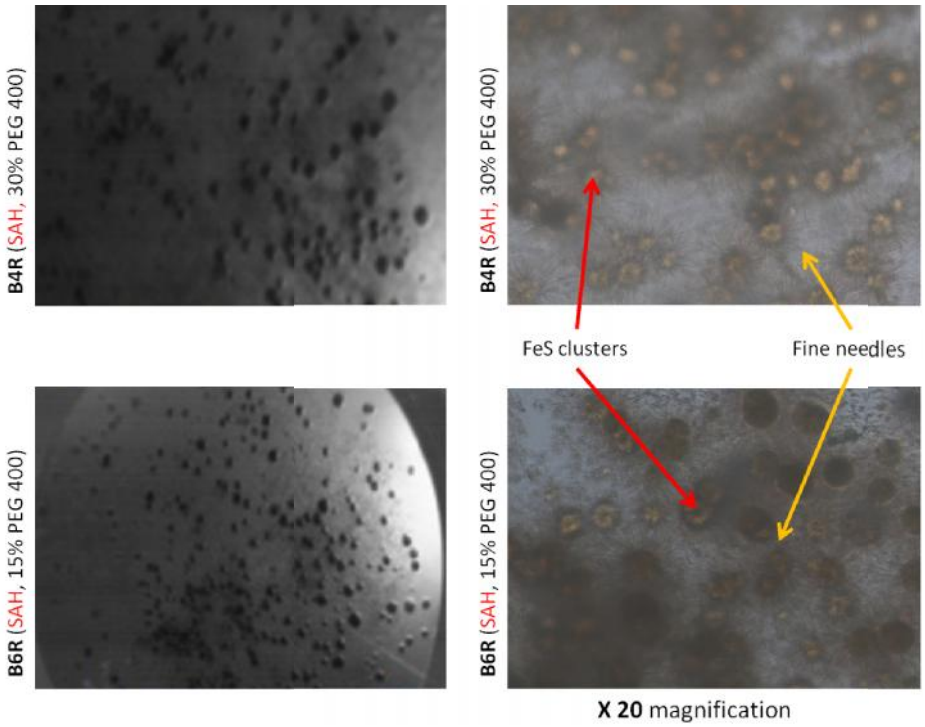

Figure 2.45 *Pictures showing the identified [Fe-S] clusters and the formed fine needles which occur when SAH is the co-substrate.*

Having obtained a promising set of conditions the next task was to optimize these to try and make the observed globules form more defined crystals and to try and grow these into bigger crystals. The initial attempt was to see if the LipA concentration could influence the formation of crystals, the crystallization solutions were set-up as shown in Table A.5 in Appendix 1. The changes in the LipA concentration did not seem to affect the formation of the globules, but at higher concentrations the LipA simply precipitated out. It was decided to screen various precipitants (Tables A.3 and A.4) to see if any could help in making the observed globules develop into well defined crystals. This was not achieved; the formation of the globules was not affected by the precipitants screened. Another approach was to try the seeding of crystals to try and grow bigger crystals. In this approach the identified conditions from Table A.1 in which globules were obtained were used in seeding experiments. The buffer used was TRIS buffer (100 mM, pH 8.1). Fresh solutions of Table A.1 were prepared and in addition to the LipA solution 1 L of the globule forming solutions were added to the mixtures. This did not lead to the formation of better defined crystals.

2.6 Comments and Conclusions

The primary aim of this project as described in the Aims and Objectives (Section 1.7) was to study the reaction kinetics of the LipA mediated conversion of octanoyl substrates into lipoyl products. This main objective would be achieved firstly by expressing, purifying and then isolating the LipA. Then secondly, synthesizing and purifying peptide analogues of the enzyme's natural substrate. Finally, after reconstituting the LipA to give an active form, this would be used in *in vitro* assays with the peptide analogues to study the reaction.

The work described in this thesis details how the *lipA* gene from *Sulfolobus solfataricus* was expressed in *E. coli* cells and was subsequently purified under anaerobic conditions and isolated. Also, it is detailed how the inactive LipA was reconstituted and then used in activity assays. After the successful expression and purification of the enzyme the next step was to synthesize the substrates for the enzyme. Two types of substrates were prepared, the octanoylated peptide substrate analogues corresponding to the identified E_2 domain sequence in LipA from the archaeon *S. solfataricus* P2 and the fluorescently labelled octanoylated peptide substrate analogues Schemes 2.2 and 2.3). These synthetic substrates were prepared by applying solid phase peptide synthesis procedures.

During the conversion of octanoyl substrates to lipoyl products, the breakdown of AdoMet produces AdoH and Met as by-products. The experimental section of this thesis describes assays in which the inhibitory effect of both these by-products on LipA was investigated. It was observed from these experiments that AdoH and Met have a synergistic inhibitory effect on the LipA mediated formation of the lipoyl product. The addition of AdoH and Met to a LipA turn over assay led to a > 50 % loss in enzymatic activity. This synergistic effect was reversed by addition of MTA/AdoHcy nucleosidase. It was observed that AdoH and Met inhibited LipA regained all its enzymatic activity (~ 100 %) in the presence of MTA/AdoHcy nucleosidase.

In order to detect the formation of intermediates during the conversion of substrates into lipoyl products, time-course assays were conducted. In these assays the reaction was "quenched" at different times after initiation and the reaction mixture analysed by LC-MS to determine the masses of its components. Two types of tripeptide substrates were used for these assays, the octanoyl substrate (EK(Oct)I) and the nonanoyl substrate (EK(Non)I). It was observed that the LipA mediated formation of lipoyl product starting with a nonanoyl substrate uses a mechanism that involves the formation of an alkene (Scheme 2.9, compound **60**) and the thietane (Scheme 2.9, compound **61** and / or **62**) intermediates. However the formation of lipoyl product starting with an octanoyl substrate utilizes a different mechanism which does not necessarily involve the formation of the alkene (Figure 2.20, compound **89** and the thietane (Figure 2.20, compound **85** and / or **86**) intermediates.

The experimental sections 3.13 and 3.14 of this thesis describe three different types of experiments that were carried out in an effort to determine the dissociation constants for the interaction of *E.coli* lipoyl synthase with AdoMet and an octanoyl substrate to the enzyme. In the first set of experiments (Sections 3.13.1 and 3.13.2) changes to the UV-visible spectrum associated with LipA were observed when AdoMet and the octanoylated substrate EK(Oct)I were added. The K_d value for the binding of SAM to reconstituted LipA was determined in two experiments to be 8.8 ± 1.3 μM and 16.2 ± 3.4 μM. In comparison, the K_d value for the binding of SAM to LipA in the presence of the co-substrate EK(Oct)I was determined in two experiments to be 3.0 ± 0.9 and 3.5 ± 1.5 μM. When comparing K_d values, a lower value indicates a stronger (tighter) binding, whilst a higher value indicates a less stronger (looser) binding. Even taking into account the margin of the errors in the values determined, it was concluded that SAM binds to LipA more tightly in the presence of the co-substrate EK(Oct)I. In the second set of experiments (Section 3.13.3) an attempt was made to use rapid equilibrium dialysis (RED) in determining the dissociation constants. However, it was not possible to carry out the desired analysis of the experiment because the substrate EK(Oct)I was being trapped within the RED device's semi-permeable membrane. In the third approach, two fluorescently versions of the pentapeptide ETEK(Oct)I were prepared (Sections

3.14.1 and 3.14.2) and these were used in fluorescence polarization assays in an effort to measure the dissociation constants. However it was not possible to detect the binding interactions between the ligand and the protein using these assays.

In another experiment a fluorescent thiol sensitive 7-(diethylamino)-N-(2-(2,5-dioxo-2,5-dihydro-1*H*-pyrrol-1-yl)ethyl)-2-oxo-2*H*-chromene-3-carboxamide (Figure 2.15, compound **61**) was used as a probe to detect the presence thiol residues in reaction mixtures. However the reaction conditions used resulted in the reduction of compound **61** to give an unwanted by product compound **66** (Figure 2.17). This meant that the fluorescent thiol sensitive probe compound 61 could not be used to cysteine residues in the LipA turn over assays.

The crystallization of reconstituted LipA in the presence of its octanoyl substrate and the co-substrate SAM was attempted. If the 3D structure of the protein could be determined it could help in understanding how the enzyme interacts with the substrates and also how the enzyme mediated reaction is carried out. The initial screening crystallization experiments (*Appendix 1*) were successful in identifying possible conditions that could give LipA crystals. It was identified that polyethylene glycol (PEG) polymer induced the formation of globules in the LipA. It was also identified that the presence of SAH instead of AdoMet gave a better defined shape and size to the globules identified as being possible hits for the crystallization of the LipA. However time restraints meant it was not possible to fully explore the assay conditions to be able to obtain large crystals that could be used for X-ray crystallography.

2.7 Proposed future experimental work in this study

The work described in this thesis highlights significant aspects of how the enzyme LipA mediates the conversion of octanoyl substrates into lipoyl products. However, some of the experiments carried out were not completed due to time restraints and so the results were at times inconclusive. This means there are still a number of possible aspects to investigate before a full understanding of the reaction mechanism and the kinetics can be attained. The derivatization of cysteine containing intermediates and/or products using thiol reactive probes is a method that could provide valuable information of the LipA mediated reaction. This is mainly because the reaction is allowed to proceed for certain time period and after that the probe is then introduced, implying that there is no interference with the enzyme or substrate and the probe is only used to detect the intermediates and/or end products. There are many thiol reactive probe that are available from different commercial sources which can be used in differing reaction conditions, and so with time, it would be possible to identify the best probes and reaction conditions to carryout time course studies on the reaction. Equilibrium dialysis offers an interesting method for studying the interactions, as the process does not interfere with these but rather it's a study of equilibrium states. The RED experiments described here were unsuccessful since the substrate used was being trapped in the dialysis membrane. An attempt at using different dialysis membranes could be made until the right type of membrane, which allows the substrate to pass through it is identified and this can be used in experiments to determine K_m, υ_{max} and K_{max}, all of which are important kinetics parameters to know. The crystallization experiments carried out for this thesis have identified the possible conditions required for the crystallization of *Sulfolobus solfataricus* P2 LipA, however these conditions are far from being the optimal conditions. There is a lot of work that can still be carried out in optimizing the identified conditions and trying to grow large, well defined crystals from the "fine needles" so far obtained.

Chapter 3: Experimental

3.1 Materials

Reagents and materials were obtained from the following suppliers: bovine serum albumin (BSA) from Advanced Protein Products (Brierly Hill, UK); Chelating Sepharose fast flow resin from GE Healthcare (Amersham, UK); pBAD/HisA, *E. coli* TOP10 and BL21(DE3) competent cells from Invitrogen (Groningen, NL). Yeast extract and tryptone were purchased from Oxoid (Basingstoke, UK). Wang resin, fluorenylmethoxycarbonyl (Fmoc) amino acids, the coupling reagents (diisopropylcarbodiimide [DIC], benzotriazolyloxy-tris-[pyrrolidino]-phosphonium hexafluorophosphate [PyBOP] and hydroxybenzotriazole [HOBt]) were purchased from Novabiochem (Nottingham, UK). (*DL*)-Lipoic acid was purchased from Sigma–Aldrich (Poole, UK). *N*,*N*-Dimethylformamide (DMF) and *N*-methylpyrrolidone (NMP) were purchased from Rathburn Chemicals (Walkerburn, UK). HEPES and dithiothreitol (DTT) were purchased from Melford Laboratories (Ipswich, UK). Iodoacetamide, TCEP, *S*-adenosylmethionine chloride (AdoMet) and 5′-deoxyadenosine (AdoH) were purchased from Sigma-Aldrich (Poole, UK). Octanoic acid, HPLC-grade acetonitrile, and all other reagents were purchased from either Fisher Scientific (Loughborough, UK) or Sigma-Aldrich (Poole, UK). NAP-10 columns were purchased from Amersham Biosciences (Buckinghamshire, UK). Supelclean ™ LC-18 solid phase extraction columns from Supelco were purchased through Sigma-Aldrich (Poole, UK). The restriction enzymes and the digestion kit were acquired from Promega (Southampton, UK). All the concentrations given are final concentrations unless otherwise stated.

3.2 Instrumentation

Anaerobic Glovebox

All experiments using LipA were carried out in an anaerobic glovebox (Belle Technology, Portesham, UK) maintained under nitrogen at less than 0.2 ppm O_2.

Freeze drying

Samples were freeze dried using a Heto Power Dry LL3000.

Centrifugation

A Thermo Scientific Sorvall Evolution RC centrifuge with an SLC-6000 or SLA-1500 fixed angle rotor (Waltham, USA) was used for all the centrifugations.

Fluorescence measurements

Fluorescence measurements (microplate) were made in a POLARstar Omega plate reader (BMG Labtech, Aylesbury, UK) or a Safire2 plate reader (Tecan Group Ltd, Reading, UK). For the POLARstar Omega an excitation wavelength of 345 nm with a bandwidth of 10 nm, an emission wavelength of 440 nm with a bandwidth of 10 nm, 10 readings per well (each measurement), and an integration time of 20 μs were used. For the Safire^2 an excitation wavelength of 625 nm with a bandwidth of 5 nm, an emission wavelength of 670 nm with a bandwidth of 10 nm, 10 readings per well (each measurement), an integration time of 20 μs, and a gain of 170 were used. Data were analysed using SigmaPlot 11 (Systat Inc., San Jose, CA).

NMR

^{1}H NMR and ^{13}C NMR spectra were recorded using either a Bruker AC300 FT-NMR spectrometer (^{1}H, 300 MHz), a Bruker DPX 400 spectrometer (^{1}H, 400 MHz) or a Varian Innova 600 spectrometer (^{1}H, 600 MHz). COSY spectra were used for assignment of peptide ^{1}H NMR and HMQC spectra were used for assignment of ^{13}C NMR data.

Mass spectroscopy

Electrospray mass spectra were recorded on a Waters ZMD single quadrupole mass spectrometer. High resolution electrospray mass spectra were recorded on a Bruker Apex IIIFT-ICR mass spectrometer.

HPLC

Reversed-phase HPLC analysis was carried out on a Gilson 321 workcenter equipped with a dual wavelength UV-visible detector and a Shimadzu RF-10Axl fluorescence detector. For analytical HPLC methods; chromatograms were collected and analyzed using the Gilson Unipoint software (Gilson).

LC-MS

Reversed-phase HPLC analysis was carried out on a Gilson system workcenter and LCMS experiments coupled this HPLC via a 1:4 split into a Thermo Finnigan Surveyor MSQ electrospray mass spectrometer. The data were collected and processed using the XCalibur software system.

Fermentation

Fermentation was carried out in an Incubator Shaker Innova^{TM}4400 (New Brunswick Scientific).

UV-visible spectroscopy

UV-visible spectra of *S. solfataricus* LipA (1 mg/ml) were recorded with an Ocean Optics (Duiven, The Netherlands) USB2000 spectrophotometer using a light source Mini-D2-GS connected by optical fibres P-400-2-UV/SR to a cuvette holder inside the glove box.

3.3 The expression and purification of LipA

3.3.1 Preparation of media

2YT (1 L) media was prepared by mixing bacto-yeast extracts (10 g), bacto-tryptone (16 g), NaCl (5 g) in water (~ 500 mL). The pH of the mixture was adjusted to ~ 7.5 with 5M NaOH, and the volume of the mixture was made up to 1 L with distilled water. The media were sterilised by autoclaving on a 3 h water cycle. When preparing 5 L of 2YT media the total amount of each component in the mixture was simply increased to five times the values given here.

SOC (1 L) media was prepared by mixing bacto-yeast extracts (20 g), bacto-tryptone (5 g), and NaCl (5M, 2 mL) in distilled water (~ 900 mL). Thereafter KCl (1 M, 2.5 mL) was added followed by $MgSO_4$ (1 M, 10 mL), $MgCl_2$ (1M, 10 mL) and filter-sterilised glucose (2M, 10 mL). The volume of the mixture was adjusted to one litre with distilled water and after that sterilised by autoclaving on a 3 h water cycle.

3.3.2 Preparation of Buffers

Three different buffers A, B and C, all at pH = 7.5 were prepared by mixing the components as shown in Table 3.1. These buffers were degassed by bubbling nitrogen gas for 2 h, after which the containers were left open in an anaerobic glove box for over 24 h.

Table 3.1 *The different components of the buffers used for the purification of LipA.*

	Buffer A	**Buffer B**	**Buffer C**
Glycerol	10 % w/v (100 g)	10 % w/v (100 g)	10 % w/v (100 g)
HEPES	25 mM (5.96 g)	25 mM (5.96 g)	25 mM (5.96 g)
NaCl	500 mM (29 g)	500 mM (29 g)	100 mM (5.8 g)
Imidazole	500 mM (29 g)	250 mM (17 g)	-
pH of Buffer	7.5	7.5	7.5

3.3.3 Plasmids

The pBADHis derived vector pMK024 (pBADHis (lipAHis, iscSUA, hscBA, fdx)) was constructed by Dr Marco Kriek. This plasmid encodes the His tagged *lipA* gene from *Sulfolobus solfotaricus* (ORF no. SSO3158) and the *isc*, *hsc* and *fdx* genes. The plasmid also possesses an ampicillin resistance marker.

3.3.4 Transformation of Top 10 and BL21(DE3) competent cells

E. coli TOP 10 and BL21(DE3) competent cells were transformed with the plasmid pMK024 as follows. Cells and plasmid were incubated on ice for 15 min, after which period plasmid (1.0 μL) was added to the cells (50 μL). The resulting mixture was placed on ice for a further 30 min and then heat shocked in a water bath (42 ^{o}C, 45 s). The mixture was then placed on ice for 3 min and then SOC media (250 μL) was added. After that, the mixture was agitated at 190 rpm and 37 ^{o}C for an hour. Aliquots of cells (40 μL) were plated out onto ampicillin (100 mg/L) containing agar plates, which were then incubated at 37 ^{o}C for 12 h.

3.3.5 Mini-prep isolation of plasmid DNA

Plasmid DNA was extracted from overnight cell cultures of transformed cell colonies, using the Wizard® Plus SV Miniprep DNA purification system. Overnight cell culture (10 mL) was centrifuged (15 min, 4000 rpm), after which the supernatant was discarded and the pellet resuspended in cell resuspension solution (CRS). Cell lysis solution (CLS, 250 μL) was added and the mixture was tipped over several times to mix. Alkaline protease solution (APS, 10 μL) was added, mixed, and the mixture was incubated (5 min, room temp). Neutralisation solution (NSB, 350 μL) was added to the mixture which was then centrifuged at 13200 rpm for 15 min at room temperature. The lysate was decanted into a spin column in a collection tube and centrifuged at 13200 rpm for one min. The flow-through was discarded. The spin column was washed with an ethanol containing wash solution (750 μL) and centrifuged at 13200 rpm for one min. The flow-through was discarded, and the spin

column was washed again with the ethanol containing wash solution (250 μL). After the flow-through was discarded the spin column was dried by centrifuging (2 min, 13200 rpm, at room temperature). The DNA was eluted by placing the spin column in a new sterile 1.5 ml microcentrifuge tube, adding nuclease-free water (100 μL) and centrifuging (13200 rpm and room temperature) for 1 min. The DNA was stored at –20 °C.

3.3.6 Restriction enzymes digestions

The plasmid digestion was carried out using the Promega restriction enzymes digestion kit as follows: plasmid DNA (5 μL) was mixed with the selected 10 x buffer (1μL) solution for the enzymes, BSA (1μL, 1mg/mL), and each of the restriction enzymes (0.5 μL) needed for the digestion. The total volume was then made up to 10 μL with sterile water. The reaction mixture was incubated in a water bath (37 ^{o}C, 1 h 15 min). Samples were loaded on an agarose gel, which was set up across a constant voltage of 120 V for 1 h. The gel was developed in ethidium bromide and visualized using a UV lamp.

3.3.7 Cell growth and protein expression

Freshly prepared 2YT media (10 mL) containing ampicillin (100 mg/L) was inoculated with either single cell colonies from an agar plate grown overnight (37 ^{o}C and 190 rpm) or cells from a glycerol frozen cell stock. A New Brunswick Scientific BioFlo 110 ® fermentor (5 L) was used for the large-scale expression of the transformed cells in 2YT media. A fresh 2YT medium (5L) with ampicillin (100 mg/L) was inoculated using the overnight cultures. The bacterial cell cultures were then incubated at 37 ^{o}C and 190 rpm until the measured optical density (at 600 nm) for the mixture was between 0.8 and 1.0. Filter sterilised arabinose solution (20% w/v, 10 mL/L) was added to the mixture to induce protein expression. Growth was continued at 27 ^{o}C, 190 rpm for 4 h and cells were harvested by centrifugation

(Beckman JLA 10,500 rotor; 6000 rpm; 4 ^{o}C; 15 min) and the resulting cell pellets were stored at −80 ^{o}C.

3.3.8 Anaerobic purification of LipA [136]

Cell paste (30 - 40 g) was resuspended in anaerobic buffer A (3 mL/g of cells). Benzonase (4 µL, 25 U/µL) and lysozyme (10 mg) were added and the suspension was mixed on a magnetic stirrer for 1 h. The cells were lysed by sonication (10 mins, 1 s pulse). The lysate was centrifuged (13200 rpm, 4 ^{o}C, 30 min) and the supernatant was applied to a nickel-charged affinity column (Chelating Sepharose FF) equilibrated in buffer A. The column was washed with buffer A (five column volumes) and the protein was eluted with buffer B. The LipA containing fractions, observed by their characteristic black colour and monitored by recording a UV absorption chart were combined, concentrated to 20 mL (~10 mg/mL) and applied to an S-75 gel filtration column (33 × 750 mm) equilibrated with anaerobic buffer C. The purified protein was eluted with buffer C and the LipA containing fractions were identified by their characteristic deep black colour, and also monitored by recording a UV absorption chart and further characterised by SDS-PAGE were stored at 80 ^{o}C in 10 mL aliquots.

3.3.9 Preparation of agarose gel

Agarose gels (1% (w/v)) were prepared by mixing agarose powder and tris-acetate-EDTA (TAE) (1M) solution. Two sizes of gel were prepared, 140 mL volume (1.4 g of agarose) or 40 mL volume (0.4 g of agarose). The appropriate amount of agarose powder was dissolved in TAE and the solution was heated in a microwave oven and then poured onto a mould. A plastic comb with the wanted total number of wells was placed into the solution. The solution was then allowed to set in the cold room (4 ^{o}C).

3.3.10 SDS-PAGE electrophoresis

A 15% resolving gel (10 mL, 5 mL per plate) and a stacking gel were prepared by mixing the gel components as shown in Table 3.2. The resolving gel (5 mL) was poured into the gel cassette and its surface was covered with a thin layer of isopropanol (50%). The gel was allowed to set after which the thin layer of isopropanol was carefully removed. The stacking gel was prepared and applied on top of the resolving gel and a plastic comb was inserted into the gel solution. The gel was left to set for 1 h, the comb was removed and the wells were washed with distilled water.

Table 3.2 *Preparation of the loading and stacking gel for SDS gel analysis.*

	Stacking gel (mL)	**Resolving gel (mL)**
H_2O	3.4	4.0
30% Acrylamide / bis acrylamide mix	0.83	3.3
1.5 M Tris buffer (pH 8.8) or (pH 6.8)	0.630	2.500
10% SDS	0.050	0.100
10% Ammonium persulfate	0.050	0.100
TEMED	0.002	0.004

3.3.11 Sulfide analysis

Sulfide analysis was carried out according to the method of Beinert.[156]

3.3.12 Iron content analysis

Iron content analysis was carried out according to the method of Fish.[201] ***Solution A*** was prepared by mixing equal amounts of concentrated HCl (1 mL in 10 mL of water) and $KMnO_4$ (450 μg in 10 mL of water). ***Solution B*** was prepared by mixing ferrozine (80 mg), neocuproine (80 mg), ascorbic acid (8.0 g) and ammonium acetate (9.7 g). Water was added to make the final volume of the solution 25 mL. Standard Fe-solutions were prepared by dissolving $FeSO_4.7H_2O$ (50 mg) in water (10 mL), to give a concentration of 5 mg/mL solution. 100 μL of this solution was diluted to 10 mL in water to give a 50 μg/mL solution. Serial dilution of this solution in buffer D was carried out as shown in the Table 3.3.

Table 3.3 *Preparation of standard Fe^{2+} solutions for iron content analysis.*

Volume of buffer D	**Volume of Fe^{2+} (50 «g/mL) solution**	**Concentration of Fe^{2+} («M)**	**$A_{562\ nm}$**
600	400	71.94	0.475
650	350	62.95	0.435
700	300	53.96	0.380
750	250	44.96	0.305
800	200	35.97	0.235
850	150	26.98	0.219
900	100	17.99	0.158
950	50	8.99	0.087
970	30	5.40	0.054
990	10	1.80	0.045

Solution A (500 μL) was added to the samples and these were heated at 60 ^{o}C for 2 h. Thereafter solution B (100 μL) was added to the sample solutions and the mixture was left for 15 min. The absorbance at 562 nm was recorded for the standard Fe-solutions and the protein samples. A linear plot of the absorbance of each standard Fe-solution as a function of its theoretical concentration was made. The equation for this line was of the form $\boldsymbol{y = mx + c}$ where the absorbance at 562 nm is y, the protein concentration is x and the intercept is c. This equation was used to calculate the concentration of the protein sample based on the measured absorbance. When the absorbance of the test sample was outside of the absorbance range for the standards, then the assay was repeated with a more appropriate dilution.

3.3.13 Determination of protein concentration

Protein concentrations were determined using the method described by Bradford [202], and having bovine serum albumin (BSA) as a standard. The Bradford reagent was prepared by dissolving Coomassie Brilliant Blue G-250 (100 mg) in 95% ethanol (50 mL) and adding 85% (w/v) phosphoric acid (100 mL). When the dye had completely dissolved this solution was diluted to one litre and filtered through a Whatman paper.

3.3.14 Reconstitution of Lip A

UV spectrum of LipA (250-700 nm) was recorded from which the A_{420}/A_{280} ratio was calculated. A NAP-10 column was equilibrated with Buffer D (25 mM HEPES, pH 7.5), and LipA (1 mL ~20 mg/ mL, ~0.6 mM) was applied to the column and eluted with Buffer D. A Bradford assay [202] was used to determine the protein concentration. DTT (5mM final concentration) was added to the LipA, and the mixture was incubated for 30 min at room temperature. $FeCl_3$ (5 mole equivalent) was added to the LipA followed by the drop-wise addition of $Na_2S.9H_2O$ (10 mole equiv.). The mixture was incubated at room temperature for 90 min. The mixture was then centrifuged at 10,000 rpm.

3.4 Testing fluorophores for stability in the presence of sodium dithionite

6-Carboxyfluorescein, 3-bromomethyl-7-methoxy-1,4-benzoxazin-2-one, coumarin 343, rhodamine B, *N*-(iodoacetaminoethyl)-1-naphthylamine-5-sulfuric acid, 4-bromomethyl-6,7-dimethoxycoumarin and 7-mercapto-4-methylcoumarin (Chapter 2, Scheme 2.2) were tested for stability in the presence of sodium dithionite as follows. Stock solutions of reactants were prepared as shown in Table 3.4, and thereafter, the solutions were added to a cuvette in the volumes shown. The total final volume was 500 μL. The cuvette was placed into a fluorescence detector, and the change in the reaction mixture's fluorescence intensity was recorded over a period of 30 min. The control experiments were set up using the same reagents and conditions except that no sodium dithionite was added to the mixture.

Table 3.4 *Testing fluorophores for stability in the presence of sodium dithionite.*

Compound	**Stock solution**	**Final Concentration**	**Final volume Ε«L)**
Water	-	-	300
DTT	10 mM	1 mM	50
Fluorophore	500 μM	50 μM	50
Sodium dithionite	10 mM	1 mM	50
HEPES Buffer (25mM, pH 7.5)	250 mM	25 mM	50

Preparation of dry ethanol

Iodine (0.5 g) was added to magnesium turning (5.0 g), followed by commercial absolute alcohol (75 mL). The mixture was warmed to dissolve all the iodine and then heating was continued until the magnesium turnings were converted to ethoxide. After this more absolute alcohol (900 mL) was added and the mixture was refluxed for 30 min. The ethanol was then distilled into a sealed, oxygen free dry storage vessel.

3.5 Synthesis of 7-(diethylamino)-2-oxo-2H-chromene-3-carboxylic acid (38) [203]

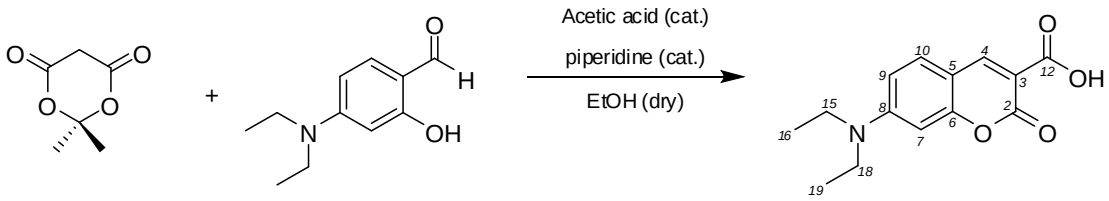

2,2-Dimethyl-1,3-dioxane-4,6-dione (1.87 g, 13.0 mmol) and 4-(diethylamino)-salicyclaldehyde (2.50 g, 13.0 mmol) were dissolved in ethanol (20.0 mL). Thereafter piperidine (50 µL) and glacial acetic acid (30 µL) were added to the reaction mixture which was then stirred at room temperature for 48 h and then finally refluxed for a further 4 h. The product was precipitated as an orange powder (Yield 3.09 g, 91 %); m.p. 220.5 – 226.5 ^{o}C (lit. m.p. 228.9 – 230.85 ^{o}C).[203] $\mathbf{R_f}$ 0.50 (chloromethane /methanol, 9:1), **ES-MS:** *m/z* 284 ($[M+Na]^+$, 100 %), 262 ($[M+H]^+$, 18 %). **^{1}H NMR** (300MHz, $CDCl_3$) δ = 12.4 (1H, br s, OH), 8.66 (1H, s, H-4), 7.44 (1H, d, $J_{10,9}$ = 8.5 Hz, H-10), 6.75 (1H, d, $J_{9,10}$ = 8.5 Hz, H-9), 6.54 (1H, s, H-7), 3.48 (2H, q, $J_{15,16}$ = 7.3 Hz, H-15), 3.48 (2H, q, $J_{18,19}$ = 7.3 Hz, H-18), 1.26 (3H, t, $J_{16,15}$ = 7.3 Hz, H-16), 1.26 (3H, t, $J_{19,18}$ = 7.3 Hz, H-19). **^{13}C NMR** (75 MHz, $CDCl_3$) δ = 165.5 (C-12), 164.4 (C-6), 158.0 (C-2), 153.8 (C-8), 150.3 (C-4), 132.0 (C-10), 111.0 (C-3), 108.6 (C-5), 105.6 (C-9), 96.9 (C-7), 45.4 (C-18), 45.4 (C-15), 12.4 (C-19), 12.4 (C-16).

The spectroscopic data corresponds to that found in literature.[204]

3.6 Solid phase peptide synthesis of the peptide substrate analogues

3.6.1 *Synthesis of Octanoyl chloride* [205]

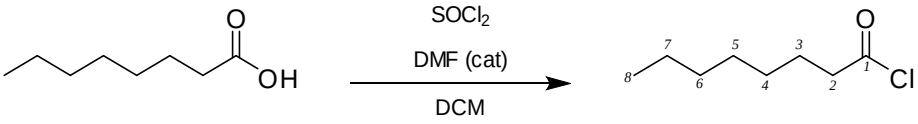

octanoic acid — octanoyl chloride

Octanoic acid (2.00 g, 0.014 mol) was added to DCM (7.0 mL) and the mixture was stirred under N_2 gas (5 min). Thionyl chloride (2.40 g, 0.020 mol) was added to the mixture, followed by DMF (1.0 mL). The reaction mixture was then stirred overnight. Evaporating the solvent *in vacuo* gave a crude product from which the octanoyl chloride was purified by micro-distillation. A yellowish liquid was obtained for the purified octanoyl chloride (Yield 2.00 g, 88 %); b.p. (70 – 74 ^{o}C, 10 mmHg), (lit. b.p. 73 ^{o}C, 10 mmHg). $\neg_{max}/cm^{-1}$ (KBr) 2927 (CH_2), 2858 (CH_2) and 1795 (C=O). ^{1}H NMR (300MHz, $CDCl_3$) δ = 2.88 (2H, t, $J_{2,3}$ = 7.3 Hz, H-2), 1.71 (2H, quin, $J_{3,2}$ = 7.3 Hz, $J_{3,5}$ = 6.8 Hz, H-3), 1.40 - 1.23 (8H, m, H-4, 5, 6, 7), 0.87 (3H, t, $J_{8,7}$ = 6.8 Hz, H-8). **^{13}C NMR** (75 MHz, $CDCl_3$) δ = 173.8 (C-1), 47.1 (C-2), 31.5 (C-6), 28.7 (C-5), 28.4 (C-4), 25.0 (C-3), 22.5 (C-7), 14.0 (C-8).

3.6.2 Coupling of Octanoyl chloride to Fmoc-Ly-OH

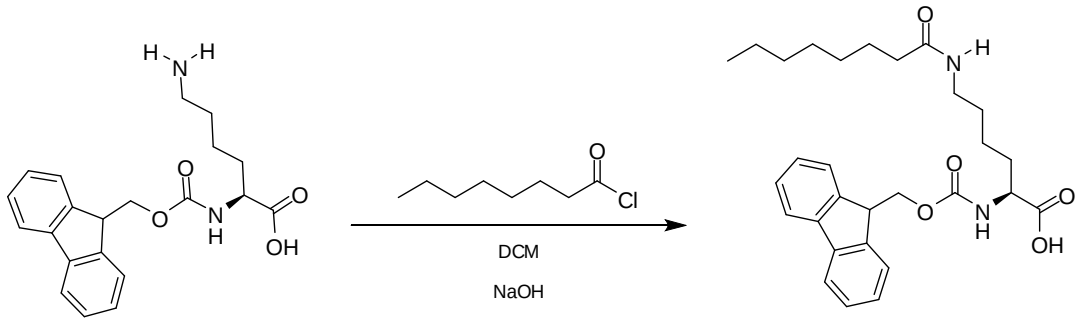

Fmoc - Lys - OH

Fmoc - Lys (Oct) - OH

Fmoc-Lys-OH (0.378 g, 1.03 mmol) was suspended in DCM (5 mL) and then NaOH (2M, 3.00 mL) solution was added to the suspension. The reaction mixture was stirred for 5 min, after which octanoyl chloride (0.25 g, 1.54 mmol, 260 μL) was slowly added. The mixture was then stirred for 3 h at room temperature. The organic phase was separated and washed with NaOH solution (3x 5 mL), dried on $MgSO_4$ and concentrated *in vacuo* to give a yellow solid. This solid was not soluble in common solvents making it difficult to characterise by the conventional procedures. A sample of the solid was sent for analysis by MALDI TOF mass spectrometry. The spectrum obtained did not contain show signals expected for the title compound. Rather it indicated the presence of some unidentified compound(s). IR analysis of the aqueous phase indicated the presence of octanoyl chloride: $\neg_{max}/cm^{-1}$ (KBr) 2927 (CH_2), 2858 (CH_2) and 1795 (C=O). After this, the aqueous solution was acidified with HCl (2M) to a pH ~ 6 inducing precipitation of a whitish solid. The white solid was collected by filtration and the filtrate analysed by ESI mass spectroscopy. This analysis indicated the presence of Lys-OH (**ES-MS:** *m/z* = 317 the $[M+H]^+$ ion), the product of Fmoc-deprotection of Fmoc- Lys-OH. It was concluded that the basic conditions for the Schotten-Baumann procedure were sufficient to cause the deprotection of the Fmoc group from Fmoc- Lys-OH. Therefore the Schotten-Baumann approach was deemed unsuitable for use in the coupling of octanoic acid during the synthesis of octanoylated peptides. An alternative approach was to use the orthogonal Dde protection of the lysine residue which would allow for the coupling of octanoic acid to be carried to the Fmoc protected α-amino acids.

3.6.3 *Loading of Fmoc-Ile-OH onto the Wang resin.*

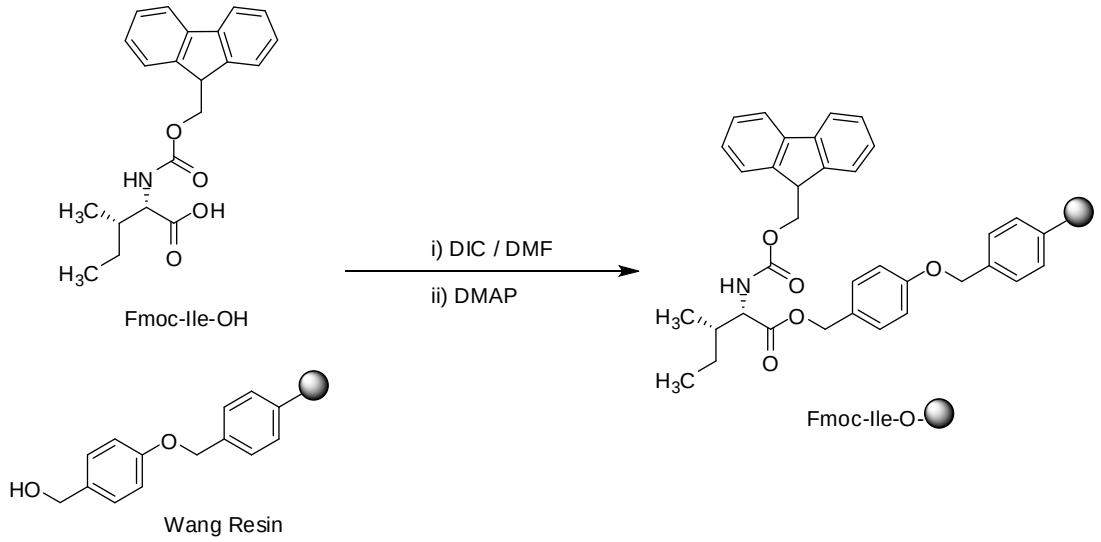

Fmoc-Ile-OH (2.24 g, 6.34 mmol) was added to DMF (10 mL) and stirred. DIC (0.50 mL, 3.20 mmol) was added to the mixture which was stirred for a further 10 min. The reaction mixture was then added to Wang resin (1.84 g, 0.44 mmol/g) previously swelled in DMF for 30 min. Then DMAP (0.054 g, 0.4 mmol) was added to the reaction mixture. The flask was placed in an ultrasonic bath (2 h, room temperature) after which the resin was filtered, washed alternately with DCM (3 x 30 mL), DMF (3 x 30 mL) and diethyl ether (3 x 30 mL) and was finally dried *in vacuo*. 3.00 g of resin was obtained.

3.6.4 Capping of the resin's unreacted groups

Pyridine (1.00 mL, 12.40 mmol) and benzoyl chloride (1.00 mL, 8.60 mmol) were added to DCM (30 mL) and the mixture was cooled to 0 ^{o}C. Loaded Wang resin (1.54 g) was added to the solution and the resulting mixture was agitated in an ultrasonic bath (15 min, room temperature). The resin was filtered, washed alternately with DCM (3 x 30 mL) and diethyl ether (3 x 30 mL) and then dried *in vacuo*. This capped resin (2.20g) was stored at –20 ^{o}C.

3.6.5 Determining loading of resin (Quantitative Fmoc Test

Piperidine in DMF (20%, v/v; 1.5 mL) was added to an accurately weighed-out amount of resin (<5 mg) and the mixture was allowed to settle for 15 min. The resin was then filtered through a glass pipette (with a glass wool plug) and the filtrate was diluted to 25 mL with the 20% piperidine in DMF solution. The absorbance at 302 nm (A_{302}) was recorded using the 20% piperidine/DMF as the blank and equation 3.1 was used to determine the loading yield. The loading achieved on the Wang resin was 0.35 mmol/g, which was a yield of 75 %.

$$Loading\ (mmol/g) = \left[\frac{(A_{302} \times V)}{(\varepsilon_{302} \times M)}\right] \times 1000 \qquad (equation\ 3.1)\ [206]$$

A_{302} = absorbance of the piperidyl-fulvene adduct

V = the final total volume (25 mL)

M = accurately weighed out mass of resin

ε_{302} = Molar extinction co-efficient of the piperidyl-fulvene adduct at 302 nm (7800 $M^{-1}cm^{-1}$)

3.6.6 The Ninhydrin test (Kaiser Test) [207, 208]

The following three test solutions were prepared: **Solution A:** ninhydrin (1.25 g) was dissolved in ethanol (25 mL) (5% w/v). **Solution B:** phenol (20 g) was dissolved in ethanol (5 mL) (4:1). **Solution C:** KCN (32 mg) was dissolved in water (50 mL) then 1 mL of this solution was diluted to 50 mL with pyridine. The test was carried out by adding 5 drops of a solution prepared by mixing the above in the following ratio; Solution A: Solution B: Solution C (2: 1: 1) to the test-sample in a small glass tube and heating the tube to 100 ^{o}C for 5 min. A positive result was a blue colour indicating the presence of free amines on the peptide (*i.e.* complete deprotection or incomplete coupling). A negative result was when the resin did not change colour (*i.e.* incomplete deprotection or complete coupling).

3.6.7 *Synthesis of 2-acetyldimedone (Dde)*

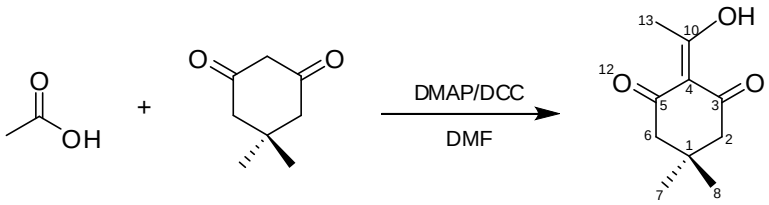

Glacial acetic acid (6.75 mL, 0.095 mol) was added to DMF (220 mL) and stirred. Dimedone (14.00 g, 0.10 mol) was added to the mixture followed by DCC (25.00 g, 0.13 mol) and then DMAP (11.50 g, 0.10 mol). The reaction mixture was stirred for 48 h at room temperature generating a white precipitate that was removed by filtration. DMF in the filtrate was removed by azeotropic distillation with toluene (100 mL) and evaporated on a rotary evaporator. The residue was redissolved in a minimum amount of ethyl acetate (15 mL) and the resulting solution was washed with 1M $KHSO_4$ (4 x 50 mL). The aqueous solution was acidified with 5M HCl and then extracted with DCM (3 x 15 mL). The organic layer was dried over $MgSO_4$, concentrated in *vacuo* and purified by column chromatography silica (ethyl acetate: hexane (1:4)) to give 2-acetyldimedone (Yield 8.35 g, 48 %) as a white solid, m.p. 34.0 – 42.0 ^oC (lit. m.p. 36 – 40 ^oC). $\mathbf{R_f}$ 0.32 (ethyl acetate/hexane, 4:1), **ES-MS:** *m/z* 183.2 ([M+H], 100%). $^{\mathbf{1}}\mathbf{H}$ **NMR** (300 MHz, $CDCl_3$) δ = 2.61 (3H, s, H-13), 2.54 (2H, s, H-6), 2.37 (2H, s, H-2), 1.08 (6H, s, H-8, H-7). $^{\mathbf{13}}\mathbf{C}$ **NMR** (75 MHz, $CDCl_3$) δ = 202.4 (C-10), 197.9 (C-3), 195.2 (C-5), 112.3 (C-4), 52.4 (C-2), 46.8 (C-6), 30.6 (C-13), 28.5 (C-1), 28.2 (C-8, C-7).

3.6.8 Preparation of Fmoc-Lys(Dde)-OH

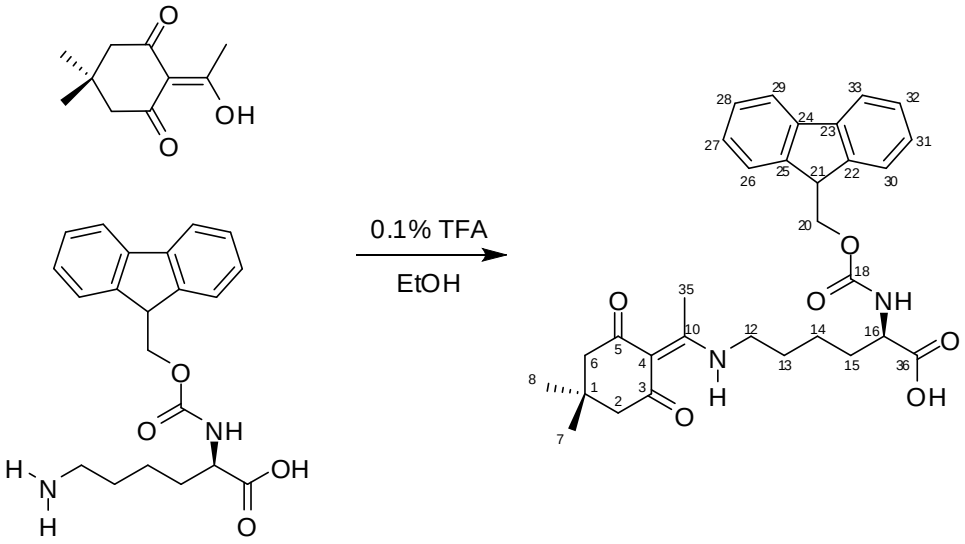

Fmoc-Lys-OH (1.53 g, 4.20 mmol) was added to Dde (1.60 g, 8.78 mmol) followed by ethanol (20 mL) and the resultant mixture was stirred to mix. After this, TFA (0.03 mL, 0.40 mmol) was added and then the reaction mixture was refluxed for 72 h. The solvent was then evaporated and the orange residue obtained was redissolved in minimal ethyl acetate (10 mL). The resultant solution was washed with 1M $KHSO_4$ (2 x 20 mL) and then dried over $MgSO_4$. The solvent was removed in vacuo to give yellow oil which was redissolved in ethyl acetate (10 mL). Drop-wise addition of the reaction mixture into ice cold hexane (20 mL) yielded the product as a white solid which was collected by filtration, washed with hexane (3 x 15 mL) and finally vacuum dried (Yield 2.12 g, 95%), m.p. 76.0 – 82.5 ^{o}C (lit. m.p. 80.0 ^{o}C). $\mathbf{R_f}$ 0.20 (methanol, acetic acid, 4:1). **ES-MS:** *m/z* 533 ($[M+H]^+$, 75 %); 555 ($[M+Na]^+$, 21 %). **^{1}H NMR** (300MHz, $CDCl_3$) δ = 7.75 (1H, d, $J_{33,32}$ = 7.3 Hz, H-33), 7.74 (1H, d, $J_{29,28}$ = 7.3 Hz, H-29), 7.56 (1H, d, $J_{30,31}$ = 7.3 Hz, H-30), 7.56 (1H, d, $J_{26,27}$ = 7.3 Hz, H-26), 7.30 (1H, dd, $J_{32,31}$ = 7.5 Hz, $J_{32,33}$ = 7.3 Hz, H-32), 7.30 (1H, dd, $J_{28,27}$ = 7.5 Hz, $J_{28,29}$ = 7.3 Hz, H-28), 7.21 (1H, dd, $J_{31,32}$ = 7.4 Hz, $J_{31,30}$ = 7.3 Hz, H-31), 7.21 (1H, dd, $J_{27,28}$ = 7.5 Hz, $J_{27,26}$ = 7.3 Hz, H-27), 4.49 (1H, t, $J_{16,15}$ = 8.6 Hz, H-16), 4.24 (2H, d, $J_{20,21}$ = 6.6 Hz, H-20), 3.93 (1H, t, $J_{21,20}$ = 6.6 Hz, H-21), 3.40 (2H, t, $J_{12,13}$ = 7.1 Hz, H-12), 2.34 (1H, s, H-6), 2.34 (1H, s, H-2), 2.17 (3H, s, H-35), 2.08 (1H, t, J = 7.6 Hz, H-15), 1.82 (2H, quin, $J_{13,14}$ = 7.3 Hz, J = 7.1 Hz, H-13), 1.18 (2H, quin, J = 7.6 Hz, $J_{14,13}$ = 7.3 Hz, H-14), 1.11 (3H, s, H-7), 0.95 (3H, s, H-8). **^{13}C NMR** (75 MHz, $CDCl_3$) δ = 198.3 (C-3, C-5), 174.4 (C-10), 174.0 (C-36), 156.1 (C-

18), 143.8 (C-25), 141.2 (C-24, C-23), 127.7 (C-28, C-32), 127.0 (C-27, C-31), 125.1 (C-26, C-30), 119.9 (C-29, C-33), 107.8 (C-4), 67.0 (C-20), 53.4 (C-16), 52.3 (C-6, C-2), 47.1 (C-21), 43.3 (C-12), 31.9 (C-15, C-13), 30.1 (C-1), 28.3, 28.1 (C-8, C-7), 22.4 (C-14), 18.2 (C-35).

3.6.9 Coupling of Fmoc-Lys(Dde)-OH to Ile-Wang resin

Fmoc-Lys(Dde)-OH (1.04 g, 1.95 mmol) and HOBt (0.26g, 1.98 mmol) were dissolved in a minimal amount of DMF (5 mL) . DIC (0.25 g, 1.95 mmol) was added and the solution was stirred for approximately 5 min by which time a white precipitate was beginning to form in the flask. The activated amino acid solution was then added to the peptidyl resin in the reaction vessel and the mixture was agitated for 1 h. The resin was then filtered, washed with DMF (3 x 10 mL) and the ninhydrin test used to confirm completion the coupling reaction.

3.6.10 Dde deprotection

A mixture of imidazole (0.96 g, 1.35 mmol) and hydroxylamine hydrochloride (1.32 g, 1.80 mmol) suspended in *N*-methylpyrrolidone (5.00 mL) was agitated in an ultrasonic bath to dissolve the solid. DMF (1.00 mL) was added then the resultant solution was added to the peptidyl resin (1.00 g). After agitation in an ultrasonic bath for 3 h, the resin was dried by filtration and washed repeatedly with DMF (10 mL, 5 x 1 min). The presence of free amino groups was confirmed by the Ninhydrin test on a sample of the resin.

3.6.11 Coupling of octanoic acid

Octanoic acid (0.47 g, 3.20 mmol) was dissolved in DMF (10 mL). PyBoP (1.61 g, 3.09 mmol) and diisopropylethylamine (DIPEA) (0.50 mL, 2.90 mmol) were added and the resultant mixture was added to the peptidyl resin. The suspended resin was

agitated for 1 h and then filtered and washed with DMF (3 x 10 mL). Completion of the coupling reaction was confirmed using the Kaizer test.

3.6.12 Coupling of Fmoc-Glu(tBu)-OH

Fmoc-Glu(O*t*Bu)-OH (0.83 g, 1.95 mmol) and HOBt (0.26 g, 1.98 mmol) were dissolved in a minimal amount of DMF. DIC (0.25 g, 1.95 mmol) was added and the solution was stirred until a white precipitate was beginning to form in the flask. The activated amino acid solution was then added to the peptidyl resin and the mixture was agitated for 1 h. The resin was then filtered, washed with DMF (3 x 10 mL) and the Ninhydrin test was used to confirm completion of the coupling.

3.6.13 Coupling of Fmoc-Thr(tBu)-OH

Fmoc-Thr(*t*Bu)-OH (0.78 g, 1.95 mmol) and HOBt (0.26g, 1.98 mmol) were dissolved in a minimal amount of DMF (5 mL). DIC (0.25 g, 1.95 mmol) was added and the solution was stirred until a white precipitate was formed in the flask. The activated amino acid solution was then added to the peptidyl resin in the reaction vessel and the mixture was agitated for 1 h. The resin was then filtered, washed with DMF (3 x 10 mL) and the Ninhydrin test was then used to confirm completion of the coupling.

3.6.14 Cleavage of peptides from the resin

The peptidyl resin was put into a flask and a mixture of anisole/water/TFA (1: 1: 9) (5 mL) was added and the resin was stirred (2 h), after which time the liquid was drained. The resin was washed with TFA (3x 7.5 mL). The peptide was precipitated by adding the mixture into diethyl ether (10 mL). The resultant suspension was centrifuged (3000 rpm, 5 min) to separate the peptide as the pellet.

3.6.15 Preparation of the tripeptide substrate analogues

The basic procedure used to prepare the fluorescent pentapeptide was applied in the synthesis of the tripeptide substrate analogues. For all the peptides synthesized the common steps used were until Dde deprotection after which the difference lay in whether octanoic acid or nonanoic acid was coupled. Thereafter for the tripeptides one more amino acid (Fmoc-Glu(*t*Bu)-OH) was coupled whilst for the pentapeptide two more amino acids, (Fmoc-Thr(*t*Bu)-OH and Fmoc-Glu(*t*Bu)-OH) were coupled, and the fluorescent coumarin was attached. The tripeptides were analysed by HPLC and purified either preparatively on an HPLC or using a prepacked Supelclean ™ LC-18 solid phase extraction column.

3.6.16 Synthesis of octanoyl tripeptide (Glu-Lys(Oct)-Ile-OH)

Fmoc-Ile-OH (2.27 g, 6.42 mmol) was loaded onto Wang resin and followed by the coupling of Fmoc-Lys(Dde)-OH (0.72 g, 1.36 mmol, and 4 eq). Thereafter Dde deprotection was carried out to afford the coupling of octanoic acid (0.52 mL; 0.47g; 3.26 mmol) to the lysine residue. The third amino acid, Fmoc-Glu(*t*Bu)-OH (1.00 g, 2.36 mmol) was then coupled to complete the synthesis of the octanoyl tripeptide. Trifluoroacetic acid was used to cleave the peptide from the resin using and the crude product was obtained upon evaporating the acid *in vacuo*. The tripeptide was analysed by HPLC and either purified preparatively on an HPLC column or purified using a prepacked Supelclean ™ LC-18 solid phase extraction column.

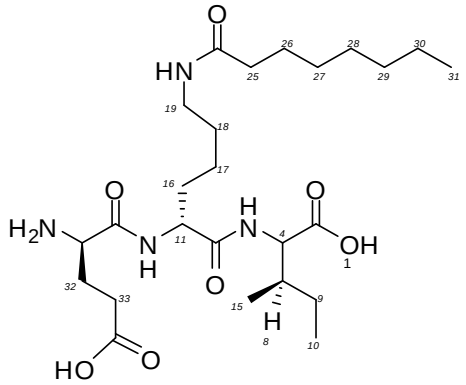

(**39**)

EK(Oct)I

The product was obtained as a white solid (Yield 198.9 mg, 29 %). Rf 0.14(reverse phase, acetonitrile/water 1:1); **ES-MS:** *m/z* 515 ($[M+H]^+$, 100 %), 539 ($[M+Na]^+$, 40 %). **^{1}H NMR** (300MHz, D_2O) δ = 4.57 (1H, dd, $J_{11,16}$ = 15.0 Hz, J = 7.2 Hz, H-11), 4.42 (1H, dd, J = 8.6 Hz, $J_{4,8}$ = 6.7 Hz, H-4), 3.36 (1H, t, $J_{23,32}$ = 8.4 Hz, H-23), 2.67 (2H, t, $J_{19,18}$ = 6.8 Hz, H-19), 2.45 (1H, t, $J_{32,33}$ = 7.2 Hz, H-32), 2.25 (2H, t, $J_{25,26}$ = 7.7 Hz, H-25), 2.14 – 1.93 (5H, m, H-8, H-16, H-32, H-33), 1.57 – 1.56 (4H, m, H-18, H-26), 1.45 – 1.32 (11H, m, H-9, H-17, H-27, H-28), H-29, H-30), 0.88 (3H, d, $J_{15,8}$ = 6.3 Hz, H-15), 0.89 (3H, t, $J_{10,9}$ = 7.1 Hz, H-10), 0.87 (3H, t, $J_{31,30}$ = 6.8 Hz, H-31).

3.6.17 Synthesis of nonanoyl tripeptide (Glu-Lys(Non)- Ile-OH)

The first amino acid Fmoc-Ile-OH (2.27 g, 6.42 mmol) was loaded onto the Wang resin, followed by the coupling of Fmoc-Lys(Dde)-OH (0.72 g, 1.36 mmol, 4 eq). After the Dde deprotection, nonanoic acid (0.68 mL; 4.3mmol) was coupled to the lysine residue. Fmoc-Glu(*t*Bu)-OH (1.00 g, 2.36 mmol) was then coupled to complete the synthesis of the tripeptide which was then cleaved from the resin using trifluoroacetic acid to give a white crude product (Yield 45 mg, 35 %). The tripeptide was analysed by HPLC and either purified preparatively on an HPLC or purified using a prepacked Supelclean ™ LC-18 solid phase extraction column.

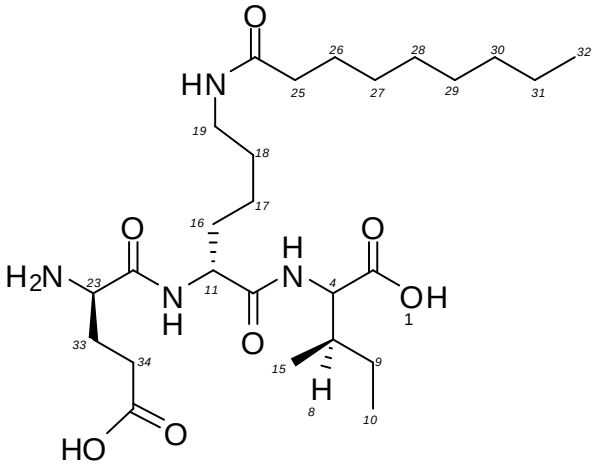

(**41**)

EK(Non)I

R_f 0.20 (reverse phase, acetonitrile/water 1:1); **ES-MS:** *m/z* 529 ($[M+H]^+$, 100 %), 551 ($[M+Na]^+$, 40 %). **^{1}H NMR** (300MHz, D_2O) δ = 4.57 (1H, t, $J_{11,16}$ = 6.3 Hz, H-11), 4.42 (1H, d, $J_{4,8}$ = 6.0 Hz, H-4), 4.25 (1H, t, $J_{23,33}$ = 8.2 Hz, H-23), 3.36 (2H, t, $J_{19,18}$ = 6.7 Hz, H-19), 2.67 (2H, $J_{33,34}$ = 7.0 Hz, H-33), 2.41 (2H, t, $J_{25,26}$ = 7.7 Hz, H-25), 2.33 (2H, d, $J_{34,33}$ = 7.0 Hz, H-34), 1.86 (2H, q, $J_{8,9}$ = 8.5 Hz, H-8), 1.76 (1H, t, $J_{16,17}$ = 7.6 Hz, H-16), 1.58 (2H, quin, $J_{26,25}$ = 7.7 Hz, J = 7.5 Hz, H-26), 1.46 (2H, quin, $J_{18,17}$ = 7.3 Hz, J = 6.8 Hz, H-18), 1.43 (1H, q, $J_{9,10}$ = 7.1 Hz, H-9), 1.35 – 1.27 (2H, m, H-17, H-27, H-28, H-29), 1.25 (2H, q, $J_{31,30}$ = 7.4 Hz, J = 6.8 Hz, H-31), 1.22 (2H, d, $J_{30,29}$ = 7.4 Hz, H-30), 0.92 (3H, t, $J_{10,9}$ = 7.1 Hz, H-10), 0.89 (3H, d, $J_{15,8}$ = 6.3 Hz, H-15), 0.83 (3H, t, $J_{32,31}$ = 6.8 Hz, H-32).

3.6.18 Synthesis of the octanoyl tetrapeptide (Thr-Glu-Lys(Oct)-Ile-OH)

The octanoyl tetrapeptides was prepared using the general solid phase peptide protocol. After the Fmoc-deprotection of Fmoc-Ile-Wang resin (1.00 g, 0.25 mmol/g), Fmoc-Lys(Dde)-OH (0.40 g, 3 equiv) was coupled. The Dde protecting group was then removed and followed by the coupling of the octanoic acid (0.18 mL, 5 equivalents) to the lysine side chain. The third amino acid Fmoc-Glu(*t*Bu)-OH (1.00 g, 2.36 mmol) and the fourth amino acid Fmoc-Thr(*t*Bu)-OH (0.78 g, 1.95 mmol) were then coupled to complete the synthesis of the compound. Trifluoroacetic acid was used to cleave the peptide from the resin using and the crude product was obtained upon evaporating the acid *in vacuo*. The tetrapeptide was analysed by HPLC and either purified preparatively on an HPLC column or purified using a prepacked Supelclean ™ LC-18 solid phase extraction column. The tetrapeptide was eluted in water/acetonitrile (9:1) and the required fractions were pooled then the solvent was removed by freeze drying.

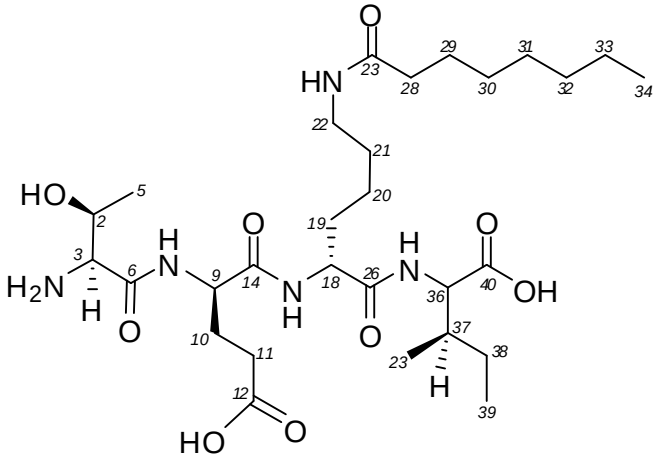

(**41**)

TEK(Oct)I

A white solid (Yield 116.4 mg, 50 %); $\mathbf{R_f}$ 0.20 (reverse phase, acetonitrile / water (1:3). **ES-MS**: *m/z* 616 ($[M+H]^+$, 100%), 638 ($[M+Na]^+$, 45 %).**^{1}H NMR** (300MHz, D_2O) δ = 4.55 (1H, dd, $J_{9,10}$ = 9.0 Hz, J = 4.5 Hz, H-9), 4.36 (1H, dd, $J_{18,19}$ = 6.7 Hz, J = 8.6 Hz, H-18), 4.22 (1H, dd, J = 8.6 Hz, $J_{36,37}$ = 6.7 Hz, H-36), 4.20 (1H, dq, $J_{2,5}$ = 6.0 Hz, J = 3.0 Hz, H-2), 3.88 (1H, td, J = 8.1 Hz, J = 3.0 Hz, H-3), 2.98 (2H, td, $J_{22,21}$ = 6.8 Hz, J = 5.4 Hz, H-22), 2.30 (2H, t, $J_{11,10}$ = 6.7 Hz, H-11), 2.17 (2H, t, $J_{28,29}$ = 7.7 Hz, H-28), 1.86 (1H, s, H-37), 1.94 (1H, t, $J_{10,11}$ = 6.7 Hz, H-10), 1.63

(2H, t, $J_{19,20}$ = 7.6 Hz, H-19), 1.57 – 1.35 (6H, m, H-21, H-29, H-30), 1.29 (3H, d, $J_{5,2}$ = 6.1 Hz, H-5), 1.23 - 1.18 (8H, m, H-20, H-31, H-32, H-33), 1.21 (2H, q, $J_{38,39}$ = 7.1 Hz, H-38), 0.95 (3H, d, $J_{42,37}$ = 6.3 Hz, H-42), 0.89 (3H, t, $J_{39,38}$ = 7.1 Hz, H-39), 0.85 (3H, t, $J_{34,33}$ = 6.8 Hz, H-34). **^{13}C NMR** (100 MHz, D_2O) δ = 176.4 (C-14), 176.0 (C-24), 174.9 (C-40), 173.5 (C-12), 172.2 (C-26), 171.6 (C-6), 69.1 (C-2), 59.6 (C-36), 58.7 (C-3), 52.6 (C-9), 52.3 (C-18), 40.3 (C-22), 37.3 (C-28), 36.4 (C-37), 31.2 (C-32), 30.9 (C-19), 30.3 (C-11), 29.2 (C-30), 28.5 (C-31), 28.5 (C-21), 27.1 (C-10), 26.9 (C-29), 30.8 (C-38), 30.5 (C-20), 30.4 (C-33), 18.3 (C-5), 15.0 (C-42), 14.3 (C-34), 12.7 (C-39).

3.6.19 Preparation of the octanoyl pentapeptide (Glu-Thr-Glu-Lys(Oct)-Ile-OH)

The first amino acid Fmoc-Ile-OH (2.27 g, 6.42 mmol) was loaded onto the Wang resin, followed by the coupling of Fmoc-Lys(Dde)-OH (0.72 g, 1.36 mmol, 4 eq). After the Dde deprotection had been carried out octanoic acid (0.18 mL, 5 equivalents) was coupled to the lysine residue. Fmoc-Glu(*t*Bu)-OH (1.00 g, 2.36 mmol) was then coupled to the growing chain. The fourth and fifth amino acids i.e. Fmoc-Thr(*t*Bu)-OH (0.78 g, 1.95 mmol) and Fmoc-Glu(*t*Bu)-OH (1.00 g, 2.36 mmol) respectively were coupled to complete the synthesis of the pentapeptide. The pentapeptide ETEK(Oct)I was then cleaved from the resin using trifluoroacetic acid.

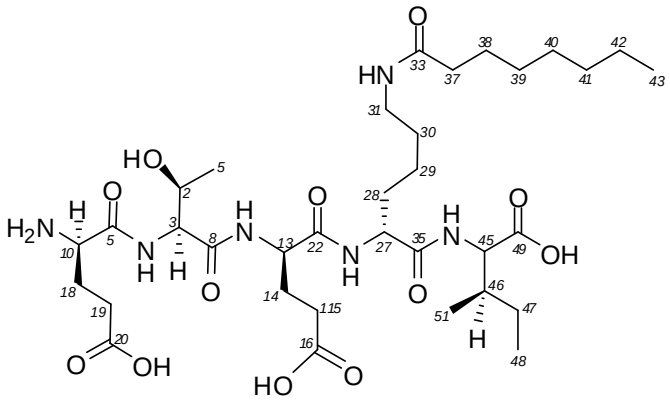

(**42**)

ETEK(Oct)I

This compound was obtained as a white solid (Crude Yield 108 mg, 35 %). **R_f** = 0.22 (acetonitrile: water, 2:1). **ES-MS:** m/z 859 ([M+TFA]$^-$, 35 %), 746 ([M+H]$^+$, 36.5 %);

767.6 ([M+Na]$^+$, 100 %).**^{1}H NMR** (400MHz, D_2O) δ = 4.39 (1H, d, $J_{3,2}$ = 4.8 Hz, H-3), 4.37 (1H, t, $J_{13,14}$ = 7.9 Hz, H-13), 4.20 (1H, d, J = 9.0 Hz, $J_{45,46}$ = 6.6 Hz, H-45), 4.21 (1H, t, $J_{27,28}$ = 7.2 Hz, H-27), 4.12 (1H, qt, $J_{2,7}$ = 6.4 Hz, J = 5.1 Hz, J = 4.8 Hz, H-2), 3.96 (1H, td, $J_{10,18}$ = 8.4 Hz, J = 4.3 Hz, H-10), 2.98 (2H, td, $J_{31,30}$ = 6.8 Hz, J = 5.4 Hz, H-31), 2.24 (2H, t, $J_{15,14}$ = 6.7 Hz, H-15), 2.05 (2H, dt, $J_{18,10}$ = 9.1 Hz, $J_{18,19}$ = 7.3 Hz, H-18), 2.17 (2H, t, $J_{37,38}$ = 7.5 Hz, H-37), 2.15 (2H, t, $J_{19,18}$ = 7.0 Hz, H-19), 1.93 (1H, m, H-46), 1.90 (2H, m, H-14), 1.68 (2H, m, H-28), 1.57 (2H, quin, $J_{38,37}$ = 7.7 Hz, J = 7.5 Hz, H-38), 1.46 (2H, quin, $J_{30,29}$ = 7.3 Hz, J = 6.8 Hz, H-30), 1.35 – 1.22 (8H, m, H-29, H-39, H-41, H-42), 1.21 (2H, q, $J_{47,48}$ = 7.2 Hz, H-47), 1.18 (2H, t, $J_{40,41}$ = 7.4 Hz, H-40), 1.13 (3H, d, $J_{7,2}$ = 6.4 Hz, H-7), 0.88 (3H, d, $J_{51,46}$ = 6.7 Hz, H-51), 0.88 (3H, t, $J_{48,47}$ = 7.2 Hz, H-48), 0.87 (3H, t, $J_{43,42}$ = 6.8 Hz, H-43).

3.7 Purification of peptides

3.7.1 Prepacked column purification of peptides

Aliquots of the crude tripeptide (50 mg) were dissolved in water/acetonitrile (2:1) and purified by reverse phase chromatography on a Supelclean ™ LC-18 solid phase extraction column. Peptides were eluted in a water/acetonitrile (9:1) gradient from 10% acetonitrile to 40 % acetonitrile and the required fractions were pooled and then the solvent was removed by freeze-drying.

3.7.2 Preparative HPLC purification of peptides

Crude tripeptide was dissolved in water/acetonitrile, 2:1 (5.0 mg/mL of peptide) and 200µl aliquots were purified by HPLC on a reversed phase Phenomenex Gemini C18 (5 µm, 150 × 10 mm) column with UV detection at 230 nm. The mobile phase was a mixture of 20 mM ammonium bicarbonate, pH 7 (pump A) and acetonitrile (pump B), beginning with 30 % organic and 70 % aqueous for 5 min at 2 mL /min followed by a 15 min linear gradient to 75 % acetonitrile. The gradient was raised to 100 % organic and 0 % aqueous in 1 min and maintained for 5 min followed by return to initial conditions over 1 min. Each injection was complete in 37 min. This was

repeated with further aliquots of crude peptide (19 × 200µL) then the required fractions were pooled and the solvent was removed by freeze-drying.

3.7.3 HPLC Analysis of peptides

Crude tripeptide was dissolved in water/acetonitrile, 2:1 (5.0 mg/mL of peptide) and 50µl aliquots were analysed by HPLC on a reversed phase Phenomenex Luna C18 (5 µm, 150 × 4.6 mm) column with UV detection at 230 nm. The mobile phase was a mixture of 20 mM ammonium bicarbonate, pH 7 (pump A) and acetonitrile (pump B), beginning with 30 % organic and 70 % aqueous for 5 min at 2 mL/min followed by a 15 min linear gradient to 75 % acetonitrile. The gradient was raised to 100 % organic and 0 % aqueous in 1 min and maintained for 5 min followed by return to initial conditions over 1 min. Each injection was complete in 37 min. This was repeated with further aliquots of crude peptide (19 × 200µL) then the required fractions were pooled and the solvent was removed by freeze-drying.

3.8 Synthesis of the fluorescent pentapeptide substrate analogues

The fluorescent pentapeptide substrates were prepared using one of two approaches. The first approach, used to prepare DECA-ETEK(Oct)I **43** involved the coupling of the fluorophore to the growing peptide chain on the resin. After this the fluorescent pentapeptide was cleaved from the resin using TFA. In the second approach the pentapeptide ETEK(Oct)I **42** was assembled and cleaved from the Wang resin. After purification the pentapeptide was then reacted with the fluorophore which allowed for the coupling to occur. This approach was used to prepare Alexa 350-ETEK(Oct)I **44** and Cy5-ETEK (Oct)I **45**.

3.8.1 Preparation of DECA-ETEK(Oct)I

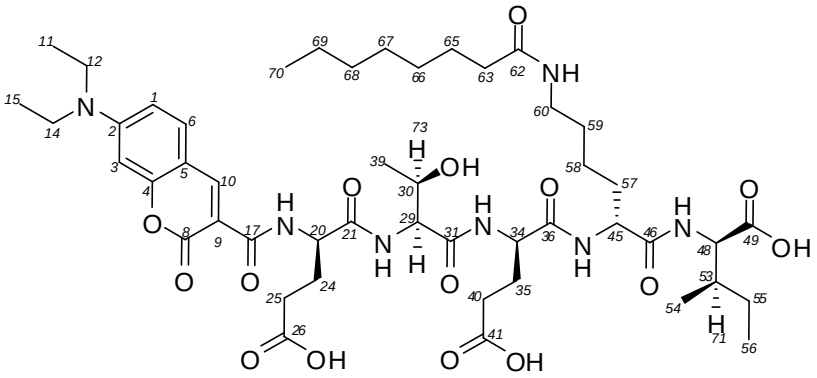

(**43**)
DECA - ETEK(Oct)I

The pentapeptide, ETEK(Oct)I was synthesized on Wang's resin using the steps shown in reaction Scheme 2.2 (described in section 3.6.19). After that the fluorophore was coupled to the pentapeptide on the resin as follows. Fmoc-Glu(tBu)-Thr(tBu)-Glu(tBu)-Lys(Oct)-Ile-resin was Fmoc-deprotected using piperidine (20%, v/v) in DMF. The coumarin, 7-(diethylamino)-2-oxo-2H-chromene-3-carboxylic acid (0.85 g, 3.25 mmol) and PyBOP (1.62, 3.10 mmol) were dissolved in DMF (5 mL). DIPEA (0.17 mL, 10 equiv.) was added and the solution was applied to the peptidyl resin. The suspended resin was agitated for 1 h and the liquid was drained. The resin was washed with DMF (3 x 10 mL) and the fluorescent pentapeptide was cleaved

from the resin using TFA. A yellowish solid was obtained for the product (Crude Yield 250 mg, 35 %). **R_f** 0.25 (acetonitrile: water, 2:1). **ES-MS:** *m/z* 1011 ($[M+Na]^+$, 41 %), 989 ($[M+H]^+$, 26 %), 514 ($[M+K+H]^{2+}$, 35 %). **^{1}H NMR** (600 MHz, DMSO-d_6) δ = 8.40 (1H, s, H-10), 7.56 (1H, d, $J_{6,1}$ = 8.5 Hz, H-6), 6.65 (1H, d, $J_{1,6}$ = 8.5 Hz, H-1), 6.41 (1H, s, H-3), 4.60 (1H, dd, $J_{20,24}$ = 11.5 Hz, *J* = 7.4 Hz, H-20), 4.50 (1H, dd, $J_{29,30}$ = 6.1 Hz, *J* = 5.6 Hz, H-29), 4.35 (1H, dd, $J_{34,35}$ = 11.5 Hz, *J* = 8.3 Hz, H-34), 4.22 (1H, ddd, $J_{45,57}$ = 15.0 Hz, *J* = 7.4 Hz, $J_{45,57}$ = 6.6 Hz, H-45), 4.15 (1H, dd, *J* = 8.6 Hz, $J_{48,53}$ = 6.6 Hz, H-48), 4.00 (1H, quind, $J_{30,39}$ = 6.1 Hz, *J* = 3.0 Hz, H-30), 3.50 (2H, q, $J_{12,11}$ = 7.2 Hz, H-12), 3.41 (2H, q, $J_{14,15}$ = 7.2 Hz, H-14), 2.90 (2H, td, $J_{60,59}$ = 6.8 Hz, *J* = 5.4 Hz, H-60), 2.36 (2H, t, $J_{25,24}$ = 7.1 Hz, H-25), 2.22 (2H, t, $J_{40,35}$ = 6.7 Hz, H-40), 2.13 (2H, t, $J_{63,65}$ = 7.7 Hz, H-63), 1.95 (2H, t, $J_{35,40}$ = 6.7 Hz, H-35), 1.90 (1H, dquind, $J_{53,55}$ = 11.0 Hz, $J_{53,48}$ = 6.6 Hz, $J_{53,54}$ = 6.4 Hz, *J* = 2.6 Hz, H-53), 1.85 (2H, t, $J_{24,25}$ = 7.2 Hz, H-24), 1.77 (2H, quin, $J_{65,63}$ = 7.7 Hz, $J_{65,66}$ = 7.5 Hz, H-65), 1.60 – 1.38 (8H, m, H-68, H-59, H-58, H-57), 1.34 (2H, tq, $J_{69,68}$ = 7.4 Hz, $J_{69,70}$ = 6.8 Hz, H-69), 1.28 (6H, t, *J* = 7.2 Hz, H-11, H-15), 1.20 – 1.13 (6H, m, H-67, H-66, H-55), 1.10 (3H, d, $J_{39,30}$ = 6.1 Hz, H-39), 1.04 (3H, d, $J_{54,53}$ = 6.4 Hz, H-54), 0.95 (6H, t, *J* = 7.0 Hz, H-56, H-70).

3.8.2 HPLC purification of fluorescent DECA-ETEK(Oct)I

A solution of the crude fluorescent pentapeptide (5.35 mg/ mL) was prepared using 0.1 % formic acid in water and 0.1 % formic acid in acetonitrile (2:5). A reversed phase Phenomenex Luna C18 (5 µm, 150 × 10 mm) column was used for the preparative HPLC purification of the fluorescent pentapeptide (250 µL aliquots), with UV detection at 223 nm and 280 nm. The mobile phase consisting of 0.1 % formic acid in water (pump A) and 0.1 % formic acid in acetonitrile (pump B) was initially run for five min at 1 mL/min (settings of 25 % organic and 75 % aqueous solutions) followed by a 15 min linear gradient to 75 % formic acid in acetonitrile. This was then raised to 100 % in 1 min and maintained for 5 min; finally the mobile phase organic concentration was dropped to 25% in 2 min and maintained. The injection was complete in 37 min. This was repeated with other aliquots of crude peptide (15 × 250 µL). The fractions isolated as having the desired peptide were pooled and the solvent was removed by freeze-drying.

3.8.3 Synthesis of amino-functionalized Cyanine-5-fluorescent dye (Cy5-ETEK(Oct)I)

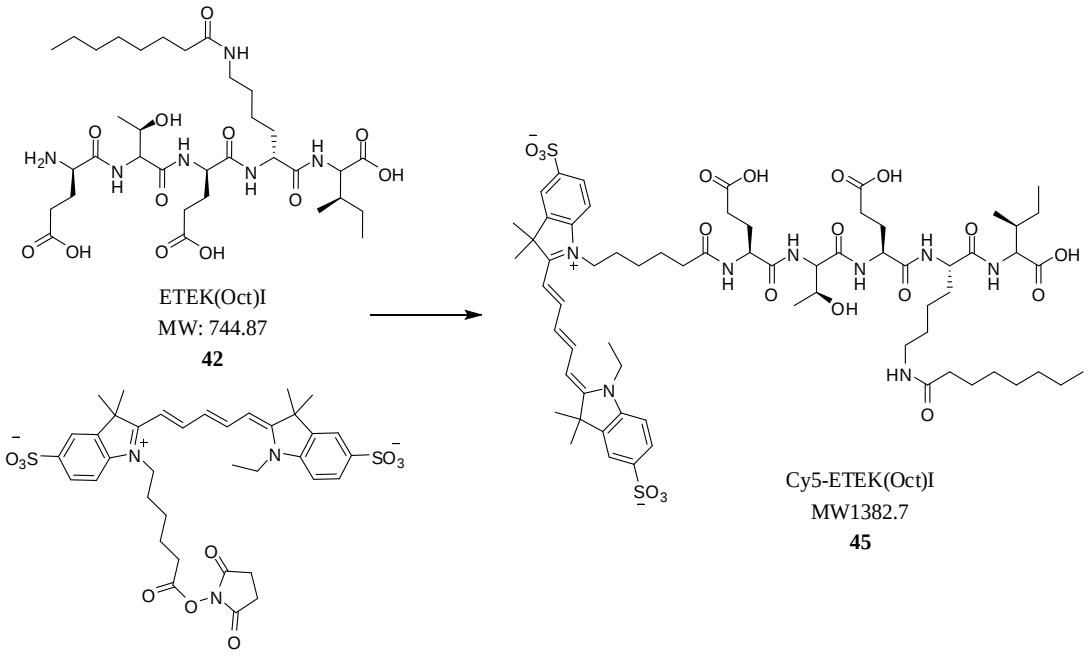

The Cy5 NHS ester **89** (4.21 mg, 5.6 mmol) was dissolved in anhydrous DMF (50 μL). Purified octanoyl-pentapeptide ETEK(Oct)I (5.00 mg, 6.7 μmol) was dissolved in anhydrous DMF (50 μL) and was then added to the Cy5 NHS ester solution. Diisopropylethylamine DIPEA (3.1 mL, 2.3 mg and 18 μmols) was added to the reaction mixture. The volume of the reaction mixture was made up to 300 mL using the anhydrous DMF. The reaction was vortexed (90 min) and thereafter kept on ice overnight. The amino functionalized Cyanine-5 fluorescent dye was purified on a gel-filtration column (1mL, NAP-10 column). **ES-MS:** *m/z* 1384.4 ($[M+H]^+$, 35 %), 692.4 9($[M+2H]$)$^{2+}$. The recorded fluorescence intensity showed a single peak for compound at wavelength range 600 nm – 680 nm.

3.8.4 Synthesis of amino functionalized Alexa-350 fluorescent dye (Alexa 350-ETEK(Oct)I)

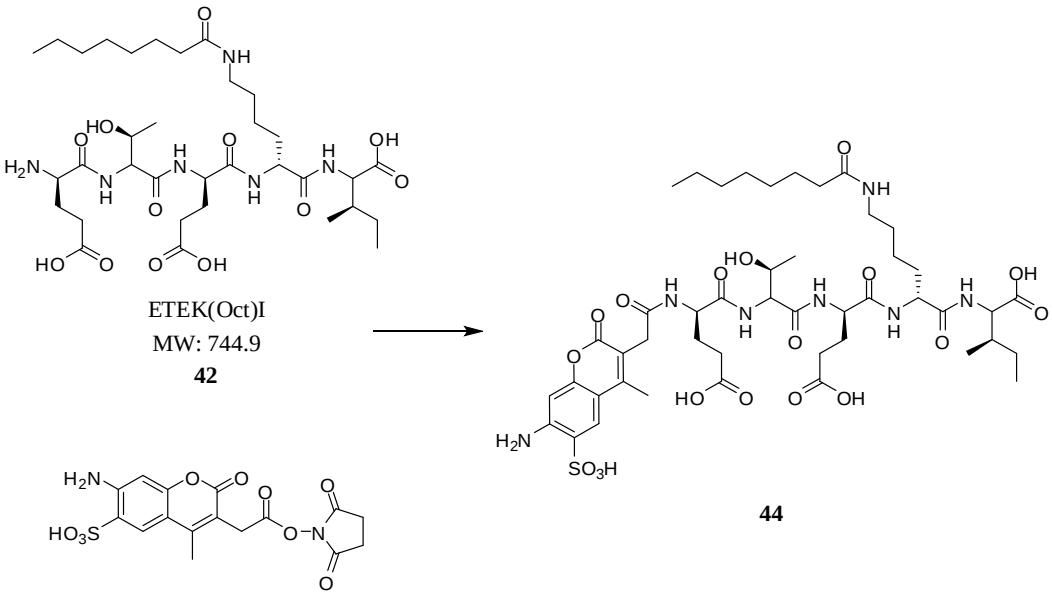

Purified octanoyl-pentapeptide ETEK(Oct)I (11.2 mg, 15 μmol) was dissolved anhydrous dimethylformamide (DMF (100 μL)). Alexa Fluor® 350 carboxylic acid succinimidyl ester (5 mg, 12 μmol) was dissolved in anhydrous DMF (100 μL) and added to the peptide solution in a vial. The volume of the reaction mixture was made up to 250 μL with anhydrous DMF and a magnetic bar was placed in the vessel which was covered with black insulation tape to prevent light passing into it. The reaction mixture was stirred for 5h at room temperature. The reaction was quenched by injecting the mixture into a preparative HPLC column from which the desired compound was purified and subsequently characterized by ESI-mass spectral analysis and by observing the fluorescence intensity for the compound. **ES-MS:** *m/z* 520.9 ($[M+2H]^{2+}$, 85 %). The recorded fluorescence intensity showed a single peak for compound at wavelength range 330 nm – 400 nm. The HPLC analysis at 220 nm gives one major peak corresponding to the compound.

3.9 The Synthesis of Alexa 350

3.9.1 Preparation of 3-carbethoxyaminophenol [209, 210]

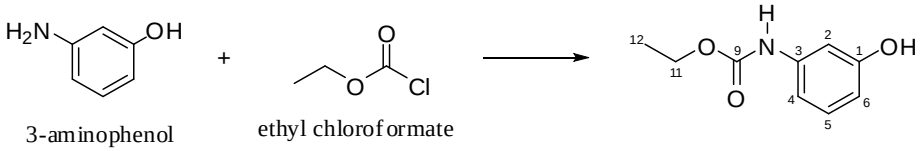

3-aminophenol ethyl chloroformate 3-carbethoxyaminophenol

Ethyl acetate (40 mL) was heated to reflux and then 3-amino-phenol (5.65 g, 52 mmol) was added. The mixture was refluxed for five minutes after which ethyl chloroformate (3 mL, 30 mmol) was added dropwise over 15 min whilst refluxing. Thereafter the reaction mixture was refluxed for a further 20 min and then cooled to room temperature. The resultant suspension was filtered and the collected solid washed with ethyl acetate (3 x 15 mL). The filtrate was left at room temperature overnight and the solvent removed *in vacuo*. The white solid obtained was washed with petroleum ether (40 – 60 ^{o}C) (3 x 15mL) and dried *in vacuo*. (Yield 4.8 g, 88 %), m.p. 92 – 96 ^{o}C. **ES-MS:** *m/z* 182 $([M+H]^{+}$, 75 %); 204 $([M+Na]^{+}$, 21 %). **^{1}H NMR** (300MHz, DMSO-d_6) δ = 7.09 (1H, d, $J_{2,6}$ = 2.6 Hz, H-2), 6.94 (1H, t, $J_{5,4}$ = 8.1 Hz, $J_{5,6}$ = 7.9 Hz, H-5), 6.84 (1H, d, $J_{4,5}$ = 8.1 Hz, H-4), 6.39 (1H, dd, $J_{6,5}$ = 7.9 Hz, $J_{6,2}$ = 2.6 Hz, H-6), 4.10 (2H, q, $J_{11,12}$ = 7.3 Hz, H-11), 1.35 (3H, t, $J_{12,11}$ = 7.3 Hz, H-12). **^{13}C NMR** (75 MHz, DMSO-d_6) δ = 157.7 (C-1), 153.4 (C-9), 140.3 (C-3), 129.3 (C-5), 109.4 (C-4), 109.0 (C-6), 105.3 (C-2), 60.0 (C-11), 14.5 (C-12).

3.9.2 Preparation of ethyl (7-[(ethoxycarbonyl)amino]-4-methyl-2-oxo-2H-chromen-3-yl)acetate [210]

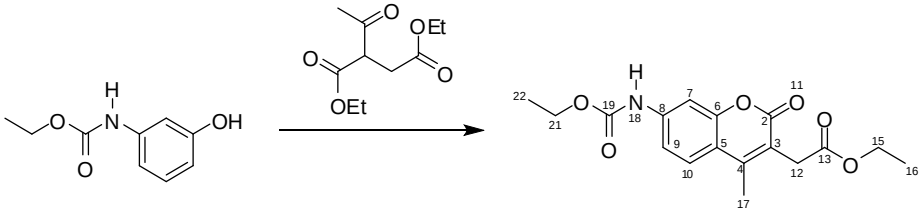

H_2SO_4 (75%, 50 mL) was added to 3-carbethoxyaminophenol (4.24 g, 23.4 mmol), followed by diethyl-2-acetyl succinate (5.07 g, 23.4 mmol). The reaction mixture was stirred at room temperature for 4 h. Ice-cold water (150 mL) was added to the reaction mixture and the suspension formed was filtered. The filter cake was washed thoroughly with ice-cold water until the washings were neutral. The filter cake was then washed with absolute alcohol (100 mL) and dried *in vacuo*. (Yield 7.1 g, 91 %), m.p. 285 – 295 ^{o}C. **ES-MS:** *m/z* 334 ($[M+H]^+$, 100 %); 357 ($[M+Na]^+$, 50 %). **^{1}H NMR** (300 MHz, DMSO-d_6) δ = 7.75 (1H, s, H-7), 7.49 (1H, d, $J_{9,10}$ = 9.0 Hz, H-9), 7.45 (1H, d, $J_{10,9}$ = 9.0 Hz, H-10), 4.21 (2H, q, $J_{21,22}$ = 7.2 Hz, H-21), 4.05 (2H, q, $J_{15,16}$ = 7.0 Hz, H-15), 3.57 (2H, s, H-12), 2.37 (3H, s, H-17), 1.30 (3H, t, $J_{22,21}$ = 7.2 Hz, H-22), 1.13 (3H, t, $J_{16,15}$ = 7.0 Hz, H-16). **^{13}C NMR** (75 MHz, DMSO-d_6) δ = 170.1 (C-13), 153.3 (C-2), 152.5 (C-6), 149.2 (C-19), 145.4 (C-4), 142.4 (C-8), 126.3 (C-10), 121.8 (C-3), 116.8 (C-9), 114.4 (C-5), 104.1 (C-7), 60.7 (C-21), 60.4 (C-15), 32.6 (C-12), 14.9 (C-17), 14.4 (C-22), 14.0 (C-16).

3.9.3 Preparation of 7-carbethoxyamido-4-methylcoumarin-3-acetic acid

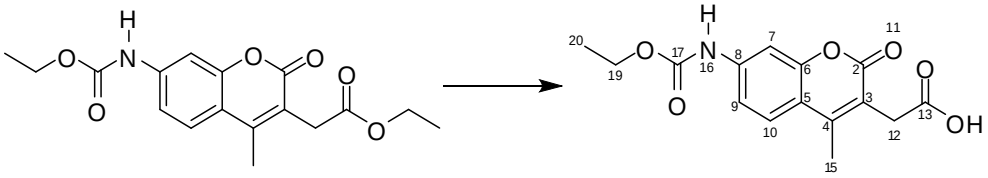

Crude 7-carboethoxyamido-4-methylcoumarin-3-ethyl-acetate (500 mg, 1.5 mmol) was refluxed for 2 h with 10% methanolic potassium hydroxide (w/v) (5 mL). The alcohol was evaporated by rotatory evaporation. 2M HCl was added slowly to give a precipitate which was filtered off and washed with cold distilled water until the washing was free of acid, and dried *in vacuo*. The crude product was purified on a silica column using an ethyl acetate: MeOH solvent system with a MeOH gradient from 0 % to 30 %. Fractions containing the desired product were pooled together and freeze dried. (Crude Yield 205.8 mg, 45 %); m.p. 245 – 250 ^{o}C. $\mathbf{R_f}$ 0.30 (ethyl acetate: methanol 9:1). **ES-MS:** *m/z* 306.3 ($[M+H]^+$, 100 %); 328.3 ($[M+Na]^+$, 50 %). **^{1}H NMR** (300 MHz, DMSO-d_6) δ = 7.73 (1H, d, $J_{9,10}$ = 8.8 Hz, H-9), 7.56 (1H, s, H-7), 7.41 (1H, d, $J_{10,9}$ = 8.8 Hz, H-10), 4.17 (2H, q, $J_{19,20}$ = 6.5 Hz, H-19), 3.56 (2H, s, H-12), 2.35 (3H, s, H-15), 1.26 (3H, t, $J_{20,19}$ = 7.0 Hz, H-20). **^{13}C NMR** (75 MHz, DMSO-d_6) δ = 171.5 (C-13), 160.8 (C-2), 153.3 (C-17), 152.4 (C-6), 148.7 (C-4), 142.2 (C-8), 126.1 (C-10), 117.4 (C-5), 114.5 (C-3), 114.3 (C-9), 104.1 (C-7), 60.6 (C-19), 32.8 (C-12), 14.9 (C-15), 14.4 (C-20).

3.9.4 Preparation of 7-amino-4-methylcoumarin-3-acetic acid (AMCA)

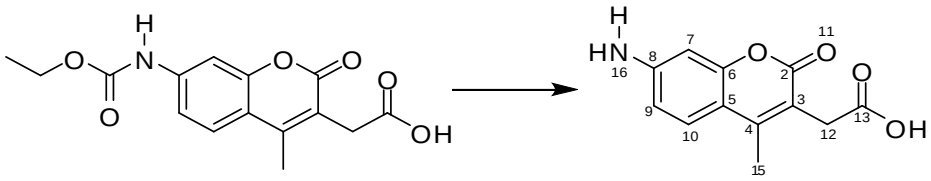

Glacial acetic acid (1.12 mL), concentrated H_2SO_4 (1 mL) and 7-carbethoxyamido-4-methylcoumarin-3-acetic acid (65 mg, 0.21 mmol) were refluxed for 3 h. After being cooled at 25 ^oC the mixture was poured into 7.5 mL of an ice-water mixture, then warmed to 70 ^oC and treated with Celite (1:1). After being filtered, warmed and washed with 10 mL of hot water, the filtrate was cooled at room temperature to crystallize. The 7-amino-4-methylcoumarin-3-acetic acid crystals were filtered, washed with cold distilled water and then with cold ethanol. The crystals were dried *in vacuo* to give the product (Yield 36.4 g, 75 %). **ES-MS:** *m/z* 234.2 ($[M+H]^+$, 100 %); 256.2 ($[M+Na]^+$, 10 %); 297.2 ($[M+Na+CH_3CN]$, 80 %). **^{1}H NMR** (300 MHz, DMSO-d_6) δ = 7.46 (1H, d, $J_{10,9}$ = 8.8 Hz, H-10), 6.60 (1H, d, $J_{9,10}$ = 8.8 Hz, H-9), 6.45 (1H, s, H-7), 3.51 (2H, s, H-12), 2.28 (3H, s, H-15). **^{13}C NMR** (75 MHz, DMSO-d_6) δ = 172.3 (C-13), 161.5 (C-2), 154.5 (C-6), 152.6 (C-8), 149.8 (C-4), 126.5 (C-10), 118.1 (C-3), 111.7 (C-5), 109.5 (C-9), 98.8 (C-7), 32.7 (C-12), 14.9 (C-15).

3.9.5 Sulfonation of 7-amino-4-methyl-6-sulfocoumarin-3-acetic acid (Alexa 350)

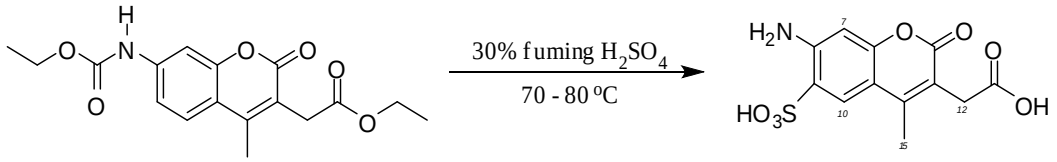

Powdered 7-carboethoxyamido-4-methylcoumarin-3-ethyl-acetate (500 mg, 1.5 mmol) was added in small portions to ice cold 30% fuming sulfuric acid (4 mL). After the addition was completed the reaction mixture was stirred for 1 h at 0 °C, warmed to room temperature for 2 hrs, and was then stirred for 3 days at 80 °C. The solution was cooled to room temperature and poured into crushed ice (4 g). The mixture was left overnight and the resultant precipitate was collected by suction filtration. The precipitate was resuspended in water (5 mL), and the pH of the suspension was adjusted to 5 by adding 2M NaOH. The resultant mixture was poured into methanol (25 mL) and the suspension was isolated by filtration. The filtrate was evaporated to dryness to give crude product which was further purified on a SEPHADEX LH-20 resin column eluting with water to give 3.75 mg (0.8%) of pure Compound. **ES-MS:** *m/z* 314.3 ($[M+H]^+$, 35 %); 326.3 ($[M+Na]^+$, 34 %); 356.3 ($[M+H^+ + CH_3CN]$, 80 %). **^{1}HNMR** (300 MHz, DMSO-d_6) δ = 7.84 (1H, s, H-10), 6.49 (1H, s, H-7), 5.18 (br s, 2H), 3.52 (2H, s, H-12), 2.50 (3H, s, H-15). The compound was being retained on the ion exchange column. An attempt was made to retrieve the trapped compound by gradually lowering the pH of the mobile phase (this was done by slowly increasing the concentration of acetic acid from 1% to 40 %). However, very little of the target compound was obtained in this way and it was decided to instead purchase the compound from commercial sources.

3.10 Thiol reactive compound experiments

3.10.1 Synthesis of thiol reactive maleimide coumarin

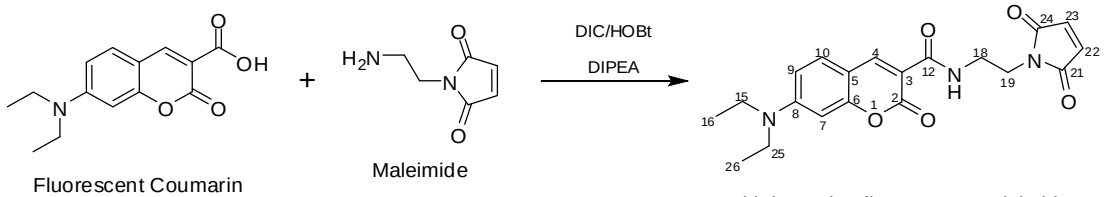

Fluorescent Coumarin + Maleimide → Thiol reactive fluorescent maleimide

The fluorescent coumarin (131.9 mg, 5.1 x 10^{-4} mol, 1.5 molar equiv.) and HOBt (82 mg, 6.1 x 10^{-4} mol) and were dissolved in a minimal amount of dry DMF (4 mL). Diisopropylcarbodiimide (92 μL) was added and the reaction mixture was stirred for about 30 min to allow for activation to occur. N-(2-aminoethyl) maleimide (47.5 mg, 3.4 x 10^{-4} mol) and diisopropylethylamine (100 μL) were added and the reaction mixture was stirred at room temperature for 12 h. The reaction was worked up using a 1:1 mixture of sodium bicarbonate: diethyl ether and the aqueous layer was washed with diethyl ether (4 X 10 mL). The organic layer was dried over $MgSO_4$ and the mixed fraction was evaporated on a rotatory evaporator. The crude product was purified on a silica column using a CH_2Cl_2: MeOH solvent system with MeOH gradient from 0% to 3%. Fractions containing the title compound were pooled together and freeze dried. (Yield 46.9 mg, 36%), m.p. 178 – 182 ^{o}C. **ES-MS**: *m/z* 384 ($[M+H]^+$, 75 %); 406 ($[M+Na]^+$, 21 %). **^{1}H NMR** (300 MHz, $CDCl_3$)) δ = 8.69 (1H, s, H-4), 7.45 (1H, d, $J_{10,9}$ = 8.6 Hz, H-10), 6.79 (2H, s, H-23, H-22), 6.67 (1H, d, $J_{9,10}$ = 8.5 Hz, H-9), 6.57 (1H, s, H-7), 3.81 (2H, t, $J_{19,18}$ = 5.8 Hz, H-19), 3.65 (2H, q, $J_{18,19}$ = 5.8 Hz, H-18), 3.46 (2H, q, $J_{15,16}$ = 7.0 Hz, H-15), 3.46 (2H, q, $J_{25,26}$ = 7.0 Hz, H-25), 1.25 (3H, t, $J_{26,25}$ = 7.1 Hz, H-26), 1.25 (3H, t, $J_{16,15}$ = 7.1 Hz, H-16). **^{13}C NMR** (75 MHz, $CDCl_3$) δ = 173.0 (C-24, C-21), 165.5 (C-12), 160.0 (C-2), 158.0 (C-6), 154.2 (C-8), 145.4 (C-4), 138.4 (C-23, C-22), 133.5 (C-10), 121.0 (C-3), 105.0 (C-5, C-9), 90.0(C-7), 42.0 (C-25, C-15), 37.5 (C-18), 36.0 (C-19), 11.5 (C-26, C-16).

3.10.2 Test for reaction of maleimide compound with thiols

Stock solutions of TCEP (4.8 mM), lipoic acid (80 μM) and the thiol reactive maleimide coumarin (4.8 mM) were prepared in ammonium bicarbonate buffer (25 mM, pH 7.5). Lipoic acid (20 μL) was added to ammonium bicarbonate buffer (140 μL). TCEP (20 μL) was added to the reaction vessel and the mixture was incubated at room temperature for 1 h. Thereafter thiol reactive maleimide coumarin (20 μL) was added and the reaction vessel was incubated at room temperature for 3h.

Table 3.5 *The reaction conditions for the maleimide reaction with thiols.*

	+Ve Assay	**- Thiol**	**- TCEP**	**- Maleimide**
Buffer	140 μL	160 μL	160 μL	160 μL
Thiol (800 μM)	20 μL	0	20 μL	20 μL
TCEP (4.8 mM)	20 μL	20 μL	0	20 μL
Maleimide (5.4 mM)	20 μL	20 μL	20 μL	0

+Ve assay = positive assay (the assay in which all components were added).

-Thiol = negative assay in which the thiol (e.g. ~-lipoic acid) was excluded.

-TCEP = negative assay in which the TCEP was excluded.

-Maleimide = negative assay in which the thiol reactive maleimide coumarin was excluded.

The Table 3.5 shows the full set of assay conditions in which the maleimide coumarin (61) was reacted with the thiol. In the main assay the thiol used was α-lipoic acid. The Table 3.5 also shows the various negative controls that were carried out as well alongside the positive assay. The reaction mixture was then analysed by mass spectroscopy and HPLC to determine the components after the reaction time.

3.11 Product Inhibition Assays.

Assays to test the product inhibitory effect of AdoH and methionine on the LipA catalysed conversion of octanoyl substrates into lipoyl products were set up in the anaerobic glove-box by mixing the components as shown in the Tables 3.6 to 3.11. A summary of the results of these assays is given in Table 2.3.

Table 3.6 *The positive EK(Oct)I turnover Assay*

Compound	Stock solution	Final Concentration	Final volume («L)
Lip A	250 μM	100 μM	80
SAM-Chloride	33 mM	1 mM	6.1
EK(Oct)I	500 μM	50 μM	20
Sodium dithionite	10 mM	1 mM	20
HEPES buffer	25mM, pH 7.5	-	73.9
Total Volume			200

In the positive EK(Oct)I turnover assay LipA (100μM) was mixed with SAM-chloride (1mM), EK(Oct)I (50 μM) (octanoyl tripeptide **39**, Scheme 2.2) and sodium dithionite (1 mM), in HEPES buffer (pH 7.5, 25 mM) in the volumes shown in Table 3.6. The assay mixture was incubated in a water bath (37 ^{o}C, 30 min), after which neat TFA was added to precipitate the LipA and stop the enzyme catalysed reaction. The precipitated protein was separated from the supernatant by centrifugation (12 500 rpm, 15 min). Thereafter the supernatant was analysed by injecting a sample (100 μL) into the LC-MS, from which it was possible to characterise components of the supernatant by identifying the observed mass ions. The computer program Xcalibur was used to quantify the area corresponding to the identified mass ions. The fraction of Lipoyl product was determined to be 0.82.

To test the inhibitory effect of AdoH and methionine on the LipA mediated production of the lipoyl product, assays were prepared as shown in Table 3.7 – Table 3.9. Each of the product inhibition assays was incubated alongside the positive assay in the water bath after which period the protein LipA in the assays was precipitated by adding neat TFA (25 μL). The supernatants were analysed by injecting 100 μL samples into the LC-MS. The area under the identified mass ion peaks was determined using the computer program Xcalibur.

Table 3.7 *The effect of DOA and Met on the LipA catalyzed reaction.*

Compound	**Stock solution**	**Final Concentration**	**Final volume («L)**
Lip A	250 μM	100 μM	80
SAM-Chloride	33 mM	1 mM	6.1
EK(Oct)I	500 μM	50 μM	20
Sodium dithionite	10 mM	1 mM	20
DOA	10 mM	1mM	20
Met	10 mM	1mM	20
HEPES buffer	25mM, pH 7.5	-	33.9
Total Volume			200

Table 3.7 shows the assay preparation which was used to determine what the effect of adding AdoH and Met to the positive would be. The fraction of Lipoyl product was determined to be 0.30. Table 3.8 shows the assay in which AdoH, Met and *Pfs* were all added to the positive assay. This assay was used to determine if the addition of Pfs would reverse the effects of AdoH and Met on the positive assay. The fraction of Lipoyl product was determined to be 0.84.

Table 3.8 *The combined effect of DOA, Met and Pfs on the LipA catalyzed reaction.*

Compound	Stock solution	Final Concentration	Final volume («L)
Lip A	250 µM	100 µM	80
SAM-Chloride	33 mM	1 mM	6.1
EK(Oct)I	500 µM	50 µM	20
Sodium dithionite	10 mM	1 mM	20
DOA	10 mM	1mM	20
Met	10 mM	1mM	20
Pfs	125 µM	10 µM	16
HEPES buffer	25mM, pH 7.5	-	17.9
Total volume			200

The assay of Table 3.9 was used to test the effect of the *Pfs* protein on the positive LipA assay. The fraction of Lipoyl product was determined to be 0.95.

Table 3.9 *The effect of Pfs on the LipA catalyzed reaction.*

Compound	Stock solution	Final Concentration	Final volume («L)
Lip A	250 µM	100 µM	80
SAM-Chloride	33 mM	1 mM	6.1
EK(Oct)I	500 µM	50 µM	20
Sodium dithionite	10 mM	1 mM	20
Pfs	125 µM	10µM	16
HEPES buffer	25mM, pH 7.5	-	57.9
Total Volume			200

The negative control assays were prepared as shown in Table 3.10and Table 3.11 Each of the negative control assays was incubated alongside the positive assay in the water bath after which period the protein LipA in the assays was precipitated by adding neat TFA (25 mL). The supernatants were analysed by injecting 100 µL samples into the LC-MS. The area under the identified mass ion peaks was determined using the computer program Xcalibur. For the assay of Table 3.10 the fraction of Lipoyl product was found to be 0.01, whilst for the assay of Table 3.11 the fraction was found to be 0.00.

Table 3.10 *No SAM negative control.*

Compound	**Stock solution**	**Final Concentration**	**Final volume E«L)**
Lip A	250 µM	100 µM	80
EK(Oct)I	500 µM	50 µM	20
Sodium dithionite	10 mM	1 mM	20
HEPES buffer	25mM, pH 7.5	-	80
Total Volume			200

Table 3.11 *No Sodium dithionite negative control.*

Compound	**Stock solution**	**Final Concentration**	**Final volume E«L)**
Lip A	250 µM	100 µM	80
SAM-Chloride	33 mM	1 mM	6.1
EK(Oct)I	500 µM	50 µM	20
HEPES buffer	25mM, pH 7.5	-	93.9
Total Volume			200

3.12 Detection of the EK(Non)I products and intermediates

The nonanoyl tripeptide substrate analogue EK(Non)I (compound **11**, Scheme 2.2) was used in assays with reconstituted LipA as shown in Table 3.12. EK(Non)I (50 μM) was mixed with SAM-chloride (1mM), LipA (100μM) and sodium dithionite (1 mM), in Ammonium bicarbonate buffer (pH 7.5, 25 mM) in the volumes shown. The assay mixture was incubated in a water bath (37 ^{o}C, 30 min), after which the neat TFA (25 μL) was added to stop the enzyme catalysed reaction. The precipitated protein was separated from the supernatant by centrifugation (12 500 rpm, 30 min). Aliquots (80 μL) of the supernatant were analysed on the LCMS for products and intermediates. Enough assays were carried out to enable the collection of 1.5 mL of the supernatant and this was analysed by High Resolution Mass Spectroscopy.

Table 3.12 *The positive EK(Non)I Assay.*

Compound	Stock solution	Final Concentration	Final volume («L)
Lip A	250 μM	100 μM	160
SAM-Chloride	33 mM	1 mM	12.2
EK(Non)I	500 μM	50 μM	40
Sodium dithionite	10 mM	1 mM	40
Buffer	25mM, pH 7.5	-	147.8
Total Volume			400

The negative control assays were prepared by mixing the components in Table 3.12 but in one of these assays there was no EK(Non)I present; the volume was made up with buffer. In the other negative control assay the LipA was removed from the assay and the volume was made up with buffer. The reaction in the negative control assays was stopped by adding neat TFA (25 μL). The precipitated protein was separated from the supernatant by centrifugation (12 500 rpm, 30 min). Aliquots (80 μL) of the supernatant were analysed on the LCMS for products and intermediates.

3.13 Determination of binding constant Kd for SAM by UV-visible spectroscopy

3.13.1 UV-visible spectral changes observed following the addition of SAM to reconstituted LipA in the presence of EK(Oct)I

Reconstituted LipA (15 μM) was mixed with the octanoyl tripeptide substrate EK(Oct)I (200 μM), and SAM (concentration increasing from 0 – 500 μM) was added in small aliquots. After each addition of SAM, the protein mixture was stirred for 5 min and the UV- visible spectrum was recorded. The absorbencies at 400 nm were plotted against the concentration of SAM in the reaction mixture. This data was fitted to an exponential linear function $y = y_0 + ae^{-bx} + cx$, from which the constants a, b, c and y_0 were determined. These constants were then used to fit the data to a ligand substrate binding function $y = \frac{B_{max}x}{K_D + x} + N_s x$ from which was the binding constant K_d and the constant B_{max} were determined. The data was analysed and reprocessed using the computer software SigmaPlot®.

3.13.2 UV- visible spectral changes observed following the addition of SAM to reconstituted LipA

SAM (concentration increasing from 0 – 400 μM) was added in small aliquots to reconstituted LipA (15 μM). After each addition of SAM the protein mixture was stirred for 5 min and the UV- visible spectrum was recorded. The absorbencies at 400 nm were plotted against the concentration of SAM in the reaction mixture. This data was fitted to an exponential linear function $y = y_0 + ae^{-bx} + cx$, from which the constants a, b, c and y_0 were determined. These constants were then used to fit the data to a ligand substrate binding function $y = \frac{B_{max}x}{K_D + x} + N_s x$ from which was the binding constant K_D and the constant B_{max} were determined. The data was analysed and reprocessed using the computer software SigmaPlot®.

3.13.3 The Rapid Equilibrium Dialysis (RED) experiments

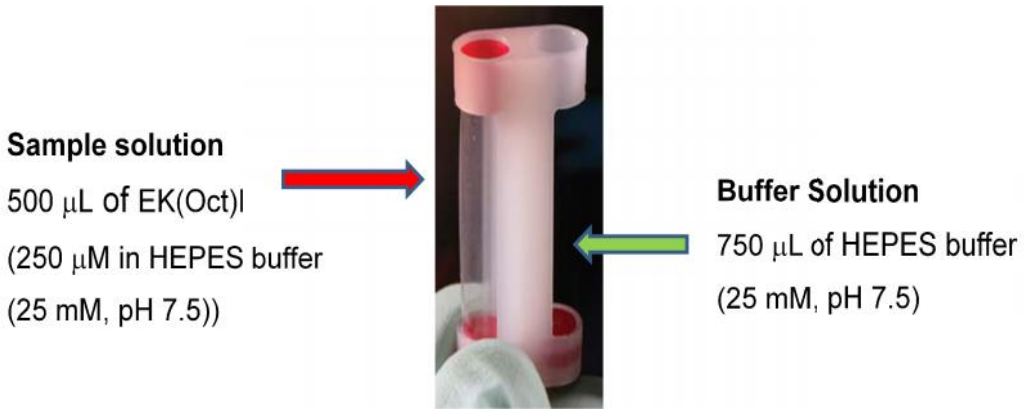

Figure 3.1 *Picture showing how the assay solutions were prepared in the RED inserts*

The rapid equilibrium dialysis assays were prepared in the RED device whose picture is shown in Figure 2.29. The picture in Figure 3.1 shows an RED device insert and how the different components of the assay were placed in it. A 250 μM solution of the tripeptide EK(Oct)I in HEPES buffer (25 mM, pH 7.5) was prepared. 500 μL of this solution was placed into the sample chamber of the RED device. Reconstituted LipA (150 μM) was prepared following the general procedure for reconstitution (Experimental section 3.3.14). 75 μL of this LipA solution was placed into the buffer chamber. The buffer solution was made up to 750 μL with HEPES buffer (25 mM, pH 7.5). The RED device was sealed using self-adhesive tape and incubated at 37 ^{o}C in a warm water bath for 6 h. Every 30 min 20 μL samples were collected from both chambers of the device and each sample was diluted to 80 μL in HEPES buffer (25 mM, pH 7.5). These samples were analysed by HPLC.

3.14 Alexa Fluor® 350 and Cy5 LipA binding constant (Kd) Assays

3.14.1 LipA Binding Assays using Alexa350-ETEK(Oct)I

Stock solutions of SAM (2 μM) and the amino-functionalised Alexa 350 fluorescent dye pentapeptide (Alexa350-ETEK(Oct)I) (200 nM) were prepared. LipA was reconstituted using the standard procedure and concentrated to 20 mg/mL. 4.0 μL drops of the pentapeptide (final concentration of 10 nM) were placed in 12 wells of a 96 well plate. Thereafter 20.0 μL of SAM (final concentration of 500 nM) was added to each of the wells. Different solutions of LipA (final concentrations ranging from 1nM to 100 μM) were prepared in HEPES buffer (25 mM, pH 7.5) and added to the 12 wells as shown in Table 3.13. The reaction mixtures were allowed to equilibrate for 30 min. Thereafter the fluorescence intensity and the fluorescence polarisation of the reaction mixtures were recorded on the plate reader. The second set of assays was prepared in exactly the same manner as above but without adding SAM. The volume of the mixtures was made up by adding an equivalent amount of buffer, as shown in Table 3.14.

3.14.2 LipA Binding Assays using Cy5-ETEK(Oct)I

Stock solutions of SAM (2 μM) and the amino-functionalized Cy5-fluorescent dye pentapeptide (Cy5-ETEK(Oct)I) (200 nM) were prepared. LipA was reconstituted using the standard procedure and concentrated to 20 mg/mL. 4.0 μL drops of the pentapeptide (final concentration of 10 nM) were placed in 12 wells of a 96 well plate. Thereafter 20.0 μL of SAM (final concentration of 500 nM) was added to each of the wells. Different solutions of LipA (final concentrations ranging from 1nM to 100 μM) were prepared in HEPES buffer (25 mM, pH 7.5) and added to the 12 wells as shown in Table 3.15 The reaction mixtures were equilibrated for 30 min after which the fluorescence intensity and the fluorescence polarization data for the reaction mixtures were recorded on the plate reader. The second set of assays was prepared in exactly the same manner but without adding SAM, instead making up the volume by adding an equivalent amount of buffer, as shown in Table 3.16.

Table 3.13 *A table showing the concentrations of the components of the assay set up on 96 well plate to determine binding constant (Kd) using the prepared fluorescent peptide Alexa350-ETEK(Oct)I in the presence of SAM.*

Well number	**1**	**2**	**3**	**4**	**5**	**6**	**7**	**8**	**9**	**10**	**11**	**12**
[Alexa350-ETEK(Oct)I] (nM)	10	10	10	10	10	10	10	10	10	10	10	10
[SAM] («M)	0.5	0.5	0.5	0.5	0.5	0.5	0.5	0.5	0.5	0.5	0.5	0.5
[Final LipA] (nM)	0	0.1	1	10	50	100	200	500	1000	10000	50000	100000
Total Volume (µL)	80	80	80	80	80	80	80	80	80	80	80	80

Table 3.14 *A table showing the concentrations of the components of the assay set up on 96 well plate to determine binding constant (K_d) using the prepared fluorescent peptide Alexa350-ETEK(Oct)I in the absence of SAM.*

Well number	**1**	**2**	**3**	**4**	**5**	**6**	**7**	**8**	**9**	**10**	**11**	**12**
[Alexa350 ETEK(Oct)I] (nM)	10	10	10	10	10	10	10	10	10	10	10	10
[Final LipA] (nM)	0	0.1	1	10	50	100	200	500	1000	10000	50000	100000
Total Volume (µL)	80	80	80	80	80	80	80	80	80	80	80	80

Table 3.15 *Table showing the concentrations of the components of the assay set up on 96 well plate to determine binding constant (Kd) using the prepared fluorescent peptide Cy5-ETEK(Oct)I in the presence of SAM.*

Well number	1	2	3	4	5	6	7	8	9	10	11	12
[Cy5-ETEK(Oct)I] (nM)	10	10	10	10	10	10	10	10	10	10	10	10
[SAM] («M)	0.5	0.5	0.5	0.5	0.5	0.5	0.5	0.5	0.5	0.5	0.5	0.5
[Final LipA] nM	0	0.1	1	10	50	100	200	500	1k	10k	50k	100k
Total Volume (µL)	80	80	80	80	80	80	80	80	80	80	80	80

Table 3.16 *Table showing the concentrations of the components of the assay set up on 96 well plate to determine binding constant (Kd) using the prepared fluorescent peptide Cy5-ETEK(Oct)I in the absence of SAM.*

Well number	1	2	3	4	5	6	7	8	9	10	11	12
[Cy5-ETEK(Oct)I] (nM)	10	10	10	10	10	10	10	10	10	10	10	10
[Final LipA] nM	0	0.1	1	10	50	100	200	500	1k	10k	50k	100k
Total Volume (µL)	80	80	80	80	80	80	80	80	80	80	80	80

3.15 Crystallization of LipA

3.15.1 Preparation of the cover-slips

Cover-slips were washed thoroughly in distilled water and placed on a plastic rack. Most of the water was shaken off and the cover-slips were dried under a stream of blowing hot air. The circumferences of all the wells of a 24-well Linbro plate were greased with vacuum grease after which the plate was degassed in the anaerobic glove box for at least 24 h.

3.15.2 Preparation of precipitant solutions

Three buffer solutions; Phosphate buffer (100 mM, pH 6.6), TRIS buffer (100 mM, pH 8.1) and HEPES Buffer (100 mM, pH 7.5) were prepared in water. These solutions were degassed for 30 min by bubbling nitrogen gas, and then were transferred into an anaerobic glove-box where they kept open for at least 24 h.

3.15.3 Preparation of the peptide, SAM and SAH stock solutions

LipA was purified on an S-75 gel purification column using the standard procedure outlined in Section 3.3.8. The protein was then reconstituted using the standard procedure detailed in Section 3.3.14 thereafter concentrated to ~ 0.75 mM in HEPES buffer (25 mM, pH 7. 5). A solution of tripeptide EK(Oct)I (3.9 mM in HEPES buffer) was prepared and divided into 25 μL aliquots. A solution of S-adenosyl methionine chloride (70 mM in HEPES buffer (25 mM, pH 7. 5)) was prepared and divided into 20 μL aliquots. Another solution of S-adenosyl homocysteine (20 mM) in HEPES buffer (25 mM, pH 7. 5) was also prepared.

3.15.4 Preparation of the complex peptide solution

The stock peptide solution for setting up the crystallization assays was prepared by mixing LipA (75 μL, 0.75 mM) and EKO(ct)I (25 μL, 3.9 mM). This mixture was shaken a several times and then SAM chloride (8 μL, 70 mM) was added, and the resultant mixture was shaken further. The different precipitant solutions shown in the Table A.1 – A.5 were mixed in the 24 well Linbro plates.

3.15.5 Setting the crystallization assay

The complex protein solution (2.5 μL) was pipetted onto the centre of a cover-slip. Then the precipitant (2.5 μL) was pipetted-out from the Linbro plate well and applied to the centre of the protein drop on the cover-slip. The cover-slip was then carefully placed over the well so as to seal the well (helped by the vacuum grease which had been applied around the edges of the well). In a variation of the complex peptide mixture, the 20 mM SAH was added to the mixture in place of the 70 mM SAM. The schematic diagram of Figure 3.2 shows the cross section of each well of the Linbro plate and how precipitants and the complex protein mixtures were placed. The cover-slip and the drops were placed over the wells so as to obtain hanging crystallisation drops. The diagram in Figure 3.2 shows how two hanging-drops (i) containing SAM and (ii) containing SAH and sodium dithionite were set side by side over one well.

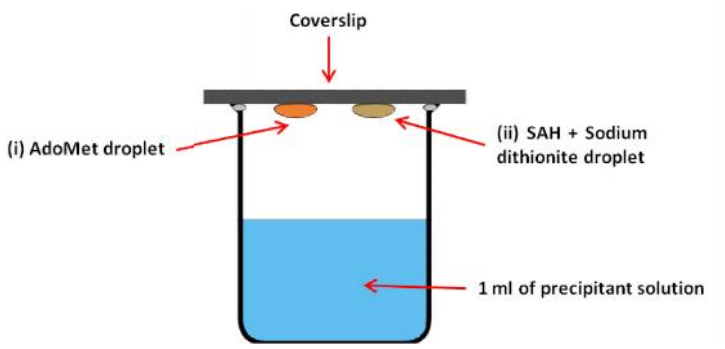

Figure 3.2 *A schematic diagram showing the cross section of one of the wells of the 24 well Linbro plate when set up for the crystallisation assay. The precipitant solutions were 1 mL of either Phosphate buffer (100 mM, pH 6.6) or TRIS buffer (100 mM, pH 8.1) or HEPES Buffer (100 mM, pH 7.5). The droplets were prepared on the cover slips by placing LipA (75 «L, 75 «M) with or without EK(Oct)I (22 «L, 3.9 mM). Droplet (i) contained SAM (8 «L, 70 mM) and droplet (ii) contained SAH (8 «L, 21 mM) and sodium dithionite (2 «L, 2mM..*

Appendix 1

Table A.1 *The initial conditions screened for the crystallization of E.coli LipA. Three buffers were used, phosphate buffer (100 mM, pH 6.6), HEPES buffer (100 mM, pH 7.5) and TRIS buffer (100 mM, pH 8.1).*

	1	2	3	4	5	6
A	Buffer 2.6 M $(NH_4)_2SO_4$ 0.5 µL LipA mixt.	Buffer 2.2 M $(NH_4)_2SO_4$ 1.0 µL LipA mixt.	Buffer 1.8 M $(NH_4)_2SO_4$ 1.5 µL LipA mixt.	Buffer 1.8 M Li_2SO_4 2.0 µL LipA mixt	Buffer 1.6 M Li_2SO_4 2.5 µL LipA mixt	Buffer 1.4 M Li_2SO_4 3.0 µL LipA mixt.
B	Buffer 2.6 M HCOONa 0.5 µL LipA mixt.	Buffer 2.0 M HCOONa 1.0 µL LipA mixt.	Buffer 1.6 M HCOONa 1.5 µL LipA mixt.	Buffer 30% PEG 400 2.0 µL LipA mixt	Buffer 20% PEG 400 2.5 µL LipA mixt	Buffer 15% PEG 400 3.0 µL LipA mixt.
C	Buffer 30% PEG 1500 0.5 µL LipA mixt.	Buffer 20% PEG 1500 1.0 µL LipA mixt.	Buffer 15% PEG 1500 1.5 µL LipA mixt.	Buffer 26% PEG 4000 2.0 µL LipA mixt.	Buffer 16% PEG 4000 2.5 µL LipA mixt.	Buffer 12% PEG 4000 3.0 µL LipA mixt.
D	Buffer 19.5% PEG 8000 0.5 µL LipA mixt.	Buffer 12% PEG 8000 1.0 µL LipA mixt.	Buffer 9% PEG 8000 1.5 µL LipA mixt.	Buffer 10% isopropanol 2.0 µL LipA mixt.	Buffer 5% isopropanol 2.5 µL LipA mixt.	Buffer 2% isopropanol 3.0 µL LipA mixt

Table A.2 *Testing the effect changing the concentration of PEG polymer has the formation of possible E.coli LipA crystals*.

	1	**2**	**3**	**4**	**5**	**6**
A	100 mM TRIS pH 8.1 15 % PEG 400 2.5 µL LipA mixt.	100 mM TRIS pH 8.1 20 % PEG 400 2.5 µL LipA mixt.	100 mM TRIS pH 8.1 25 % PEG 400 2.5 µL LipA mixt.	100 mM TRIS pH 8.1 30% PEG 400 2.5 µL LipA mixt.	100 mM TRIS pH 8.1 40 % PEG 400 2.5 µL LipA mixt.	100 mM TRIS pH 8.1 50 % PEG 400 2.5 µL LipA mixt.
B	100 mM TRIS pH 8.1 15 % PEG 1500 2.5 µL LipA mixt.	100 mM TRIS pH 8.1 20 % PEG 1500 2.5 µL LipA mixt.	100 mM TRIS pH 8.1 25 % PEG 1500 . 2.5 µL LipA mixt.	100 mM TRIS pH 8.1 30% PEG 1500 2.5 µL LipA mixt.	100 mM TRIS pH 8.1 35 % PEG 1500 2.5 µL LipA mixt.	100 mM TRIS pH 8.1 40 % PEG 1500 2.5 µL LipA mixt.
C	100 mM TRIS pH 8.1 15 % PEG 4000 2.5 µL LipA mixt.	100 mM TRIS pH 8.1 18 % PEG 4000 2.5 µL LipA mixt.	100 mM TRIS pH 8.1 20 % PEG 4000 2.5 µL LipA mixt.	100 mM TRIS pH 8.1 25 % PEG 4000 2.5 µL LipA mixt.	100 mM TRIS pH 8.1 28 % PEG 4000 2.5 µL LipA mixt.	100 mM TRIS pH 8.1 30 % PEG 4000 2.5 µL LipA mixt.
D	100 mM TRIS pH 8.1 9 % PEG 8000 2.5 µL LipA mixt. .	100 mM TRIS pH 8.1 12 % PEG 8000 2.5 µL LipA mixt.	100 mM TRIS pH 8.1 15 % PEG 8000 2.5 µL LipA mixt.	100 mM TRIS pH 8.1 18 % PEG 8000 2.5 µL LipA mixt.	100 mM TRIS pH 8.1 21 % PEG 8000 2.5 µL LipA mixt.	100 mM TRIS pH 8.1 27 % PEG 8000 2.5 µL LipA mixt.

Table A.3 *Testing the effect of additives on the crystallization 1*

	1	2	3	4	5	6
A	40 % PEG 4000 Water	40 % PEG 4000 Water	40 % PEG 4000 10 mM Sodium formate Water	40 % PEG 4000 1 M Sodium formate Water	40 % PEG 4000 10 mM Sodium Acetate Water	40 % PEG 4000 1 M Sodium Acetate Water
B	40 % PEG 4000 10 mM Ammonium Sulfate Water	40 % PEG 4000 1M Ammonium Sulfate Water	40 % PEG 4000 10 mM Lithium Sulfate Water	40 % PEG 4000 1M Lithium Sulfate Water	40 % PEG 4000 200 mM Magnesium chloride Water	40 % PEG 4000 2M Magnesium chloride Water
C	40 % PEG 4000 200 mM Sodium chloride Water	40 % PEG 4000 2M Sodium chloride Water	40 % PEG 4000 100 mM Taurine Water	40 % PEG 4000 1M Taurine Water	40 % PEG 4000 50 mM Ethylene diamine Water	40 % PEG 4000 250 mM Ethylene diamine Water
D	40 % PEG 4000 50 mM Pyridine Water	40 % PEG 4000 250 mM Pyridine Water	40 % PEG 4000 100 mM Sucrose Water	40 % PEG 4000 1M Sucrose Water	40 % PEG 4000 50 mM tri-butyl amine Water	40 % PEG 4000 250 mM tri-butyl amine Water

Table A.4 *Testing the effect of additives on the crystallization 2.*

	1	**2**	**3**	**4**	**5**	**6**
A	15 % PEG 400 2.5 µL LipA mixt. 1,8Diaminooctane (1 mM)	15 % PEG 400 2.5 µL LipA mixt. 1,8Diaminooctane (20 mM)	15 % PEG 400 2.5 µL LipA mixt. Fructose (10 mM)	15 % PEG 400 2.5 µL LipA mixt. Fructose (100 mM)	15 % PEG 400 2.5 µL LipA mixt. Arabinose (10 mM)	15 % PEG 400 2.5 µL LipA mixt. Arabinose (100 mM)
B	15 % PEG 400 2.5 µL LipA mixt. Ethanolamine (10 mM)	15 % PEG 400 2.5 µL LipA mixt. Ethanolamine (100 mM)	15 % PEG 400 2.5 µL LipA mixt. 4-Dimethylaminopyridine (10 mM)	15 % PEG 400 2.5 µL LipA mixt. 4-Dimethylaminopyridine (100 mM)	15 % PEG 400 2.5 µL LipA mixt. N-Methylmorpholin ε-N-oxide (10 mM)	15 % PEG 400 2.5 µL LipA mixt. N-Methylmorpholin ε-N-oxide (100 mM)
C	15 % PEG 400 2.5 µL LipA mixt. HEPES (2mM)	15 % PEG 400 2.5 µL LipA mixt. HEPES (20 mM)	15 % PEG 400 2.5 µL LipA mixt. 1,2-Dimethoxyethane (1% w/v)	15 % PEG 400 2.5 µL LipA mixt. 1,2-Dimethoxyethane (5 % w/v)	115 % PEG 400 2.5 µL LipA mixt. Glycolic acid (10 mM)	15 % PEG 400 2.5 µL LipA mixt. Glycolic acid (100 mM)
D	15 % PEG 400 2.5 µL LipA mixt. Imidazole (10 mM)	15 % PEG 400 2.5 µL LipA mixt. Imidazole (100 mM)	15 % PEG 400 2.5 µL LipA mixt. Piperidine (10 mM)	15 % PEG 400 2.5 µL LipA mixt. Piperidine (100 mM)	15 % PEG 400 2.5 µL LipA mixt. tri-Sodium citrate (25 mM)	15 % PEG 400 2.5 µL LipA mixt. tri-Sodium citrate (250 mM)

Table A.5 *The effect of altering the concentration of LipA on the formation of crystals was also investigated.*

	1	**2**	**3**	**4**	**5**	**6**
A	100 mM TRIS pH 8.1 2.6 M $(NH_4)_2SO_4$ 0.5 µL LipA mixt.	100 mM TRIS pH 8.1 2.2 M $(NH_4)_2SO_4$ 1.0 µL LipA mixt.	100 mM TRIS pH 8.1 1.8 M $(NH_4)_2SO_4$ 1.5 µL LipA mixt.	100 mM TRIS pH 8.1 1.8 M Li_2SO_4 2.0 µL LipA mixt	100 mM TRIS pH 8.1 1.6 M Li_2SO_4 2.5 µL LipA mixt	100 mM TRIS pH 8.1 1.4 M Li_2SO_4 3.0 µL LipA mixt.
B	100 mM TRIS pH 8.1 2.6 M HCOONa 0.5 µL LipA mixt.	100 mM TRIS pH 8.1 2.0 M HCOONa 1.0 µL LipA mixt.	100 mM TRIS pH 8.1 1.6 M HCOONa 1.5 µL LipA mixt.	100 mM TRIS pH 8.1 30% PEG 400 2.0 µL LipA mixt	100 mM TRIS pH 8.1 20% PEG 400 2.5 µL LipA mixt	100 mM TRIS pH 8.1 15% PEG 400 3.0 µL LipA mixt.
C	100 mM TRIS pH 8.1 30% PEG 1500 0.5 µL LipA mixt.	100 mM TRIS pH 8.1 20% PEG 1500 1.0 µL LipA mixt.	100 mM TRIS pH 8.1 15% PEG 1500 1.5 µL LipA mixt.	100 mM TRIS pH 8.1 26% PEG 4000 2.0 µL LipA mixt.	100 mM TRIS pH 8.1 16% PEG 4000 2.5 µL LipA mixt.	100 mM TRIS pH 8.1 12% PEG 4000 3.0 µL LipA mixt.
D	100 mM TRIS pH 8.1 19.5% PEG 8000 0.5 µL LipA mixt.	100 mM TRIS pH 8.1 12% PEG 8000 1.0 µL LipA mixt.	100 mM TRIS pH 8.1 9% PEG 8000 1.5 µL LipA mixt.	100 mM TRIS pH 8.1 10% isopropanol 2.0 µL LipA mixt.	100 mM TRIS pH 8.1 5% isopropanol 2.5 µL LipA mixt.	100 mM TRIS pH 8.1 2% isopropanol 3.0 µL LipA mixt

List of References

1. Booker SJ, Cicchillo RM, Grove TL: **Self-sacrifice in radical S-adenosylmethionine proteins**. *Current Opinion in Chemical Biology* 2007, **11**(5):543 - 552.
2. Reed LJ, Hackert ML: **Structure-function relationships in dihydrolipoamide acyltransferases**. *Journal of Biological Chemistry* 1990, **265**(16):8971 - 8974.
3. Miller JR, Busby RW, Jordan SW, Cheek J, Henshaw TF, Ashley GW, Broderick JB, Cronan JE, Jr., Marletta MA: **Escherichia coli LipA is a lipoyl synthase: in vitro biosynthesis of lipoylated pyruvate dehydrogenase complex from octanoyl-acyl carrier protein**. *Biochemistry* 2000, **39**(49):15166 - 15178.
4. Fontecave M, Ollagnier-de-Choudens S, Mulliez E: **Biological radical sulfur insertion reactions**. *Chemical Reviews* 2003, **103**(6):2149-2166.
5. Hayden MA, Huang I, Bussiere DE, Ashley GW: **The Biosynthesis of Lipoic Acid - Cloning of *lip*, a Lipoate Biosynthetic Locus of *Escherichia-Coli***. *Journal of Biological Chemistry* 1992, **267**(14):9512 - 9515.
6. Fontecave M, Ollagnier-de-Choudens S, Mulliez E: **Biological Radical Sulfur Insertion Reactions**. *Chemical Reviews* 2003, **103**(6):2149 - 2166.
7. Frey PA, Hegeman AD, Ruzicka FJ: **The Radical SAM Superfamily**. *Critical Reviews in Biochemistry and Molecular Biology* 2008, **43**(1):63-88.
8. Choi-Rhee E, Cronan JE: **A Nucleosidase Required for In Vivo Function of the S-Adenosyl-L-Methionine Radical Enzyme, Biotin Synthase**. *Chemistry & Biology* 2005, **12**(5):589 - 593.
9. Parry RJ: **Biosynthesis of some sulfur-containing natural products investigations of the mechanism of carbon-sulfur bond formation**. *Tetrahedron* 1983, **39**(8):1215 - 1238.
10. Chiang P, Gordon R, Tal J, Zeng G, Doctor B, Pardhasaradhi K, McCann P: **S-Adenosylmethionine and methylation**. *The Journal of the Federation of American Societies for Experimental Biology* 1996, **10**(4):471 - 480.
11. Cantoni GL: **Biological Methylation: Selected Aspects**. *Annual Review of Biochemistry* 1975, **44**(1):435 - 451.

12. Fontecave M, Atta M, Mulliez E: **S-adenosylmethionine: nothing goes to waste**. *Trends in Biochemical Sciences* 2004, **29**(5):243 - 249.
13. Stubbe J, van der Donk WA: **Protein Radicals in Enzyme Catalysis**. *Chemical Reviews* 1998, **98**(2):705 - 762.
14. Jarrett JT: **The generation of 5'-deoxyadenosyl radicals by adenosylmethionine-dependent radical enzymes**. *Current Opinion in Chemical Biology* 2003, **7**(2):174 - 182.
15. Layer G, Heinz DW, Jahn D, Schubert W-D: **Structure and fuction of radical SAM enzymes**. *Current Opinion in Chemical Biology* 2004, **8**:468 - 476.
16. Fontecave M, Mulliez E, Ollagnier-de-Choudens S: **Adenosylmethionine as a source of 5'-deoxyadenosyl radicals**. *Current Opinion in Chemical Biology* 2001, **5**(5):506 - 512.
17. Sofia HJ, Chen G, Hetzler BG, Reyes-Spindola JF, Miller NE: **Radical SAM, a novel protein superfamily linking unresolved steps in familiar biosynthetic pathways with radical mechanisms: functional characterization using new analysis and information visualization methods**. *Nucleic Acids Research* 2001, **29**(5):1097 - 1106.
18. Booker SJ, Grove TL: **Mechanistic and functional versatility of radical SAM enzymes**. *F1000 Biology Reports*, **2**:52 - 63.
19. Frey PA, Hegeman AD, Ruzicka FJ: **The Radical SAM Superfamily**. *Critical Reviews in Biochemistry and Molecular Biology* 2008, **43**(1):63 - 88.
20. Duschene KS, Veneziano SE, Silver SC, Broderick JB: **Control of radical chemistry in the AdoMet radical enzymes**. *Current Opinion in Chemical Biology* 2009, **13**(1):74 - 83.
21. Chirpich TP, Zappia V, Costilow RN, Barke HA: **Lysine 2,3-aminomutase. Purification and properties of a pyridoxal phosphate and S-adenosylmethionine-activated enzyme**. *Journal of Biological Chemistry* 1970, **245**:1778 - 1789.
22. Cosper NJ, Booker SJ, Ruzicka F, Frey PA, Scott RA: **Direct FeS Cluster Involvement in Generation of a Radical in Lysine 2,3-Aminomutase**. *Biochemistry* 2000, **39**(51):15668 - 15673.
23. Hanzelmann P, Schindelin H: **Crystal structure of the S-adenosylmethionine-dependent enzyme MoaA and its implications for**

molybdenum cofactor deficiency in humans. *Proceedings of the National Academy of Sciences of the United States of America* 2004, **101**(35):12870 - 12875.

24. Layer G, Moser J, Heinz DW, Jahn D, Schubert WD: **Crystal structure of coproporphyrinogen III oxidase reveals cofactor geometry of radical SAM enzymes**. *The European Molecular Biology Organization Journal* 2003, **22**:6214 – 6224.
25. Kozbial P, Mushegian A: **Natural history of S-adenosylmethionine-binding proteins**. *BMC Structural Biology* 2005, **5**(1):19 - 45.
26. Vey JL, Drennan CL: **Structural Insights into Radical Generation by the Radical SAM Superfamily**. *Chemical Reviews*, **111**(4):2487 - 2506.
27. Marsh ENG, Patwardhan A, Huhta MS: **S-Adenosylmethionine radical enzymes**. *Bioorganic Chemistry* 2004, **32**(5):326 - 340.
28. Wang SC, Frey PA: **S-adenosylmethionine as an oxidant: the radical SAM superfamily**. *Trends in Biochemical Sciences* 2007, **32**(3):101 - 110.
29. Challand MR, Driesener RC, Roach PL: **Radical S-adenosylmethionine enzymes: Mechanism, control and function**. *Natural Product Reports* 2011, **28**:1696 - 1721.
30. Frey PA, Magnusson OT: **S-adenosylmethionine: a wolf in sheep's clothing, or a rich man's adenosylcobalamin**. *Chemical Reviews* 2003, **103**:2129.
31. Nesbitt NM, Cicchillo RM, Lee K-H, Grove TL, Booker SJ: **Lipoic acid biosynthesis**. *Oxidative Stress and Disease* 2008, **24**:11 - 55.
32. Buckel W, Golding BT: **Radical Enzymes in Anaerobes**. *Annual Review of Microbiology* 2006, **60**(1):27 - 49.
33. Bryant P, Kriek M, Wood RJ, Roach PL: **The activity of a thermostable lipoyl synthase from Sulfolobus solfataricus with a synthetic octanoyl substrate**. *Analytical Biochemistry* 2006, **351**(1):44 - 49.
34. Frey PA, Reed GH: **Radical Mechanisms in Adenosylmethionine- and Adenosylcobalamin-Dependent Enzymatic Reactions**. *Current Opinion in Chemical Biology* 2000, **382**:6 - 14.
35. Chirpich TP, Zappia V, Costilow RN, Barker HA: **Lysine 2,3-Aminomutase**. *Journal of Biological Chemistry* 1970, **245**(7):1778 - 1789.

36. Lieder KW, Booker S, Ruzicka FJ, Beinert H, Reed GH, Frey PA: **S-Adenosylmethionine-Dependent Reduction of Lysine 2,3-Aminomutase and Observation of the Catalytically Functional Iron−Sulfur Centers by Electron Paramagnetic Resonance**. *Biochemistry* 1998, **37**(8):2578 - 2585.

37. Frey PA: **The role of radicals in enzymatic processes**. *The Chemical Record* 2001, **1**(4):277 - 289.

38. Marsh ENG, Drennan CL: **Adenosylcobalamin-dependent isomerases: new insights into structure and mechanism**. *Current Opinion in Chemical Biology* 2001, **5**(5):499 - 505.

39. Banerjee R: **Radical Carbon Skeleton Rearrangements: Catalysis by Coenzyme B12-Dependent Mutases**. *Chemical Reviews* 2003, **103**(6):2083 - 2094.

40. Johnson MK: **Iron-sulfur proteins: new roles for old clusters**. *Current Opinion in Chemical Biology* 1998, **2**(2):173 - 181.

41. Chen D, Walsby C, Hoffman BM, Frey PA: **Coordination and Mechanism of Reversible Cleavage of S-Adenosylmethionine by the [4Fe-4S] Center in Lysine 2,3-Aminomutase**. *Journal of the American Chemical Society* 2003, **125**(39):11788 - 11789.

42. Walsby CJ, Hong W, Broderick WE, Cheek J, Ortillo D, Broderick JB, Hoffman BM: **Electron-Nuclear Double Resonance Spectroscopic Evidence That S-Adenosylmethionine Binds in Contact with the Catalytically Active [4Fe-4S]$^{+}$ Cluster of Pyruvate Formate-Lyase Activating Enzyme**. *Journal of the American Chemical Society* 2002, **124**(12):3143 - 3151.

43. Cosper MM, Jameson GNL, Davydov R, Eidsness MK, Hoffman BM, Huynh BH, Johnson MK: **The [4Fe-4S]$^{2+}$ Cluster in Reconstituted Biotin Synthase Binds S-Adenosyl-l-methionine**. *Journal of the American Chemical Society* 2002, **124**(47):14006 - 14007.

44. Krebs C, Broderick WE, Henshaw TF, Broderick JB, Huynh BH: **Coordination of Adenosylmethionine to a Unique Iron Site of the [4Fe-4S] of Pyruvate Formate-Lyase Activating Enzyme: A Mössbauer Spectroscopic Study**. *Journal of the American Chemical Society* 2002, **124**(6):912 - 913.

45. Marquet A: **Enzymology of carbon-sulfur bond formation**. *Current Opinion in Chemical Biology* 2001, **5**(5):541 - 549.

46. Zhao X, Miller JR, Jiang Y, Marletta MA, Cronan JE: **Assembly of the Covalent Linkage between Lipoic Acid and Its Cognate Enzymes**. *Chemical Biology* 2003, **10**(12):1293 - 1302.

47. Lin S, Hanson RE, Cronan JE: **Biotin Synthesis Begins by Hijacking the Fatty Acid Synthetic Pathway**. *Nature Chemical Biology* 2010, **6**(9):682 - 688.

48. Cheek J, Broderick JB: **Adenosylmethionine-Dependent Iron-Sulfur Enzymes: Versatile Clusters in a Radical New Role.** *Journal of Biological Inorganic Chemistry* 2001, **6**:209 - 226.

49. Ollagnier-de-Choudens S, Mulliez E, Fontecave M: **The PLP-dependent biotin synthase from Escherichia coli: mechanistic studies**. *Federation of European Biochemical Societies (FEBS) Letters* 2002, **532**(3):465 - 468.

50. Parry RJ, Kunitani MG: **Biotin biosynthesis. 1. The incorporation of specifically tritiated dethiobiotin into biotin**. *Journal of the American Chemical Society* 1976, **98**(13):4024 - 4026.

51. Frappier F, Jouany M, Marquet A, Olesker A, Tabet JC: **On the mechanism of the conversion of dethiobiotin to biotin in E. coli. Studies with deuterated precursors using tandem mass spectroscopic (MS-MS) techniques**. *The Journal of Organic Chemistry* 1982, **47**(12):2257 - 2261.

52. Guillerm G, Frappier F, Gaudry M, Marquet A: **On the mechanism of conversion of dethiobiotin to biotin in Escherichia coli**. *Biochimie* 1977, **59**(1):119 - 121.

53. Frey PA, Magnusson OT: **S-adenosylmethionine: a wolf in sheep's clothing, or a rich man's adenosylcobalamin**. *Chem Rev* 2003, **103**:2129.

54. Trainor DA, Parry RJ, Gitterman A: **Biotin biosynthesis. 2. Stereochemistry of sulfur introduction at C-4 of dethiobiotin**. *Journal of the American Chemical Society* 1980, **102**(4):1467 - 1468.

55. Florentin D, Tse Sum Bui B, Marquet A, Ohshiro T, Izumi Y: **On the mechanism of biotin synthase of Bacillus sphaericus.** *Acad Sci Paris, Life Sci* 1994, **317**(6):485 - 488.

56. Ifuku O, Kishimoto J, Haze S, Yanagi M, Fukushima S: **Conversion of dethiobiotin to biotin in cell-free extracts of Escherichia coli.** *Bioscience, Biotechnology, and Biochemistry* 1992, **56**(11):1780 -1785.

57. Birch OM, Fuhrmann M, Shaw NM: **Biotin Synthase from Escherichiacoli, an Investigation of the Low Molecular Weight and Protein Components Required for Activity inVitro**. *Journal of Biological Chemistry* 1995, **270**(32):19158 - 19165.

58. Frey PA, Magnusson OT: **S-Adenosylmethionine: A Wolf in Sheep's Clothing, or a Rich Man's Adenosylcobalamin?** *Chemical Reviews* 2003, **103**(6):2129 - 2148.

59. Sanyal I, Cohen G, Flint DH: **Biotin Synthase: Purification, Characterization as a [2Fe-2S]Cluster Protein, and in vitro Activity of the Escherichia coli bioB Gene Product**. *Biochemistry* 1994, **33**(12):3625 - 3631.

60. Méjean A, Tse Sum Bui B, Florentin D, Ploux O, Izumi Y, Marquet A: **Highly purified biotin synthase can convert dethiobiotin into biotin in the absence of any other protein, in the presence of photoreduced deazaflavin**. *Biochemical and Biophysical Research Communications* 1995, **217**(3):1231 - 1237.

61. Jarrett JT: **The novel structure and chemistry of iron-sulfur clusters in the adenosylmethionine-dependent radical enzyme biotin synthase**. *Archives of Biochemistry and Biophysics* 2005, **433**(1):312 - 321.

62. Escalettes F, Florentin D, Tse Sum Bui B, Lesage D, Marquet Ae: **Biotin Synthase Mechanism: Evidence for Hydrogen Transfer from the Substrate into Deoxyadenosine**. *Journal of the American Chemical Society* 1999, **121**(15):3571 - 3578.

63. Guianvarc'h D, Florentin D, Tse Sum Bui B, Nunzi F, Marquet A: **Biothin synthase, a new member of the family of enzymes which uses S-adenosylmethionine as a source of deoxyadenosyl radical**. *Biochemical and Biophysical Research Communications* 1997, **236**(2):402 - 406.

64. Shaw NM, Birch OM, Tinschert A, Venetz V, Dietrich R, Savoy LA: **Biotin synthase from Escherichia coli: isolation of an enzyme-generated intermediate and stoichiometry of S-adenosylmethionine use.** *Biochemical Journal* 1998 **330**(3):1079 -1085.

65. Escalettes F, Florentin D, Tse Sum Bui B, Lesage D, Marquet A: **Biotin Synthase Mechanism: Evidence for Hydrogen Transfer from the Substrate into Deoxyadenosine.** *Journal of the American Chemical Society* 1999, **121**(15):3571 - 3578.

66. Becker A, Fritz-Wolf K, Kabsch W, Knappe J, Schultz S, Wagner AFV: **Structure and mechanism of the glycyl radical enzyme pyruvate formate-lyase**. *Nature Structural and Molecular Biology* 1999, **6**(10):969 - 975.

67. Marquet A, Frappier F, Guillerm G, Azoulay M, Florentin D, Tabet JC: **Biotin biosynthesis: synthesis and biological evaluation of the putative intermediate thiols**. *Journal of the American Chemical Society* 1993, **115**(6):2139 - 2145.

68. Mejean A, Bui BTS, Florentin D, Ploux O, Izumi Y, Marquet A: **Highly Purified Biotin Synthase Can Transform Dethiobiotin into Biotin in the Absence of Any Other Protein, in the Presence of Photoreduced Deazaflavin**. *Biochemical and Biophysical Research Communications* 1995, **217**(3):1231-1237.

69. Duin EC, Lafferty ME, Crouse BR, Allen RM, Sanyal I, Flint DH, Johnson MK: **[2Fe-2S] to [4Fe-4S] Cluster Conversion in Escherichia coli Biotin Synthase**. *Biochemistry* 1997, **36**(39):11811 - 11820.

70. Benda R, Tse Sum Bui B, Schuenemann V, Florentin D, Marquet A, Trautwein AX: **Iron Sulfur Clusters of Biotin Synthase In Vivo: A Mossbauer Study**. *Biochemistry* 2002, **41**(50):15000 - 15006.

71. Ollagnier-de Choudens S, Sanakis Y, Hewitson KS, Roach P, Baldwin JE, Munck E, Fontecave M: **Iron-Sulfur Center of Biotin Synthase and Lipoate Synthase**. *Biochemistry* 2000, **39**(14):4165 - 4173.

72. Ugulava NB, Gibney BR, Jarrett JT: **Iron−Sulfur Cluster Interconversions in Biotin Synthase: Dissociation and Reassociation of Iron during Conversion of [2Fe-2S] to [4Fe-4S] Clusters.** *Biochemistry* 2000, **39**(17):5206 - 5214.

73. Ugulava NB, Gibney BR, Jarrett JT: **Biotin Synthase Contains Two Distinct Iron-Sulfur Cluster Binding Sites: Chemical and Spectroelectrochemical Analysis of Iron-Sulfur Cluster Interconversions**. *Biochemistry* 2001, **40**(28):8343 - 8351.

74. DeMoll E, White RH, Shive W: **Determination of the metabolic origins of the sulfur and 3'-nitrogen atoms in biotin of Escherichia coli by mass spectrometry.** *Biochemistry* 1984, **23**(3):558 - 562.

75. Ohshiro T, Yamamoto M, Tse Sum Bui B, Florentin D, Marquet A, Izumi Y: **Enzymatic conversion of dethiobiotin to biotin in cell free extracts of a bacillus sphaericus bioB transformant**. *Biosci Biotechnol, Biochem* 1994, **58**(9):1738 - 1741.

76. Sanyal I, Gibson KJ, Flint DH: **Escherichia coliBiotin Synthase: An Investigation into the Factors Required for Its Activity and Its Sulfur Donor.** *Archives of Biochemistry and Biophysics* 1996, **326**(1):48 - 56.

77. Ugulava NB, Sacanell CJ, Jarrett JT: **Spectroscopic Changes during a Single Turnover of Biotin Synthase: Destruction of a [2Fe-2S] Cluster Accompanies Sulfur Insertion** *Biochemistry* 2001, **40**(28):8352 - 8358.

78. Tse Sum Bui B, Florentin D, Fournier F, Ploux O, Méjean A, Marquet A: **Biotin synthase mechanism: on the origin of sulphur**. *Federation of European Biochemical Societies (FEBS) Letters* 1998, **440**(1-2):226 - 230.

79. Tse Sum Bui B, Escalettes F, Chottard G, Florentin D, Marquet A: **Enzyme-mediated sulfide production for the reconstitution of [2Fe−2S] clusters into apo-biotin synthase of Escherichia coli**. *European Journal of Biochemistry* 2000, **267**(9):2688 - 2694.

80. Kiyasu T, Asakura A, Nagahashi Y, Hoshino T: **Contribution of Cysteine Desulfurase (NifS Protein) to the Biotin Synthase Reaction of Escherichia coli.** *Journal of Bacteriology* 2000, **182**:2879 - 2885.

81. Gibson KJ, Pelletier DA, Turner IM: **Transfer of Sulfur to Biotin from Biotin Synthase (BioB protein)**. *Biochemical and Biophysical Research Communications* 1999, **254**(3):632 - 635.

82. Ugulava NB, Surerus KK, Jarrett JT: **Evidence from Mossbauer Spectroscopy for Distinct [2Fe-2S]2+ and [4Fe-4S]2^{+} Cluster Binding Sites in Biotin Synthase from Escherichia coli**. *Journal of the American Chemical Society* 2002, **124**(31):9050 - 9051.

83. McIver L, Baxter RL, Campopiano DJ: **Identification of the [Fe-S] Cluster-binding Residues of Escherichia coli Biotin Synthase**. *Journal of Biological Chemistry* 2000, **275**(18):13888 - 13894.

84. Broach RB, Jarrett JT: **Role of the [2Fe-2S]2+ Cluster in Biotin Synthase: Mutagenesis of the Atypical Metal Ligand Arginine 260**. *Biochemistry* 2006, **45**(47):14166 - 14174.

85. Hewitson KS, Baldwin JE, Shaw NM, Roach PL: **Mutagenesis of the proposed iron-sulfur cluster binding ligands in Escherichia coli biotin synthase**. *Federation of European Biochemical Societies (FEBS) Letters* 2000, **466**(2-3):372 - 376.

86. Ollagnier-de Choudens S, Sanakis Y, Hewitson KS, Roach P, Münck E, Fontecave M: **Reductive Cleavage of S-Adenosylmethionine by Biotin Synthase from Escherichia coli**. *Journal of Biological Chemistry* 2002, **277**(16):13449 - 13454.

87. Hewitson K, Ollagnier-De Choudens S, Sanakis Y, Shaw NM, Baldwin JE, Munck E, Roach PL, Fontecave M: **The iron-sulfur center of biotin synthase: site directed mutants**. *Journal of Biological Inorganic Chemistry* 2002, **7**(1):83 - 93.

88. Berkovitch F, Nicolet Y, Wan JT, Jarrett JT, Drennan CL: **Crystal Structure of Biotin Synthase, an S-Adenosylmethionine-Dependent Radical Enzyme**. *Science* 2004, **303**(5654):76 - 79.

89. Mislow K, Meluch WC: **The Configuration of (+)-a-Lipoic Acid.** . *Journal of the American Chemical Society* 1956, **78**(10):2341 - 2342.

90. Cremer DR, Rabeler R, Roberts A, Lynch B: **Long-term safety of [alpha]-lipoic acid (ALA) consumption: A 2-year study**. *Regulatory Toxicology and Pharmacology* 2006, **46**(3):193 - 201.

91. Spalding MD, Prigge ST: **Lipoic Acid Metabolism in Microbial Pathogens**. *Microbiology and Molecular Biology Reviews* 2010, **74**(2):200 - 228.

92. Billgren ES, Cicchillo RM, Nesbitt NM, Booker SJ: **7.07 - Lipoic Acid Biosynthesis and Enzymology**. In: *Comprehensive Natural Products II.* Edited by Editors-in-Chief: Lew M, Hung-Wen L. Oxford: Elsevier; 2010: 181 - 212.

93. Patel M, Harris R: **Mammalian alpha-keto acid dehydrogenase complexes: gene regulation and genetic defects**. *The Journal of The Federation of American Societies for Experimental Biology* 1995, **9**(12):1164 - 1172.

94. Perham RN: **Swinging Arms and Swinging Domains in Multifunctional Enzymes Catalytic Machines for Multistep Reactions**. *Annual Review of Biochemistry* 2000, **69**(1):961-1004.

95. Hassan BH, Cronan JE: **Protein-Protein Interactions in Assembly of Lipoic Acid on the 2-Oxoacid Dehydrogenases of Aerobic Metabolism**. *Journal of Biological Chemistry* 2011, **286**(10):8263 - 8276.

96. Berg A, Vervoort J, De Kok A: **Three-Dimensional Structure in Solution of the N-Terminal Lipoyl Domain of the Pyruvate Dehydrogenase Complex from Azotobacter vinelandii**. *European Journal of Biochemistry* 1997, **244**(2):352 - 360.

97. Cronan JE, Zhao X, Jiang Y: **Function, attachment and synthesis of lipoic acid in Escherichia coli**. *Advances in Microbiological Physiology* 2005, **50**:103 - 146.

98. Kikuchi G, Motokawa Y, Yoshida T, Hiraga K: **Glycine cleavage system: reaction mechanism, physiological significance, and hyperglycinemia**. *Proceedings of the Japan Academy, Series B* 2008, **84**(7):246 - 263.

99. Douce R, Bourguignon J, Neuburger M, Rébeillé F: **The glycine decarboxylase system: a fascinating complex**. *Trends in Plant Science* 2001, **6**(4):167-176.

100. Douce R, Neuburger M: **Biochemical dissection of photorespiration**. *Current Opinion in Plant Biology* 1999, **2**(3):214 - 222.

101. Fujiwara K, Okamura-Ikeda K, Motokawa Y: **Expression of mature bovine H-protein of the glycine cleavage system in Escherichia coli and in vitro lipoylation of the apoform**. *Journal of Biological Chemistry* 1992, **267**(28):20011 - 20016.

102. Reed LJ, DeBusk BG, Gunsalus IC, Schnakenberg GHF: **Chemical Nature of a-Lipoic acid**. *Journal of the American Chemical Society* 1951, **73**(12):5920 - 5920.

103. Reed LJ, Gunsalus IC, Schnakenberg GHF, Soper QF, Boaz HE, Kern SF, Parke TV: **Isolation, Characterization and Structure of α-Lipoic Acid**. *Journal of the American Chemical Society* 1953, **75**(6):1267 - 1270.

104. Bullock MW, Brockman JA, Patterson EL, Pierce JV, Stokstad ELR: **Synthesis of compounds in the thioctic acid series**. *Journal of the American Chemical Society* 1952, **74**(13):3455 - 3455.

105. Parry RJ: **Biosynthesis of lipoic acid. 1. Incorporation of specifically tritiated octanoic acid into lipoic acid**. *Journal of the American Chemical Society* 1977, **99**(19):6464 - 6466.

106. White RH: **Stable isotope studies on the biosynthesis of lipoic acid in Escherichia coli**. *Biochemistry* 1980, **19**(1):15 - 19.

107. Marquet A, Tse Sum Bui B, Florentin D: **Biosynthesis of Biotin and Lipoic Acid**. *Vitamins and Hormones* 2001, **61**:51 - 101.

108. Parry RJ, Trainor DA: **Biosynthesis of lipoic acid. 2. Stereochemistry of sulfur introduction at C-6 of octanoic acid**. *Journal of the American Chemical Society* 1978, **100**(16):5243 - 5244.

109. Mislow K, Meluch WC: **The Stereochemistry of α-Lipoic Acid**. *Journal of the American Chemical Society* 1956, **78**(22):5920 - 5923.

110. White RH: **Stoichiometry and stereochemistry of deuterium incorporated into fatty acids by cells of Escherichia coli grown on [methyl-2H^3]acetate**. *Biochemistry* 1980, **19**(1):9 - 15.

111. White RH: **Biosynthesis of lipoic acid: extent of incorporation of deuterated hydroxy- and thiooctanoic acids into lipoic acid**. *Journal of the American Chemical Society* 1980, **102**(21):6605 - 6607.

112. Vise AB, Lascelles J: **Some Properties of a Mutant Strain of Escherichia coli which Requires Lysine and Methionine or Lipoic Acid for Growth**. *Journal of General Microbiology* 1967, **48**(1):87 - 93.

113. Herbert AA, Guest JR: **Biochemical and Genetic Studies with Lysine + Methionine Mutants of Escherichia coli: Lipoic Acid and a-Ketoglutarate Dehydrogenase-less Mutants.** *Journal of General Microbiology* 1968, **53**(3):363 - 381.

114. Brookfield DE, Green J, Ali ST, Machado RS, Guest JR: **Evidence for two protein-lipoylation activities in Escherichia coli**. *Federation of European Biochemical Societies (FEBS) Letters* 1991, **295**(1-3):13 - 16.

115. Reed KE, Cronan JE, Jr.: **Lipoic acid metabolism in Escherichia coli: sequencing and functional characterization of the lipA and lipB genes**. *Journal of Bacteriology* 1993, **175**(5):1325 - 1336.

116. Jordan SW, Cronan JE, Jr.: **Biosynthesis of lipoic acid and posttranslational modification with lipoic acid in Escherichia coli**. *Methods in Enzymology* 1997, **279**:176 - 183.

117. Vanden Boom TJ, Reed KE, Cronan JE, Jr.: **Lipoic acid metabolism in Escherichia coli: isolation of null mutants defective in lipoic acid biosynthesis, molecular cloning and characterization of the E. coli lip locus, and identification of the lipoylated protein of the glycine cleavage system**. *Journal of Bacteriology* 1991, **173**(20):6411 - 6420.

118. Hayden MA, Huang I, Bussiere DE, Ashley GW: **The biosynthesis of lipoic acid. Cloning of lip, a lipoate biosynthetic locus of Escherichia coli**. *Journal of Biological Chemistry* 1992, **267**(14):9512 - 9515.

119. Hayden MA, Huang IY, Iliopoulos G, Orozco M, Ashley GW: **Biosynthesis of lipoic acid: Characterization of the lipoic acid auxotrophs Escherichia coli W1485-lip2 and JRG33-lip9**. *Biochemistry* 1993, **32**(14):3778 - 3782.

120. Morris TW, Reed KE, Cronan JE, Jr.: **Identification of the gene encoding lipoate-protein ligase A of Escherichia coli. Molecular cloning and characterization of the lplA gene and gene product**. *Journal of Biological Chemistry* 1994, **269**(23):16091 - 16100.

121. Busby RW, Schelvis JPM, Yu DS, Babcock GT, Marletta MA: **Lipoic Acid Biosynthesis: LipA Is an Iron−Sulfur Protein**. *Journal of the American Chemical Society* 1999, **121**(19):4706 - 4707.

122. Ollagnier-de Choudens S, Fontecave M: **The lipoate synthase from Escherichia coli is an iron-sulfur protein**. *Federation of European Biochemical Societies (FEBS) Letters* 1999, **453**(1-2):25 - 28.

123. Cicchillo RM, Lee KH, Baleanu-Gogonea C, Nesbitt NM, Krebs C, Booker SJ: **Escherichia coli lipoyl synthase binds two distinct [4Fe-4S] clusters per polypeptide**. *Biochemistry* 2004, **43**(37):11770 - 11781.

124. Jordan SW, Cronan JE, Jr.: **A new metabolic link. The acyl carrier protein of lipid synthesis donates lipoic acid to the pyruvate dehydrogenase complex in Escherichia coli and mitochondria**. *Journal of Biological Chemistry* 1997, **272**(29):17903 - 17906.

125. Gueguen V, Macherel D, Jaquinod M, Douce R, Bourguignon J: **Fatty Acid and Lipoic Acid Biosynthesis in Higher Plant Mitochondria**. *Journal of Biological Chemistry* 2000, **275**(7):5016 - 5025.

126. Wada M, Yasuno R, Jordan SW, Cronan JE, Jr., Wada H: **Lipoic acid metabolism in Arabidopsis thaliana: cloning and characterization of a**

cDNA encoding lipoyltransferase. *Plant Cell Physiology* 2001, **42**(6):650-656.

127. Zhao X, Miller JR, Jiang YF, Marletta MA, Cronan JE: **Assembly of the covalent linkage between lipoic acid and its cognate enzymes**. *Chemistry & Biology* 2003, **10**(12):1293 - 1302.
128. Booker SJ: **Unraveling the pathway of lipoic acid biosynthesis**. *Journal of Chemical Biology* 2004, **11**(1):10 - 12.
129. Miller JR, Busby RW, Jordan SW, Cheek J, Henshaw TF, Ashley GW, Broderick JB, Cronan JE, Marletta MA: **Escherichia coli LipA Is a Lipoyl Synthase: In Vitro Biosynthesis of Lipoylated Pyruvate Dehydrogenase Complex from Octanoyl-Acyl Carrier Protein**. *Biochemistry* 2000, **39**(49):15166-15178.
130. Booker SJ: **Unraveling the pathway of lipoic acid biosynthesis**. *Chemistry & Biology* 2004, **11**(1):10-12.
131. Fujiwara K, Okamura-Ikeda K, Motokawa Y: **Purification and characterization of lipoyl-AMP:N epsilon-lysine lipoyltransferase from bovine liver mitochondria**. *Journal of Biological Chemistry* 1994, **269**(24):16605 - 16609.
132. Fujiwara K, Takeuchi S, Okamura-Ikeda K, Motokawa Y: **Purification, Characterization, and cDNA Cloning of Lipoate-activating Enzyme from Bovine Liver**. *Journal of Biological Chemistry* 2001, **276**(31):28819 - 28823.
133. Zhao X, Miller JR, Jiang Y, Marletta MA, Cronan JE: **Assembly of the Covalent Linkage between Lipoic Acid and Its Cognate Enzymes**. *Chemistry & Biology* 2003, **10**(12):1293-1302.
134. Cicchillo RM, Iwig DF, Jones AD, Nesbitt NM, Baleanu-Gogonea C, Souder MG, Tu L, Booker SJ: **Lipoyl Synthase Requires Two Equivalents of S-Adenosyl-l-methionine To Synthesize One Equivalent of Lipoic Acid** *Biochemistry* 2004, **43**(21):6378 - 6386.
135. Reed LJ, Hackert ML: **Structure-function relationships in dihydrolipoamide acyltransferases**. In: *Journal of Biological Chemistry.* vol. 265; 1990: 8971 - 8974.
136. Bryant P: **Investigations into Lipoic Acid Biosynthesis** *PhD Research.* Southampton: University of Southampton; 2008.

137. Cicchillo RM, Lee K-H, Baleanu-Gogonea C, Nesbitt NM, Krebs C, Booker SJ: **Escherichia coli Lipoyl Synthase Binds Two Distinct [4Fe-4S] Clusters per Polypeptide**. *Biochemistry* 2004, **43**(37):11770 - 11781.

138. Bui BTS, Escalettes F, Chottard G, Florentin D, Marquet A: **Enzyme-mediated sulfide production for the reconstitution of [2Fe-2S] clusters into apo-biotin synthase of Escherichia coli**. *European Journal of Biochemistry* 2000, **267**(9):2688 - 2694.

139. Cicchillo RM, Booker SJ: **Mechanistic Investigations of Lipoic Acid Biosynthesis in Escherichia coli: Both Sulfur Atoms in Lipoic Acid are Contributed by the Same Lipoyl Synthase Polypeptide**. *Journal of the American Chemical Society* 2005, **127**(9):2860 - 2861.

140. Cicchillo RM, Iwig DF, Jones AD, Nesbitt NM, Baleanu-Gogonea C, Souder MG, Tu L, Booker SJ: **Lipoyl Synthase Requires Two Equivalents of S-Adenosyl-l-methionine To Synthesize One Equivalent of Lipoic Acid.** In., vol. 43; 2004: 6378-6386.

141. Douglas P, Kriek M, Bryant P, Roach PL: **Lipoyl Synthase Inserts Sulfur Atoms into an Octanoyl Substrate in a Stepwise Manner**. *Angewandte Chemie International Edition* 2006, **45**(31):5197 - 5199.

142. Phornphisutthimas S, Thamchaipenet A, Panijpan B: **Conjugation in Escherichia coli**. *Biochemistry and Molecular Biology Education* 2007, **35**(6):440 - 445.

143. Adelberg EA, Pittard J: **Chromosome Transfer in Bacterial Conjugation**. *Microbiology and Molecular Biology Reviews* 1965, **29**(2):161-172.

144. Jones D, Sneath PH: **Genetic transfer and bacterial taxonomy**. *Microbiology and Molecular Biology Reviews* 1970, **34**(1):40 - 81.

145. Mandel M, Higa A: **Calcium-dependent bacteriophage DNA infection**. *Journal of Molecular Biology* 1970, **53**(1):159 - 162.

146. Cohen SN, Chang ACY, Hsu L: **Nonchromosomal Antibiotic Resistance in Bacteria: Genetic Transformation of Escherichia coli by R-Factor DNA**. *Proceedings of the National Academy of Sciences* 1972, **69**(8):2110 - 2114.

147. Panja S, Aich P, Jana B, Basu T: **How does plasmid DNA penetrate cell membranes in artificial transformation process of Escherichia coli?** *Molecular Membrane Biology* 2008, **25**(5):411 - 422.

148. Panja S, Saha S, Jana B, Basu T: **Role of membrane potential on artificial transformation of E. coli with plasmid DNA**. *Journal of Biotechnology* 2006, **127**(1):14 - 20.

149. Michod RE, Wojciechowski MF, Hoelzer MA: **DNA Repair and the Evolution of Transformation in the Bacterium Bacillus subtilis**. *Genetics* 1988, **118**(1):31 - 39.

150. Redfield RJ: **Evolution of Bacterial Transformation: Is Sex With Dead Cells Ever Better Than No Sex at All?** *Genetics* 1988, **119**(1):213 - 221.

151. Yoshida N, Sato M: **Plasmid uptake by bacteria: a comparison of methods and efficiencies**. *Applied Microbiology and Biotechnology* 2009, **83**(5):791 - 798.

152. Kriek M, Peters L, Takahashi Y, Roach PL: **Effect of iron-sulfur cluster assembly proteins on the expression of Escherichia coli lipoic acid synthase**. *Protein Expression and Purification* 2003, **28**:241 - 245.

153. Wei H, Therrien C, Blanchard A, Guan S, Zhu Z: **The Fidelity Index provides a systematic quantitation of star activity of DNA restriction endonucleases**. *Nucleic Acids Research* 2008, **36**(9):e50.

154. Bloch KD: **Digestion of DNA with Restriction Endonucleases**. In: *Current Protocols in Protein Science*. John Wiley & Sons, Inc.; 2001: A.4I.1–A.4I.3.

155. Fish WW: **Rapid colorimetric micromethod for the quantitation of complexed iron in biological samples**. In: *Methods in Enzymology*. Edited by James F. Riordan BLV, vol. 158: Academic Press; 1988: 357 - 364.

156. Helmut B: **Semi-micro methods for analysis of labile sulfide and of labile sulfide plus sulfane sulfur in unusually stable iron-sulfur proteins**. *Analytical Biochemistry* 1983, **131**(2):373 - 378.

157. Cicchillo RM, Iwig DF, Jones AD, Nesbitt NM, Baleanu-Gogonea C, Souder MG, Tu L, Booker SJ: **Lipoyl Synthase Requires Two Equivalents of S-Adenosyl-l-methionine To Synthesize One Equivalent of Lipoic Acid**. *Biochemistry* 2004, **43**(21):6378-6386.

158. Kent SBH: **Chemical Synthesis of Peptides and Proteins**. *Annual Review of Biochemistry* 1988, **57**(1):957 - 989.

159. Nyfeler R: **Peptide Synthesis via Fragment Condensation**. In: *Methods in Molecular Biology, Vol 35; Peptide Synthesis Protocols*. Edited by

Pennington MW, Dunn BM. Totowa, NJ: Humana Press Inc.; 1994: 303 - 316.

160. Merrifield RB: **Solid Phase Peptide Synthesis. I. The Synthesis of a Tetrapeptide**. *Journal of the American Chemical Society* 1963, **85**(14):2149 - 2154.
161. Pennington MW, Byrnes ME: **Procedures to Improve Difficult Couplings**. In: *Methods in Molecular Biology, Vol 35: Peptide Synthesis Protocols.* Edited by Pennington MW, Dunn BM. Totowa, NJ: Humana Press Inc.; 1994: 1 - 16.
162. Montalbetti CAGN, Falque V: **Amide bond formation and peptide coupling**. *Tetrahedron* 2005, **61**(46):10827 - 10852.
163. Jone J: **Peptide bond formation**. In: *Amino Acid and Peptide Synthesis.* Edited by Davies SG. Oxford: Oxford Chemistry Pimers; 1997: 25 - 41.
164. Diaz-Mochon JJ, Laurent B, Mark B: **Full Orthogonality between Dde and Fmoc: The Direct Synthesis of PNA Peptide Conjugates**. *Organic Letters* 2004, **6**(7):1127 - 1129.
165. Bycroft BW, Chan WC, Chhabra SR, Hone ND: **A novel lysine-protecting procedure for continuous flow solid phase synthesis of branched peptides**. *Journal of the Chemical Society, Chemical Communications* 1993(9):778 - 779.
166. Wagner BD: **The use of coumarins as environmentally-sensitive fluorescent probes of heterogeneous inclusion systems**. *Molecules* 2009, **14**:210 - 237.
167. Leung W-Y, Trobridge PA, Haugland RP, Haugland RP, Mao F: **7-Amino-4-methyl-6-sulfocoumarin-3-acetic acid: A novel blue fluorescent dye for protein labelling**. *Bioorganic & Medicinal Chemistry Letters* 1999, **9**(15):2229 - 2232.
168. Wang H-Y, Leung W-Y, Mao F: **Sulfonated derivatives of 7-aminocoumarin**. In., vol. 5,696,157. United States Patent: Molcular Probes, Inc, Eugene, Oreg.; 1997: 1 - 40.
169. Panchuk–Voloshina N, Haugland RP, Bishop–Stewart J, Bhalgat MK, Millard PJ, Mao F, Leung W-Y, Haugland RP: **Alexa Dyes, a Series of New Fluorescent Dyes that Yield Exceptionally Bright, Photostable**

Conjugates. *The Journal of Histochemistry & Cytochemistry* 1999, **47**(9):1179 - 1188.

170. Farrar CE, Siu KKW, Howell PL, Jarrett JT: **Biotin Synthase Exhibits Burst Kinetics and Multiple Turnovers in the Absence of Inhibition by Products and Product-Related Biomolecules**. *Biochemistry* 2010, **49**(46):9985 - 9996.
171. Walter C, Frieden E: **The Prevalence and Significance of the Product Inhibition of Enzymes**. In: *Advances in Enzymology and Related Areas of Molecular Biology*. John Wiley & Sons, Inc.; 2006: 167 - 274.
172. Challand MR, Ziegert T, Douglas P, Wood RJ, Kriek M, Shaw NM, Roach PL: **Product inhibition in the radical S-adenosylmethionine family**. *Federation of European Biochemical Societies (FEBS) Letters* 2009, **583**(8):1358 - 1362.
173. Tse Sum Bui B, Lotierzo M, Escalettes F, Florentin D, Marquet A: **Further Investigation on the Turnover of Escherichia coli Biotin Synthase with Dethiobiotin and 9-Mercaptodethiobiotin as Substrates** *Biochemistry* 2004, **43**(51):16432 - 16441.
174. Choi-Rhee E, Cronan JE: **Biotin Synthase Is Catalytic In Vivo, but Catalysis Engenders Destruction of the Protein**. *Chemistry & Biology* 2005, **12**(4):461 - 468.
175. Cornell KA, Riscoe MK: **Cloning and expression of Escherichia coli 5'-methylthioadenosine/S-adenosylhomocysteine nucleosidase: Identification of the pfs gene product**. *Biochimica et Biophysica Acta (BBA) - Gene Structure and Expression* 1998, **1396**(1):8 - 14.
176. Lee JE, Cornell KA, Riscoe MK, Howell PL: **Structure of E. coli 5'-methylthioadenosine/S-adenosylhomocysteine Nucleosidase Reveals Similarity to the Purine Nucleoside Phosphorylases**. *Structure* 2001, **9**(10):941 - 953.
177. Rossi AM, Taylor CW: **Analysis of protein-ligand interactions by fluorescence polarization**. *Nature Protocols* 2011, **6**(3):365 - 387.
178. Jameson DM, Seifried SE: **Quantification of Protein–Protein Interactions Using Fluorescence Polarization**. *Methods* 1999, **19**(2):222 - 233.
179. Ugulava NB, Frederick KK, Jarrett JT: **Control of Adenosylmethionine-Dependent Radical Generation in Biotin Synthase: A Kinetic and**

Thermodynamic Analysis of Substrate Binding to Active and Inactive Forms of BioB. *Biochemistry* 2003, **42**(9):2708 - 2719.

180. **Guide to Equilibrium Dialysis** [http://www.nestgrp.com/pdf/Ap1/EqDialManual.pdf]
181. **The Thermo Scientific RED Device Systems Brochure** [http://www.piercenet.com/files/1602445_RED_DeviceBrochure.pdf]
182. Waters NJ, Jones R, Williams G, Sohal B: **Validation of a rapid equilibrium dialysis approach for the measurement of plasma protein binding**. *Journal of Pharmaceutical Sciences* 2008, **97**(10):4586 - 4595.
183. Owicki JC: **Fluorescence polarization and anisotropy in high throughput screening: perspectives and primer**. *Journal of Biomolcular Screening* 2000, **5**:297 - 306.
184. Trinquet E, Mathis G: **Fluorescence technologies for the investigation of chemical libraries**. *Molecular BioSystems* 2006, **2**(8):380 - 387.
185. Jameson DM, Ross JA: **Fluorescence polarization/anisotropy in diagnostics and imaging**. *Chemical Reviews* 2010, **110**(5):2685 - 2708.
186. Weber G: **Polarization of the fluorescence of macromolecules. 1. Theory and experimental method**. *Biochem* 1952 **51**(2):145 - 155.
187. Yengo CM, Berger CL: **Fluorescence anisotropy and resonance energy transfer: powerful tools for measuring real time protein dynamics in a physiological environment.** *Current Opinion in Pharmacology* 2010, **10**:731 - 737.
188. Mocz G: **Information Content of Fluorescence Polarization and Anisotropy**. *Journal of Fluorescence* 2006, **16**(4):511 - 524.
189. Jameson DM, Sawyer WH: **Fluorescence anisotropy applied to biomolecular interactions**. *Methods in Enzymology* 1995, **246**:283 - 301.
190. Durbin SD, Feher G: **Protein crystallisation**. *Annual Review of Physical Chemistry* 1996, **47**(1):171 - 204.
191. Naomi E C: **Turning protein crystallisation from an art into a science**. *Current Opinion in Structural Biology* 2004, **14**(5):577 - 583.
192. Ducruix A, Giegé R: **Crystallization of Nucleic Acids and Proteins**, 2 edn: Oxford University Press; 1992.
193. McPherson A: **Current approaches to macromolecular crystallization**. *European Journal of Biochemistry* 1990, **189**(1):1 - 23.

194. Giegé R, Sauter C: **Biocrystallography: Past, present, future**. *HFSP Journal* 2010, **4**(3-4):109 - 121.

195. McPherson A: **Introduction to protein crystallization**. *Methods* 2004, **34**(3):254 - 265.

196. Kundrot CE: **Which strategy for a protein crystallization project?** *Cellular and Molecular Life Sciences* 2004, **61**(5):525 - 536.

197. Naomi E C: **Methods for separating nucleation and growth in protein crystallisation**. *Progress in Biophysics and Molecular Biology* 2005, **88**(3):329 - 337.

198. Ochi T, Bolanos-Garcia VM, Stojanoff V, Moreno A: **Perspectives on protein crystallisation**. *Progress in Biophysics and Molecular Biology* 2009, **101**(1-3):56 - 63.

199. Li M, Chang W-r: **Protein crystallization**. *Photosynthesis Research* 2009, **102**(2):223 - 229.

200. Bolanos-Garcia VM, Chayen NE: **New directions in conventional methods of protein crystallization**. *Progress in Biophysics and Molecular Biology* 2009, **101**(1 - 3):3 - 12.

201. Fish WW: **Rapid colorimetric micromethod for the quantitation of complexed iron in biological samples**. *Methods in Enzymology* 1988, **158**:357 - 364.

202. Bradford MM: **A rapid and sensitive method for the quantitation of microgram quantities of protein utilizing the principle of protein-dye binding**. *Analytical Biochemistry* 1976, **72**(1-2):248 - 254.

203. Bardajee GR, Winnik MA, Lough AJ: **7-Diethylamino-2-oxo-2H-chromene-3-carboxylic acid**. *Acta Crystallographica Section E-Structure Reports Online* 2006, **E62**:3076 - 3078.

204. Luan X, Cerqueira N, Oliveira A, Raposo M, Rodrigues L, Coelho P, Oliveira-Campos A: **Synthesis of fluorescent 3-benzoxazol-2-yl-coumarins**. *Advances in Colour Science and Technology* 2002, **5**(1):18 - 23.

205. Clayden J, Greeves N, Warren S, Wothers P: **Nucleophilic substitution at the carbonyl (C=O) group.** In: *Organic Chemistry.* Oxford University Press; 2001: 276 - 300.

206. Chan WC, White PD: **Fmoc Solid Phase Peptide Synthesis: A Practical Approach**. Oxford: Oxford University Press; 2000.

207. Atherton E, Sheppard RC: ***Solid Phase Peptide Synthesis A Practical Approach***: IRL Press at Oxford University Press; 1989.

208. Kaiser E, Colescott RL, Bossinger CD, Cook PI: **Color test for detection of free terminal amino groups in the solid-phase synthesis of peptides**. *Analytical Biochemistry* 1970, **34**(2):595 - 598.

209. Robinson D: **7-Amino-4-Methyl-Coumarin-3-Carboxyalkyl derivatives and Flourescent Conjugates Thereof**. In: *United States Patent.* BioCarb AB., Lund, Sweden; 1990.

210. Feng Y, Burgess K, Pledger D, Cairns N, Linthicum DS: **A Labeled Guanidine Ligand for Studying Sweet Taste**. *Bioorganic & Medicinal Chemistry Letters* 1998, **8**(7):881 - 884.